Reverse-engineering the connectome

LAURA E. SUÁREZ
Integrated Program in Neuroscience
McGill University, Montréal, QC, Canada
August 2023

A thesis submitted to McGill University in partial fulfillment
of the requirements of the degree of
Doctor of Philosophy

© LAURA E. SUÁREZ, 2023

Abstract

A prevailing feature of biological systems is the inextricable link between structure and function: the form or shape of a structure correlates with the purpose or function of that structure. This comprehensive design principle of nature encompasses multiple scales and levels of complexity, from molecules and cells, up to organs and even entire organisms. The function of the nervous system is not an exception to this rule; its function is shaped by the structure and arrangement of neurons and neural populations. Advances in imaging technologies permit the detailed reconstruction of the anatomical connection patterns of animals' nervous system. The architecture of these comprehensive wiring diagrams, termed structural connectivity networks or connectomes, shapes the functional associations between brain areas. Inter-regional axonal projections promote signaling among distant neuronal populations, resulting in patterned neuronal co-activation and coherent dynamics. The systematic co-activation among neuronal populations, often used to map functional connectivity networks, are thought to be the neural processes that support perception, cognition and behavior. However, how computation and functional specialization emerge from the underlying structural network remains one of the central questions in neuroscience. This thesis explores the link between structure and function, with an emphasis on the information-processing of brain networks. Chapter 1 provides a brief introduction to the question of the link between structure and function in brain networks and lays out the main research questions presented throughout this thesis. Chapter 2 synthesizes the current state of knowledge linking structure and function in macro scale brain networks, reviews different models used to assess this relationship, identifies methodological research gaps and lays out potential research directions to advance the field, some of which inspired part of the work presented in this thesis. Chapter 3 challenges the traditional notion of function, understood as functional connectivity, by reconceptualizing function as a computational property. This chapter combines connectomics and reservoir computing -an artificial neural network model- to investigate the link between

macroscale connectivity and the computational properties that emerge from network dynamics in the human connectome. Results emphasize the computational relevance of the connectome's macroscale topology and its mesoscale modular organization for optimal performance at criticality. Chapter 4 expands on the previous chapter and presents a multidisciplinary framework that combines artificial neural networks and connectomics to explore structure-function relationships in brain networks. This chapter outlines the principles of reservoir computing, describes the versatility of this hybrid approach, and introduces an open-source workbench tool that allows neuroscientists to implement biological neural networks as artificial reservoirs. This work highlights the impact that this combined approach can have on our mechanistic understanding of how computations and functional specialization emerge from the brain's anatomical structure. Chapter 5 explores how connectome architecture varies over phylogeny. As animals' challenges and habitats differ, so do their physical traits and cognitive abilities. This chapter presents a comparative analysis in which we comprehensively chart connectome organization across the mammalian phylogenetic spectrum to construct data-driven phylogenetic relationships based on brain wiring. Analyses show that connectome organization conforms to traditional taxonomies based on morphology and genetics and indicate that inter-species variations are mainly driven by local connectivity profiles while hallmark global features are preserved. Finally, Chapter 6 closes with a discussion of the primary findings and contributions of this thesis and provides future directions to continue exploring the link between structure and function in both biological and artificial neural networks.

Résumé

Une caractéristique prédominante des systèmes biologiques est le lien inextricable entre la structure et la fonction : la forme d'une structure est en corrélation avec le but ou la fonction de cette structure. Ce principe de conception universel de la nature englobe de multiples échelles et niveaux de complexité, des molécules et cellules, jusqu'aux organes et même à des organismes entiers. La fonction du système nerveux n'échappe pas à cette règle ; sa fonction est façonnée par la structure et l'arrangement des neurones et des populations neuronales. Les progrès des technologies d'imagerie permettent la reconstruction détaillée des schémas de connexion anatomiques du système nerveux des animaux. L'architecture de ces schémas de câblage complets, appelés réseaux de connectivité structurelle ou connectomes, façonne les associations fonctionnelles entre les zones du cerveau. Les projections axonales interrégionales favorisent la signalisation parmi les populations neuronales distantes, donnant lieu à des modèles de co-activation neuronale et à des dynamiques cohérentes. On pense que les co-activations systématiques parmi les populations neuronales, souvent utilisées pour la cartographie des réseaux de connectivité fonctionnelle, sont les processus neuronaux qui soutiennent la perception, la cognition et le comportement. Cependant, la manière dont le calcul et la spécialisation fonctionnelle émergent du réseau structurel sous-jacent reste l'une des questions centrales des neurosciences. Cette thèse explore le lien entre structure et fonction, en mettant l'accent sur les caractéristiques du traitement de l'information des réseaux cérébraux. Le chapitre 1 propose une brève introduction sur le lien entre structure et fonction dans les réseaux cérébraux et expose les principales questions de recherche présentées tout au long de cette thèse. Le chapitre 2 synthétise l'état actuel des connaissances reliant la structure et la fonction dans les réseaux cérébraux à grande échelle, identifie les lacunes méthodologiques de la recherche et expose les orientations de recherche potentielles pour faire avancer le domaine, dont certaines ont inspiré une partie des travaux présentés dans cette thèse. Le chapitre 3 remet en question la notion traditionnelle de fonction, comprise comme

connectivité fonctionnelle, en reconceptualisant la fonction comme une propriété computationnelle. Ce chapitre combine la connectomique et l'informatique de réservoir - un modèle de réseau neuronal artificiel - pour étudier le lien entre la connectivité à grande échelle et les propriétés computationnelles qui émergent de la dynamique du réseau dans le connectome humain. Les résultats soulignent la pertinence informatique de la topologie macro-échelle du connectome et de son organisation modulaire méso-échelle pour des performances optimales à la criticité. Le chapitre 4 développe le chapitre précédent et présente un cadre multidisciplinaire qui combine des réseaux neuronaux artificiels et la connectomique pour explorer les relations structure-fonction dans les réseaux cérébraux. Ce chapitre souligne les principes de l'informatique des réservoirs, décrit la polyvalence de cette approche hybride et présente un outil open source qui permet aux neuroscientifiques d'implémenter des réseaux neuronaux biologiques en tant que réservoirs artificiels. Cette étude met en évidence l'impact que cette approche combinée peut avoir sur notre compréhension mécaniste de la façon dont les calculs émergent de la structure anatomique du cerveau. Le chapitre 5 explore les variations de l'architecture du connectome au cours de la phylogénie. Comme les défis et les habitats varient d'une espèce animale à l'autre, il en va de même pour leurs caractéristiques physiques et leurs capacités cognitives. Ce chapitre présente une analyse comparative dans laquelle nous suivons de manière exhaustive l'organisation du connectome à travers le spectre phylogénétique des mammifères pour construire des relations phylogénétiques basées sur les données et basées sur le câblage cérébral. Les analyses montrent que l'organisation du connectome est conforme aux taxonomies traditionnelles basées sur la morphologie et la génétique et indiquent que les variations interespèces sont principalement déterminées par les profils de connectivité locaux, tandis que les caractéristiques globales sont préservées. Enfin, le chapitre 6 se termine par une discussion des principaux résultats et contributions de cette thèse et fournit des orientations futures pour continuer à explorer le lien entre la structure et la fonction dans les réseaux neuronaux biologiques et artificiels.

Contents

Abstract **i**

Résumé **iii**

Contents **v**

List of Figures **ix**

List of Tables **xii**

Acknowledgements **xiii**

Contribution of authors **xvi**

1 Introduction **1**

1.1 General context 1

1.2 Objectives 2

1.3 Contributions to original knowledge 3

1.3.1 Scientific contributions 3

1.3.2 Software contributions 4

2 Review of the literature **5**

2.1 Preface 5

2.2 Abstract 6

2.3 Structure and function in brain networks 6

2.4 An imperfect correspondence 9

2.5 Models of higher-order interactions 11

2.6 Individual differences in structure-function coupling 14

2.7 Regional Heterogeneity 16

2.8 Modulating structure-function relationships . . . 18
2.9 Function or property? . . . 19
2.10 Function as computational property . . . 20
2.11 Concluding Remarks . . . 22

3 Linking structure and memory capacity in the human connectome 25
3.1 Preface . . . 25
3.2 Abstract . . . 26
3.3 Introduction . . . 27
3.4 Results . . . 29
3.4.1 Learning in neuromorphic networks . . . 29
3.4.2 Memory capacity of the human connectome . . . 30
3.4.3 Connectomes optimize computation-cost trade-offs . . . 34
3.4.4 Memory capacity of intrinsic networks . . . 35
3.4.5 Information transfer across the brain . . . 38
3.4.6 Interplay between network topology, dynamics and memory capacity 39
3.4.7 Sensitivity analysis . . . 41
3.5 Discussion . . . 43
3.6 Materials and Methods . . . 48
3.6.1 Data acquisition . . . 48
3.6.2 Structural network reconstruction . . . 49
3.6.3 Reservoir computing . . . 49
3.6.4 Intrinsic networks as functional systems . . . 52
3.6.5 Memory capacity task . . . 52
3.6.6 Bootstrap resampling . . . 53
3.6.7 Null models . . . 54
3.6.8 Wiring cost . . . 55
3.6.9 Encoding and decoding capacity . . . 55
3.6.10 Graph measures . . . 57
3.7 Data availability . . . 59
3.8 Code availability . . . 59
3.9 Acknowledgements . . . 59
3.10 Author contributions . . . 60
3.11 Competing interests . . . 60
3.12 Bibliography . . . 60

4 Linking structure and computation in brain networks **84**
4.1 Preface . . . 84
4.2 Abstract . . . 85
4.3 Introduction . . . 86
4.4 Fundamentals of reservoir computing . . . 88
4.5 The brain as a reservoir . . . 92
4.6 The `conn2res` toolbox . . . 96
4.6.1 A use-case tutorial . . . 99
4.7 Concluding remarks . . . 103
4.8 Bibliography . . . 104

5 Connectome architecture across phylogeny **116**
5.1 Preface . . . 116
5.2 Abstract . . . 117
5.3 Introduction . . . 118
5.4 Results . . . 121
5.4.1 Connectome-based inter-species distances . . . 121
5.4.2 Architectural features differentiate species . . . 122
5.4.3 Conservation of small-world architecture . . . 126
5.4.4 Conservation of edge classes across species . . . 127
5.5 Discussion . . . 129
5.6 Materials and Methods . . . 132
5.6.1 Brain samples . . . 132
5.6.2 MRI acquisition . . . 133
5.6.3 Connectome reconstruction . . . 133
5.6.4 Network generation and analysis . . . 134
5.6.5 Controlling for the scanning resolution and acquisition parameters . 135
5.6.6 Spectral distance . . . 135
5.6.7 Topological distance . . . 136
5.6.8 Small-world organization . . . 141
5.6.9 Multi-resolution community detection . . . 141
5.6.10 Classification of edges . . . 142
5.6.11 Controlling for replicas . . . 144
5.6.12 Controlling for density . . . 144
5.7 Data availability . . . 144
5.8 Code availability . . . 145

5.9 Acknowledgments 145
5.10 Bibliography 145

6 Discussion **181**
6.1 Summary of findings and contributions 181
6.2 Function as computation 184
6.2.1 Annotating artificial reservoirs 184
6.2.2 Plastic reservoirs 185
6.2.3 Promoting the synergy between AI and neuroscience 186
6.3 Linking structure to ~~function~~ computation across phylogeny 187
6.4 Conclusions 187

Bibliography **189**

List of Figures

2.1 Imperfect correspondence between structural and functional connectivity . 8
2.2 Models of higher-order interactions 10
2.3 Regional heterogeneity and annotated brain graphs 14
2.4 The ascending arousal system modulates structure-function relationships . 17
S2.1 Measuring structural and functional connectivity 23

3.1 Measuring the memory capacity of biological neural networks 31
3.2 Memory capacity of the human connectome 33
3.3 Computation *vs* wiring cost trade-off 35
3.4 Memory capacity of intrinsic networks 37
3.5 Encoding and decoding capacity of intrinsic networks 40
3.6 Contribution of network topology to memory capacity is a function of the dynamics 42
S3.1 Effect of the modular structure captured by the readout nodes 73
S3.2 Effect of the internal connectivity structure of the readout nodes 74
S3.3 A chaotic state closer to critical dynamics 75
S3.4 Effect of relative density on the memory capacity of intrinsic networks . . . 76
S3.5 Memory capacity of the human connectome - replication using thalamic input nodes 77
S3.6 Memory capacity of intrinsic networks - replication using thalamic input nodes 78
S3.7 Memory capacity of the human connectome - replication using a coarser parcellation 79
S3.8 Memory capacity of intrinsic networks - replication using a coarser parcellation 80
S3.9 Effect of the choice of activation function: hyperbolic tangent 81
S3.10 Benchmarking connectome-informed reservoirs against other reservoir computing architectures 82

4.1 Reservoir computing . . . 89
4.2 `conn2res` toolbox . . . 97
4.3 Use-case tutorial: effect of local and global dynamics on the performance of perceptual and context decision making tasks . . . 102

5.1 MaMI data set . . . 120
5.2 Spectral and topological distance between orders . . . 123
5.3 Contribution of network features . . . 125
5.4 Conservation of small-world architecture . . . 127
5.5 Contribution of edge types . . . 128
S5.1 Modularity . . . 160
S5.2 Laplacian eigenspectra . . . 161
S5.3 Distribution of local graph features across taxonomic orders . . . 162
S5.4 Distribution of global graph features across taxonomic orders . . . 163
S5.5 Cumulative distribution of binary local graph features across taxonomic orders . . . 164
S5.6 Cumulative distribution of weighted local graph features across taxonomic orders . . . 165
S5.7 Effect of using replicated samples on the topological and spectral distance between orders . . . 166
S5.8 Effect of using replicated samples on the contribution of network features . . . 167
S5.9 Changes in local topology along the frontal-occipital axis . . . 168
S5.10 Relationship between spectral and topological distance . . . 169
S5.11 Network density . . . 170
S5.12 Controlling for network density . . . 171
S5.13 Contribution of network features after controlling for connection density . . . 172
S5.14 Taxonomic order separation in low-dimensional space . . . 173
S5.15 Connectome-based clustering of mammals . . . 174
S5.16 Connection length distribution . . . 175
S5.17 Effect of (decreasing) parcellation resolution on the spectral and topological inter-species distance . . . 176
S5.18 Effect of (decreasing) parcellation resolution on the contribution of topological network features . . . 177
S5.19 Effect of (increasing) parcellation resolution on the spectral and topological inter-species distance . . . 178

S5.20Effect of (increasing) parcellation resolution on the contribution of topological network features 179
S5.21Effect of kernel density estimation (kde) on inter-species spectral distances . 180

List of Tables

S3.1 List of LIF and LSM model parameters 83

S5.1 List of animal species 154

Acknowledgements

Much of my academic, professional and personal growth during the past six years can be attributed to the mentorship and support of incredible scientists, but above all, incredible human beings that deserve to be recognized. First and foremost, I would like to thank Dr. Bratislav Mišić, my exceptional PhD supervisor. Not only are you a brilliant scientist but also a wonderful and kind human being. None of the work in this thesis would have been possible without your guidance, patience and unconditional support. Bratislav, it has been a real honor and a pleasure to work by your side. There are just not enough words to express my gratitude for everything you have done for me, and for having given me this amazing opportunity of coming to Montréal and doing my PhD under your supervision. Likewise, I would like to thank Guillaume Lajoie, my co-supervisor. Thanks for accepting to walk this journey next to Bratislav and I, and for always welcoming me into your group and making me feel like a member of the Neuro-AI Computations Research lab. Your guidance and support have been crucial for the development of the projects presented in this thesis. To my committee members, Drs. Sylvain Baillet and Blake Richards, and all my collaborators and co-authors: thank you for mentorship, guidance and support throughout these years. All your insightful thoughts and ideas were essential to ensure that the work presented here was the absolute best it could be. To my past and present colleagues in the Network Neuroscience Lab — Golia, Ross, Bertha, Zhen-Qi, Justine, Vincent, Filip, Andrea, Eric, and all others, you are "all" any PhD trainee could have asked for as lab mates. Thank you for your help, support, inspiration, and most importantly, for your friendship. You are all such wonderful people and I am hoping to keep working with you in the future. To my previous supervisor, Dr. Juan Claudio Nino, and his brilliant ex-trainee Jack Kendall. Thank you for having given me the chance to work at the NRG lab, and for introducing me to the fascinating world of neuromorphic computing. To Dr. Étienne De Villers-Sidani, my internship supervisor over the last year. Thanks for believing in me and giving me the opportunity to experience the Industry world before concluding my PhD. I am deeply grateful for your mentorship and guidance. I have learned a lot from you and from the

entire Innodem team. Special thanks to my family, in particular to my parents and my brother. Thank you for all your love and unconditional support from afar, for believing in me and for always pushing me to give the best of myself. To my amazing and inspiring friends Nazanin, Sara, Bertha, Laëtitita, Emanuelle, Claudia, Carole and Laïla. Thank you so much for your support. You were always there reaching out to me when I needed it the most. Each one of you has been crucial to make it until the end of my PhD. And last but not least, I would like to thank Ádám Demjén for being an amazing partner, for infusing my life with so much fun, peace, joy and love over the past few months, for being so supportive and understanding during the writing of this thesis and the last stages of my PhD, and for helping me keep things light, fun and smooth.

Dedicated to all latin women in
(neuro) Science

Contribution of authors

As the lead author on the manuscripts presented in chapters 2 through 5, I was responsible for overseeing all aspects of the research, including: literature review, conceptualization, experimental design, data processing, statistical analysis, visualization, interpretation of results, and writing of the manuscripts. Contributions of co-authors for these chapters are outlined below:

Chapter 3

- Ross D. Markello: writing of the manuscript
- Richard F. Betzel: writing of the manuscript
- Bratislav Misic: literature review, conceptualization, and writing of the manuscript

Chapter 3

- Blake A. Richards: editing of the manuscript
- Guillaume Lajoie: conceptualization and editing of the manuscript
- Bratislav Misic: conceptualization, interpretation of results and writing of the manuscript

Chapter 4

- Agoston Mihalik: software development and editing of the manuscript
- Filip Milisav: software development and editing of the manuscript
- Kenji Marshall: software development
- Mingze Li: software development
- Petra Vertes: editing of the manuscript
- Guillaume Lajoie: conceptualization and editing of the manuscript

- Bratislav Misic: conceptualization and writing of the manuscript

Chapter 5

- Yossi Yovel: data collection and processing
- Martijn P. van den Heuvel: editing of the manuscript
- Olaf Sporns: experimental design and editing of the manuscript
- Yaniv Assaf: data collection and processing
- Guillaume Lajoie: experimental design and editing of the manuscript
- Bratislav Misic: conceptualization, experimental design, interpretation of results and writing of the manuscript

Chapter 1

Introduction

1.1 General context

The relationship between structure and function is a ubiquitous concept in biological systems: from the conformation of proteins, diverse cell morphologies, different organ shapes, up to the biomechanics of animals' skeletons. Analogously, the function of the nervous system is shaped by the structure and arrangement of neurons and neural populations. Synaptic projections form a complex network of hierarchically nested and increasingly polyfunctional neural circuits. The dynamics that unfold upon this network are thought to support perception, cognition and behavior.

Advances in imaging technologies, such as magnetic resonance imaging, have permitted the detailed reconstruction of the connection patterns of animals' nervous system. These comprehensive wiring diagrams, often termed structural connectivity networks or connectomes, represent the physical anatomical connections between neural elements. The architecture of structural connectivity networks imparts a distinct signature on neural co-activation patterns. Inter-areal synaptic projections promote signalling and synchrony among distant neuronal populations, giving rise to coordinated spatiotemporal patterns of neural activity and coherent dynamics. The systematic co-activation among neuronal populations is used to map functional connectivity networks.

Conventionally, the link between structure and function in brain networks has been addressed through models that map structural connectivity to functional connectivity. Although these models successfully predict functional co-activation patterns as well as emergent neural dynamic phenomena, they fail to establish a direct link between these emergent functional interactions and the computations that underlie perception, cognition

and behavior. The objective of this thesis is to further improve our understanding of the relationship between structure and function, but with a notion of *function* that moves away from emergent dynamical phenomena, and redirects the focal point towards the computational and information-processing properties of the brain.

1.2 Objectives

Chapter 3 objectives

Chapter 3 challenges the traditional notion of function, conventionally understood as the systematic co-activation of regional brain activity, or functional connectivity, by directly considering function as a computational property. Combining connectomics and reservoir computing, I reconstruct human connectomes using diffusion-weighted MRI, implement them as artificial reservoirs, and train these connectome-informed reservoirs to perform a memory task. By benchmarking artificial neural networks with connectome-based architectures against random architectures, this chapter assess the functional consequences of brain network topology. Specifically, I investigate how network topology and dynamics support the memory capacity of the human connectome.

Chapter 4 objectives

Chapter 4 expands on the previous chapter and proposes a general interdisciplinary framework that combines connectomics and reservoir computing to explore how network structure and dynamics shape computation and learning in reservoirs with biologically-plausible architectures. This chapter outlines the principles of reservoir computing, describes the flexibility and versatility of this hybrid approach, and introduces `conn2res`, an open-source workbench tool that allows neuroscientists to implement biological neural networks as artificial reservoirs.

Chapter 5 objectives

Chapter 5 explores how connectome architecture varies over phylogeny. Cognitive abilities are shaped by natural selection in the same way morphological traits are. As animals' challenges and habitats differ, so do their physical traits as well as their behavioural repertoires. In this chapter I examine the hypothesis of whether variations in connectome architecture, that result from speciation events in the genome, account for cognitive

and behavioural adaptations across taxonomic orders. By comprehensively charting connectome organization across the mammalian phylogenetic spectrum, this chapter presents a comparative analysis in which I quantitatively assess inter-species connectome similarities, and construct data-driven derived phylogenetic relationships based on brain wiring. I then compare these newly derived, connectome-based phylogenetic relations against already established phylogenetic links based on morphology and genetics.

1.3 Contributions to original knowledge

Collectively, the presented research contributes to our comprehension of how structure and function are linked in brain networks from two complementary perspectives. While one improves our understanding of how connectome architecture shapes the computational and information-processing properties of the brain, the other provides insight into how inter-species variations in cognition and behavior are supported by variations in connectome architecture across the mammalian phylogenetic spectrum. Beyond this, the work presented in this thesis also makes unique technical contributions via openly-developed and freely-available software that provides researchers with easy-to-use tools and leads to a more mechanistic understanding of the link between network structure and cognitive function in biological brains. Below, I briefly highlight these distinct *scientific* and *software* contributions.

1.3.1 Scientific contributions

Chapter 3

- The interaction between macroscale network topology, mesoscale modular organization and critical dynamics confers optimal memory capacity to the human connectome.
- The modular organization of the brain, as defined by these intrinsic networks, constitutes a computationally-relevant feature of the human connectome.
- The connectome's network topology optimizes the trade-off between computational capacity and metabolic costs derived from wiring.
- The connectome supports functional specialization by promoting spatial heterogeneity of information content across functional networks.

Chapter 4

- By moving beyond the traditional notion of *function*, understood as *functional connectivity*, to a concept that is based on the computational and information-processing properties of the brain, `conn2res` sets the stage for a more mechanistic and meaningful understanding of how computation and functional specialization emerge from the brain's anatomical network structure.

Chapter 5

- Variations in connectome architecture reflect phylogeny. In other words, species with similar genetics, morphology and behavior tend to have similar connectome architecture.
- Differentiation of taxonomic orders is better explained by variations in local network topology. Conversely, global network topology appears to be conserved across species.
- Small-worldness, rich-club organization and connection-length distribution are among the global topological traits shared across mammalian species, while interspecies differences are mainly driven by variations in regional connectivity profiles.

1.3.2 Software contributions

In Chapter 4 I introduce `conn2res` (https://github.com/netneurolab/conn2res.git), an open-source Python package that allows researchers to implement artificial neural networks with connectome-informed architectures, and to train them to learn different cognitive tasks. While `conn2res` was originally created to enable the analyses discussed in Chapter 3, it can contribute more insights into the field. Therefore, the toolbox was developed to add more flexibility in terms of the network architecture and type of local dynamics that can be implemented by the artificial neural network, and it was extended to include a more comprehensive repertoire of cognitive tasks.

Chapter 2

Review of the literature

Laura E. Suárez[1], Ross D. Markello[1], Richard F. Betzel[2], & Bratislav Misic[1]

[1]McConnell Brain Imaging Centre, Montréal Neurological Institute, McGill University, Montréal, QC, Canada

[2]Psychological and Brain Sciences, Program in Neuroscience, Cognitive Science Program, Network Science Institute, Indiana University, Bloomington, IN, USA

Published in:

Trends in Cognitive Sciences: https://doi.org/10.1016/j.tics.2020.01.008

2.1 Preface

A common thread throughout this thesis is the relationship between structure and function in brain networks. Traditionally, *structure* has been linked to the anatomical connections of the brain, or structural connectivity networks, whereas *function* has been described as regional co-activation patterns of neural activity, used to map functional connectivity networks. The projects outlined in this thesis move away from this phenomenological concept of function to a notion that is closer to what we would generally consider as cognitive function and behavior. One way in which this thesis attempts to do so is by considering function as a computational property. This chapter starts by introducing the traditional interpretations of *structure* and *function* in the context of brain networks, followed by a review of the different modelling traditions used to map structural connectivity to functional connectivity. Altogether, the studies reviewed in this chapter evidence

the complexity of the structure-function relationship, suggesting that there is not a one-to-one correspondence between the two, and that other local factors, such as molecular, microstructural, morphometric and intrinsic dynamic variables, also play a role in determining how structure shapes function in the brain. This chapter also identifies several methodological gaps, one of those being the lack of a more nuanced notion of *function*, and suggests potential research directions to advance our comprehension of how structure and function are linked in biological brains. All sections in this chapter make part of a published review article, except for Section 2.10, which was added here to briefly introduce a novel modelling framework that makes emphasis on the information-processing properties of brain networks. Chapter 3 and chapter 4 were developed based on this new modelling approach. A more detailed description of the fundamentals and genesis of this approach are provided in sections 4.4 and 4.5 of chapter 4.

2.2 Abstract

Structure-function relationships are a fundamental principle of many naturally occurring systems. However, network neuroscience research suggests that there is an imperfect link between structural connectivity and functional connectivity in the brain. Here we synthesize the current state of knowledge linking structure and function in macroscale brain networks and discuss the different types of models used to assess this relationship. We argue that current models do not include the requisite biological detail to completely predict function. Structural network reconstructions enriched with local molecular and cellular metadata, in concert with more nuanced representations of functions and properties, hold great potential for a truly multiscale understanding of the structure-function relationship.

2.3 Structure and function in brain networks

The relationship between structure and function is a central concept in natural sciences and engineering. Consider how the conformation of a protein determines its chemical properties and ultimately, its biological function. The folding of the protein into a three dimensional structure promotes interactions among amino acids, allowing the protein to chemically interact with other molecules and endowing it with function. Conversely, disruption of the protein's structure results in loss of function. Tellingly, the protein is said

to be *denatured*, highlighting the idea that changing its structure has fundamentally altered its natural function.

The function of the nervous system is analogously shaped by the structure and arrangement of neurons and neuronal populations. The complex network of synaptic projections forms a hierarchy of nested and increasingly polyfunctional neural circuits that support perception, cognition and action. Modern imaging technology permits high-throughput reconstruction of neural circuits across spatiotemporal scales, and across species (Box S2.1). Through extensive international data sharing efforts, increasingly detailed reconstructions of the nervous system's connection patterns are available in humans and in multiple model organisms, including invertebrate (Chiang et al., 2011), avian (Shanahan et al., 2013), rodent (Bota et al., 2015; Oh et al., 2014) and primate species (Majka et al., 2016; Markov et al., 2012). These comprehensive wiring diagrams of the nervous system—termed **structural connectivity** (SC) networks or **connectomes**—represent the physical connections between neural elements (Sporns et al., 2005).

The emergence of network neuroscience offers an opportunity to quantify and articulate the link between the organizational features of neuronal networks and the spectrum of cortical functions. Structural connectivity networks possess distinctive and nonrandom attributes, including high local clustering and short path length, characteristic features of a small-world architecture (Watts and Strogatz, 1998). Populations with similar functional properties tend to cluster together, forming specialized modules cross-linked by hub nodes with diverse connectional fingerprints (Kötter et al., 2001; Young, 1993). The hubs of the networks are disproportionately interconnected with each other, forming a putative core (Hagmann et al., 2008) or "rich club" (Heuvel et al., 2012), an architectural feature that potentially allows signals to be sampled and integrated from specialized modules (Zamora-López et al., 2010). Finally, brain networks are spatially-embedded, with finite metabolic and material resources (Bullmore and Sporns, 2012), resulting in increased prevalence of shorter, low-cost connections (Horvát et al., 2016; Roberts et al., 2016). These organizational attributes have been replicated across a range of species and tracing techniques, suggesting common organizational principles across phylogeny (Heuvel et al., 2016).

The architecture of SC networks imparts a distinct signature on neuronal co-activation patterns. Inter-regional projections promote signaling and synchrony among distant neuronal populations, giving rise to coherent neural dynamics, measured as regional time series of electromagnetic or hemodynamic neural activity. Systematic co-activation among pairs of regions can be used to map **functional connectivity** (FC) networks. Over the past decade, these dynamics are increasingly recorded without task instruction or

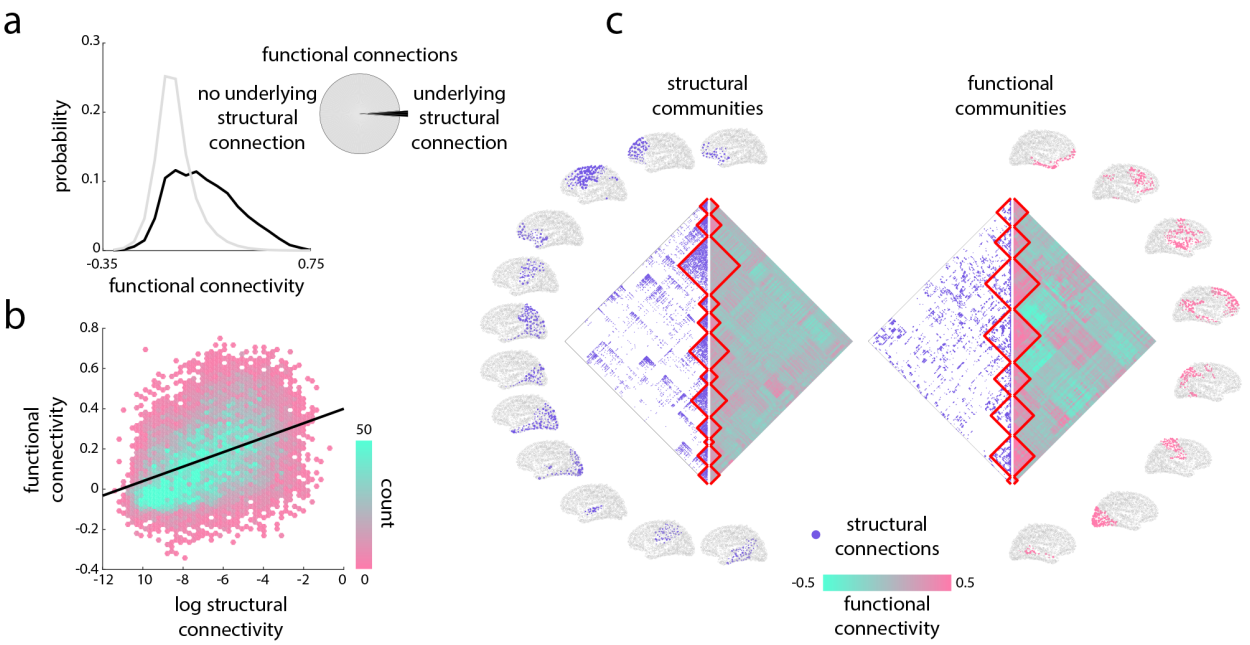

Figure 2.1: **Imperfect correspondence between structural and functional connectivity** | Despite considerable overlap, structure and function diverge both locally and globally. (a) Due to the sparse nature of structural connectivity, most functional connections are not supported by an underlying structural connection. Models of higher-order interactions are therefore necessary to make predictions about most functional connections. (b) In cases where a corresponding structural connection exists, there is a correlation between structural and functional connection weight, but these correlations are typically between $R = 0.3$ and $R = 0.7$. This means that even for this small class of connections, direct structural connectivity optimistically explains no more than 50% of the variance in functional connectivity. (c) Structure and function continue to diverge at the mesoscopic scale. Community detection for structural and functional networks typically yields different solutions; functional communities (resting state networks) tend to encompass spatially distributed systems with perceptual, cognitive and affective relevance, while structural networks tend to be more spatially constrained.

stimulation; the resulting "intrinsic" or "resting-state" FC is thought to reflect spontaneous neural activity (Biswal et al., 1995). Intrinsic FC patterns are highly organized (Bellec et al., 2010; Damoiseaux et al., 2006; Thomas Yeo et al., 2011), reproducible (Gordon et al., 2017; Noble et al., 2019) and comparable to task-driven co-activation patterns (Cole et al., 2014; Smith et al., 2009). The persistent and reproducible nature of brain activity during rest makes resting-state FC an ideal starting point to study structure-function relationships (Damoiseaux and Greicius, 2009; Honey et al., 2010).

Here we synthesize the current state of knowledge linking structure and function in macroscale brain networks. We first show that direct one-to-one links between structure and function are limited and inherently obscured by the networked nature of the brain. We survey modern quantitative methods that move away from direct correlations between

structure and function by conceptualizing function as emerging from higher-order interactions among multiple neuronal populations, with a focus on strengths, limitations and commonalities. We posit that the next steps in understanding network-level structure-function relationships must take into account regional heterogeneity by enriching network reconstructions with microscale attributes, including transcriptomic, cytoarchitectonic and neuromodulatory information. We close by highlighting emerging theories that macroscale structure-function relationships are not uniform across the brain, but vary in parallel with cytoarchitectonic and representational hierarchies.

2.4 An imperfect correspondence

Early studies emphasized correlations between structural and functional connection weights. Structural weights are correlated with functional weights (Honey et al., 2009), and nodes that are central to structural networks also tend to be central in functional networks (Honey et al., 2009). Furthermore, structurally-connected pairs of neural elements display greater functional connectivity than structurally-unconnected pairs (Honey et al., 2009; Shen et al., 2012) (Fig. 2.1a). More globally, many intrinsic functional networks—particularly the visual and somatomotor networks—are circumscribed by patterns of dense anatomical connectivity (Alves et al., 2019; Shen et al., 2012; Van Den Heuvel et al., 2009).

While structural and functional connectivity are significantly correlated, the correspondence is not perfect. Even the best-case estimates place the correlation at $R^2 \approx 0.5$ (Honey et al., 2009), which means that considerable variance (at least half) in functional connection weights is unexplained by a simple 1:1 correspondence with structure. The discrepancy widens in the case of functional connections between regions that are not structurally connected (Fig. 2.1b). A particularly salient example is the case of homotopic functional connections between corresponding structures in the two hemispheres. These are typically the strongest subset of functional connections (Mišić et al., 2014b). Interestingly, not all homotopic functional connections are supported by a direct underlying callosal projection (Shen et al., 2015), and strong homotopic functional connections may be observed even in individuals with no callosal connections (Layden et al., 2019; O'Reilly et al., 2013; Uddin et al., 2008). These examples illustrate the simple point that sustained communication via indirect anatomical connections may manifest as strong functional connectivity.

The discordance between structure and function is particularly pronounced at the mesoscopic scale. Intrinsic networks commonly observed in resting-state FC and meta-analytic co-activation cannot be recovered from structural networks (Betzel et al., 2018;

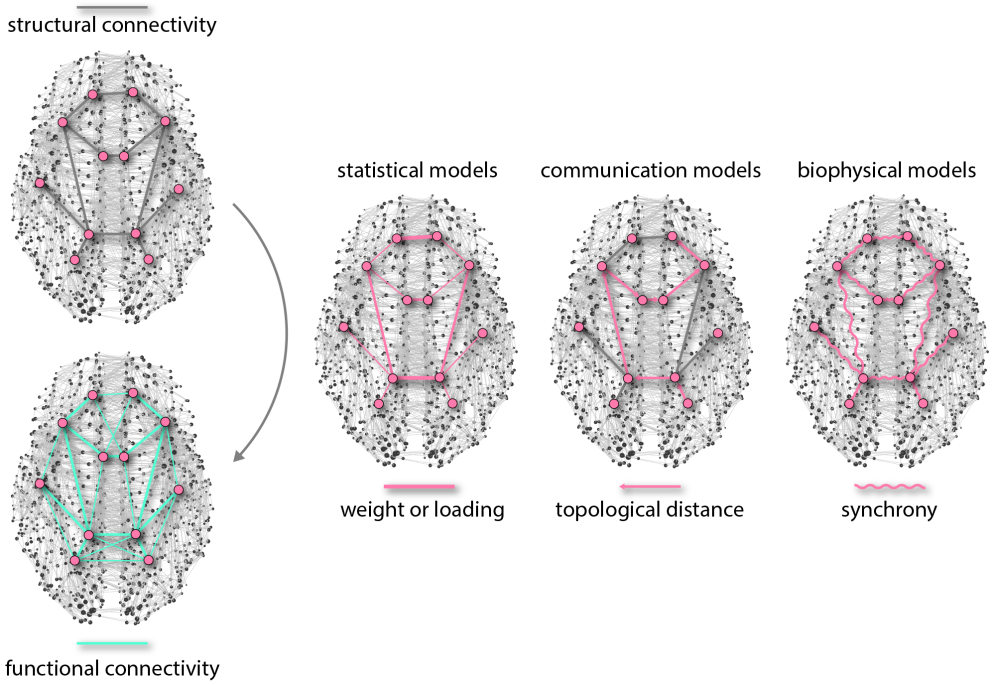

Figure 2.2: **Models of higher-order interactions** | Due to the poor direct correspondence between structural and functional connectivity, multiple models of higher-order interactions have been proposed to translate structure to function. These models entail varying assumptions and complexity. Statistical models attempt to assign weights or loadings to structural—and in some cases, functional connections—to maximize correlations between network modalities (Messé et al., 2014; Mišić et al., 2016). Communication models embody one or more signaling mechanisms, ranging between those that are fully centralized (routing) or fully decentralized (diffusion) (Crofts and Higham, 2009; Goñi et al., 2014; Graham and Rockmore, 2011; Mišić et al., 2015). Biophysical models simulate patterns of synchrony among biologically-realistic neuronal populations, thereby directly generating spontaneous or stimuluation-induced activity (Breakspear, 2017; Deco et al., 2009; Honey et al., 2007; Sanz-Leon et al., 2015).

Mišić et al., 2015) (Fig. 2.1c). While intrinsic networks can be reproducibly defined using independent component analysis (Damoiseaux et al., 2006), community detection (Power et al., 2011) or data-driven clustering (Bellec et al., 2010; Thomas Yeo et al., 2011), both in resting state recordings and in meta-analytic co-activation (Smith et al., 2009), application of comparable methods to diffusion-weighted structural connectivity or anatomical covariance networks yields networks that are more spatially contiguous (Betzel et al., 2017; Mišić et al., 2015). For example, clustering or community detection methods typically fail to identify a default mode-like structural network, perhaps because not all parts of the network are anatomically inter-connected (Honey et al., 2010).

Structural and functional networks also show global organizational differences. For example, structural networks show evidence of extensive assortative mixing, whereby

nodes with similar properties (e.g. degrees) are more likely to be connected, whereas the same is not true of functional networks (Lim et al., 2019). At the mesoscopic scale, communities or modules recovered from structural networks are assortative, while communities recovered from functional networks are disassortative (Betzel et al., 2018). In other words, in functional networks there is a pronounced affinity among nodes with dissimilar attributes. As a result, tuning community detection algorithms to be sensitive to disassortative structures improves the match between structural and functional modules (Betzel et al., 2018). Altogether, a rich body of work demonstrates discordance between SC and FC that spans multiple scales, from the embedding of individual nodes and edges to their global arrangement.

Why the discrepancy between SC and FC? Functional interactions may arise via indirect structural connections, resulting in coherent time courses among regions that are two or more synapses removed from each other. In other words, the propensity of two regional time courses to correlate is driven not only by direct signaling between them, but also by the common inputs they receive from sensory organs and from the entire network (Bettinardi et al., 2017; Damoiseaux and Greicius, 2009). A corollary is that functional interactions are much less distance-dependent than structural connections. Anatomical wiring is subject to material, spatial and metabolic constraints (Bullmore and Sporns, 2012); these pressures manifest in reduced connection probability and connection weight with increasing spatial separation (Horvát et al., 2016; Roberts et al., 2016). Although similar distance-dependence is observed for functional connectivity, its effect is weaker, ensuring systematic differences between structural and functional configurations. In the next section we consider models that translate structure to function by conceptualizing function as an emergent property of multiple structural links.

2.5 Models of higher-order interactions

As we have seen so far, there exists a non-trivial link between structural and functional connectivity, but the two are not perfectly aligned. A number of models have emerged that embody this link, including statistical models (Messé et al., 2014; Mišić et al., 2016), communication models (Crofts and Higham, 2009; Goñi et al., 2014; Graham and Rockmore, 2011; Mišić et al., 2015) and biophysical models (Breakspear, 2017; Deco et al., 2009; Honey et al., 2007; Sanz-Leon et al., 2015). Though different in their implementation and assumptions, the common idea is to emphasize collective, **higher-order interactions** among neural elements that transcends the strong local clustering and geometric dependence of

dyadic structural relationships. Here we briefly review each of these analytic strategies, with a focus on their biological interpretation and predictive utility, and most importantly, what they teach us about the nature of the structure-function relationship in the brain.

Perhaps the simplest way to link structure and function is statistically. Varying forms of reduced rank regression have emerged as particularly useful, including canonical correlation (Deligianni et al., 2016) and partial least squares (Mišić et al., 2016). In these data-driven models the objective is to simultaneously identify weighted combinations of structural and functional connections that are maximally correlated across individuals (McIntosh and Mišić, 2013) (Fig. 2.2). An appealing feature of such models is that they embody multiple structure-function modes. In other words, a particular structural configuration or subnetwork may give rise to distinct patterns of functional interactions (Mišić et al., 2016). Taking this idea further, artificial neural networks can be used to learn functional networks from structural networks. For example, a recent study used a variant of the *word2vec* algorithm to build a low-dimensional embedding representation of the connectome, and used it to train a deep neural network to predict edge-wise functional connectivity (Rosenthal et al., 2018). Altogether, statistical models offer a data-driven way to associate combinations of structural and functional connections without assuming a specific mode of interaction among neuronal populations.

Communication models emerging from network science and telecommunication engineering conceptualize functional interactions as the superposition of elementary signaling events on the underlying anatomical network (Avena-Koenigsberger et al., 2018; Graham and Rockmore, 2011) (Fig. 2.2). By explicitly formulating a model of inter-regional signaling, these models open two important questions, namely: how biologically realistic is the model, and how well does the model fit the attributes of the functional network? Early studies focused on centralized forms of communication, such as shortest path routing, whereby discrete signals travel via the shortest contiguous set of edges from a source node to a pre-specified target node. More recently, attention has shifted to decentralized mechanisms where signals diffuse through the network (Atasoy et al., 2016; Mišić et al., 2014a), often broadcast on multiple fronts (Abdelnour et al., 2014; Bettinardi et al., 2017; Mišić et al., 2015; Worrell et al., 2017). Others have considered mechanisms that are neither fully centralized nor decentralized, including communication via path ensembles (Avena-Koenigsberger et al., 2017; Crofts and Higham, 2009) or **multiplexed** strategies involving multiple mechanisms (Avena-Koenigsberger et al., 2019; Betzel et al., 2019; Goñi et al., 2014; Vazquez-Rodriguez et al., 2019). An emerging consensus is that, given the strong relationship between geometric and topological proximity in the brain, it is possible

for decentralized mechanisms to utilize the shortest path structure of the network, either by diffusion (Goñi et al., 2014) or navigation (Seguin et al., 2018). A common methodological thread in these implementations is that pairwise FC is operationalized either as a transmission event (Goñi et al., 2014) or as co-activation (Mišić et al., 2015).

The most biologically detailed and well-studied models are biophysical dynamical systems (Breakspear, 2017; Cabral et al., 2017; Deco et al., 2011). Here the collective dynamics of a **neuronal ensemble** are assumed to be sufficiently low-dimensional such that they can be described by their mean firing rate. Ensembles are coupled by empirically-determined anatomical connectivity into a spatially-discretized network or into a spatially-continuous sheet. Parameters such as conductances may be theoretically derived or empirically informed, and models may be extended to include stochastic fluctuations (Ghosh et al., 2008), time delays (Deco et al., 2011) and external stimulation (Spiegler et al., 2016). Regional time courses are described by a system of coupled differential equations that capture both local fluctuations and influence from other connected regions, exhibiting a rich repertoire of oscillations, synchrony and waves (Roberts et al., 2019) (Fig. 2.2). As a result, these models output realistic temporal waveforms (Hansen et al., 2015; Jirsa et al., 2017), power spectra (Schirner et al., 2018) and covariance patterns (Deco et al., 2009; Honey et al., 2009).

How can we compare these models and how well do they actually predict function from structure? A formal meta-analysis is challenging, as there is little consensus on important analytical choices. For instance, model fit may be reported as variance explained (Honey et al., 2009) or some form of squared error (Messé et al., 2014), and may be assessed in-sample (Mišić et al., 2016) or out-of-sample (Wang et al., 2019). Some studies focus on individual-participant estimates (Abdelnour et al., 2018; Honey et al., 2009; Proix et al., 2017), while others focus on "consensus" networks compiled from multiple individuals (Mišić et al., 2015). Among studies that focus on individuals, some report accuracies across participants (i.e. per edge) (Mollink et al., 2019), while others report accuracies across edges (i.e. per participant) (Abdelnour et al., 2018). Due to inaccuracies in computational tractography, many studies report single-hemisphere predictions (Goñi et al., 2014), while others report whole-brain predictions (Vazquez-Rodriguez et al., 2019). Finally, investigators utilize a range of parcellation schemes with differing numbers of nodes and edges (i.e. variables), making it challenging to directly compare model fits across studies. Lack of standardized reporting is not a problem specific to structure-function questions, but a more general concern in network neuroscience (Hallquist and Hillary, 2018). To our knowledge, out-of-sample prediction of functional connectivity are typically reported to be between $R = 0.3$

and $R = 0.5$, with the largest approximately $R = 0.6$ (Rosenthal et al., 2018).

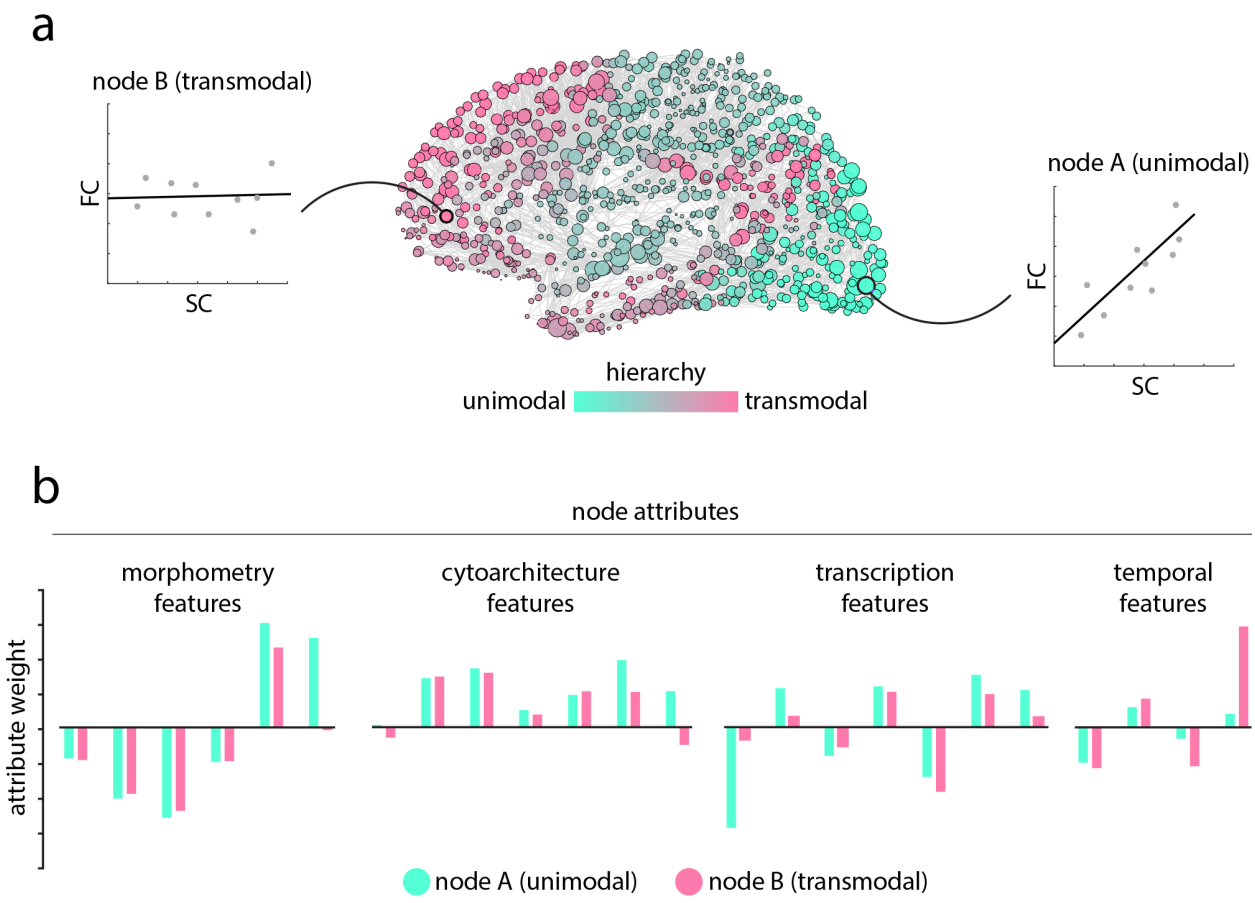

Figure 2.3: **Regional heterogeneity and annotated brain graphs** | The structure-function relationship may not be uniform across the brain, and instead may be region-specific. (a) Nodes are coloured by their position in a putative unimodal-transmodal hierarchy (Margulies et al., 2016). The structure-function relationship is stronger for nodes lower in the hierarchy than for nodes higher in the hierarchy (Baum et al., 2019; Buckner and Krienen, 2013; Demirtas et al., 2010; Preti and Van De Ville, 2019; Vazquez-Rodriguez et al., 2019; Wang et al., 2019) (b) The standard graph model of brain structure and function assumes all nodes are the same, but brain regions differ in multiple local attributes, including gene transcription, cytoarchitecture, receptor profiles and temporal dynamics. Variation in local microscale attributes may influence how neuronal populations broadcast and integrate signal traffic, resulting in regional differences in macroscale structure-function coupling.

2.6 Individual differences in structure-function coupling

Although a consensus is emerging about the relationship between structural and functional networks at the group level, much less is known about the alignment between structural and functional configurations in individuals. *A priori*, strong alignment between

structure and function appears desirable to ensure communication fidelity; a straightforward prediction would be that the correspondence between SC and FC should have behavioural consequences. Indeed, a recent study demonstrated that the extent of alignment between structure and function correlated with individual differences in cognitive flexibility (Medaglia et al., 2018). Intriguingly, and reinforcing the idea of an imperfect match between structure and function, a recent study showed that SC and FC show distinct patterns of inter-subject variance, and therefore map onto cognitive function in distinct ways (Zimmermann et al., 2018).

More broadly, individual differences in structure-function coupling provide a new opportunity to quantify the effects of manipulations and perturbations, such as cognitive tasks (Medaglia et al., 2018; Wu et al., 2019), development and aging (Baum et al., 2019; Supekar et al., 2010; Uddin et al., 2011), neurological and psychiatric diseases (Cocchi et al., 2014; Jirsa et al., 2017), and lesions (Grayson et al., 2016; Roland et al., 2017; Rosenthal et al., 2018). An important question that can be answered with this approach is whether structure and function align to the same extent in domain-general *versus* domain-specific tasks, or in task *versus* rest. Given the prominent relationship between functional configurations in task and rest (Cole et al., 2014) it seems likely they would display a similar relationship with structure. Two recent studies support this notion, showing that regional differences in structure-function coupling observed in rest (discussed in more detail in the next section) can be recapitulated using task-based functional connectivity (Baum et al., 2019) and patterns of regional activation (Wu et al., 2019).

The challenge of studying individual differences in structure-function coupling may be compounded by individual variation in functional boundaries (see *Outstanding Questions*). Applying a uniform parcellation to all participants facilitates comparisons between individuals, but entails the assumption that areas can be mapped to identical spatial locations in every participant. Recent evidence from precision mapping studies using repeated measurements in single individuals suggests that functional boundaries can systematically vary across individuals (Gordon et al., 2017; Laumann et al., 2015; Mueller et al., 2013; Wang et al., 2015), as well as within individuals but across sessions (Salehi et al., 2018). It is not difficult to imagine that structure-function relationships may not be perfectly captured if areas are misaligned across individuals. How to reconstruct networks while respecting individual differences in topographic organization remains a major question for future studies of structure-function relationships.

2.7 Regional Heterogeneity

Direct structural connectivity accounts for much of the variance observed in functional connectivity, while incorporating higher-order interactions and individual-subject variation bring the two even closer. And yet a sizable portion of variance in functional connectivity remains elusive. An emerging possibility is that macroscopic graph representations do not embody the requisite biological detail to completely predict function. The graph model deliberately abstracts away local attributes that we know to be important for neural activity and functional interactions, including transcription profiles, cytoarchitecture, receptor densities, laminar differentiation and temporal dynamics. It is easy to envision how these attributes may influence how signals are generated, routed, transformed and integrated by neuronal populations as they traverse the network, shaping the resulting functional connection patterns. In the following section we argue that the graph representation with uniform nodes leaves out important information, naturally limiting the extent to which functional connectivity can be predicted using only structural connectivity.

Multiple studies have related local molecular, microstructural, morphometric and temporal measurements to macroscale network embedding. For example, transcriptional signatures tend to covary more prominently among structurally- and functionally-connected regions (Arnatkevičiūtė et al., 2018; Fulcher and Fornito, 2016; Richiardi et al., 2015), and prediction of function from structure is enhanced by information about gene co-expression (Betzel et al., 2019). Microstructural profile covariance is also correlated with functional connectivity, including morphometric similarity (Seidlitz et al., 2018), intracortical myelination (Huntenburg et al., 2017) and laminar differentiation (Paquola et al., 2019). Recent evidence from high-resolution MRI demonstrates that activity during cognitive tasks is layer-dependent (Finn et al., 2019), suggesting that structure-function relationships may also be layer-dependent Likewise, neurotransmitter receptor distributions fundamentally shape the range and expression of functional interactions (Shine et al., 2019). Finally, the intrinsic temporal dynamics of individual regions systematically vary across neocortex (Gollo et al., 2015; Keitel and Gross, 2016; Murray et al., 2014; Shafiei et al., 2018), promoting synchrony among some neuronal populations but also restricting synchrony among others. Altogether, how local properties relate to macroscale network connectivity remains an exciting open question (Heuvel and Yeo, 2017; Larivière et al., 2018). Increasing focus on **annotated graphs**, in which nodes are labeled with additional metadata, may ultimately enrich our understanding of how local circuitry contributes to global functional patterns (Khambhati et al., 2018; Murphy et al., 2016).

If global structure-function relationships depend on microscale properties, we are presented with an intriguing possibility: the relationship between structure and function may itself be heterogeneous across the brain. In other words, structure may be more tightly coupled to function in some areas compared to others. Indeed, several recent studies, independently conducted and using different methods, have found converging evidence that structure-function relationships are organized around a **hierarchical** gradient spanning unimodal to transmodal cortex (Margulies et al., 2016; Mesulam, 1998). Specifically, structure and function appear to be tightly coupled in unimodal sensory areas, but systematically decouple towards transmodal cortex at the apex of the hierarchy (Baum et al., 2019; Paquola et al., 2019; Preti and Van De Ville, 2019; Vazquez-Rodriguez et al., 2019). This decoupling is observed over the course of normative development (Baum et al., 2019), and is observed not only for functional connectivity, but for task activation patterns as well (Wu et al., 2019). A prominent account posits that rapid evolutionary expansion of association cortices effectively untethers polysensory regions from molecular signaling gradients and canonical sensory-motor activity cascades, resulting in fundamentally different structure-function relationships along the unimodal-transmodal hierarchy (Buckner and Krienen, 2013).

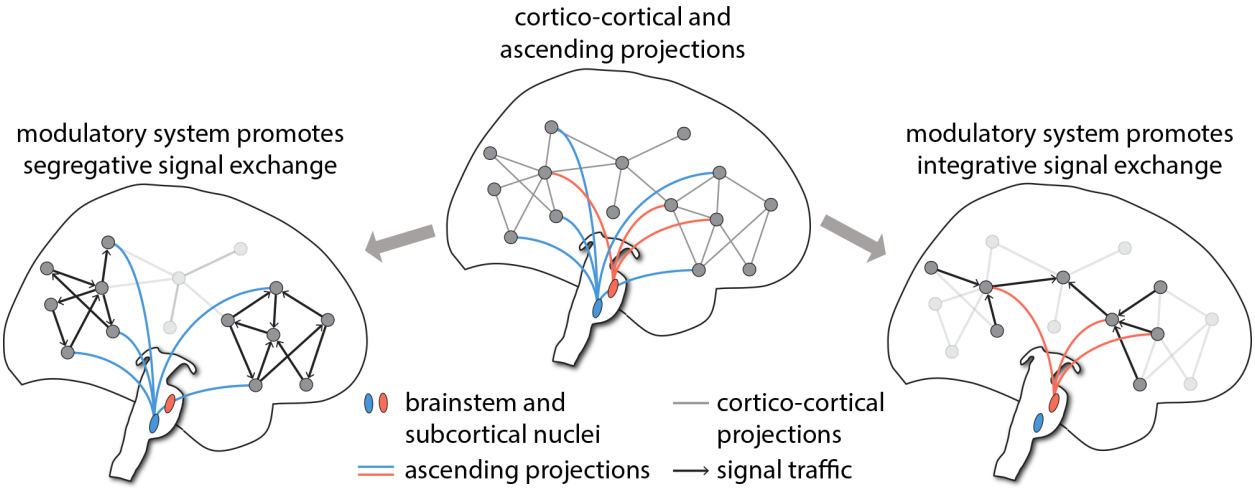

Figure 2.4: **The ascending arousal system modulates structure-function relationships** | Top: two putative arousal systems, originating from nuclei in the brainstem and subcortex and terminating at multiple cortical nodes, are shown in blue and orange. Left: modulation by the blue system promotes signal exchange within specialized, topologically-segregated populations. Right: modulation by the orange system promotes signal exchange between neuronal populations. The ascending arousal system thus modulates functional interactions on the static structural network, facilitating fluid transitions among multiple functional configurations.

The gradual decoupling of structure and function may reflect systematic hierarchical variation in laminar differentiation (Paquola et al., 2019) and cytoarchitecture (Vazquez-Rodriguez et al., 2019). Two recent computational modeling studies support this idea. In the first, microscale-related parameters of a biophysical model were allowed to differ between brain regions (Wang et al., 2019). The best-fitting model was characterized by strong recurrent connections and excitatory subcortical input in sensorimotor regions; conversely, default network regions had weak recurrent connections and excitatory subcortical inputs (Wang et al., 2019). A complementary study found that biophysical models could be fitted to functional connectivity significantly better if they were informed by hierarchical heterogeneity estimated from T1w/T2w ratios (Demirtas et al., 2010). This regional heterogeneity may reflect spatial variation in cytoarchitecture; for instance, dendritic arborization patterns support distinct algorithmic transformations of converging inputs, including selecting, routing and multiplexing information (Payeur et al., 2019). Altogether, multiple lines of evidence suggest that the present graph model with uniform nodes obscures important biological detail; an important question for future research is how to integrate node annotations in models of structure-function relationships (Khambhati et al., 2018).

2.8 Modulating structure-function relationships

Perhaps the most important annotations missing from current macroscale wiring diagrams are the neurotransmitter receptor fingerprints of each node. Modulation via ascending projections from the brainstem and subcortical nuclei alters neuronal firing rate, making neurons more or less responsive to incoming signals. The resulting adjustments in neural gain fundamentally alter how signals are routed through the network, how they are transformed, and ultimately, how they are integrated (Bell and Shine, 2016; Shine, 2019).

Zooming out and considering the network as a whole, it is easy to see that neuromodulation provides a mechanism by which a static structural network can support distinct propagation patterns (Bell and Shine, 2016; Shine, 2019). This phenomenon is observed across a variety of generic and real-world networked systems, where a single network can support distinct spatiotemporal propagation regimes depending on the interaction patterns unfolding on the network (Hens et al., 2019). An intuitive example is road traffic: depending on conditions (time of day, day of the week, weather, construction), the same road network may feature distinct traffic loads and patterns. In an analogous manner, the system of ascending neuromodulatory projections confers the capacity to translate the static anatomical network into multiple functional configurations and flexibly switch

between such configurations. Moreover, each receptor type has a specific distribution, affinity and effect on neural gain, meaning that modulation can be either targeted or diffuse, and can be exerted over a range of time scales.

Recent evidence from pharmacological modulation supports the notion that the ascending arousal system promotes distinct functional configurations (Bell and Shine, 2016; Brink et al., 2019; Shine, 2019). Functional network reconfiguration has been associated with perturbations of noradrendergic (Brink et al., 2016; Shine et al., 2018a), dopaminergic (Alavash et al., 2018; Shafiei et al., 2018) and serotonergic signaling (Deco et al., 2018; Tagliazucchi et al., 2016). In computational models, due to the complex nonlinear dynamics playing out over the connectome, even small local modulation of the excitation-inhibition equilibrium can substantially change the organization of functional interactions, promoting dynamic switching between topologically integrated and segregated states (Deco et al., 2018; Shine et al., 2018b). Unfortunately, state-of-the-art computational models rarely take neuromodulation into account, while the brainstem and subcortex are often left out of network reconstructions due to challenges in fiber tracking and parcellating some nuclei. Understanding how neuromodulation fits into the structure-function relationship is a key frontier in the field (see *Outstanding Questions*).

2.9 Function or property?

In the previous two sections we considered the possibility that network structure could be enriched by additional local information. Here we ask whether we are correctly defining network function in terms of FC. We begin by drawing the distinction between structure-*function* and structure-*property* relationships. In a complex system marked by a specific size, shape, arrangement and orientation, a property may be any measurable feature, but this is different from their purpose or function. For instance, the mass and charge of a protein are features, but the function of the protein is to bind and interact with another molecule. Although resting correlation patterns display many intuitively appealing and methodologically convenient attributes, they are likely not the primary purpose of inter-regional signaling, but rather a manifestation of that process.

This idea has already gained a footing in the field, with multiple efforts under way to understand how the structural organization of the brain can influence properties other than resting state FC. One straightforward extension is to link structure and time-varying or dynamic functional connectivity (Cabral et al., 2017; Fukushima et al., 2018). Another is to operationalize higher-order interactions among pairwise functional connections, either by

constructing hypergraphs that describe functional interactions among three or more nodes simultaneously (Gu et al., 2017) or temporal networks that capture interactions among nodes in successive time frames (Griffa et al., 2017; Mitra et al., 2015). Given the degenerate nature of functional networks (Marrelec et al., 2016), there is also increasing effort to project functional dynamics to lower-dimensional spaces or manifolds that compactly summarize time-varying interactions (Shine et al., 2019).

Taking this notion further, we envision increasing focus on properties more directly linked to internal representations and behaviour (Brown and De Bivort, 2018). For example, structural connectivity may influence the participation of individual regions in intrinsic functional networks (Zhang et al., 2016). The anatomical connectional fingerprint or embedding of some areas may predispose them to frequently switch affiliation among large-scale cognitive systems, while others may display stable or invariant affiliation with one system (Fukushima et al., 2018). Other approaches may focus directly on relating structural connectivity to task activation (Wu et al., 2019). Particularly exciting are advances in artificial intelligence, such as reservoir computing, that make it possible to implement connectomes as artificial neural networks (Kawai et al., 2019). These "neuromorphic" or "biomimetic" networks, endowed with realistic connection patterns and biophysical dynamics, can process time-varying signals and be trained on a range of tasks including speech recognition and spatial navigation, allowing researchers to directly assess the relation between anatomical connectivity and functional repertoire.

2.10 Function as computational property

In the previous section the possibility of defining function in ways that it is more directly linked to internal representations and behaviour was pointed out. Here we introduce a novel framework to explore the link between structure and function in brain networks. This new framework, motivated by the convergence of two recent technological revolutions: artificial intelligence and connectomics, aims to re-direct the focus towards the computational and information-processing aspects of biological brains.

Connectomics has facilitated the access to detailed reconstructions of the wiring patterns of the nervous system of multiple species. This has allowed researchers to formulate a variety of models that map network architecture to diverse functional phenomena, including emergent neural dynamics and functional co-activation patterns (Breakspear, 2017; Shafiei et al., 2020; Uddin, 2020), or to inter-individual differences in behavior (Melozzi et al., 2019; Mišić and Sporns, 2016; Seguin et al., 2020). Furthermore, descriptive studies

on connectomes have shown that biological neural networks display nontrivial topological attributes characteristic of complex systems (Bassett and Bullmore, 2006; Bertolero et al., 2015; Betzel et al., 2017; Chen et al., 2008; Hagmann et al., 2008; Heuvel et al., 2012; Hilgetag and Kaiser, 2004; Kaiser and Hilgetag, 2006; Liu et al., 2020; Power et al., 2011; Sporns et al., 2007; Sporns and Zwi, 2004; Towlson et al., 2013; Watts and Strogatz, 1998; Zamora-López et al., 2010). It remains unclear, however, how these organizational principles confer computational capacity to biological neural circuits. Artificial intelligence, on the other hand, has proposed numerous models aimed to tackle the problem of replicating the computations performed by biological agents and systems. The most successful models achieving or surpassing human-like intelligence are artificial neural networks, a model inspired on connectionist theories about the brain (Feldman and Ballard, 1982; Fodor and Pylyshyn, 1988). What if biologically inspired connectivity patterns could be used to inform the architecture of artificial neural networks? What if we could synthetically train these connectome-informed networks to perform a variety of real-world tasks? Could this tell us something new about our own brains? Answering these questions is not as straightforward as it seems. In most cases, the specification of the topology of artificial neural networks is ad hoc and problem-specific. Furthermore, depending on the size of the network and the complexity of the task, training these models could result computationally very expensive.

Reservoir computing, a recurrent artificial neural network model, provides an alternative solution that deals with some of these technical obstacles. This computing paradigm proposes a simple three-layer architecture consisting of an input layer, followed by an intermediate hidden layer called the *reservoir*, typically modeled as a recurrent artificial network of nonlinear units, and a readout layer (Jaeger, 2001; Lukoševičius and Jaeger, 2009; Maass et al., 2002). A characteristic feature of this approach is that learning only occurs in the connections that link the reservoir to the readout layer, hence, the connectivity of the reservoir is fixed. The computational capabilities of this model are entirely determined by the transformed representation of the inputs produced by the reservoir. Therefore, this computational paradigm offers the convenience of imposing arbitrary network architectures and dynamics on the reservoir, and of evaluating the effect of these parameters on the performance of the task at hand. This flexibility opens new and exciting opportunities. Combining the computational aspects of reservoir computing with biologically-realistic connection patterns from connectomics data, we can now explore how network architecture shapes the computational capacity of connectome-informed reservoirs, thus elucidating a new facet of the link between structure and function in brain

networks.

2.11 Concluding Remarks

Although the modern theory of structure-function relationships in the brain is still in its infancy, several of its intellectual arcs are now coming into focus. Structure leaves an indelible mark on function, but a rich literature supports the notion that the link between structural and functional connectivity is complex, precluding a simple one-to-one mapping. Emerging models emphasize higher-order interactions via anatomical links that transcend dyadic relationships, opening fundamentally new opportunities to ask how the wiring of the brain supports function. Structural network reconstructions enriched with cellular and molecular metadata, in concert with more nuanced representations of functions and properties, hold great potential for a refined and truly *multi*-scale understanding of the structure-function relationship. Altogether, the confluence of technological, analytic and theoretical advances opens fundamentally new opportunities to discover physical laws that translate structure to function in brain networks.

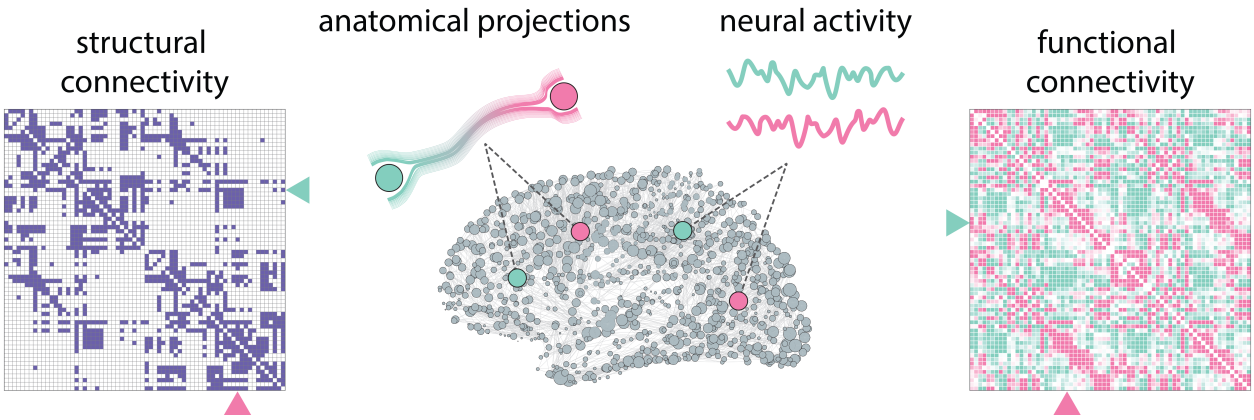

Figure S2.1: **Measuring structural and functional connectivity** | At the macroscale level, structural and functional networks are derived by first parcellating the brain into grey matter nodes. For **structural connectivity** networks, edges are defined by reconstructing white matter projections between network nodes. For **functional networks**, edges are defined by estimating statistical associations between node time courses.

BOX 1: MEASURING STRUCTURAL AND FUNCTIONAL CONNECTIVITY

Modern imaging and tracing technology allows reconstruction of brain connectomes at multiple spatial and temporal scales. Depending on the acquisition technique, network nodes may represent neurons, neuronal populations, or brain regions. Network edges represent either structural connectivity (SC) or functional connectivity (FC), and their definition and interpretation depends on the imaging modality (Figure S2.1).

Diffusion-weighted MRI is the most extensively used non-invasive *in vivo* imaging method to measure macroscale SC between brain regions. Applying tractography algorithms on an individual's DWI data, SC can be defined as either the connection probability, the number of reconstructed streamlines, or the mean fractional anisotropy across streamlines between two brain regions. This family of techniques is subject to several important limitations, most notably systematic false positives and false negatives (Maier-Hein et al., 2017; Reus and Heuvel, 2013; Thomas et al., 2014). Reconstructions are also sensitive to methodological choices, such as the location of the initial seed points and tracking algorithm employed (Schilling et al., 2019). Tracing technologies, applied to post-mortem samples, offer greater fidelity, finer spatial detail and information about directionality of

anatomical projections. Mesoscale methods reconstruct cellular connectivity by combining light microscopy with conventional or viral tracers. Microscale methods reconstruct individual synaptic contacts using electron microscopy.

MRI-based measures are also used to derive macroscale FC networks. FC is typically quantified by computing statistical associations between regional haemodynamic time courses recorded using resting state or task based functional MRI (fMRI). FMRI-based FC may primarily capture stable functional configurations, potentially limiting inferences about time-dependent functional interactions (Gratton et al., 2018) (but see (Lurie et al., 2019)). Other technologies, focusing on electromagnetic neural activity at the macroscale, offer greater potential to resolve time-dependent functional interactions, including electroencephalography, magnetoencephalography and electrocorticography. At the microscale, numerous microelectrode recording techniques allow measurement of extracellular and intracellular electrical activity. Recent advances in calcium imaging with flourescent indicators permits comprehensive *in vivo* measurement of action potentials across the entire brain in animal models (Yang and Yuste, 2017).

Altogether, exciting technological advances yield estimates of anatomical projections and functional interactions over multiple levels of description. Many of the key insights from human MRI (imperfect correspondence between structure and function, relation with spatial proximity, etc.) can be replicated by tracing studies in animal models (Hori et al., 2020) and by electrophysiological methods (Schirner et al., 2018). At the same time, recent studies suggest that tracer-based structural networks do provide better overall predictive power compared to diffusion-based structural networks, primarily because they contain information about projection directionality (Knock et al., 2009; Melozzi et al., 2019). How the structure-function relationship depends on measurement scale and technology is still not fully understood and more research is necessary to consolidate knowledge across subfields.

Chapter 3

Learning function from structure in neuromorphic networks

Laura E. Suárez[1,2], Blake A. Richards[1,2,3], Guillaume Lajoie[2,4], & Bratislav Misic[1]

[1]Montréal Neurological Institute, McGill University, Montréal, Canada

[2]Mila, Quebec Artificial Intelligence Institute, Montréal, QC, Canada

[3]School of Computer Science, McGill University, Montréal, QC, Canada

[4]Department of Mathematics and Statistics, Université de Montréal, Montréal, QC, Canada

Published in:

Nature Machine Intelligence: https://doi.org/10.1038/s42256-021-00376-1

3.1 Preface

Enough evidence supports that there is a correspondence between structure and function in brain networks, but what are the exact mechanisms and the extent of such correspondence remains unknown (Suárez et al., 2020). Conventionally, *structure* and *function* have been respectively attributed to structural and functional connectivity networks. Structural connectivity describes the anatomical projections connecting different brain regions, whereas functional connectivity captures the systematic co-activation patterns of regional brain activity. Previous reports concerning the link between structure and function in brain networks have mainly focused on statistical, communication or biophysical models that, informed by the structural connectome, aim to predict functional connectivity from structural connectivity (Suárez et al., 2020). These models have successfully reproduced

inter-regional functional interactions and other distinct dynamical phenomena, but a link connecting these emergent dynamical and functional events to cognition and behavior is still missing. Furthermore, network neuroscience has provided a framework to investigate and quantify the topological features of structural and functional connectivity networks (Bassett et al., 2018). Of particular interest are several descriptive studies on connectome architecture showing that biological neural networks display multiple nonrandom features characteristic of complex systems (Heuvel et al., 2016). Despite these insights, how specific topological attributes support cognition and behavior is still an area under research. A prominent hypothesis, however, predicts that some of these nontrivial architectural features confer computational capacity to brain networks. The work discussed in this chapter explores the relationship between structural network architecture and computational capacity in the human connectome. Specifically, I combine MRI connectomics and reservoir computing — an artificial recurrent neural network model — to investigate how memory capacity in the human connectome is jointly supported by network architecture and dynamics.

3.2 Abstract

The connection patterns of neural circuits in the brain form a complex network. Collective signaling within the network manifests as patterned neural activity, and is thought to support human cognition and adaptive behavior. Recent technological advances permit macro-scale reconstructions of biological brain networks. These maps, termed connectomes, display multiple non-random architectural features, including heavy-tailed degree distributions, segregated communities and a densely interconnected core. Yet, how computation and functional specialization emerge from network architecture remains unknown. Here we reconstruct human brain connectomes using *in vivo* diffusion-weighted imaging, and use reservoir computing to implement connectomes as artificial neural networks. We then train these neuromorphic networks to learn a memory encoding task. We show that biologically realistic neural architectures perform best when they display critical dynamics. We find that performance is driven by network topology, and that the modular organization of intrinsic networks is computationally relevant. Throughout, we observe a prominent interaction between network structure and dynamics, such that the same underlying architecture can support a wide range of memory capacity values as well as different functions (encoding or decoding), depending on the dynamical regime the network is in.

This work opens new opportunities to discover how the network organization of the brain optimizes cognitive capacity.

3.3 Introduction

The brain is a complex network of anatomically connected and functionally interacting neuronal populations. The wiring of the network allows its components to collectively transform signals representing internal states and external stimuli. Recent technological and analytic advances provide the opportunity to comprehensively map, image and trace connection patterns of nervous systems in multiple species (Heuvel et al., 2016; Insel et al., 2013), yielding high-resolution "connectomes" of individual brains (Bassett and Sporns, 2017; Sporns et al., 2005). Numerous reports have found evidence of non-random topological attributes that theoretically enhance the capacity of the network to process information (Heuvel et al., 2016), including high clustering and short path length (Bassett and Bullmore, 2006; Kaiser and Hilgetag, 2006; Sporns and Zwi, 2004; Watts and Strogatz, 1998), specialized segregated communities (Bertolero et al., 2015; Betzel et al., 2017; Chen et al., 2008; Hilgetag and Kaiser, 2004; Liu et al., 2020; Power et al., 2011), heavy-tailed degree distributions (Hagmann et al., 2008; Sporns et al., 2007), and a core of densely inter-connected hub nodes (Heuvel et al., 2012; Towlson et al., 2013; Zamora-López et al., 2010). The wiring patterns needed to support these attributes entail energetic and metabolic cost, yielding an economic trade-off between efficient information transmission and minimal wiring cost (Bullmore and Sporns, 2012). Despite these insights, the link between macroscale connectivity structure and the computational properties that emerge from network activity is not well understood.

How does the organization of the brain confer computational capacity? One way to address this question is to relate structural connectivity to neural dynamics and emergent patterns of functional connectivity (Breakspear, 2017; Shafiei et al., 2020; Suárez et al., 2020; Uddin, 2020). Another is to relate structural connectivity to individual differences in behaviour (Melozzi et al., 2019; Mišić and Sporns, 2016; Seguin et al., 2020). Although both paradigms inform us about functional consequences of network organization, they do not explicitly consider how network organization supports information processing (Ju and Bassett, 2020). An alternative way to conceptualize structure-function relationships is to directly consider function as a computational property. Modern artificial intelligence algorithms offer new ways to link structure and function, by conceptualizing function as a computational property (Richards et al., 2019).

A prominent paradigm to understand how artificial recurrent neural networks extract information from a continuous stream of external stimuli is reservoir computing (Lukoševičius and Jaeger, 2009). Also known as *echo-state networks* or *liquid state machines* (Jaeger, 2001; Maass et al., 2002), this computational schema typically uses randomly connected recurrent neural networks, but arbitrary network architectures can also be used. The networks are trained in a supervised manner to learn representations of external time-varying stimuli, and can be adapted to a wide range of tasks, including speech recognition (Skowronski and Harris, 2007; Verstraeten et al., 2006, 2005), motor learning (Ijspeert, 2008; Li and Jaeger, 2011; Salmen and Ploger, 2005), natural language processing (Homma and Hagiwara, 2013; Tong et al., 2007), working memory (Pascanu and Jaeger, 2011; Strock et al., 2018) and spatial navigation (Antonelo and Schrauwen, 2014; Sussillo and Abbott, 2009). A significant benefit of the reservoir framework is that arbitrary dynamics can be super-imposed on the network, providing a tool to investigate how network organization and dynamics jointly support learning and functional specialization.

Here we combine connectomics and reservoir computing to investigate the link between network organization, dynamics and computational properties in human brain networks. We construct neuromorphic artificial neural networks endowed with biologically realistic connection patterns derived from diffusion weighted imaging. We then train these connectome-informed reservoirs to perform a memory capacity task (Jaeger, 2002). To evaluate how memory capacity depends on both network structure and dynamics, we parametrically tune the dynamical state of the network, driving the network to transition between stable, critical and chaotic dynamics. We assess memory capacity of empirically-derived connectomes against four null models, and show that the underlying topology and modular structure of the brain enhance memory capacity in the context of critical dynamics. Throughout the report, we focus on the role of *intrinsic networks* (Bellec et al., 2010; Damoiseaux et al., 2006; Power et al., 2011; Schaefer et al., 2018; Smith et al., 2009; Thomas Yeo et al., 2011): large-scale functional systems of the brain thought to be the putative building blocks of higher cognition (Bertolero et al., 2015, 2018; Uddin et al., 2019). Finally, we systematically investigate how memory capacity depends on the interaction between specific network attributes and dynamics.

3.4 Results

3.4.1 Learning in neuromorphic networks

Reservoir computing was initially proposed as a computational framework to model how cortical circuits extract information from the spatiotemporal patterns of neural activity elicited by continuous streams of external stimuli (Buonomano and Maass, 2009). Nowadays reservoir computing is primarily used as an artificial recurrent neural network architecture in its own right (Lukoševičius and Jaeger, 2009). In its simplest form, the "vanilla" reservoir computing architecture consists of a recurrent network of interacting nonlinear neurons, known as the *reservoir*, and a linear readout module. In the present report, we use empirically-derived patterns of human brain connectivity to constrain the connections within the reservoir. Specifically, we apply deterministic streamline tractography on diffusion spectrum MRI data ($n = 66$ subjects. Data source: https://doi.org/10.5281/zenodo.2872624) to reconstruct individual high-resolution human connectomes (1015 nodes; 1000 cortical and 15 subcortical regions). To reduce the impact of false positives and false negatives, we generate group-level consensus networks that retain the topological characteristics of individual subject networks (Betzel et al., 2018; Reus and Heuvel, 2013; Roberts et al., 2017).

We use the reservoir framework to quantify the capacity of individual brain regions to encode temporal information during a memory capacity task (Fig. 3.1a), hereinafter referred to as memory task. In this task a uniformly distributed temporal signal is introduced into the reservoir through a set of input nodes (blue). The signal propagates through the network, giving rise to complex patterns of neural activity across the reservoir. The activity time-series of a set of readout nodes (purple) within the reservoir are then used to train a readout linear unit to reproduce a delayed version of the input signal. Performance in this task thus depends on the ability of the readout nodes to encode the temporal properties of the external stimuli. In other words, the ability of the readout nodes to represent past inputs in their current activation states, which we refer to as *memory capacity*, is proportional to the performance of the network in the memory task (see *Methods* for details). The memory capacity of a network – its ability to encode past input history in its ongoing dynamics – emerges as a result of feedback input from previous time steps via recurrent connections (Elman, 1990, 1991).

We selected readout nodes using intrinsic networks, (Bellec et al., 2010; Damoiseaux et al., 2006; Power et al., 2011; Smith et al., 2009; Thomas Yeo et al., 2011) (Fig. 3.1b). Intrinsic

networks are a connectivity-based partition of the brain into groups of areas with coherent time courses and similar function (Wig, 2017). As such, they are thought to represent the putative building blocks of higher cognition, and provide a convenient and cognitively meaningful way to divide the brain into large-scale systems. In the present study, we measured the memory capacity of the brain across seven intrinsic networks reported by Yeo, Krienen and colleagues (Thomas Yeo et al., 2011). Subcortical regions were set as input nodes for all experiments (results using alternative input nodes are shown in *Sensitivity Analysis*). To provide confidence intervals for the memory capacity estimates of intrinsic networks, we generate 1000 group-consensus matrices by bootstrap resampling individual subjects (see *Methods* for details).

The computational properties of the reservoir depend on both its architecture and its dynamics (Büsing et al., 2010; Mastrogiuseppe and Ostojic, 2018). Here, the reservoir consists of a recurrent neural network of discrete-time, nonlinear units with a hyperbolic tangent activation function. We parametrically tune the dynamics of the reservoir by scaling the largest eigenvalue of the connectivity matrix (parameter α; see *Methods*). The dynamics of the reservoir are considered to be stable when $\alpha < 1$, and chaotic when $\alpha > 1$. When $\alpha \approx 1$ the dynamics are said to be critical or at the edge of chaos (Seung, 1996). Fig. 3.1c shows the mean (solid lines) memory capacity and the standard deviation (shaded regions) across samples for each of the seven intrinsic networks as a function of α. As expected, memory capacity is greater when the dynamics of the reservoir are stable ($\alpha < 1$), and decreases as the dynamics evolve towards a chaotic state ($\alpha > 1$) (Seung, 1996). Maximal memory capacity is attained when the dynamics of the reservoir are at the transition between the stable and chaotic regimes ($\alpha \approx 1$). This general behaviour is observed across all intrinsic networks, with more prominent differences between them in the chaotic regime. The greater within-network variability in memory capacity at $\alpha > 1$ is consistent with the notion that the system is in a chaotic state, while capacity in the stable regime is less variable.

3.4.2 Memory capacity of the human connectome

We first assess how memory capacity depends on connectome architecture and dynamics. We average memory capacity across intrinsic networks to provide an overall estimate for the memory capacity of the connectome. Fig. 3.2a shows the distribution of mean memory capacity as a function of α. Consistent with the results from the previous section, we find the greatest performance close to the edge of chaos, with memory capacity generally > 0.8

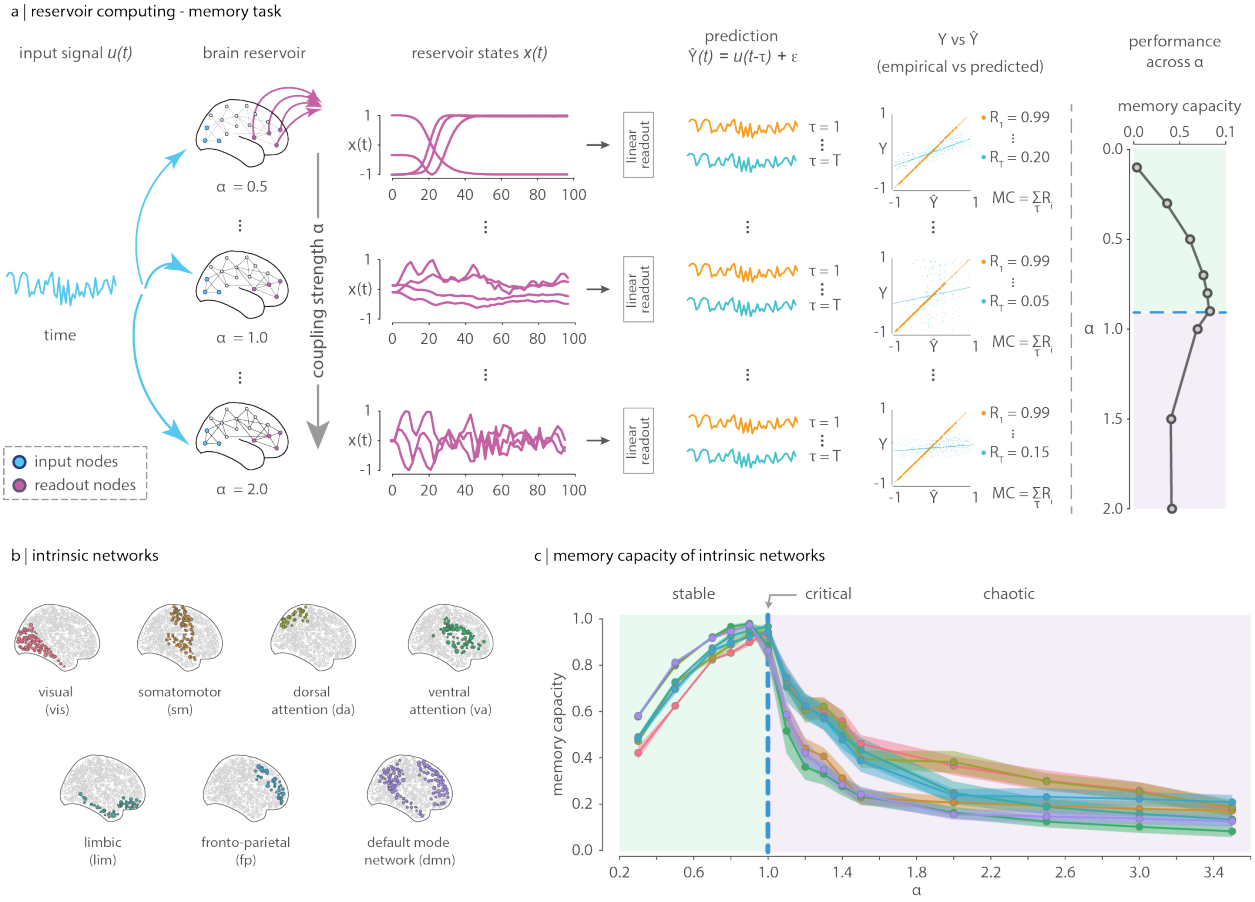

Figure 3.1: **Measuring the memory capacity of biological neural networks** | By using biologically-inspired connectivity measures obtained from MRI connectomics data, we leverage reservoir computing models to investigate the effect of network architecture on the encoding capacity of large-scale brain networks in a memory task. (a) Toy figure illustrating the memory capacity task. In this task, a uniform random input signal ($u(t)$) is introduced to the reservoir through a set of input nodes (blue nodes). The input signal propagates through the network, activating the states of the units within the reservoir. The activation states (reservoir states $x(t)$) of the readout nodes (purple nodes) are then retrieved from the reservoir, and are used to train a linear model to reproduce a delayed version of the input signal at different time lags ($Y = u(t - \tau)$). Memory capacity (MC) is estimated as the sum across time lags (τ) of the absolute correlation (R) between the predicted ($\hat{Y}$) and the time-lagged target signal (Y). The dynamics of the reservoir are controlled with α, a parameter that scales the spectral radius (largest eigenvalue) of the connectivity matrix, while uniformly modifying its coupling strength. A memory capacity estimate is obtained for every value of α. (b) Lateral projection (right hemisphere) of the Yeo-Krienen intrinsic network partition (Thomas Yeo et al., 2011). The procedure described in (a) was independently applied to each of the seven intrinsic networks. (c) Distribution (across samples) of memory capacity as a function of α for each intrinsic network.

at α values close to 1. We next ask how performance depends on network topology and on the modular organization captured by the intrinsic networks.

To assess the extent to which memory capacity depends on the underlying network topology, we construct a population of null networks by randomly rewiring pairs of edges in the structural network, preserving the density, degree sequence and the intrinsic network label assignment of the nodes ((Maslov and Sneppen, 2002); Fig. 3.2b). Using this null model, we perform the same memory task to measure the memory capacity of each of the seven intrinsic networks, and then average across them to provide a network-level memory capacity estimate. We apply this procedure on 1,000 rewired networks to construct a distribution of the memory capacity of the network under the null hypothesis that network-level memory capacity is independent of the underlying connectivity patterns. We then compare brain networks against the rewired models using the Wilcoxon-Mann-Whitney two-sample rank-sum test. We find that empirical brain networks have significantly better performance than rewired networks at criticality (medians in empirical and rewired networks are 0.91 and 0.77, respectively, $P_{rewired} < 10^{-4}$ two-tailed, and common-language effect size = 99%; Fig. 3.2a); at other dynamical regimes (stable and chaotic), the connectome generally has lower capacity. These results suggest that connectome topology optimally functions as a reservoir when dynamics are critical or at the edge of chaos.

The rewiring of empirical networks, however, not only destroys the underlying network topology, but also the structure of the readout nodes imposed by the intrinsic network partition. This raises a new question: is memory capacity driven by the fact that readout nodes represent modules in the connectome? To investigate this, we apply the Louvain community detection algorithm on both the empirical and the rewired networks, and use this optimized partition to select new sets of readout nodes. Fig. S3.1 compares memory capacity of empirical and rewired networks using the optimized and the intrinsic network partitions. Results show that increasing the modularity score derived from the partition imposed by the readout nodes does not necessarily translate into better memory capacity for the empirical or the rewired networks, suggesting that memory capacity is not strictly driven by the fact that readout nodes represent the partition of the connectome with maximum modularity. Note however, that this result does not preclude the possibility that there exists an optimal – but not necessarily maximal – modularity that enhances memory capacity by striking a balance between segregation and integration (Rodriguez et al., 2019).

We thus next seek to directly assess whether the partition of the connectome into intrinsic networks enhances memory capacity. To do so, we use a spatially-constrained label-permutation null model that randomly permutes intrinsic network labels while

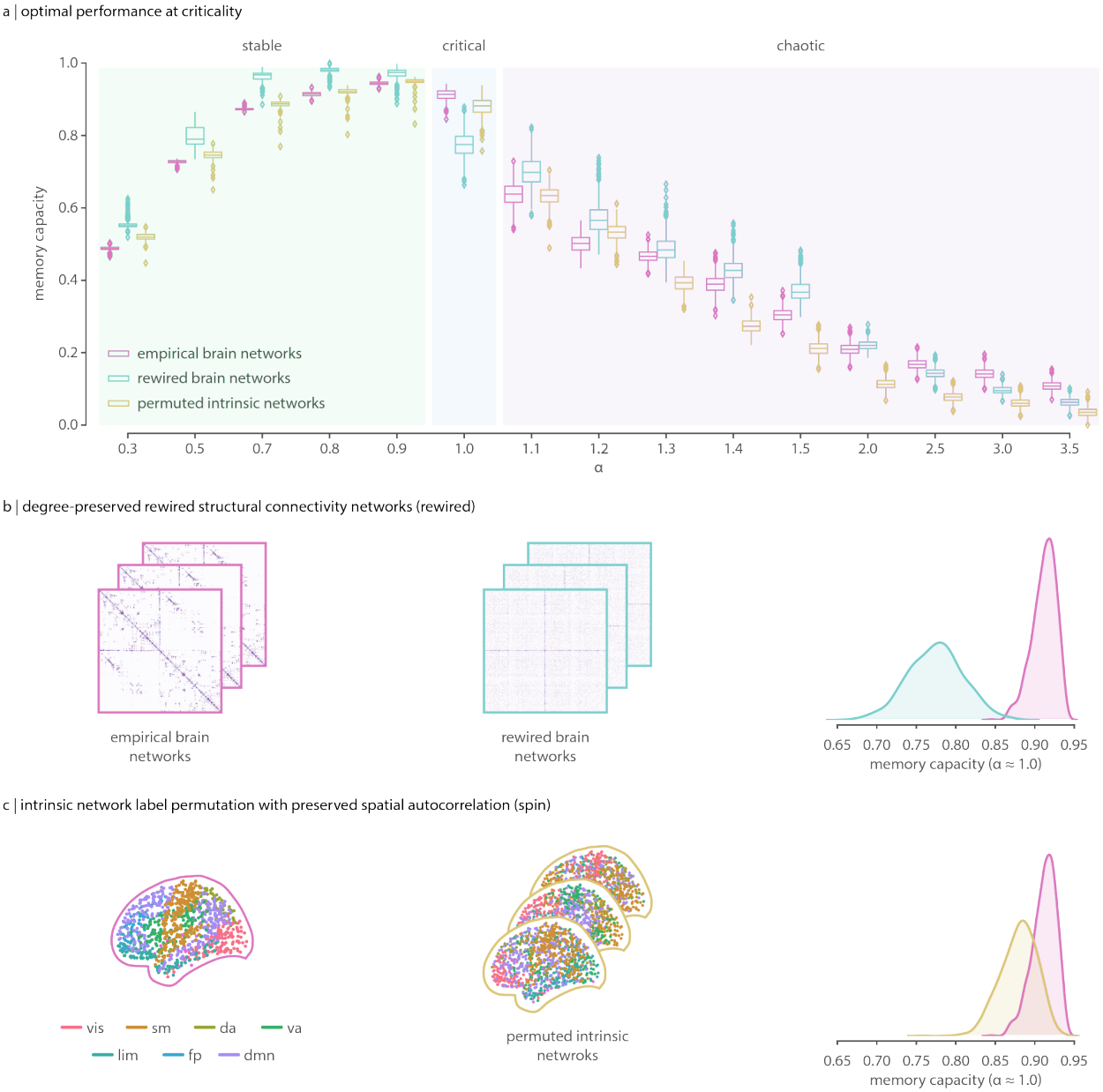

Figure 3.2: **Memory capacity of the human connectome** | (a) Boxplots show the distribution of mean memory capacity (averaged across intrinsic networks) for families of empirical (magenta) and null (cyan and yellow) network models, as a function of α. At the critical point ($\alpha \approx 1$), empirical networks perform significantly better compared to the alternative null models ((b) and (c); cyan and yellow, respectively). (b) To determine whether memory capacity depends on the underlying connectivity structure, empirical networks are compared against a family of rewired networks constructed by randomly swapping pairs of edges while preserving network size, density, degree sequence and node-level intrinsic-network assignment (cyan in panel (a); denoted by $P_{rewired}$) (Maslov and Sneppen, 2002). The distributions show the memory capacity of the empirical (magenta) and rewired (cyan) brain networks at the critical point. (c) To evaluate whether the partition of the connectome into seven intrinsic networks is relevant for the task at hand, empirical networks are compared against a family of nulls with the same underlying connectivity but arbitrary modular structure assigned by randomly permuting intrinsic network labels, while preserving their spatial autocorrelation (yellow in panel (a); denoted by P_{spin}) (Alexander-Bloch et al., 2018; Markello and Misic, 2021). The distributions show the memory capacity of the empirical (magenta) and label-permutation (yellow) models at the critical point. Boxes represent the quartiles of each distribution, and whiskers extend up to 1.5× the interquartile range. Points beyond the whiskers are determined to be outliers.

preserving their spatial autocorrelation. We generate 1,000 permutations to construct a distribution of the memory capacity of the network under the null hypothesis that the memory capacity of the connectome depends on its intrinsic network structure, and not on trivial differences in size, coverage or symmetry of intrinsic networks (Alexander-Bloch et al., 2018; Markello and Misic, 2021) (Fig. 3.2c). Again, we use the Wilcoxon-Mann-Whitney two-sample rank-sum test to compare the empirical intrinsic network partition against the spatially-constrained permutation model. We find that, at criticality, the partition provided by empirical intrinsic networks significantly outperforms the spatially-constrained label-permutation model (medians in the empirical and permuted partitions are 0.91 and 0.88, respectively, $P_{spin} < 10^{-4}$ two-tailed, and common-language effect size = 88%; Fig. 3.2a). This suggests that intrinsic networks constitute a computationally relevant feature of the human connectome (Bertolero et al., 2015, 2018).

The results presented so far highlight the importance of intrinsic networks for the memory capacity of the connectome. However, it is still unclear whether memory capacity is determined by the internal connectivity structure of intrinsic networks, or by the external connectivity of intrinsic networks with the rest of the brain. To investigate this, we construct a new family of rewired nulls, one per intrinsic network. In this type of null model, we allow all the connections to be rewired except those within a particular intrinsic network, thus preserving the internal connectivity structure of the intrinsic networks while randomizing the topology of the rest of the network. Fig. S3.2 shows a comparison between the memory capacity of empirical and rewired networks. As before, empirical intrinsic networks perform significantly better than their rewired counterparts at criticality, suggesting that their memory capacity is not uniquely driven by their internal connectivity structure, but rather emerges from external connections and interactions with the rest of the connectome.

Collectively, these four null models suggest that the global topology of the connectome supports memory capacity and that intrinsic networks act as computational building blocks. Importantly, computation in the connectome is supported by connectivity between intrinsic networks, consistent with the notion that cognition emerges from the continuous interaction of functionally specialized modules in the brain (Crossley et al., 2013; Shine et al., 2018).

3.4.3 Connectomes optimize computation-cost trade-offs

Previously, we observed that the human connectome outperforms the rewired model only when the dynamics are critical. In the stable and chaotic regimes, randomly rewired

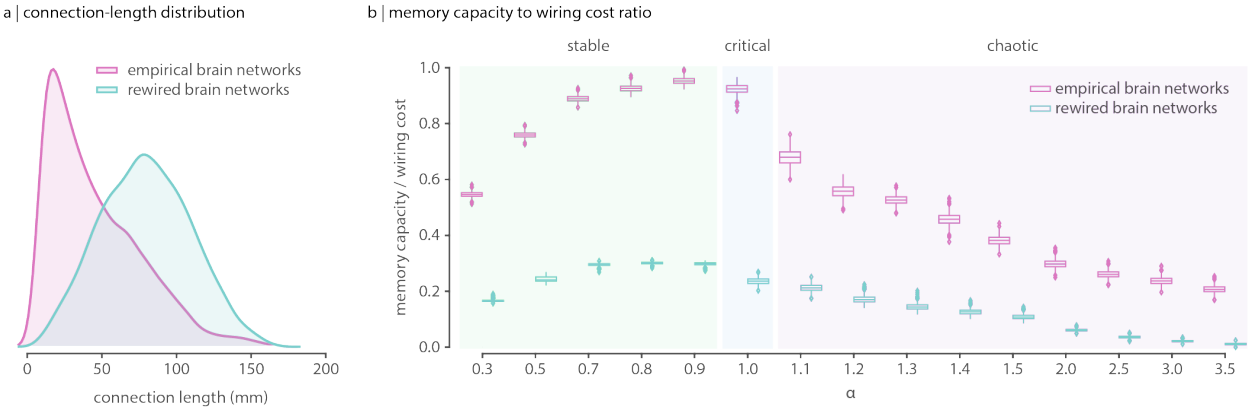

Figure 3.3: **Computation *vs* wiring cost trade-off** | (a) Connection-length distribution of empirical (magenta) vs rewired networks (cyan). Euclidean distance between brain regions was used as a proxy for connection length. (b) Boxplots show the distribution of memory capacity to wiring cost ratio (averaged across intrinsic networks) for the empirical (magenta) and rewired (cyan) networks. When we account for the wiring cost, empirical networks outperform rewired networks across all dynamical regimes. Boxes represent the quartiles of each distribution, and whiskers extend up to 1.5× the interquartile range. Points beyond the whiskers are determined to be outliers.

networks outperform the empiricallly-derived architecture (Fig.3.2a). However, this null model does not account for the fact that the brain is a spatially-embedded network, with finite metabolic and material resources (Bullmore and Sporns, 2012; Stiso and Bassett, 2018). As a result, brain networks are characterized by a prevalence of shorter, low-cost connections (Horvát et al., 2016; Roberts et al., 2016); by contrast, the random flipping of edges in rewired networks skews the connection length distribution towards longer connections resulting in networks with greater wiring cost than empirical brain networks (Fig.3.3a) (Betzel and Bassett, 2018; Betzel et al., 2017). Fig.3.3b shows memory capacity of empirical and rewired networks, normalized by wiring cost, estimated as the sum of the connection lengths weighted by connectivity values. When we account for the cost of wiring, empirical connectomes outperform rewired networks across the three dynamical regimes, suggesting that brain network topology optimizes the trade-off between computational capacity and cost.

3.4.4 Memory capacity of intrinsic networks

We next investigate the memory capacity of individual intrinsic networks. Fig. 3.4a shows the distribution of memory capacity of intrinsic networks, as well as the corresponding null distributions generated by rewiring and spatially-constrained label permutation. Performance is stratified according to dynamical regime, from stable (mean performance

for $\alpha = [0.3, 0.5, 0.7, 0.8, 0.9]$) to critical (performance for $\alpha \approx 1.0$) to chaotic (mean performance for $\alpha = [1.5, 2.0, 2.5, 3.0, 3.5]$). To establish a clearer distinction between the critical and the chaotic regimes, we selected α values above 1.5 to characterize chaotic dynamics (results for intermediate values of α in the range 1.1 to 1.5 are provided in Fig.S3.3). Throughout subsequent analyses, dynamical regimes are defined using the same ranges across α values provided here.

We then compare the performance of empirical intrinsic networks against their analogues in the rewired and label-permutation null models. Consistent with the intuition developed from the global performance shown in the previous section, we find significantly greater memory capacity for most intrinsic networks in the critical regime, at the edge of chaos (mean memory capacity > 0.9 for all networks), but poorer or inconsistently better performance in the stable and chaotic regimes (across dynamical regimes, Wilcoxon–Mann–Whitney two-sample rank-sum test: $P_{rewired} < 0.05$ and $P_{spin} < 0.05$ two-tailed, compared to the rewired and the label-permutation models, respectively).

How do intrinsic networks compare with each other in terms of memory capacity? Making direct comparisons between intrinsic networks is challenging, as memory capacity will be partially driven by features such as network size (i.e., number of nodes) and number of internal connections (Hopfield, 1982; Zylberberg and Strowbridge, 2017). To account for differences among networks due to density, we normalize their memory capacity by their relative connection density (see Fig.S3.4).

Fig. 3.4b shows the density-normalized network-specific memory capacity at each of the three dynamical regimes. In the critical regime, we observe few differences among networks, with the greatest memory capacity in the limbic network, perhaps reflecting an anatomically-mediated predisposition for memory encoding (Neves et al., 2008; Scoville and Milner, 1957; Wills et al., 2005). In the stable and chaotic regimes we observe diametrically opposite ordering, such that networks with greater capacity in the stable regime have lower capacity in the chaotic regime, and vice versa. This suggests an interplay between network topology, dynamics and memory capacity, a phenomenon we study in greater detail in a subsequent section. Interestingly, the order of intrinsic networks' memory capacity resembles the unimodal-transmodal hierarchy (Huntenburg et al., 2018; Margulies et al., 2016; Mesulam, 1994; Mesulam, 1998), differentiating sensory networks (visual and somatomotor) from association networks (default and frontoparietal), suggesting a potential link between the hierarchical organization of the cortex and cognitive capacity (Taylor et al., 2015; Zamora-López et al., 2010).

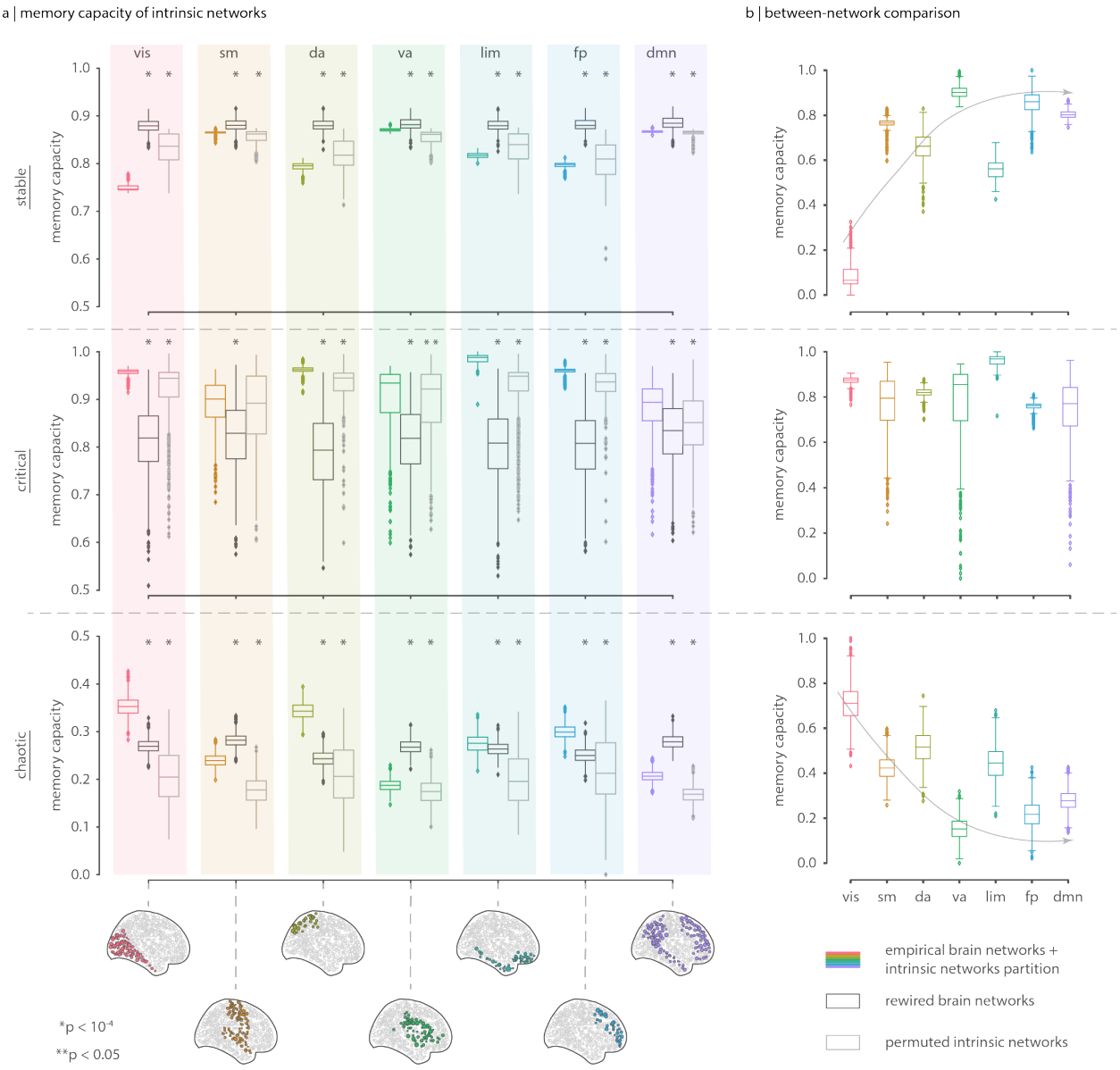

Figure 3.4: **Memory capacity of intrinsic networks** | (a) Boxplots show the distribution of the mean memory capacity (averaged across α values corresponding to each regime) for each intrinsic network, stratified by dynamical regime. At the critical point, memory capacity of empirical intrinsic networks is consistently and significantly higher compared to their analogues in the rewired and label permutation models. (b) To compare intrinsic networks directly, beyond the effects of network size and connection density, relative density was linearly regressed out from the memory capacity estimates of each intrinsic network (see Fig. S3.4 for further details). Memory capacity was scaled between 0 and 1 using the minimum and maximum values within each dynamical regime. When compared to each other, memory capacity is homogeneous across intrinsic networks in the critical regime but heterogeneous in the stable and chaotic regimes. Boxes represent the quartiles of each distribution, and whiskers extend up to 1.5× the interquartile range. Points beyond the whiskers are determined to be outliers.

3.4.5 Information transfer across the brain

The performance of intrinsic networks in the memory task provides a measure of how the macroscopic human connectome supports temporal information storage. This metric, however, tells us little about how information changes as it travels from one region to the other in the brain. We thus next investigate how temporal information content (i.e., memory capacity) is transformed as signals propagate through the connectome during learning. Specifically, we compare the encoding and decoding capacity of intrinsic networks (Fig. 3.5a). We define the encoding capacity of an intrinsic network as the memory capacity when nodes in that intrinsic network are used as readout nodes. We define the decoding capacity of an intrinsic network as the memory capacity when the directly connected neighbours of that intrinsic network are used as readout nodes.

Differences between encoding and decoding capacity quantify the extent to which temporal information content is transformed as signals travel through an intrinsic network (Shine et al., 2020). To determine whether encoding and decoding are statistically different from one another, we conduct a two-tailed, one-sample t-test under the null hypothesis that the mean of the difference between encoding and decoding capacity is equal to zero ($H_0 : \mu_{enc.-dec.} = 0$). Across all dynamical regimes, the encoding - decoding differences of intrinsic networks are significantly different from zero ($P < 10^{-4}$, Bonferroni corrected). Fig. 3.5b shows the effect size of the difference between the encoding and decoding capacity of intrinsic networks across dynamical regimes. We quantify effect size as the Cohen's D estimator consistent with a one-sample t-test for means ($H_0 : \mu_{enc.-dec.} = 0$). We use this measure to compare the empirical network against the rewired and label-permutation models. Importantly, across all intrinsic networks and dynamical regimes, we observe significantly greater asymmetry between encoding and decoding for the empirical connectome compared to the rewired and spatially-constrained null models. This suggests that the brain's connectivity – particularly its modular organization – promotes functional heterogeneity and specialization of intrinsic networks.

At criticality – when overall connectome performance is optimal – we observe smaller but significant differences between encoding and decoding. The reduction in the difference between encoding and decoding capacity at the critical point suggests a homogenization of information content across the connectome (integration). At the same time, the magnitude of the difference between encoding and decoding is significant (minimum absolute effect size > 0.25), indicating a heterogeneous distribution of information across functional networks (segregation). In other words, at the critical point, there exists a balance between integration and segregation of the information across the connectome (Sporns, 2013; Sporns

et al., 2004). Interestingly, the intrinsic network with the greatest difference between encoding and decoding capacity at criticality is the limbic network, again suggesting an anatomical basis for the well-studied involvement of this network in memory function (Neves et al., 2008; Scoville and Milner, 1957; Wills et al., 2005).

Finally, it is noteworthy that most intrinsic networks are computationally flexible, performing better as decoders in the stable regime (*decoding* $>$ *encoding*), and better as encoders in the chaotic regime (*decoding* $<$ *encoding*). This is the case for all intrinsic networks (visual, somatomotor, dorsal attention, limbic and fronto-parietal; Fig. 3.5b), except the ventral attention and the default mode networks. Interestingly, the default mode network is the only one that acts as a decoder in both the stable and the chaotic regimes, while its encoding capacity is expressed only at criticality, consistent with contemporary theories that this network supports global monitoring and information integration (Dohmatob et al., 2020). Overall, results suggest that topology and dynamics interact to support switching of the direction in which temporal information content accumulates in intrinsic networks, endowing these networks with computational flexibility.

3.4.6 Interplay between network topology, dynamics and memory capacity

A recurring theme in the previous sections was that memory capacity depends on the interaction between network topology and dynamics. Here we relate memory capacity to multiple (local- and global-level) attributes of the connectome graph across the three dynamical regimes. Fig. 3.6a shows the distribution of correlations between memory capacity and local graph attributes; attributes are first computed for individual nodes and then averaged within intrinsic networks. Fig. 3.6b shows the correlations between memory capacity and global graph attributes. All graph properties were computed using the weighted structural connectivity network. Briefly, graph attributes include measures of connectedness (strength), clustering, centrality (betweenness), connection diversity (participation), global efficiency (characteristic path length), and modularity (see *Methods* for definitions).

We note three key results. First, we observe moderate to high correlations between graph attributes and memory capacity, suggesting that network structure influences performance. Second, the direction of that influence depends on the dynamics, with correlation signs switching from one regime to another. In other words, structure does not simply drive dynamics, and thus performance. Rather, structure and dynamics interact to drive

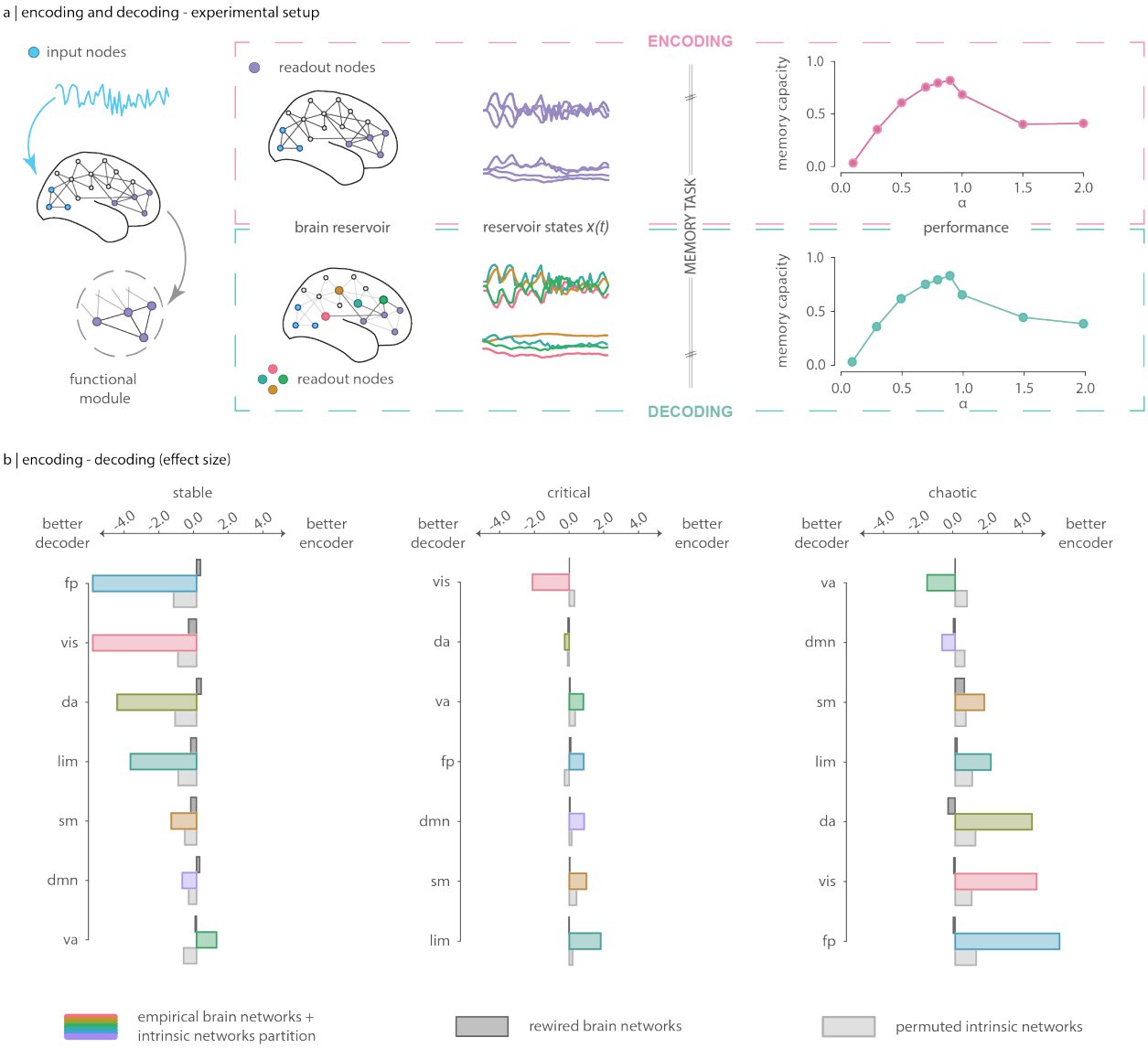

Figure 3.5: **Encoding and decoding capacity of intrinsic networks** | The difference between the encoding and decoding capacity of an intrinsic network quantifies the extent to which information is transformed as it propagates through the network. (a) The encoding (decoding) capacity of a network is equivalent to its memory capacity when it operates as an encoder (decoder). The coding role of the network is determined by the selection of the readout nodes. In the encoding setup (top panel) readout nodes are the nodes that belong to the network; they are a proxy for the information *sent* by the network. In the decoding setup (bottom panel) readout notes correspond to the direct neighbours of the network; they are a proxy for the information *received* by the network. (b) Bar plots show the effect size of the difference between encoding and decoding, quantified as the *Cohen's D* estimator consistent with a 1-sample *t*-test. Compared to the rewired and spatially-constrained null models, the human connectome presents overall a higher encoding - decoding asymmetry.

performance. Third, at criticality, memory capacity is much less dependent on the topology, compared to the stable and chaotic regimes, where the correlations are typically greater. That is, at criticality, memory capacity transcends topological features and becomes more dependent on global network dynamics.

3.4.7 Sensitivity analysis

Throughout our analyses, subcortical regions, which include structures such as the thalamus, the basal ganglia, the hippocampus, the amygdala and the brain stem, served as input nodes in all experiments. Nevertheless, not all these regions necessarily constitute biologically plausible relay stations for incoming sensory signals. Among the subcortical structures, the thalamus is known to play an important role in relaying sensory and motor signals from the rest of the body to the cerebral cortex and to other cortical structures (Sherman and Guillery, 2002). Therefore, we repeated all analyses using an alternative experimental set up that uses the left and right thalamus as input nodes. Results are shown in Figs. S3.5 and S3.6. Although memory capacity estimates change from one type of experimental set up to the other, the human brain network still displays maximum and optimal memory capacity in the critical state compared to the rewired ($P_{rewired} = 0.0$ and common-language effect size = 99% two-tailed, Wilcoxon-Mann-Whitney two-sample rank-sum test) and label-permutation ($P_{spin} = 0.0$ and common-language effect size = 99% two-tailed, Wilcoxon-Mann-Whitney two-sample rank-sum test) models. This is true for the whole brain, as well as for individual intrinsic networks, with even stronger effect sizes compared with the original analyses.

Likewise, all analyses presented thus far were conducted on a fine grained, high-resolution parcellation of the brain. We repeated our analyses at a lower resolution parcellation (448 cortical and 15 subcortical regions) to assess the extent to which our results depend on network scale. Results are shown in Figs. S3.7 and S3.8. At this coarser parcellation, the overall memory capacity of the brain in the critical state is again statistically higher compared to the rewired and label-permutation models.

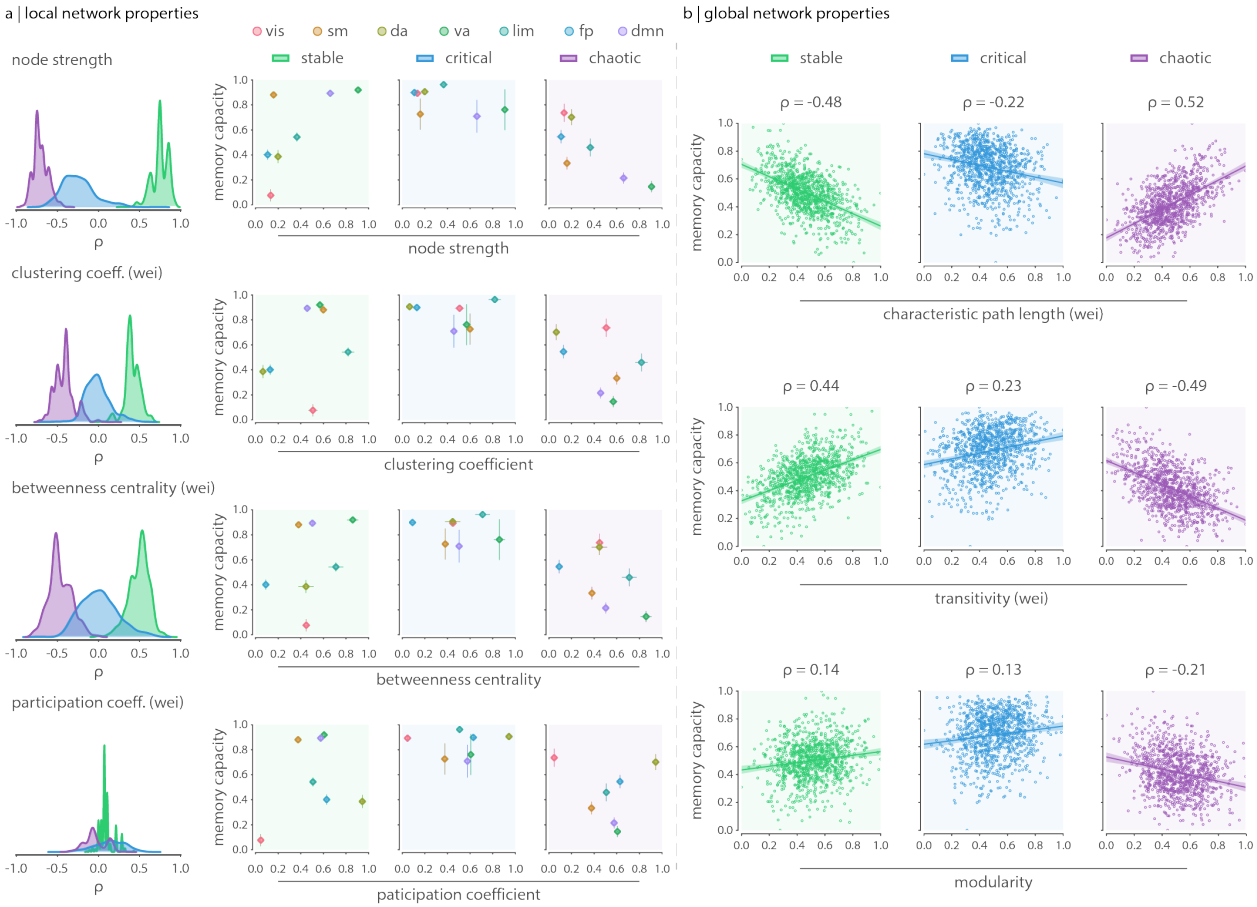

Figure 3.6: **Contribution of network topology to memory capacity is a function of the dynamics** | Local and global topological attributes interact with network dynamics to shape the memory capacity of the human connectome. (a) Correlation between local network attributes and memory capacity across intrinsic networks, stratified by dynamical regime (stable: green, critical: blue, and chaotic: purple). Local network features, including **node strength**, **clustering coefficient**, **betweenness centrality** and **participation coefficient**, were estimated at the node level and then averaged within each intrinsic network. (Right column) Scatter plots show the relationship between memory capacity (y-axis) and average local network attributes (x-axis) across intrinsic networks; markers (error bars) represent the mean (standard deviation) across samples. Each coloured marker corresponds to an intrinsic network. (Left column) Distribution (across samples) of the Spearman's rank correlation between memory capacity and average local network attributes across intrinsic networks. (b) Correlation between global network attributes and memory capacity in the human connectome, stratified by dynamical regime (stable: green, critical: blue, and chaotic: purple). Global network features include **characteristic path length**, **transitivity** and **modularity**. Scatter plots show the relationship between memory capacity (y-axis) and global network attributes (x-axis) across samples; the corresponding Spearman's rank correlation is indicated on the top of each scatter plot.

3.5 Discussion

In the present report we used reservoir computing to study how network structure and dynamics shape learning and computations in networks with architectures based on the human connectome. Using neuromorphic neural networks, we show that empirically-derived architectures perform best at criticality, maximizing temporal memory capacity relative to their wiring cost. We find that performance is driven by network topology, and that the modular organization of intrinsic networks is computationally relevant. Throughout, we observe a prominent interaction between network structure and dynamics, such that the same underlying architecture can support a wide range of learning capacities across dynamical regimes.

By studying artificial neural networks with connectome-based architectures, we begin to reveal the functional consequences of brain network topology. Numerous studies point to a unique set of organizational features of brain networks (Bassett et al., 2011; Heuvel et al., 2016; Rubinov and Sporns, 2010; Sporns et al., 2005), but how these features influence the neural computations that support cognition remains unknown. By training networks with biologically-realistic connectivity to perform a simple memory task, we show that connectomes achieve superior performance compared to populations of networks with identical low-level features (density, degree sequence) but randomized high-level topology. In a similar fashion, two recent studies explore the effect of biologically-instantiated connectivity from different primate species on the performance of artificial neural networks (Damicelli et al., 2022; Goulas et al., 2021). Importantly, this hybrid approach can be implemented at multiple spatial scales, from large-scale brain networks, to the level of cortical microcircuits (Haeusler and Maass, 2007).

The present work highlights a symbiotic relationship between structure and dynamics. Namely, the unique topological features of the brain support optimal performance only when dynamics are critical, but not when they are stable or chaotic. Multiple accounts posit that the brain, akin to many other naturally occurring complex systems, operates at the interface of order and disorder. In this critical regime, at the "edge of chaos", dynamic transitions are optimized, and thought to confer adaptive benefits, including greater dynamic range and selective enhacement of weak inputs (Haldeman and Beggs, 2005; Shew et al., 2009; Vázquez-Rodríguez et al., 2017). In addition, multiple empirical studies have demonstrated that neural dynamics exhibit fluctuations consistent with a networked system at criticality (Cocchi et al., 2017; Deco and Jirsa, 2012; Kitzbichler et al., 2009; Tagliazucchi et al., 2012). We also observe that the interaction between topology and dynamics

shapes how information accumulates in the connectome. Interestingly, the direction in which information accumulates in non-critical regimes mirrors the characteristic ordering of intrinsic networks along the unimodal-transmodal hierarchy (Huntenburg et al., 2018; Margulies et al., 2016; Mesulam, 1994; Mesulam, 1998), suggesting a possible mechanism to flexibly switch between bottom-up and top-down information flow.

In the context of reservoir computing, a link between the computational power of the reservoir and the edge of chaos has been established in multiple theoretical studies (Bertschinger and Natschläger, 2004; Langton, 1990; Legenstein and Maass, 2007a,b). The reservoir has the potential to work as a universal function approximator as long as it can hold (memorize) and nonlinearly transform (separate distinct classes) information about past and present external stimuli in its high-dimensional transient states (Maass and Markram, 2004). The balance between these two properties, namely the *fading memory property*, which is enhanced by stable dynamics, and the *separation property*, which is supported by chaotic dynamics, is optimal at the edge of chaos. At this critical point, where the transition between stable and chaotic dynamics occurs, the perfect balance between order and disorder delivers the optimal trade-off between memory and separation. The fact that brain networks perform better at criticality (compared to the rewired network model) suggests that network topology may be configured to negotiate that optimal trade-off between these two computational properties, and therefore maximize computational capacity.

Computational power and information processing, however, might not be the only features that brain networks seem to optimize. The brain is a spatially embedded network with finite metabolic and material resources, and as such, there are physical demands that biological networks should satisfy (Bullmore and Sporns, 2012). For instance, the growth and maintenance of axonal projections entails material and energetic costs. These wiring costs increase with the length of inter-neuronal connections and manifest as a prevalence of short-range connections (Horvát et al., 2016; Roberts et al., 2016). Therefore, studies of the computational, topological and dynamical features of the brain must also consider the cost imposed by its geometrical constraints (Betzel et al., 2016; Betzel et al., 2017; Kaiser and Hilgetag, 2006). A salient finding in the present report is that, when wiring cost is taken into account, brain networks outperform randomized networks in all dynamical regimes. The fact that empirical networks achieve higher computational power per unit cost compared to the rewired networks supports the idea that brain networks are highly economical: they maximize adaptive value while minimizing wiring cost (Bassett et al., 2010).

The present paradigm could be used to systematically map combinations of network attributes and dynamical regimes to a range of computational functions, and may ultimately help to identify design principles for engineering better networks and circuits. In particular, this paradigm presents a new direction for designing neuromorphic or biomimetic computing architectures (Tanaka et al., 2019). These include reservoirs built from analog circuits (Appeltant et al., 2011; Li et al., 2018; Soriano et al., 2014; Zhao et al., 2016), field-programmable gate arrays (FPGA; (Alomar et al., 2014; Antonik, 2018; Antonik et al., 2015; Wang et al., 2017)), very large-scale integration circuits (VLSI; (Petre and Cruz-Albrecht, 2016; Polepalli et al., 2016; Roy et al., 2014)), memristive networks (Bennett et al., 2017; Du et al., 2017; Kendall et al., 2018; Kulkarni and Teuscher, 2012; Sillin et al., 2013; Suárez et al., 2018; Yang et al., 2016), and photonic or opto-electronic devices (Katumba et al., 2017, 2018; Laporte et al., 2018; Vandoorne et al., 2008, 2014; Zhang et al., 2014). The architectures of these systems rarely take advantage of emerging understanding of connection patterns in biological networks. Due to their physical nature, neuromorphic systems are conditioned by similar spatial, material and energetic costs as biological neural networks. Because of this, the cost-effective design of these information processing systems could benefit from insights gained about the economical organization of brain networks (Bassett et al., 2010; Bullmore and Sporns, 2012). We envision that the present work serves as a foundation for future efforts to design biologically-inspired neuromorphic architectures.

More broadly, the present work addresses the question of the structure-function relationship in the brain, but with a focus on computation. Over the past 20 years, multiple forward models have been proposed to link structural connection patterns to functional connection patterns (Suárez et al., 2020), including statistical models (Messé et al., 2014; Mišić et al., 2016), communication models (Crofts and Higham, 2009; Goñi et al., 2014; Graham and Rockmore, 2011; Mišić et al., 2015) and neural mass models (Breakspear, 2017; Deco et al., 2009; Honey et al., 2007; Sanz-Leon et al., 2015). These models have been successful in predicting an array of empirical phenomena, including static and dynamic functional connectivity (Honey et al., 2010). However, these models are largely phenomenological, and focused on predicting an emergent property of the system (intrinsic functional connectivity), rather than explaining how the system computes and approximates functions in the external environment. The present work represents a step towards mapping network structure more directly to its computational function. Along these lines, several recent reports have investigated the computational advantages provided by different network architectures. By systematically varying topological features akin to those found in biological brain networks, these studies have assessed the effect

of specific topological attributes on the computational capacity of reservoir networks across different tasks. For instance, Rodriguez and colleagues show that the mesoscale modular structure of the reservoir shapes signal propagation dynamics and determines performance in a memory capacity task (Rodriguez et al., 2019). Likewise, Aceituno and colleagues show that the frequency domain of the reservoir's units can be modified in a task-specific manner by introducing cycles of various lengths into the network, boosting performance in multiple tasks (Aceituno et al., 2020). These reports - which highlight general design principles for recurrent neural networks - suggest that the performance of the connectome may be shaped by mesoscale structure and higher-order interactions that simultaneously take place among more than two nodes, such as motifs (Shen et al., 2012; Sporns and Kötter, 2004), cycles and cavities (Bettinardi et al., 2017; Sizemore et al., 2018).

Training both empirical and null networks allows us to identify topological features of connectomes that are important for memory capacity and to rule out those that are not. The poor performance of randomly rewired networks suggests that low-level properties such as degree sequence and density do not influence learning, and point to higher-order properties such as mesoscale organization (Fig. 3.2 and Fig. 3.4). Empirical networks outperform label-permutation nulls with the same underlying topology but a different mesoscale organization, confirming that mesoscale organization defined by intrinsic networks shapes learning (Fig. 3.2 and Fig. 3.4). Indeed, selecting readout modules using a partition optimized for the connectome – rather than intrinsic networks derived from resting-state fMRI – lowers performance, pointing to a singular computational role of intrinsic networks (Fig. S3.1). The overall high performance of the intrinsic network partition is potentially explained by the fact that the intrinsic networks reflect the underlying mesoscale organization of structural networks but do not have maximal modularity, balancing segregation and integration. This finding is also consistent with theoretical results, which show that in non-biological recurrent neural networks there exists an optimal, but not maximal, modularity for memory capacity, providing a computational infrastructure that can simultaneously support a range of localized and distributed operations (Rodriguez et al., 2019). Interestingly, rewiring the network while preserving the internal structure of readout modules lowers memory capacity, suggesting that the performance of biological connectomes is not driven by the internal structure of intrinsic networks, but rather how they are topologically arranged with respect to one another (Fig. S3.2). Collectively, these comparisons emphasize the influence of higher-order interactions on memory capacity. Therefore, identifying structural features that support the memory capacity of a particular intrinsic network requires considering the higher-order interactions that simultaneously

take place among multiple nodes and networks (Aceituno et al., 2020). As a salient example, we find that the limbic network consistently presents the greatest memory capacity, and the greatest difference between encoding and decoding, suggesting that the enhanced memory capacity of this network naturally arises from its connections and interactions with other networks (Neves et al., 2008; Scoville and Milner, 1957; Wills et al., 2005).

In particular, we provide evidence that the intrinsic networks of the brain constitute computationally relevant systems. Despite their widespread use as a frame of reference in cognitive neuroscience, their precise cognitive function is not completely understood. Although they are typically labeled based on prior domain knowledge from functional neuroanatomy (Uddin et al., 2019), these networks are primarily defined as groups of neuronal populations with coherent time courses. Multiple studies have reported correlations between the expression of these networks and individual differences in behaviour (Medaglia et al., 2018), but how they contribute to computation in the brain is unknown. The present results demonstrate that imposing this intrinsic network partition on the structural connectome yields better performance, implying that these networks represent computationally distinct components of the connectome (Bertolero et al., 2015; Haimovici et al., 2013).

Biologically-informed reservoirs can be extended to investigate a wider range of cortical functions to further our understanding on how functional specialization emerges from network structure. By training brain-inspired network architectures to implement other types of tasks, we can probe other modes or classes of computation. For example, temporal-sequence learning tasks, mimicking speech recognition, depend on the network's ability to occupy multiple states and match these states to the signal inputs, thus accessing a different computational property. We thus envision future efforts to link architecture and computation in brain networks, analogous to modern meta-analytic methods that map regional activation to cognitive tasks (Dockès et al., 2020; Fox and Lancaster, 2002; Poldrack and Yarkoni, 2016; Yarkoni et al., 2011). Mapping network structure and dynamics to fundamental blocks of computation may allow us to build a comprehensive structural-functional ontology, relating network structure to computational properties and, ultimately, to cognitive function.

We finally note that the present results should be interpreted with respect to several limitations. First, to focus on the question of how network structure influences learning, we implemented a model with simple, homogeneous dynamics across the entire network. Future work should explore the role of heterogeneous dynamics (Demirtaş et al., 2019;

Wang et al., 2019). Second, the present dynamics do not depend on time-delayed transmission, allowing us to focus only on network structure, but ignoring the role of network geometry in learning (Stiso and Bassett, 2018). Third, we used computational tractometry to reconstruct connectomes from diffusion weighted imaging, a technique prone to false positives and negatives (Maier-Hein et al., 2017; Reus and Heuvel, 2013; Thomas et al., 2014). Although we implemented steps to focus on highly-reproducible consensus features of these networks, future experiments could be designed around networks reconstructed using invasive methods with greater fidelity, such as tract tracing.

Despite common roots, modern neuroscience and artificial intelligence have followed diverging paths. Technological, analytic and theoretical advances present a unique opportunity for convergence of these two vibrant scientific disciplines. From the connectomics perspective, this work opens fundamentally new opportunities to discover how cognitive capacity emerges from the links and interactions between brain areas. From the artificial intelligence perspective, reverse-engineering biological brain networks may ultimately generate insights and novel design principles for re-engineering artificial brain-inspired networks and systems.

3.6 Materials and Methods

3.6.1 Data acquisition

Informed written consent in accordance with institutional guidelines (protocol approved by the Ethics Committee of Clinical Research of the Faculty of Biology and Medicine, University of Lausanne, Switzerland, #82/14, #382/11, #26.4.2005) was obtained for all subjects. A total of N = 66 healthy young adults (16 females, 25.3 ± 4.9 years old) were scanned at the Department of Radiology, University Hospital Center and University of Lausanne. The scans were performed in 3-Tesla MRI scanner (Trio, Siemens Medical, Germany) using a 32-channel head-coil. The protocol included (1) a magnetization-prepared rapid acquisition gradient echo (MPRAGE) sequence sensitive to white/gray matter contrast (1 mm in-plane resolution, 1.2 mm slice thickness), (2) a diffusion spectrum imaging (DSI) sequence (128 diffusion-weighted volumes and a single b0 volume, maximum b-value 8000 s/mm^2, $2.2 \times 2.2 \times 3.0$ mm voxel size), and (3) a gradient echo EPI sequence sensitive to BOLD contrast (3.3 mm in-plane resolution and slice thickness with a 0.3 mm gap, TR 1920 ms, resulting in 280 images per participant). Participants were not subject to any overt task demands during the fMRI scan.

3.6.2 Structural network reconstruction

Grey matter was parcellated into 68 cortical plus 15 subcortical nodes according to the Desikan-Killiany atlas (Desikan et al., 2006). Cortical regions were then further divided into 1000 approximately equally-sized nodes (Cammoun et al., 2012). Structural connectivity was estimated for individual participants using deterministic streamline tractography. The procedure was implemented in the Connectome Mapping Toolkit (Daducci et al., 2012), initiating 32 streamline propagations per diffusion direction for each white matter voxel. Structural connectivity between pairs of regions was defined as the number of streamlines normalized by the mean length of streamlines and mean surface area of the two regions, termed fiber density (Hagmann et al., 2008). This normalization compensates for the bias toward longer fibers during streamline reconstruction, as well as differences in region size.

To mitigate concerns about inconsistencies in reconstruction of individual participant connectomes (Jones et al., 2013; Thomas et al., 2014), as well as the sensitive dependence of network measures on false positives and false negatives (Zalesky et al., 2016), we adopted a group-consensus approach (Betzel et al., 2018; Reus and Heuvel, 2013; Roberts et al., 2017). In constructing a consensus adjacency matrix, we sought to preserve (a) the density and (b) the edge length distribution of the individual participants matrices (Betzel et al., 2016; Betzel et al., 2018; Mišić et al., 2015). We first collated the extant edges in the individual participant matrices and binned them according to length. The number of bins was determined heuristically, as the square root of the mean binary density across participants. The most frequently occurring edges were then selected for each bin. If the mean number of edges across participants in a particular bin is equal to k, we selected the k edges of that length that occur most frequently across participants. To ensure that inter-hemispheric edges are not under-represented, we carried out this procedure separately for inter- and intra-hemispheric edges. The binary density for the final whole-brain matrix was 2.5% on average. The weight associated with each edge was then computed as the mean weight across all participants.

3.6.3 Reservoir computing

We used reservoir computing to measure the encoding capacity of large-scale brain networks in a memory task. In its simplest form, the reservoir computing architecture consists of an input layer, followed by a recurrent neural network (the *reservoir*), and a readout module, which is typically a linear model. Given an input and a target signal, a learning task consists of approximating the target signal through a linear combination of the states

of the readout nodes within the reservoir. The latter are activated by the propagation of the external input signal, introduced to the reservoir through a set of input nodes. Fig. 3.1a illustrates the paradigm.

Briefly, reservoir computing relies on the two following mechanistic principles: *i)* the complex interactions within the reservoir perform a nonlinear projection of the input into a higher dimensional space; this has the potential to convert nonlinearly separable problems into linearly separable ones; and *ii)* the recurrent nature of the connections within the reservoir endows the network's states with a temporal memory. These two properties, which also depend on the dynamics of the reservoir, are critical as they constitute some of the basic computational building blocks of more complex tasks. Therefore, if these two properties exist, the reservoir has the potential to serve as a universal function approximator (Maass et al., 2002).

In the present report, we used a high-resolution human brain connectome reconstructed from diffusion-weighted imaging to constrain the connections within the reservoir. Throughout all experiments, we used all subcortical regions as input nodes, and a subset of cortical regions as readout nodes that were defined based on the Yeo-Krienen intrinsic network partition (Thomas Yeo et al., 2011). Details about network dynamics, training of the network, and the memory task are described below.

Reservoir dynamics

The reservoir consists of an artificial recurrent neural network of sigmoid units. Each unit receives one or more inputs and sums them to produce an output. Each input is separately weighted, and the sum is passed through a nonlinear activation function. The dynamics of the reservoir are thus governed by the following discrete-time, firing-rate neuron model:

$$\mathbf{x}(t+1) = \tanh(\mathbf{W_{in}}\mathbf{u}(t+1) + \mathbf{W}\mathbf{x}(t)) \tag{3.1}$$

where $\mathbf{x}(t)$ represents the vector of activation states of the nodes inside the reservoir (*reservoir states*). The vector $\mathbf{u}(t) = (u_1(t),,u_K(t))$ is a K-dimensional ($K = 15$) input signal weighted by the input matrix $\mathbf{W_{in}}$ (with constant value $\mathbf{W_{in}} = 0.0001$). Finally, the matrix $\mathbf{W}$ represents the connection weights within the reservoir, i.e., the brain connectivity measures obtained from diffusion MRI data.

For comparison, we performed the same analysis shown in Fig. 3.2 using a nonlinear threshold activation function for the reservoir's units. Specifically, if the weighted sum of the inputs to a unit is greater than or equal to a preset threshold, then the unit's activation

state is 1, and 0 otherwise. The threshold was set to 1.0 and the constant input matrix $\mathbf{W_{in}} = 0.1$. Results are shown in Fig. S3.9.

Furthermore, for comparison to other traditional reservoir computing forms, we benchmarked the memory capacity of the connectome-informed reservoirs against that of a random recurrent network of leaky integrator neurons and a random recurrent network of spiking neurons. Details about the parameters of these models are provided in Table S3.1, and results are shown in Fig. S3.10.

Stability of reservoir dynamics

We parametrically tuned the dynamics of the reservoir by uniformly scaling the connection weights so that the spectral radius (that is, the modulus of the leading eigenvalue) of the connectivity matrix is either below, at, or greater than 1 (Seung, 1996). Specifically, we first scaled the weights of the connectivity matrix between 0 and 1, and then we divided by its spectral radius. The latter operation transforms the spectral radius of the connectivity matrix to 1. To gradually modified the spectral radius, we multiplied the connectivity matrix by a wide range of α values ([0.3, 0.5, 0.7, 0.8, 0.9, 1.0, 1.1, 1.2, 1.3, 1.4, 1.5, 2.0, 2.5, 3.0, 3.5]), being α the tuning parameter. The matrix $\mathbf{W}$ in Eqn. 3.1 can then be expressed as:

$$\mathbf{W} = \alpha \frac{\mathbf{W_0}}{\rho(\mathbf{W_0})} \tag{3.2}$$

where $\mathbf{W_0}$ is the original weighted connectivity matrix scaled between 0 and 1 and $\rho(\mathbf{W_0})$ is the spectral radius of $\mathbf{W_0}$. Reservoir dynamics are stable for $\alpha < 1$, and chaotic for $\alpha > 1$. When $\alpha \approx 1$, dynamics are said to be critical, or at the *edge of chaos*, a transition point between stable and chaotic dynamics (Seung, 1996).

Readout module

The role of the readout module is to approximate the target signal $\mathbf{y}(t)$, specific to the task at hand, through a linear combination of the activation states of the output nodes within the reservoir, $\mathbf{x_{out}}(t)$. That is:

$$\hat{\mathbf{y}}(t) = f(\mathbf{W_{out}}\mathbf{x_{out}}(t)) \tag{3.3}$$

where $\mathbf{W_{out}}$ is the matrix of weights that connect the readout nodes to the readout module. Using the target signal $\mathbf{y}(t)$, these weights are trained in a supervised manner. In principle,

learning can be attained using any type of linear regression model. Here, f represents the ordinary least squares estimator.

3.6.4 Intrinsic networks as functional systems

The paradigm proposed here (Fig. 3.1a) is part of a more extensive effort to develop a framework to investigate structure-function relationships across the brain (*function* understood from a computational point of view). Specifically, this framework aims to further our understanding on how functional specialization emerges from the underlying network structure. To investigate the effects of network structure on the emergence of the spectrum of cortical functions, we need a convenient and biologically meaningful way to divide the cortex into its functional systems. Here we used a functional connectivity-based partition known as *intrinsic networks*.

Intrinsic networks, often known as *resting-state networks* in the cognitive neuroscience literature, consist of brain regions that exhibit high levels of synchronized BOLD activity (Wig, 2017). It has been hypothesized that the organization of the brain into these segregated systems or modules supports functional specialization (Wig, 2017). These internally coherent and co-fluctuating networks are associated with individual differences in task activation and behaviour, including perception, cognition and action (Cole et al., 2014; Medaglia et al., 2018). In the present study, we applied the intrinsic network partition derived by Yeo, Krienen and colleagues (Thomas Yeo et al., 2011). Briefly, the partition was obtained by applying a clustering algorithm to voxel-level functional connectivity estimated from resting-state functional MRI data.

The partition proposed by Yeo, Krienen and colleagues consists of seven non-overlapping intrinsic networks, namely: visual (vis; 151 nodes), somatomotor (sm; 219 nodes), dorsal attention (da; 58 nodes), ventral attention (va; 130 nodes), limbic (lim; 101 nodes), frontoparietal (fp; 64 nodes) and default-mode (dmn; 277 nodes); each spanning cortical regions of varying size. These networks have been consistently replicated in multiple studies using different data acquisitions, anatomical parcellations and analysis techniques (Damoiseaux et al., 2006).

3.6.5 Memory capacity task

Using the experimental paradigm described above, we estimated the encoding capacity of each intrinsic network in a memory task. In this task, the readout module is trained to approximate a delayed version of the input signal at different time-lags. In other words,

$\mathbf{y}(t) = \mathbf{u}(t-\tau)$, where $\mathbf{y}(t)$ is the target signal, $\mathbf{u}(t)$ is the input signal, and τ is the parameter that controls for the amount of memory required by the task. Therefore, there are as many linear units in the readout module as there are time-lags (one for every value of τ), and each linear unit is independently trained from one another.

We generated 4100 points of a uniformly distributed input signal ($\mathbf{u}(t) \sim \text{Uniform}(-1, 1)$). We introduced this signal to the reservoir through a set of input nodes corresponding to all 15 subcortical regions. We then recorded, for the same length of time, the activation states of the readout nodes (these activation states are represented by $\mathbf{X_{out}}$ in Eqn. 3.3). We used 2050 time points of the recorded activation states to train a linear regression model to reproduce the same input signal at different time lags (see *Readout module* for details); τ was monotonically increased in one-size steps in the range [1, 16]. The remaining 2050 time points were used to test the performance. For every τ, a performance score was computed as the absolute value of the Pearson's correlation between the target $\mathbf{y}(t)$ and the predicted signal $\hat{\mathbf{y}}(t)$. Memory capacity (MC) was then estimated as the sum of the performance score across all time delays:

$$MC = \sum_{\tau} |\rho(\mathbf{y}, \hat{\mathbf{y}})| \tag{3.4}$$

The magnitude of MC is proportional to the ability of the reservoir's activation states to encode both past and present input stimuli.

The procedure above was repeated for every value of the parameter α (see *Stability of reservoir dynamics* for details), and for every intrinsic network. In this way, the net result is a memory capacity per intrinsic network as a function of the α.

3.6.6 Bootstrap resampling

We bootstrapped individual connectivity matrices to provide a reliable estimate for the memory capacity of each intrinsic network. Specifically, we generated 1000 (sub)samples by randomly selecting, without replacement, 40 out of 66 individual connectivity matrices. For each drawn subset, we generated a group-consensus structural connectivity matrix (see *Structural network reconstruction* for details), and we applied the procedure described in the previous section. In this way, we constructed a distribution for the memory capacity of each functional system at every value of the parameter α (Fig. 3.1c).

3.6.7 Null models

We benchmarked the memory capacity of intrinsic networks against two different types of null models. The first null model evaluates the extent to which memory capacity measures depend on the underlying network connectivity. To do so, we used the method proposed in (Maslov and Sneppen, 2002), available in the Python version of the Brain Connectivity Toolbox (https://github.com/aestrivex/bctpy; (Rubinov and Sporns, 2010)). This method systematically destroys network topology by randomly swapping pairs of edges (10 swaps per edge), while preserving network size, degree distribution, density, and node-level, intrinsic-network assignment (Fig. 3.2b). This method guarantees the connectedness of the resulting rewired network, that is, every node can be reached by every other node in the network.

The second null model assesses whether the partition of the connectome into seven intrinsic networks is relevant for the performance in the memory task. We used a spatially-constrained, label-permutation null model that randomly permutes intrinsic network labels while preserving their spatial embedding and autocorrelation (Fig. 3.2c; (Alexander-Bloch et al., 2018; Markello and Misic, 2021)). This method creates a surface-based representation of our parcellations by applying the Lausanne atlas to the FreeSurfer *fsaverage* surface using files obtained from the Connectome Mapper toolkit (https://github.com/LTS5/cmp) (Daducci et al., 2012). The *fsaverage* surface is then projected onto a sphere to define spatial coordinates for each parcel; vertices on the sphere are assigned based on the closest distance to the center-of-mass of each parcel. New spatial coordinates are generated by applying randomly-sampled rotations. Finally, node-labels are then reassigned based on that of the closest resulting parcel. Importantly, this procedure was performed at the parcel resolution rather than the vertex resolution to ensure that parcel sizes were not changed during the rotation and reassignment procedure. This method is available in the module *stats* of the Netneurotools python package (https://netneurotools.readthedocs.io/en/latest/index.html).

These models were applied on a consensus structural connectivity matrix reconstructed from the individual matrices of all 66 subjects. A null distribution with 1000 iterations was built for each model. We used the Wilcoxon-Mann-Whitney two-sample rank-sum test to assess the statistical significance of the human connectome's memory capacity estimates against the null models.

3.6.8 Wiring cost

Euclidean distance was used as a proxy for white matter tract length. We estimated the distance between every pair of brain regions that are physically connected by a structural connection. The total wiring cost for the network was then estimated as the sum of the connection lengths weighted by the connectivity values; the latter are proportional to the number of streamlines between brain regions. Same conclusions can be drawn when the mean or median of the connection length distribution are used instead (not shown in the present report).

3.6.9 Encoding and decoding capacity

Broadly speaking, any communication scheme is characterized by the presence of two agents: the *encoder*, whose role is to *encode* and *send* a message, and the *decoder*, who is in charge of *receiving* and *decoding* the message. In such scheme, the capacity of the encoder agent to cipher – or encode – the message is bound to the information it *sends*, and the capacity of the decoder agent to decipher – or decode – the message is bound to the information it *receives*. Following a similar logic, we operationalized the *encoding* and *decoding* capacity of an intrinsic network as the memory capacity of the information *sent* and *received* by the network, respectively. This translates into two different experimental set ups, namely *encoding* and *decoding*, which conceptually diverge in the role played by the network (i.e., encoder or decoder), and pragmatically differ in the way readout nodes are selected. For *encoding*, the signals generated by the nodes of the network are used as a proxy for the information *sent* by the network. For *decoding*, the signals generated by the directly connected neighbour nodes of the network are used as a proxy for the information *received* by the network.

Encoding - decoding: interpretation

To quantify how temporal information content is transformed as it flows through a particular functional network, we considered the difference between its encoding and decoding capacity ($encoding - decoding$). A large difference between encoding and decoding indicates that the memory content of the information traveling from the rest of the brain to an intrinsic network has undergone a significant transformation. If the difference between encoding and decoding is positive ($encoding > decoding$; good encoder), this suggests that the interaction between intrinsic network connectivity and dynamics enhances the memory content of the signal within the network to perform the task at hand. Conversely, a negative

difference between encoding and decoding (*encoding* $<$ *decoding*; good decoder) suggests that the interaction between extrinsic network connectivity and dynamics rather favours the memory content of the signals coming to the network. Summing up, the magnitude of the difference between the encoding and decoding capacity of a network is proportional to the memory content gained or lost by the signal as information propagates through the network. The sign of the difference tells us the direction in which this transformation occurred, in other words, whether the signal gained (positive) or lost (negative) temporal content as it travels from the rest of the brain to a particular functional network.

The concepts of encoding and decoding here proposed are conceptually similar to the *information storage* and *information transfer* proposed by Boedecker and colleagues (Boedecker et al., 2012). These measures directly quantify the amount of information (in bits) that is present in the past state of a single unit and its neighbors, respectively, that is relevant to predicting its future state. Our measures, however, do not quantify information in bits. The encoding and decoding capacities indirectly quantify the amount of information contained in each intrinsic network and its neighbors, respectively, by assessing how well their current state can be used to predict past input states. The topological scale at which these measures are implemented is also different: Boedecker and colleagues implement these measures at the level of individual nodes, whereas we apply these measures at the level of intrinsic networks.

Encoding - decoding: implementation

The selection of the readout nodes in the experimental set up is what ultimately determines the *coding* paradigm. In the encoding set up, readout nodes correspond to the nodes within the network, whereas in the decoding setup, readout nodes correspond to the direct neighbours of the network. In the latter case, because the number of neighbour regions (i.e., directly connected nodes that do not belong to the network) is in all cases higher than the amount of regions within each intrinsic network, these differences should be accounted for when estimating their encoding and decoding capabilities. To do so, we first derived the between-network connectivity profile of every node in the network under examination. Based on these node-level connectivity profiles, we estimated the proportion of connections from every other network (within-network connections were excluded). Next, we randomly draw as many neighbour regions as nodes within the network in such a way that the proportions previously estimated were preserved. The selected nodes were then used as output nodes in the decoding experimental set up. To avoid biases towards

a particular set of output nodes, the same process was repeated 100 times to get a stable estimate of the decoding capacity of every intrinsic network.

It is important to note, however, that the metric here proposed, i.e., the difference between encoding and decoding capacity, assumes that signals propagate in a particular direction. Because MRI-based structural networks do not contain information about the directionality of anatomical projections (Knock et al., 2009; Melozzi et al., 2019), our network model is undirected and thus considers that information travels bidirectionally.

3.6.10 Graph measures

We explored the effects of the interaction between network topology and dynamics on the memory capacity of intrinsic networks. To do so, we correlated local and global network topological attributes with the memory capacity of the brain's intrinsic networks. Local topological attributes included: (1) node strength, (2) clustering coefficient, (3) node-betweenness centrality and (4) participation coefficient. These local features were first estimated at the node level using the weighted adjacency matrix, and then averaged within each intrinsic network. Global topological features included: (1) characteristic path length, (2) transitivity and (3) modularity. Global features were estimated at the network level, and then correlated with the average memory capacity across intrinsic networks. To calculate all graph topological metrics we used a Python version of the Brain Connectivity Toolbox (`https://github.com/aestrivex/bctpy`; (Rubinov and Sporns, 2010)). Definitions of these topological metrics can be found below.

- *Node strength:* in undirected networks, node strength is defined as the sum of the weights of the connections that go from a node to every other node in the network.
- *Clustering coefficient:* the local clustering of a node is the proportion of connections between the nodes within its neighbourhood divided by the total number of possible connections between them (Onnela et al., 2005).
- *Node betweenness centrality:* the betweenness centrality of a node is the fraction of all shortest paths in the network that contain the node. Nodes with a high value of betweeness centrality participate in a large number of shortest paths (Brandes, 2001).
- *Participation coefficient:* the participation coefficient is a measure of the distribution of a node's connections among the communities of the network. If the participation coefficient is 0, the connections of a node are entirely restricted to its community. The closer the participation coefficient is to 1, the more evenly distributed are the

connections of the node among all communities (Guimera and Amaral, 2005). Mathematically, the participation coefficient P of node i is given by:

$$P_i = 1 - \sum_{c=1}^{C} \left(\frac{S_{is}}{S_i} \right)^2 \tag{3.5}$$

where S_{is} corresponds to the sum of the weights of the connections from node i to nodes in community c, S_i is the strength of node i, and C is the total number of communities. This measure requires a previously established community structure as input. Here, we estimated the participation coefficient of individual brain regions using the proposed intrinsic-network partition.

- *Characteristic path length:* the characteristic path length is a measure of efficiency and is defined as the average shortest path length of the network. The distance matrix on which shortest paths are computed must be a connection-length matrix, typically obtained via a mapping from weight to length. Here we used the inverse of the connection-weight matrix as the distance matrix. In this way, strong (weak) connections are naturally interpreted as shorter (longer) distances (Dijkstra et al., 1959; Watts and Strogatz, 1998).

- *Transitivity:* a network's transitivity is the ratio of triangles to triplets (open and closed) in the network. A triplet consists of three nodes that are connected by either two (open) or three (closed) undirected connections (Onnela et al., 2005; Rubinov and Sporns, 2010; Watts and Strogatz, 1998).

- *Modularity:* is a measure that relates the number of within-network connections to all connections in the network; it quantifies the strength of segregation into distinct networks. The higher the modularity, the stronger is the segregation/separation between modules (Good et al., 2010; Leicht and Newman, 2008; Reichardt and Bornholdt, 2006). Mathematically, the modularity Q of a network can be expressed as:

$$Q = \sum_{i=1}^{m} (e_{ii} - a_i^2) \tag{3.6}$$

where e_{ii} is the fraction of all connections that link two nodes within module i, a_i is the fraction of connections that connect a node in module i to any other node, and m is the total number of modules. As with the participation coefficient, this

measure requires a previously established community structure as input. We used the intrinsic-network partition for this purpose.

3.7 Data availability

The source dataset from University of Lausanne is available at https://doi.org/10.5281/zenodo.2872624. To facilitate the reproducibility of this work, the data ready to run the code is publicly available on Zenodo (https://doi.org/10.5281/zenodo.4776453).

3.8 Code availability

All code used for data processing, simulation, analysis, and figure generation is publicly available on GitHub and Zenodo (https://github.com/netneurolab/suarez_neuromorphicnetworks; https://doi.org/10.5281/zenodo.4776829) (Suárez, 2021), and is built on top of the following open-source Python packages: reservoir (https://github.com/estefanysuarez/reservoir; https://doi.org/10.5281/zenodo.4913398), Netneurotools (https://github.com/netneurolab/netneurotools), Numpy (Harris et al., 2020; Oliphant, 2006; Walt et al., 2011), Scipy (Virtanen et al., 2020), Pandas (McKinney et al., 2010), Scikit-learn (Pedregosa et al., 2011), bctpy (https://github.com/aestrivex/bctpy) (Rubinov and Sporns, 2010), NetworkX (Hagberg et al., 2008), Matplotlib (Hunter, 2007), and Seaborn (Waskom et al., 2016).

3.9 Acknowledgements

We thank Ross Markello, Bertha Vazquez-Rodriguez, Golia Shafiei, Vincent Bazinet, Justine Hansen and Zhen-Qi Liu for insightful comments on the manuscript. BM acknowledges support from the Natural Sciences and Engineering Research Council of Canada (NSERC Discovery Grant RGPIN #017-04265), from the Canada Research Chairs Program, from the Canada First Research Excellence Fund, awarded to McGill University for the Healthy Brains for Healthy Lives initiative, and from the Brain Canada Future Leaders Fund. GL acknowledges support from NSERC (Discovery Grant RGPIN-2018-04821), FRQS (Research Scholar Award Junior 1 LAJGU0401-253188), and CIFAR (Canada CIFAR AI Chair). BAR acknowledges support from NSERC (NSERC Discovery Grant RGPIN 2020-05105), Healthy Brains, Healthy Lives (New Investigator Start-up, 2b-NISU-8), and funding from

CIFAR (Learning in Machines and Brains Program, Canada CIFAR AI Chair). ES acknowledges support from the Fonds de Recherche du Québec - Nature et Technologies (FRQNT) Strategic Clusters Program (2020-RS4-265502 - Centre UNIQUE - Union Neurosciences and Artificial Intelligence - Quebec) and the Fonds de Recherche du Québec - Nature et Technologies (FRQNT).

3.10 Author contributions

Conceptualization - LES, GL, BM; Methodology - LES; Formal Analysis - LES; Writing - Original Draft - LES, BM; Writing - Review and Editing - BAR, GL; Funding Acquisition - BM.

3.11 Competing interests

The authors declare no competing interests.

3.12 Bibliography

Aceituno, P. V., G. Yan, and Y.-Y. Liu (2020). "Tailoring Echo State Networks for Optimal Learning". *Iscience*, 23(9), p. 101440.

Alexander-Bloch, A. F. et al. (2018). "On testing for spatial correspondence between maps of human brain structure and function". *Neuroimage*, 178, pp. 540–551.

Alomar, M. L. et al. (2014). "Low-cost hardware implementation of reservoir computers". In: *2014 24th International Workshop on Power and Timing Modeling, Optimization and Simulation (PATMOS)*. IEEE, pp. 1–5.

Antonelo, E. A. and B. Schrauwen (2014). "On learning navigation behaviors for small mobile robots with reservoir computing architectures". *IEEE transactions on neural networks and learning systems*, 26(4), pp. 763–780.

Antonik, P. (2018). *Application of FPGA to Real-Time Machine Learning: Hardware Reservoir Computers and Software Image Processing*. Springer.

Antonik, P. et al. (2015). "FPGA implementation of reservoir computing with online learning". In: *24th Belgian-Dutch Conference on Machine Learning*.

Appeltant, L. et al. (2011). "Information processing using a single dynamical node as complex system". *Nature communications*, 2(1), pp. 1–6.

Bassett, D. S. and O. Sporns (2017). "Network neuroscience". *Nature neuroscience*, 20(3), pp. 353–364.

Bassett, D. S., P. Zurn, and J. I. Gold (2018). "On the nature and use of models in network neuroscience". *Nature Reviews Neuroscience*, 19(9), pp. 566–578.

Bassett, D. S. et al. (2010). "Efficient physical embedding of topologically complex information processing networks in brains and computer circuits". *PLoS Comput Biol*, 6(4), e1000748.

Bassett, D. S. et al. (2011). "Conserved and variable architecture of human white matter connectivity". *Neuroimage*, 54(2), pp. 1262–1279.

Bassett, D. S. and E. Bullmore (2006). "Small-world brain networks". *The neuroscientist*, 12(6), pp. 512–523.

Bellec, P. et al. (2010). "Multi-level bootstrap analysis of stable clusters in resting-state fMRI". *NeuroImage*, 51(3), pp. 1126–1139.

Bennett, C. H., D. Querlioz, and J.-O. Klein (2017). "Spatio-temporal learning with arrays of analog nanosynapses". In: *2017 IEEE/ACM International Symposium on Nanoscale Architectures (NANOARCH)*. IEEE, pp. 125–130.

Bertolero, M. A., B. T. Yeo, and M. D'Esposito (2015). "The modular and integrative functional architecture of the human brain". *Proc Natl Acad Sci USA*, 112(49), E6798–E6807.

Bertolero, M. A. et al. (2018). "A mechanistic model of connector hubs, modularity and cognition". *Nat Hum Behav*, 2(10), pp. 765–777.

Bertschinger, N. and T. Natschläger (2004). "Real-time computation at the edge of chaos in recurrent neural networks". *Neural computation*, 16(7), pp. 1413–1436.

Bettinardi, R. G. et al. (2017). "How structure sculpts function: unveiling the contribution of anatomical connectivity to the brain's spontaneous correlation structure". *Chaos: An Interdisciplinary Journal of Nonlinear Science*, 27(4), p. 047409.

Betzel, R. F. and D. S. Bassett (2018). "Specificity and robustness of long-distance connections in weighted, interareal connectomes". *Proceedings of the National Academy of Sciences*, 115(21), E4880–E4889.

Betzel, R. F. et al. (2016). "Generative models of the human connectome". *NeuroImage*, 124, pp. 1054–1064.

Betzel, R. F. et al. (2017). "The modular organization of human anatomical brain networks: Accounting for the cost of wiring". *Net Neurosci*, 1(1), pp. 42–68.

Betzel, R. F. et al. (2018). "Distance-Dependent Consensus Thresholds for Generating Group-Representative Structural Brain Networks". *Net Neurosci*, 3(2), pp. 475–496.

Boedecker, J. et al. (2012). "Information processing in echo state networks at the edge of chaos". *Theory in Biosciences*, 131(3), pp. 205–213.

Brandes, U. (2001). "A faster algorithm for betweenness centrality". *Journal of mathematical sociology*, 25(2), pp. 163–177.

Breakspear, M. (2017). "Dynamic models of large-scale brain activity". *Nat Neurosci*, 20(3), p. 340.

Bullmore, E. and O. Sporns (2012). "The economy of brain network organization". *Nat Rev Neurosci*, 13(5), p. 336.

Buonomano, D. V. and W. Maass (2009). "State-dependent computations: spatiotemporal processing in cortical networks". *Nature Reviews Neuroscience*, 10(2), p. 113.

Büsing, L., B. Schrauwen, and R. Legenstein (2010). "Connectivity, dynamics, and memory in reservoir computing with binary and analog neurons". *Neural computation*, 22(5), pp. 1272–1311.

Cammoun, L. et al. (2012). "Mapping the human connectome at multiple scales with diffusion spectrum MRI". *J Neurosci Meth*, 203(2), pp. 386–397.

Chen, Z. J. et al. (2008). "Revealing modular architecture of human brain structural networks by using cortical thickness from MRI". *Cerebral cortex*, 18(10), pp. 2374–2381.

Cocchi, L. et al. (2017). "Criticality in the brain: A synthesis of neurobiology, models and cognition". *Progress in neurobiology*, 158, pp. 132–152.

Cole, M. W. et al. (2014). "Intrinsic and task-evoked network architectures of the human brain". *Neuron*, 83(1), pp. 238–251.

Crofts, J. J. and D. J. Higham (2009). "A weighted communicability measure applied to complex brain networks". *J Roy Soc Interface*, 6(33), pp. 411–414.

Crossley, N. A. et al. (2013). "Cognitive relevance of the community structure of the human brain functional coactivation network". *Proceedings of the National Academy of Sciences*, 110(28), pp. 11583–11588.

Daducci, A. et al. (2012). "The connectome mapper: an open-source processing pipeline to map connectomes with MRI". *PLoS ONE*, 7(12), e48121.

Damicelli, F., C. C. Hilgetag, and A. Goulas (2022). "Brain connectivity meets reservoir computing". *PLoS Computational Biology*, 18(11), e1010639.

Damoiseaux, J. et al. (2006). "Consistent resting-state networks across healthy subjects". *Proc Natl Acad Sci USA*, 103(37), pp. 13848–13853.

Deco, G. and V. K. Jirsa (2012). "Ongoing cortical activity at rest: criticality, multistability, and ghost attractors". *Journal of Neuroscience*, 32(10), pp. 3366–3375.

Deco, G. et al. (2009). "Key role of coupling, delay, and noise in resting brain fluctuations". *Proc Natl Acad Sci USA*, 106(25), pp. 10302–10307.

Demirtaş, M. et al. (2019). "Hierarchical heterogeneity across human cortex shapes large-scale neural dynamics". *Neuron*, 101(6), pp. 1181–1194.

Desikan, R. S. et al. (2006). "An automated labeling system for subdividing the human cerebral cortex on MRI scans into gyral based regions of interest". *NeuroImage*, 31(3), pp. 968–980.

Dijkstra, E. W. et al. (1959). "A note on two problems in connexion with graphs". *Numerische mathematik*, 1(1), pp. 269–271.

Dockès, J. et al. (2020). "NeuroQuery, comprehensive meta-analysis of human brain mapping". *eLife*, 9, e53385.

Dohmatob, E., G. Dumas, and D. Bzdok (2020). "Dark control: The default mode network as a reinforcement learning agent". *Hum Brain Mapp*.

Du, C. et al. (2017). "Reservoir computing using dynamic memristors for temporal information processing". *Nature communications*, 8(1), pp. 1–10.

Elman, J. L. (1990). "Finding structure in time". *Cognitive science*, 14(2), pp. 179–211.

— (1991). "Distributed representations, simple recurrent networks, and grammatical structure". *Machine learning*, 7(2), pp. 195–225.

Fox, P. T. and J. L. Lancaster (2002). "Mapping context and content: the BrainMap model". *Nature Reviews Neuroscience*, 3(4), pp. 319–321.

Goñi, J. et al. (2014). "Resting-brain functional connectivity predicted by analytic measures of network communication". *Proc Natl Acad Sci USA*, 111(2), pp. 833–838.

Good, B. H., Y.-A. De Montjoye, and A. Clauset (2010). "Performance of modularity maximization in practical contexts". *Physical Review E*, 81(4), p. 046106.

Goulas, A., F. Damicelli, and C. C. Hilgetag (2021). "Bio-instantiated recurrent neural networks: Integrating neurobiology-based network topology in artificial networks". *Neural Networks*, 142, pp. 608–618.

Graham, D. and D. Rockmore (2011). "The packet switching brain". *J Cogn Neurosci*, 23(2), pp. 267–276.

Guimera, R. and L. A. N. Amaral (2005). "Functional cartography of complex metabolic networks". *nature*, 433(7028), pp. 895–900.

Haeusler, S. and W. Maass (2007). "A statistical analysis of information-processing properties of lamina-specific cortical microcircuit models". *Cerebral cortex*, 17(1), pp. 149–162.

Hagberg, A., P. Swart, and D. S Chult (2008). *Exploring network structure, dynamics, and function using NetworkX*. Tech. rep. Los Alamos National Lab.(LANL), Los Alamos, NM (United States).

Hagmann, P. et al. (2008). "Mapping the structural core of human cerebral cortex". *PLoS Biol*, 6(7), e159.

Haimovici, A. et al. (2013). "Brain organization into resting state networks emerges at criticality on a model of the human connectome". *Physical review letters*, 110(17), p. 178101.

Haldeman, C. and J. M. Beggs (2005). "Critical branching captures activity in living neural networks and maximizes the number of metastable states". *Physical review letters*, 94(5), p. 058101.

Harris, C. R. et al. (2020). "Array programming with NumPy". *Nature*, 585(7825), pp. 357–362.

Heuvel, M. P. Van den, E. T. Bullmore, and O. Sporns (2016). "Comparative connectomics". *Trends Cognitive Science*, 20(5), pp. 345–361.

Heuvel, M. P. van den et al. (2012). "High-cost, high-capacity backbone for global brain communication". *Proc Natl Acad Sci USA*, 109(28), pp. 11372–11377.

Hilgetag, C. C. and M. Kaiser (2004). "Clustered organization of cortical connectivity". *Neuroinformatics*, 2(3), pp. 353–360.

Homma, Y. and M. Hagiwara (2013). "An echo state network with working memories for probabilistic language modeling". In: *International Conference on Artificial Neural Networks*. Springer, pp. 595–602.

Honey, C. J., J.-P. Thivierge, and O. Sporns (2010). "Can structure predict function in the human brain?" *NeuroImage*, 52(3), pp. 766–776.

Honey, C. J. et al. (2007). "Network structure of cerebral cortex shapes functional connectivity on multiple time scales". *Proc Natl Acad Sci USA*, 104(24), pp. 10240–10245.

Hopfield, J. J. (1982). "Neural networks and physical systems with emergent collective computational abilities". *Proceedings of the national academy of sciences*, 79(8), pp. 2554–2558.

Horvát, S. et al. (2016). "Spatial embedding and wiring cost constrain the functional layout of the cortical network of rodents and primates". *PLoS Biol*, 14(7), e1002512.

Huntenburg, J. M., P.-L. Bazin, and D. S. Margulies (2018). "Large-scale gradients in human cortical organization". *Trends in cognitive sciences*, 22(1), pp. 21–31.

Hunter, J. D. (2007). "Matplotlib: A 2D graphics environment". *Computing in science & engineering*, 9(3), pp. 90–95.

Ijspeert, A. J. (2008). "Central pattern generators for locomotion control in animals and robots: a review". *Neural networks*, 21(4), pp. 642–653.

Insel, T. R., S. C. Landis, and F. S. Collins (2013). "The NIH brain initiative". *Science*, 340(6133), pp. 687–688.

Jaeger, H. (2001). "The "echo state" approach to analysing and training recurrent neural networks-with an erratum note". *Bonn, Germany: German National Research Center for Information Technology GMD Technical Report*, 148(34), p. 13.

— (2002). "Short term memory in echo state networks. gmd-report 152". In: *GMD-German National Research Institute for Computer Science (2002), http://www.faculty.jacobs-university.de/hjaeger/pubs/STMEchoStatesTechRep.pdf*. Citeseer.

Jones, D., T. Knösche, and R Turner (2013). "White matter integrity, fiber count, and other fallacies: the do's and don'ts of diffusion MRI". *NeuroImage*, 73, pp. 239–254.

Ju, H. and D. S. Bassett (2020). "Dynamic representations in networked neural systems". *Nat Neurosci*, pp. 1–10.

Kaiser, M. and C. C. Hilgetag (2006). "Nonoptimal component placement, but short processing paths, due to long-distance projections in neural systems". *PLoS Comput Biol*, 2(7), e95.

Katumba, A. et al. (2017). "A multiple-input strategy to efficient integrated photonic reservoir computing". *Cognitive Computation*, 9(3), pp. 307–314.

Katumba, A. et al. (2018). "Low-loss photonic reservoir computing with multimode photonic integrated circuits". *Scientific reports*, 8(1), pp. 1–10.

Kendall, J. D., J. C. Nino, and L. E. Suárez (2018). *Deep learning in bipartite memristive networks*. US Patent App. 15/985,212.

Kitzbichler, M. G. et al. (2009). "Broadband criticality of human brain network synchronization". *PLoS Comput Biol*, 5(3), e1000314.

Knock, S. et al. (2009). "The effects of physiologically plausible connectivity structure on local and global dynamics in large scale brain models". *J Neurosci Meth*, 183(1), pp. 86–94.

Kulkarni, M. S. and C. Teuscher (2012). "Memristor-based reservoir computing". In: *2012 IEEE/ACM international symposium on nanoscale architectures (NANOARCH)*. IEEE, pp. 226–232.

Langton, C. (1990). "Computation at the edge of chaos: Phase transition and emergent computation". *Physica D: nonlinear phenomena*, 42, pp. 12–37.

Laporte, F. et al. (2018). "Numerical demonstration of neuromorphic computing with photonic crystal cavities". *Optics express*, 26(7), pp. 7955–7964.

Legenstein, R. and W. Maass (2007a). "Edge of chaos and prediction of computational performance for neural circuit models". *Neural Networks*, 20(3), pp. 323–334.

— (2007b). "What makes a dynamical system computationally powerful". *New directions in statistical signal processing: From systems to brain*, pp. 127–154.

Leicht, E. A. and M. E. Newman (2008). "Community structure in directed networks". *Physical review letters*, 100(11), p. 118703.

Li, J. et al. (2018). "A deep learning based approach for analog hardware implementation of delayed feedback reservoir computing system". In: *2018 19th International Symposium on Quality Electronic Design (ISQED)*. IEEE, pp. 308–313.

Li, J. and H. Jaeger (2011). "Minimal Energy Control of an ESN Pattern Generator". In:

Liu, Z.-Q., Y.-Q. Zheng, and B. Misic (2020). "Network topology of the marmoset connectome". *Network Neurosci*, (-), pp. 1–26.

Lukoševičius, M. and H. Jaeger (2009). "Reservoir computing approaches to recurrent neural network training". *Computer Science Review*, 3(3), pp. 127–149.

Maass, W. and H. Markram (2004). "On the computational power of circuits of spiking neurons". *Journal of computer and system sciences*, 69(4), pp. 593–616.

Maass, W., T. Natschläger, and H. Markram (2002). "Real-time computing without stable states: A new framework for neural computation based on perturbations". *Neural computation*, 14(11), pp. 2531–2560.

Maier-Hein, K. H. et al. (2017). "The challenge of mapping the human connectome based on diffusion tractography". *Nat Commun*, 8(1), p. 1349.

Margulies, D. S. et al. (2016). "Situating the default-mode network along a principal gradient of macroscale cortical organization". *Proceedings of the National Academy of Sciences*, 113(44), pp. 12574–12579.

Markello, R. D. and B. Misic (2021). "Comparing spatial null models for brain maps". *NeuroImage*, p. 118052.

Maslov, S. and K. Sneppen (2002). "Specificity and stability in topology of protein networks". *Science*, 296(5569), pp. 910–913.

Mastrogiuseppe, F. and S. Ostojic (2018). "Linking connectivity, dynamics, and computations in low-rank recurrent neural networks". *Neuron*, 99(3), pp. 609–623.

McKinney, W. et al. (2010). "Data structures for statistical computing in python". In: *Proceedings of the 9th Python in Science Conference*. Vol. 445. Austin, TX, pp. 51–56.

Medaglia, J. D. et al. (2018). "Functional alignment with anatomical networks is associated with cognitive flexibility". *Nat Hum Behav*, 2(2), p. 156.

Melozzi, F. et al. (2019). "Individual structural features constrain the functional connectome". *Proc Natl Acad Sci USA*, 116, pp. 26961–26969.

Messé, A. et al. (2014). "Relating structure and function in the human brain: relative contributions of anatomy, stationary dynamics, and non-stationarities". *PLoS Comput Biol*, 10(3), e1003530.

Mesulam, M (1994). "Neurocognitive networks and selectively distributed processing." *Revue neurologique*.

Mesulam, M.-M. (1998). "From sensation to cognition." *Brain*, 121(6), pp. 1013–1052.

Mišić, B. and O. Sporns (2016). "From regions to connections and networks: new bridges between brain and behavior". *Curr Opin Neurobiol*, 40, pp. 1–7.

Mišić, B. et al. (2015). "Cooperative and competitive spreading dynamics on the human connectome". *Neuron*, 86(6), pp. 1518–1529.

Mišić, B. et al. (2016). "Network-level structure-function relationships in human neocortex". *Cerebral Cortex*, 26(7), pp. 3285–3296.

Neves, G., S. F. Cooke, and T. V. Bliss (2008). "Synaptic plasticity, memory and the hippocampus: a neural network approach to causality". *Nature Reviews Neuroscience*, 9(1), pp. 65–75.

Oliphant, T. E. (2006). *A guide to NumPy*. Vol. 1. Trelgol Publishing USA.

Onnela, J.-P. et al. (2005). "Intensity and coherence of motifs in weighted complex networks". *Physical Review E*, 71(6), p. 065103.

Pascanu, R. and H. Jaeger (2011). "A neurodynamical model for working memory". *Neural networks*, 24(2), pp. 199–207.

Pedregosa, F. et al. (2011). "Scikit-learn: Machine learning in Python". *Journal of machine Learning research*, 12, pp. 2825–2830.

Petre, P. and J. Cruz-Albrecht (2016). "Neuromorphic mixed-signal circuitry for Asynchronous Pulse Processing". In: *2016 IEEE International Conference on Rebooting Computing (ICRC)*. IEEE, pp. 1–4.

Poldrack, R. A. and T. Yarkoni (2016). "From brain maps to cognitive ontologies: Informatics and the search for mental structure". *Annual Review of Psychology*, 67, pp. 587–612.

Polepalli, A., N. Soures, and D. Kudithipudi (2016). "Digital neuromorphic design of a liquid state machine for real-time processing". In: *2016 IEEE International Conference on Rebooting Computing (ICRC)*. IEEE, pp. 1–8.

Power, J. D. et al. (2011). "Functional network organization of the human brain". *Neuron*, 72(4), pp. 665–678.

Reichardt, J. and S. Bornholdt (2006). "When are networks truly modular?" *Physica D: Nonlinear Phenomena*, 224(1-2), pp. 20–26.

Reus, M. A. de and M. P. van den Heuvel (2013). "Estimating false positives and negatives in brain networks". *NeuroImage*, 70, pp. 402–409.

Richards, B. A. et al. (2019). "A deep learning framework for neuroscience". *Nat Neurosci*, 22(11), pp. 1761–1770.

Roberts, J. A. et al. (2016). "The contribution of geometry to the human connectome". *NeuroImage*, 124, pp. 379–393.

Roberts, J. A. et al. (2017). "Consistency-based thresholding of the human connectome". *NeuroImage*, 145, pp. 118–129.

Rodriguez, N., E. Izquierdo, and Y.-Y. Ahn (2019). "Optimal modularity and memory capacity of neural reservoirs". *Network Neuroscience*, 3(2), pp. 551–566.

Roy, S., A. Banerjee, and A. Basu (2014). "Liquid state machine with dendritically enhanced readout for low-power, neuromorphic VLSI implementations". *IEEE transactions on biomedical circuits and systems*, 8(5), pp. 681–695.

Rubinov, M. and O. Sporns (2010). "Complex network measures of brain connectivity: uses and interpretations". *Neuroimage*, 52(3), pp. 1059–1069.

Salmen, M. and P. G. Ploger (2005). "Echo state networks used for motor control". In: *Proceedings of the 2005 IEEE international conference on robotics and automation*. IEEE, pp. 1953–1958.

Sanz-Leon, P. et al. (2015). "Mathematical framework for large-scale brain network modeling in The Virtual Brain". *NeuroImage*, 111, pp. 385–430.

Schaefer, A. et al. (2018). "Local-global parcellation of the human cerebral cortex from intrinsic functional connectivity MRI". *Cereb Cortex*, 28(9), pp. 3095–3114.

Scoville, W. B. and B. Milner (1957). "Loss of recent memory after bilateral hippocampal lesions". *Journal of neurology, neurosurgery, and psychiatry*, 20(1), p. 11.

Seguin, C., Y. Tian, and A. Zalesky (2020). "Network communication models improve the behavioral and functional predictive utility of the human structural connectome". *Network Neuroscience*, (X), pp. 1–40.

Seung, H. S. (1996). "How the brain keeps the eyes still". *Proceedings of the National Academy of Sciences*, 93(23), pp. 13339–13344.

Shafiei, G. et al. (2020). "Topographic gradients of intrinsic dynamics across neocortex". *bioRxiv*.

Shen, K. et al. (2012). "Information processing architecture of functionally defined clusters in the macaque cortex". *J Neurosci*, 32(48), pp. 17465–17476.

Sherman, S. M. and R. Guillery (2002). "The role of the thalamus in the flow of information to the cortex". *Philosophical Transactions of the Royal Society of London. Series B: Biological Sciences*, 357(1428), pp. 1695–1708.

Shew, W. L. et al. (2009). "Neuronal avalanches imply maximum dynamic range in cortical networks at criticality". *Journal of neuroscience*, 29(49), pp. 15595–15600.

Shine, J. M. et al. (2018). "The modulation of neural gain facilitates a transition between functional segregation and integration in the brain". *eLife*, 7, e31130.

Shine, J. M. et al. (2020). "Topological Augmentation of Latent Information Streams in Feed-Forward Neural Networks". *bioRxiv*.

Sillin, H. O. et al. (2013). "A theoretical and experimental study of neuromorphic atomic switch networks for reservoir computing". *Nanotechnology*, 24(38), p. 384004.

Sizemore, A. E. et al. (2018). "Cliques and cavities in the human connectome". *Journal of computational neuroscience*, 44(1), pp. 115–145.

Skowronski, M. D. and J. G. Harris (2007). "Automatic speech recognition using a predictive echo state network classifier". *Neural networks*, 20(3), pp. 414–423.

Smith, S. M. et al. (2009). "Correspondence of the brain's functional architecture during activation and rest". *Proc Natl Acad Sci USA*, 106(31), pp. 13040–13045.

Soriano, M. C. et al. (2014). "Delay-based reservoir computing: noise effects in a combined analog and digital implementation". *IEEE transactions on neural networks and learning systems*, 26(2), pp. 388–393.

Sporns, O. (2013). "Network attributes for segregation and integration in the human brain". *Current opinion in neurobiology*, 23(2), pp. 162–171.

Sporns, O., C. J. Honey, and R. Kötter (2007). "Identification and classification of hubs in brain networks". *PloS one*, 2(10), e1049.

Sporns, O. and R. Kötter (2004). "Motifs in brain networks". *PLoS Biol*, 2(11), e369.

Sporns, O., G. Tononi, and R. Kötter (2005). "The human connectome: a structural description of the human brain". *PLoS Comput Biol*, 1(4), e42.

Sporns, O. and J. D. Zwi (2004). "The small world of the cerebral cortex". *Neuroinformatics*, 2(2), pp. 145–162.

Sporns, O. et al. (2004). "Organization, development and function of complex brain networks". *Trends in cognitive sciences*, 8(9), pp. 418–425.

Stiso, J. and D. S. Bassett (2018). "Spatial embedding imposes constraints on neuronal network architectures". *Trends in cognitive sciences*, 22(12), pp. 1127–1142.

Strock, A., N. P. Rougier, and X. Hinaut (2018). "A simple reservoir model of working memory with real values". In: *2018 International Joint Conference on Neural Networks (IJCNN)*. IEEE, pp. 1–8.

Suárez, L. E. (2021). *Code for: Learning function from structure in neuromorphic networks*. Version 0.0.1-alpha.

Suárez, L. E., J. D. Kendall, and J. C. Nino (2018). "Evaluation of the computational capabilities of a memristive random network (MN3) under the context of reservoir computing". *Neural Networks*, 106, pp. 223–236.

Suárez, L. E. et al. (2020). "Linking structure and function in macroscale brain networks". *Trends in Cognitive Sciences*, 24(4), pp. 302–315.

Sussillo, D. and L. F. Abbott (2009). "Generating coherent patterns of activity from chaotic neural networks". *Neuron*, 63(4), pp. 544–557.

Tagliazucchi, E. et al. (2012). "Criticality in large-scale brain fMRI dynamics unveiled by a novel point process analysis". *Frontiers in physiology*, 3, p. 15.

Tanaka, G. et al. (2019). "Recent advances in physical reservoir computing: A review". *Neural Networks*, 115, pp. 100–123.

Taylor, P et al. (2015). "The global landscape of cognition: hierarchical aggregation as an organizational principle of human cortical networks and functions". *Scientific reports*, 5(1), pp. 1–18.

Thomas, C. et al. (2014). "Anatomical accuracy of brain connections derived from diffusion MRI tractography is inherently limited". *Proc Natl Acad Sci USA*, 111(46), pp. 16574–16579.

Thomas Yeo, B. et al. (2011). "The organization of the human cerebral cortex estimated by intrinsic functional connectivity". *J Neurophysiol*, 106(3), pp. 1125–1165.

Tong, M. H. et al. (2007). "Learning grammatical structure with echo state networks". *Neural networks*, 20(3), pp. 424–432.

Towlson, E. K. et al. (2013). "The rich club of the C. elegans neuronal connectome". *J Neurosci*, 33(15), pp. 6380–6387.

Uddin, L. Q. (2020). "Bring the noise: Reconceptualizing spontaneous neural activity". *Trends Cogn Sci*.

Uddin, L. Q., B. T. Yeo, and R. N. Spreng (2019). "Towards a universal taxonomy of macro-scale functional human brain networks". *Brain topography*, pp. 1–17.

Vandoorne, K. et al. (2008). "Toward optical signal processing using photonic reservoir computing". *Optics express*, 16(15), pp. 11182–11192.

Vandoorne, K. et al. (2014). "Experimental demonstration of reservoir computing on a silicon photonics chip". *Nature communications*, 5(1), pp. 1–6.

Vázquez-Rodríguez, B. et al. (2017). "Stochastic resonance at criticality in a network model of the human cortex". *Scientific reports*, 7(1), pp. 1–12.

Verstraeten, D., B. Schrauwen, and D. Stroobandt (2006). "Reservoir-based techniques for speech recognition". In: *The 2006 IEEE International Joint Conference on Neural Network Proceedings*. IEEE, pp. 1050–1053.

Verstraeten, D. et al. (2005). "Isolated word recognition with the liquid state machine: a case study". *Information Processing Letters*, 95(6), pp. 521–528.

Virtanen, P. et al. (2020). "SciPy 1.0: fundamental algorithms for scientific computing in Python". *Nature methods*, 17(3), pp. 261–272.

Walt, S. v. d., S. C. Colbert, and G. Varoquaux (2011). "The NumPy array: a structure for efficient numerical computation". *Computing in science & engineering*, 13(2), pp. 22–30.

Wang, P. et al. (2019). "Inversion of a large-scale circuit model reveals a cortical hierarchy in the dynamic resting human brain". *Sci Adv*, 5(1), eaat7854.

Wang, Q. et al. (2017). "Energy efficient parallel neuromorphic architectures with approximate arithmetic on FPGA". *Neurocomputing*, 221, pp. 146–158.

Waskom, M. et al. (2016). "seaborn: v0. 7.0 (January 2016)". *zenodo10*, 5281.

Watts, D. J. and S. H. Strogatz (1998). "Collective dynamics of small-world networks". *Nature*, 393(6684), p. 440.

Wig, G. S. (2017). "Segregated systems of human brain networks". *Trends in cognitive sciences*, 21(12), pp. 981–996.

Wills, T. J. et al. (2005). "Attractor dynamics in the hippocampal representation of the local environment". *Science*, 308(5723), pp. 873–876.

Yang, X., W. Chen, and F. Z. Wang (2016). "Investigations of the staircase memristor model and applications of memristor-based local connections". *Analog Integrated Circuits and Signal Processing*, 87(2), pp. 263–273.

Yarkoni, T. et al. (2011). "Large-scale automated synthesis of human functional neuroimaging data". *Nature Methods*, 8(8), p. 665.

Zalesky, A. et al. (2016). "Connectome sensitivity or specificity: which is more important?" *NeuroImage*, 142, pp. 407–420.

Zamora-López, G., C. Zhou, and J. Kurths (2010). "Cortical hubs form a module for multisensory integration on top of the hierarchy of cortical networks". *Front Neuroinform*, 4, p. 1.

Zhang, H. et al. (2014). "Integrated photonic reservoir computing based on hierarchical time-multiplexing structure". *Optics express*, 22(25), pp. 31356–31370.

Zhao, C. et al. (2016). "Novel spike based reservoir node design with high performance spike delay loop". In: *Proceedings of the 3rd ACM International Conference on Nanoscale Computing and Communication*, pp. 1–5.

Zylberberg, J. and B. W. Strowbridge (2017). "Mechanisms of persistent activity in cortical circuits: possible neural substrates for working memory". *Annual review of neuroscience*, 40.

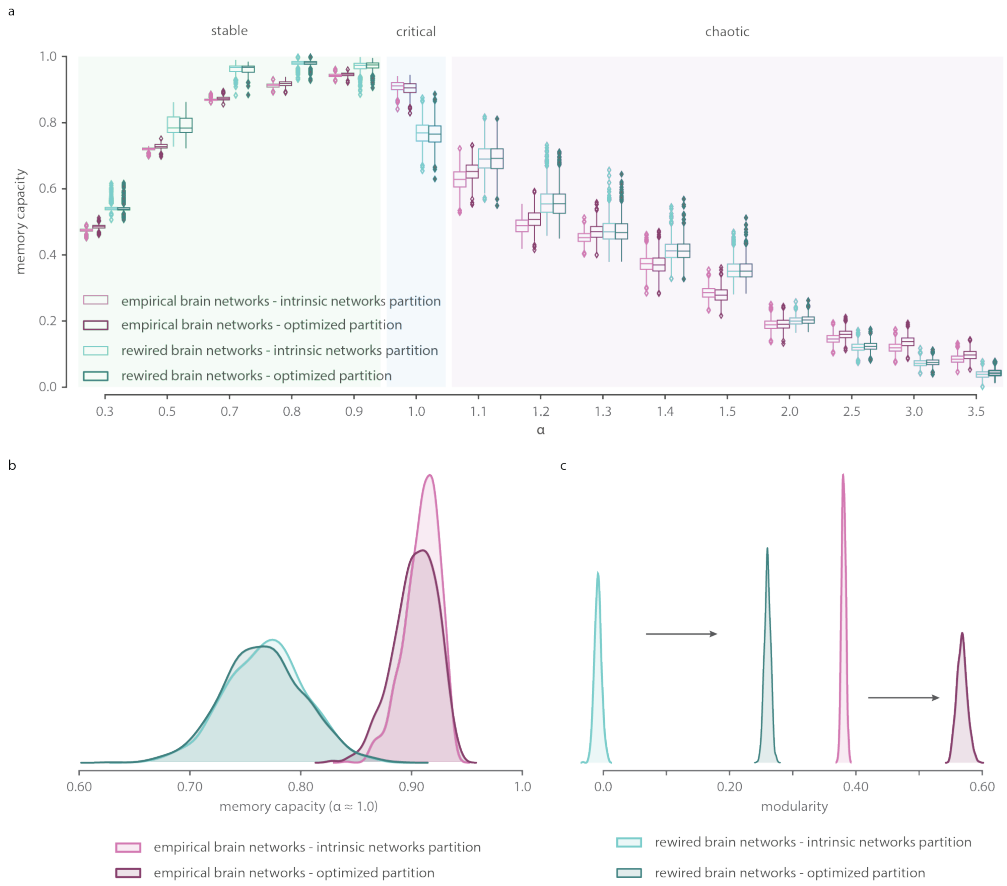

Figure S3.1: **Effect of the modular structure captured by the readout nodes** | To test whether the modular structure imposed by the selection of the readout nodes contributes to greater memory capacity, we applied the Louvain community detection algorithm on the empirical and the rewired networks, and used this optimized partition to select a new set of readout nodes (optimized partition). To make the partitions comparable, the intrinsic network partition was provided as the initial community affiliation vector parameter. (a) Comparison between the memory capacity of empirical and rewired networks using the optimized and the intrinsic network partitions for the selection of the readout nodes. When all α values are considered, the optimized modular structure of the readout nodes does not significantly impact the memory capacity of the rewired networks compared to when the intrinsic network partition is used, suggesting that the selection of readout nodes based on a partition that maximizes the modularity score is not a determining factor for the memory capacity of these networks. (b) At the critical point, the optimized partition does not translate into greater performance for the rewired networks compared to the empirical ones (Wilcoxon-Mann-Whitney two-sample rank-sum test: medians in empirical and rewired networks (using the optimized partition) are 0.90 and 0.76, respectively, $P = 0.0$ two-tailed, and common-language effect size = 99%). Furthermore, the fact that the optimized partition lowers the performance of empirical networks relative to the intrinsic network partition emphasizes the computational role of intrinsic networks (Wilcoxon-Mann-Whitney two-sample rank-sum test: medians in empirical networks using the intrinsic network and the optimized partition are 0.91 and 0.90, respectively, $P < 10^{-4}$ two-tailed, and common-language effect size = 59%). (c) Comparison of the modularity scores derived from the optimized and the intrinsic network partitions for the empirical and the rewired networks. There is a significant improvement in the modularity of both the empirical and the rewired networks. To quantify how different the partitions are, we calculated the mean normalized mutual information score (averaged across samples) between the intrinsic network partition and the optimized partition. We obtained scores of 0.563 ± 0.016 and 0.099 ± 0.007 for the empirical and the rewired brain networks, respectively. A normalized mutual information score close to 1.0 (0.0) means that the partitions are very similar (different). [Note: for the community detection, we used the *community_louvain* algorithm of the Brain Connectivity Toolbox - bctpy: https://github.com/aestrivex/bctpy].

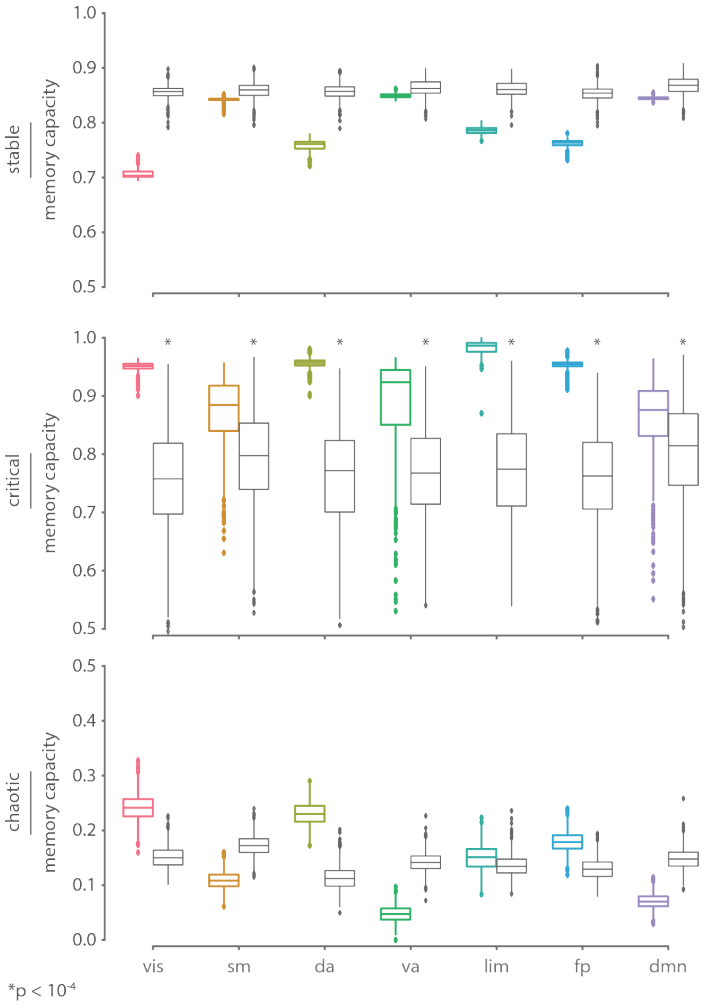

Figure S3.2: **Effect of the internal connectivity structure of the readout nodes** | To test whether the memory capacity of intrinsic networks is driven by their internal connectivity structure, a new family of rewired nulls, one per intrinsic network, was constructed. In this null model, all the connections are allowed to be rewired except those within a particular intrinsic network, thus preserving the internal connectivity structure of intrinsic networks while destroying the topology of the rest of the network. (a) Comparison of the memory capacity of empirical and rewired networks, for each intrinsic network separately, stratified by dynamical regime. For brevity, only the mean memory capacity (averaged across α values) within each dynamical regime is shown, but conclusions are the same if memory capacity is considered at each α value for the stable and the chaotic regimes; at the critical point only $\alpha \approx 1$ is considered. Importantly, at criticality, empirical intrinsic networks perform significantly better than their rewired counterparts. This suggests that the memory capacity of intrinsic networks is not uniquely driven by their internal connectivity patterns, but rather emerges as a result of the interaction of the network with the other networks, orchestrated by the global network topology of the connectome. Overall, these results emphasize the importance of considering the higher-order, between-network interactions that take place thanks to the embedding of a particular intrinsic network in the connectome for the identification of the structural features that enhance its memory capacity. Finally, these results are consistent with the idea that cognition is supported by the continuous interaction of functionally specialized modules in the brain.

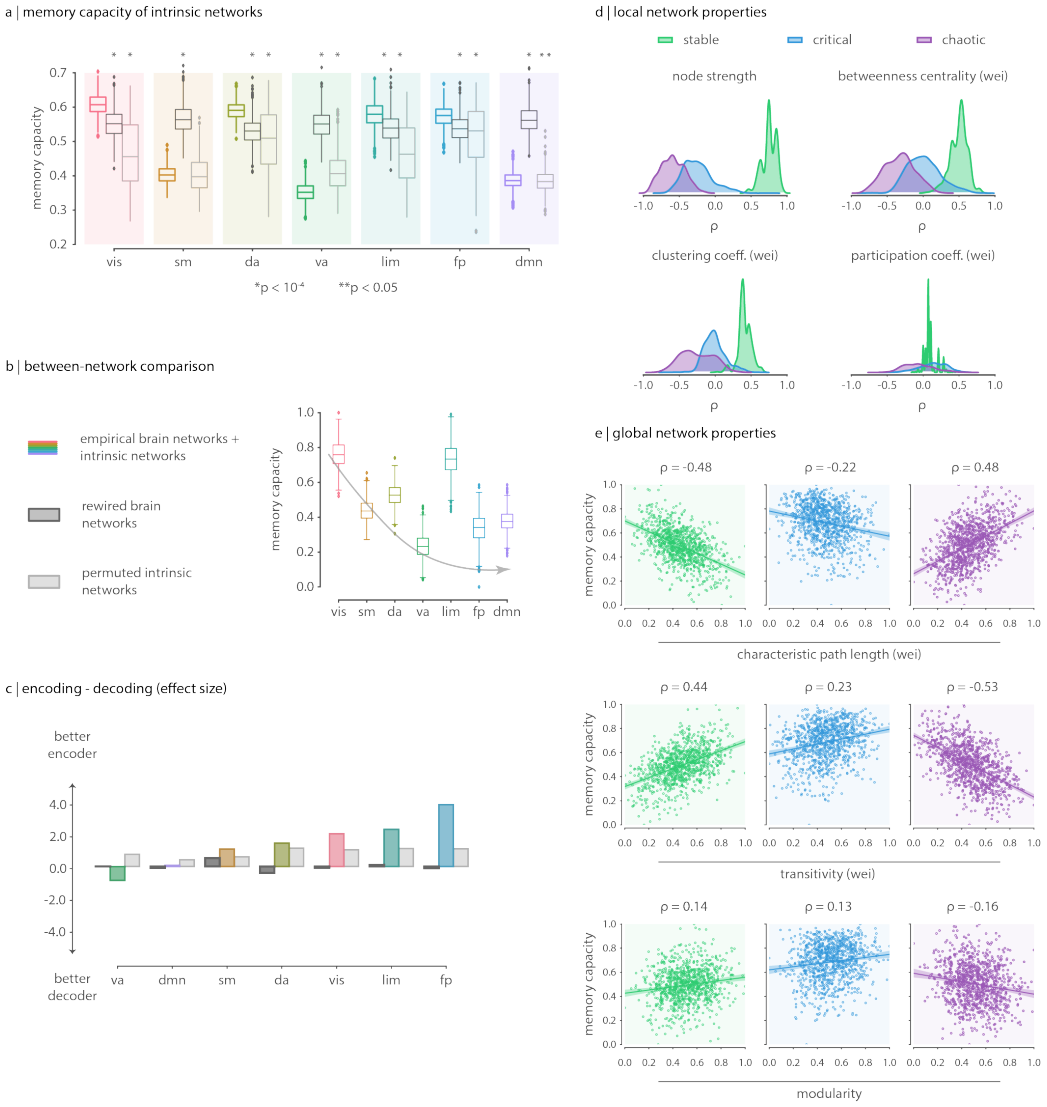

Figure S3.3: **A chaotic state closer to critical dynamics** | Results in the chaotic regime were replicated for alpha values in the range $\alpha = [1.1, 1.2, 1.3, 1.4, 1.5]$. (a) Memory capacity of intrinsic networks compared to the rewired and label-permutation models. (b) Between network comparison of memory capacity estimates after the removal (through linear regression) of relative connection density effects. (c) Difference between encoding and decoding of intrinsic networks. Relationship between memory capacity and (e) local and (f) global network properties.

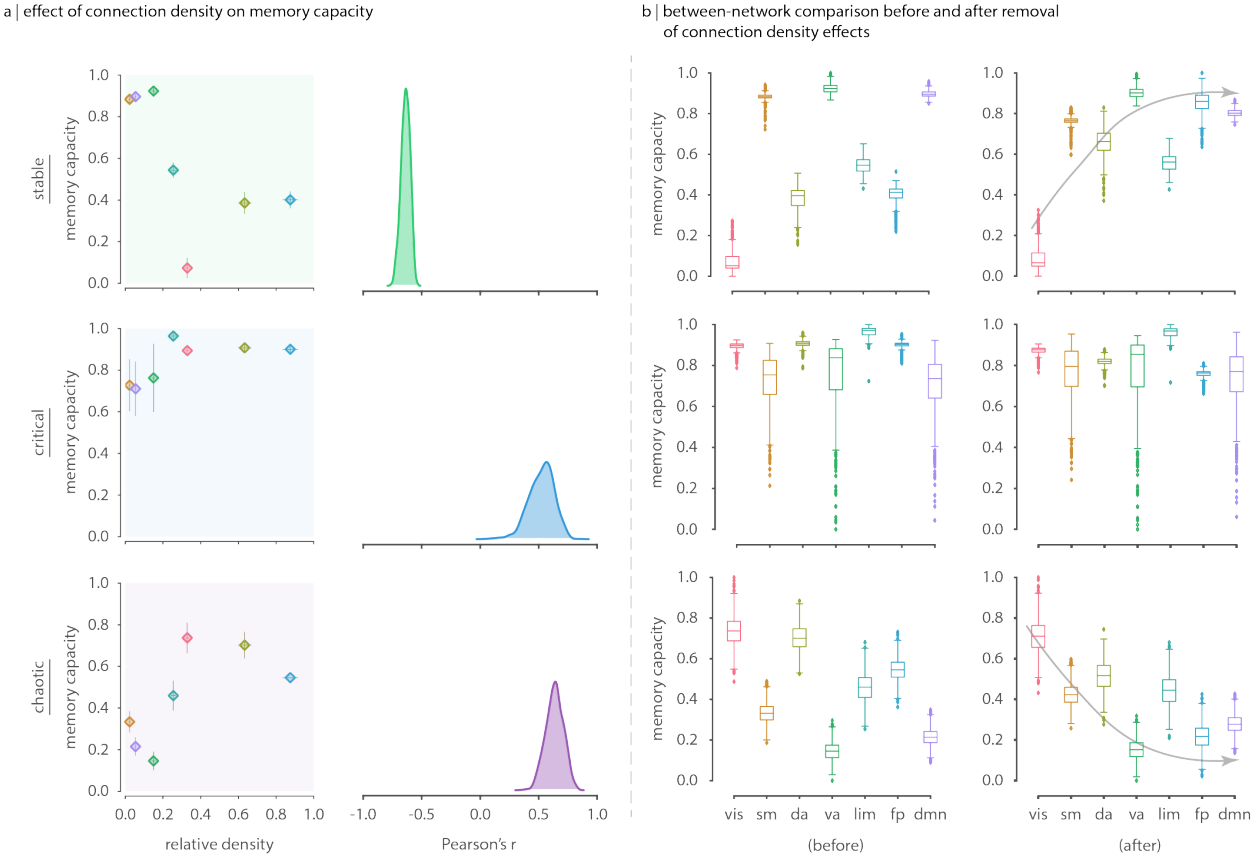

Figure S3.4: **Effect of relative density on the memory capacity of intrinsic networks** | The relative density of an intrinsic network is defined as the ration of the number of internal connections to the total number of possible connections within the intrinsic network. (a) The left column shows the relationship between memory capacity and relative density across dynamical regimes (markers represent the mean values across samples and error bars correspond to their standard deviation). The right column shows the distribution (across samples) of the Pearson's correlation between the memory capacity of intrinsic networks and their relative density. (b) Memory capacity of intrinsic networks before (left column) and after (right column) removing the effects of relative density. Given the high average values of the Pearson's correlation between memory capacity and relative density, relative density effects were regressed out using a linear model.

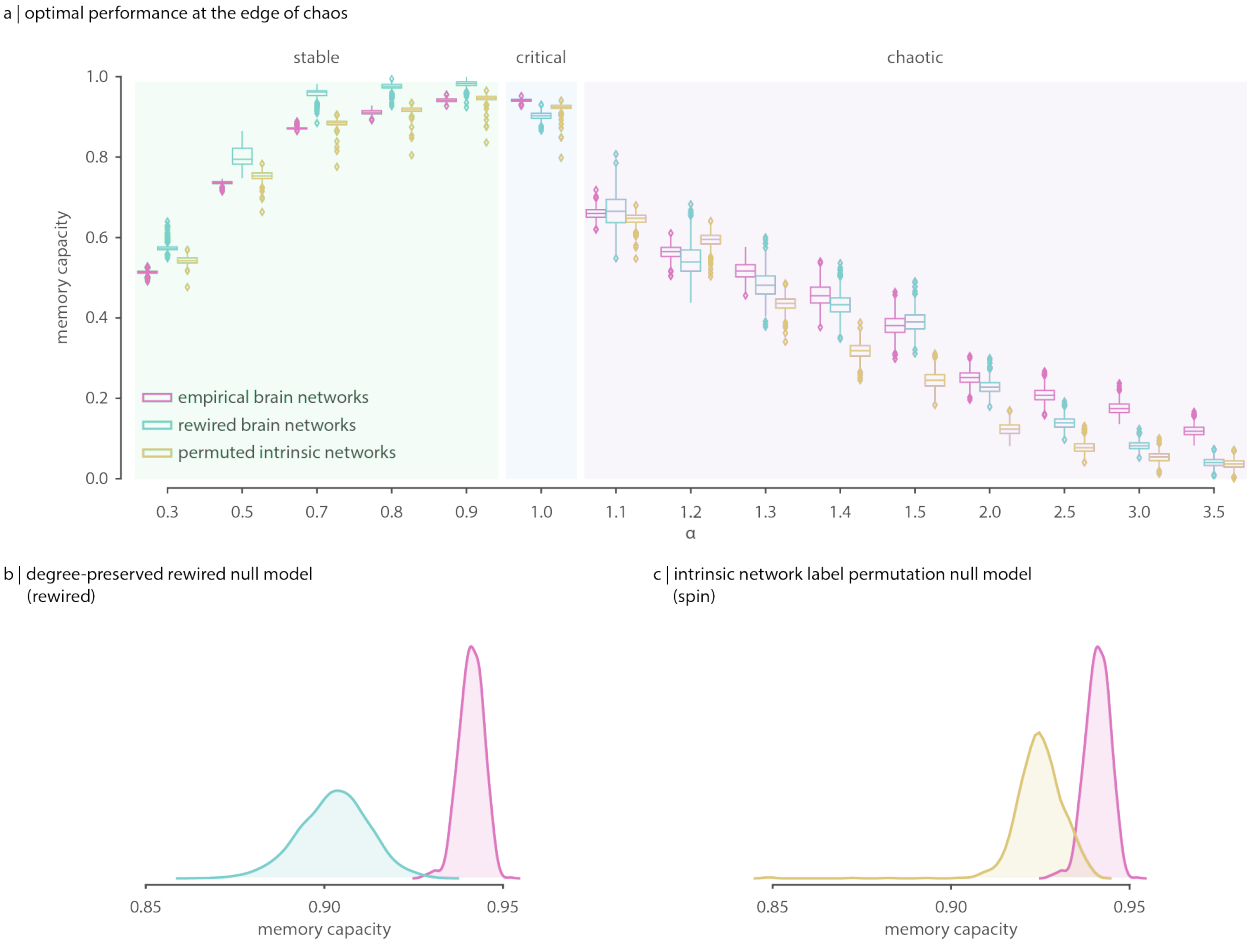

Figure S3.5: **Memory capacity of the human connectome - replication using thalamic input nodes** | Analyses were replicated considering thalamic subcortical regions as input nodes. (a) Distribution (across samples) of the memory capacity of the human connectome (magenta) as a function of the dynamics. Similar to the experimental set up where all subcortical regions are used as input nodes (Fig. 1), the estimated memory capacity of the human connectome is maximum and optimal at the critical point ($\alpha \approx 1$). (b) Distribution of the memory capacity of the empirical network (magenta; median = 0.94) vs. the rewired network model (cyan; median = 0.90, $P_{rewired} = 0.0$ and common-language effect size = 99% two-tailed, Wilcoxon-Mann-Whitney two-sample rank-sum test) at the critical state. (c) Distribution of the memory capacity of the empirical network (magenta) vs. the label-permutation model (yellow; median = 0.92, $P_{spin} = 0.0$ and common-language effect size = 99% two-tailed, Wilcoxon-Mann-Whitney two-sample rank-sum test) at the critical state.

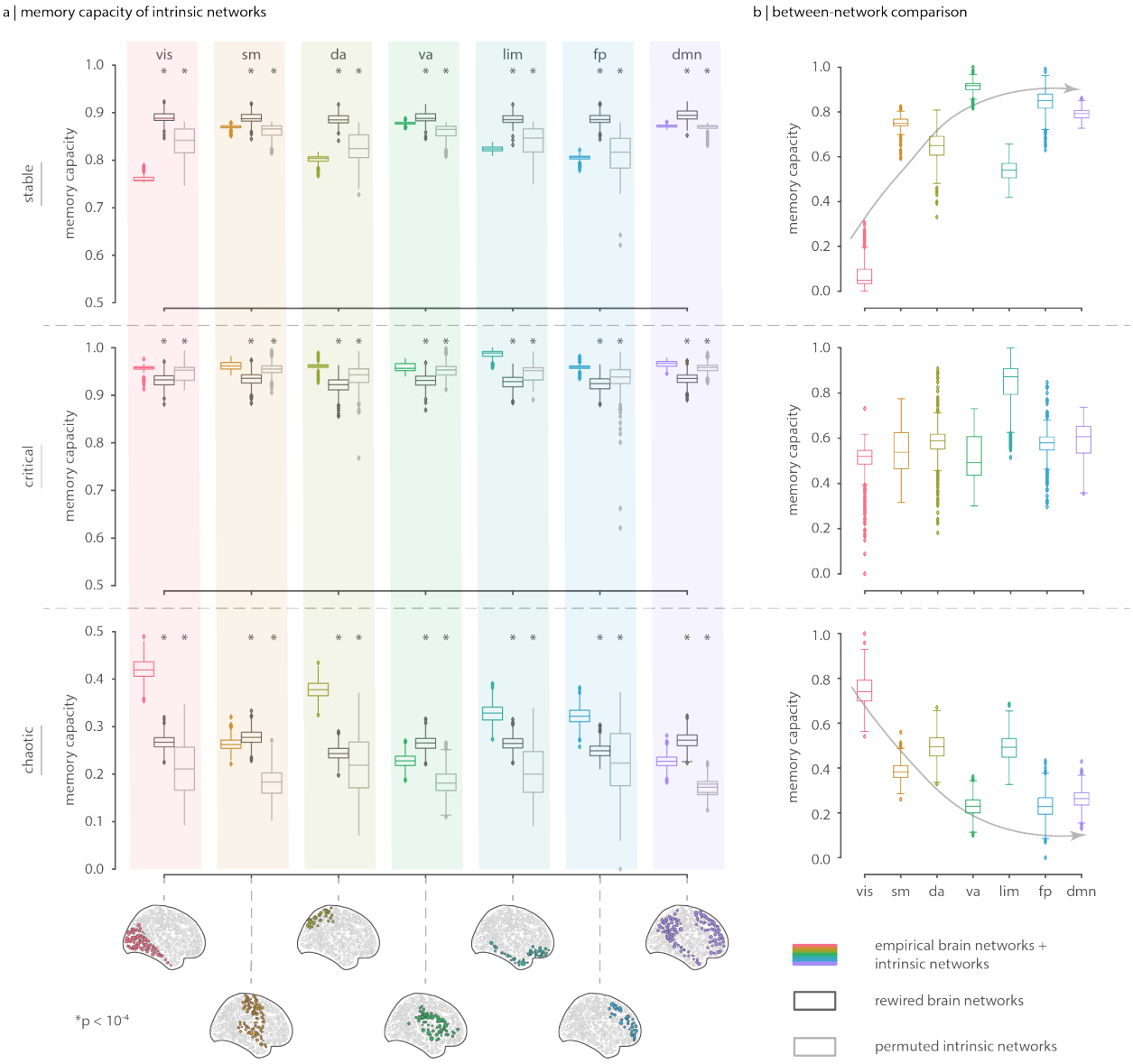

Figure S3.6: **Memory capacity of intrinsic networks - replication using thalamic input nodes** | Analyses were replicated considering thalamic subcortical regions as input nodes. (a) Memory capacity of intrinsic networks across dynamical regimes. At the critical state, memory capacity estimates on the empirical network are consistently and significantly higher and optimal across functional systems, compared to the rewired and spatially-constrained null models. (b) Comparison across intrinsic networks, after linearly regressing out the effect of relative connection density on memory capacity estimates. When compared to each other, memory capacity is in general quite homogeneous across functional systems in the critical regime, except for the limbic system, for which memory capacity is the highest, maybe reflecting an anatomically-mediated predisposition for memory encoding. In the stable and chaotic regimes, on the other hand, the axis along which memory capacity estimates fluctuate broadly resembles the unimodal-transmodal hierarchy, differentiating again somatosensory from higher-order association areas.

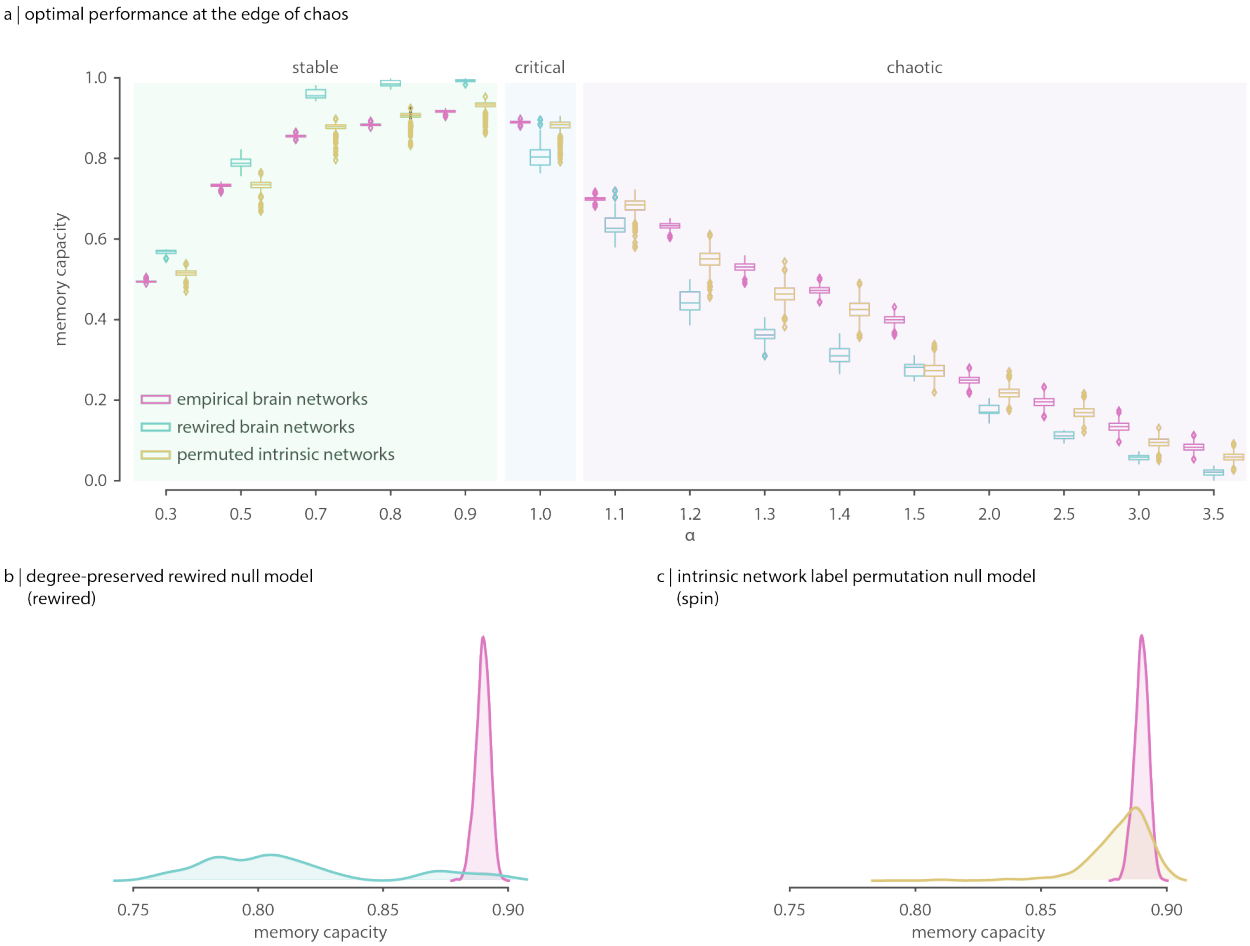

Figure S3.7: **Memory capacity of the human connectome - replication using a coarser parcellation** | Analyses were replicated using a lower resolution parcellation with 448 cortical and 15 subcortical regions. (a) Distribution (across samples) of the memory capacity of the human connectome (magenta) as a function of the dynamics. Similar to the high-resolution network, the estimated memory capacity of the human connectome is maximum and optimal at the critical point ($\alpha \approx 1$). (b) Distribution of the memory capacity of the empirical network (magenta; median = 0.89) vs. the rewired network model (cyan; median = 0.80, $P_{rewired} = 10^{-4}$ and common-language effect size = 95% two-tailed, Wilcoxon-Mann-Whitney two-sample rank-sum test) at the critical state. (c) Distribution of the memory capacity of the empirical network (magenta) vs. the label-permutation model (yellow; median = 0.88, $P_{spin} = 10^{-4}$ and common-language effect size = 75% two-tailed, Wilcoxon-Mann-Whitney two-sample rank-sum test) at the critical state.

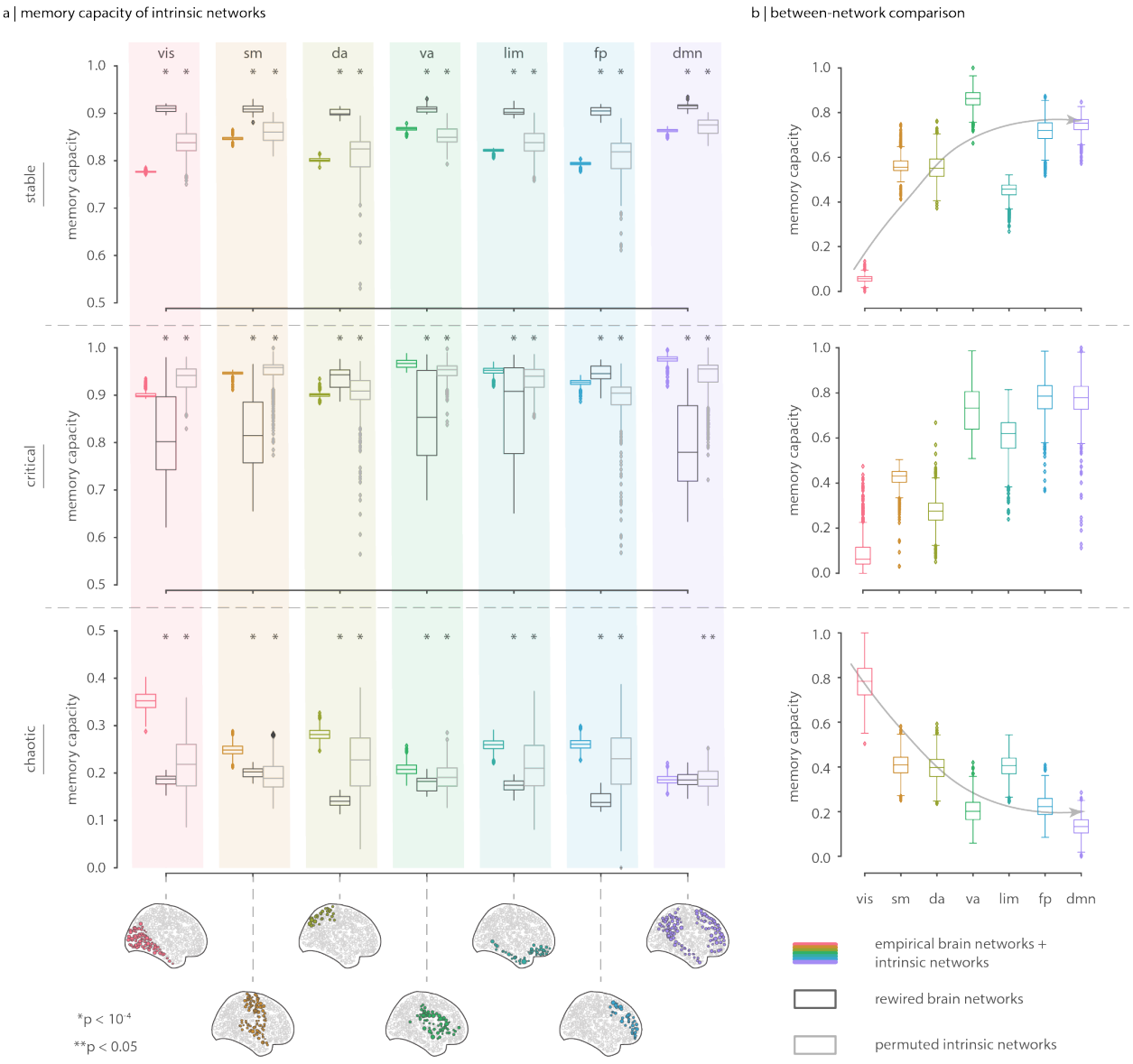

Figure S3.8: **Memory capacity of intrinsic networks - replication using a coarser parcellation** | Analyses were replicated using a lower resolution parcellation (448 cortical and 15 subcortical regions). (a) Memory capacity of intrinsic networks across dynamical regimes. In contrast to the high resolution network, at the critical state, memory capacity estimates on the empirical network are significantly different but not consistently higher across all functional systems, compared to the rewired and the spatially-constrained label permutation models. (b) Comparison across intrinsic networks, after linearly regressing out the effect of relative connection density on memory capacity estimates. At the critical state, contrary to what occurs in the high resolution network (in which there are small differences in memory capacity across functional systems), there is a higher differentiation across intrinsic networks' memory capacity, and a more prominent difference between lower somatosensory and higher association areas. The same type of differentiation is present in the stable and chaotic regimes, but in opposing directions with respect to each other. In the stable regime, memory capacity estimates follow the same trend observed in the critical state, in which somatosensory areas are on average lower compared to higher association areas. The opposite is observed in the chaotic regime: lower somatosensory areas present on average higher memory capacity compared to higher association areas.

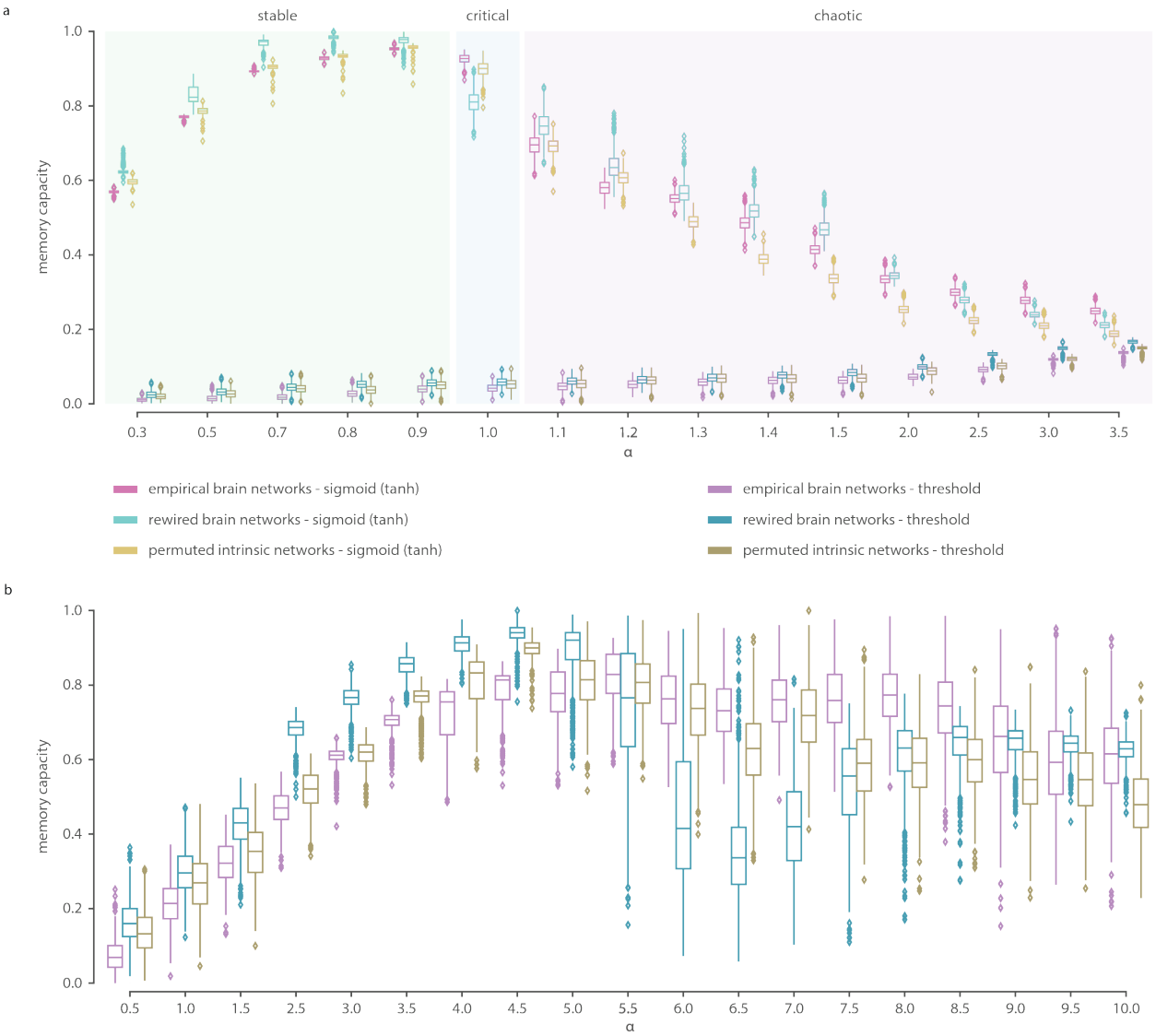

Figure S3.9: **Effect of the choice of activation function: hyperbolic tangent *vs* threshold** | For comparison, the same set of experiments were performed using threshold instead of hyperbolic tangent nonlinearity for the units in the reservoir. Specifically, if the weighted sum of the inputs to a unit is greater than the threshold θ, then the unit's activation state is 1, and 0 otherwise (binary unit). We set the threshold $\theta = 1$. (a) Comparison of the memory capacity between the hyperbolic tangent and the threshold models as a function of α. (b) Memory capacity of the threshold model for an extended set of α values. Differences in the behavior between the hyperbolic tangent and the threshold models makes it difficult to apply the same principles to determine the range of α values corresponding to the critical regime. It is worth noting that networks with hyperbolic tangent activation function display overall greater memory capacity compared to networks with threshold units, regardless of the value of α (memory capacity values in panel (a) were scaled between 0 and 1 using the minimum and maximum values obtained across models, whereas values in panel (b) were scaled using the minimum and maximum values obtained for the threshold model; therefore they are not directly comparable). This can be explained by the fact that threshold units can only display binary states, and therefore have less capacity compared to units with hyperbolic tangent nonlinearity, which can display a larger range of states, akin to populations of neurons in the brain.

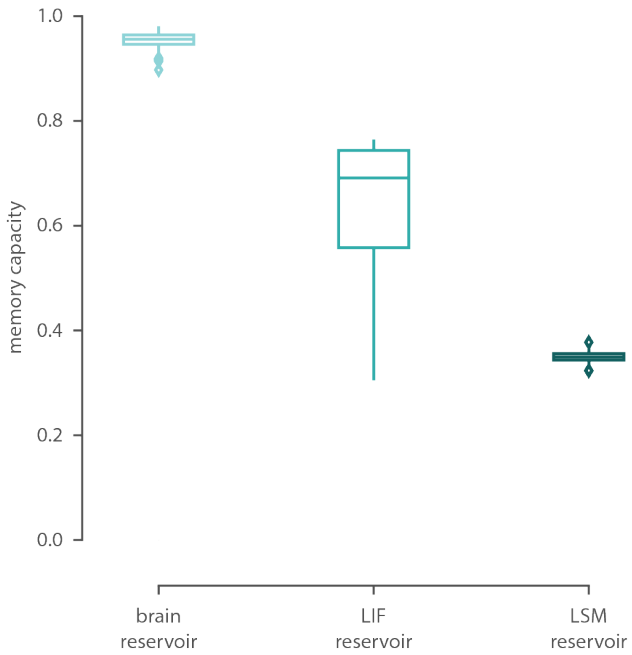

Figure S3.10: **Benchmarking connectome-informed reservoirs against other reservoir computing architectures** | We benchmarked the memory capacity of connectome-informed reservoirs against that of a random recurrent network of leaky-integrator neurons (LIF), and a random recurrent network of spiking neurons (integrate-and-fire), also known as liquid state machine (LSM). In both cases, networks were generated using the binomial model of Erdös-Rényi, with an approximate density of $\rho = 0.025$, comparable to empirical brain networks. The parameters for each neuron and synapse model are presented in Table S3.1. For the comparison, we selected the distribution of memory capacity values at the critical point (i.e., $\alpha \approx 1.0$), which is the point at which connectome-informed reservoirs outperform the rewired and label permutation models. Nevertheless, connectome-informed reservoirs outperformed the LIF and LSM models regardless of the dynamical regime.

Table S3.1: **List of LIF and LSM model parameters** | List of parameter values used for the leaky-integrate-and-fire (LIF) and the liquid state machine (LSM) models.

	Leaky-Integrate-and-Fire (LIF)	**Liquid State Machine (LSM)**
Python Package	Oger https://github.com/nschaetti/Oger	PyNEST + NEST https://github.com/IGITUGraz/LSM
Neuron model and parameters	Leaky integrator neuron: standard Echo State Network node (i.e., nonlinear units with hyperbolic tangent activation function) with a leak term (*LeakyReservoirNode* class).	Integrate-and-fire neuron with exponential-shaped postsynaptic currents (*'iaf_psc_exp'* neuron model).
	Leak rate (**leak_rate**) = 0.4	Membrane capacitance (**C_m**) = 30
	-	Membrane time constant (**tau_m**) = 10 ms
	-	Time constant - exc. synapses (**tau_syn_ex**) = 3.0 ms
	-	Time constant - inh. synapses (**tau_syn_in**) = 2.0 ms
	-	Threshold voltage (**V_th**) = 15 mV
	-	Reset voltage (**V_reset**) = 13.8 mV
	-	External current (**I_e**) = 4.5 pA
Synapse model and parameters	Static synapses. The weights were drawn from a uniform distribution with minimum value -1.0 and maximum value 1.0.	Static synapses. The weights were drawn from a Normal distribution with mean J and standard deviation 0.7J. The value of J depends on whether the synapses connects two excitatory neurons (J_EE = 50.0), two inhibitory neurons (J_IE=-200.0), one excitatory to an inhibitory neuron (J_EI = 250) or one inhibitory neuron to an excitatory neuron (J_IE = -200.0). Synaptic strength is in pA.
Network parameters	The reservoir contains 1015 units, out of which 15 correspond to input units, and the remaining 1000 correspond to readout units.	The reservoir contains 1265 units: 1015 excitatory neurons, 15 of which correspond to input nodes, and the remaining 1000 correspond to readout nodes; and 250 inhibitory neurons. We used 250 inhibitory neurons to keep the 80/20 excitatory/inhibitory ratio traditionally used for the construction of LSMs.

Chapter 4

`conn2res`: A toolbox for connectome-based reservoir computing

Laura E. Suárez[1,2], Agoston Mihalik[3], Filip Milisav[1], Kenji Marshall[1], Mingze Li[1], Petra Vertes[3], Guillaume Lajoie[2,4], & Bratislav Misic[1]

[1]McConnell Brain Imaging Centre, Montréal Neurological Institute, McGill University, Montréal, Canada

[2]Mila, Quebec Artificial Intelligence Institute, Montréal, QC, Canada

[3]Department of Psychiatry, University of Cambridge, Cambridge, United Kingdom

[4]Department of Mathematics and Statistics, Université de Montréal, Montreal, QC, Canada

4.1 Preface

In the previous chapter, I combined reservoir computing and connectomics data to investigate how a specific computational property, such as memory capacity, is supported by the synergetic cooperation between network structure and dynamics in the human connectome. In this chapter, I expand this hybrid approach between artificial intelligence and neuroscience, and present a generic framework to explore how network architecture and dynamics jointly support computation and functional specialization in biological connectomes. Specifically, I extend this framework to accommodate connectome architectures obtained from any imaging modality, different types of local dynamics, and a more comprehensive collection of cognitive tasks. By shifting the focus towards the computational and information-processing properties of the brain, this interdisciplinary approach will

provide new and more mechanistic insights about the structure-function coupling in biological brains. One could envision, for instance, training connectome-informed reservoirs on various cognitive tasks spanning a broad range of computational properties across different cognitive domains. By doing so, the framework here proposed would allow us to build a comprehensive structural-functional ontology, relating network structure and dynamics to fundamental blocks of computation and, ultimately, getting a step closer to understanding cognitive function and behavior. This chapter describes the fundamentals of reservoir computing, and outlines multiple research directions in which this combined approach can help us address different aspects of the multi-faceted link between structure and function in brain networks. Importantly, the work discussed in this chapter focuses on the development of an open-source Python toolbox, `conn2res`, making this framework available to the wide neuroscience community, and contributing to the cross-pollination of ideas between neuroscience and artificial intelligence (Prince et al., 2021). This work will be submitted for publication.

4.2 Abstract

The connection patterns of neural circuits in the brain form a complex network. How signaling in these circuits manifest as complex cognition and adaptive behaviour remains the central question in neuroscience. Concomitant advances in connectomics and artificial intelligence open fundamentally new opportunities to understand how connection patterns shape computational capacity in biological brain networks. Reservoir computing is a versatile paradigm that uses nonlinear dynamics of high-dimensional dynamical systems to perform computations and approximate cognitive functions. Here we present `conn2res`: an open-source Python toolbox for implementing biological neural networks as artificial neural networks. `conn2res` is modular, allowing arbitrary architectures and arbitrary dynamics to be imposed. This allows researchers to input connectomes reconstructed using multiple techniques, from tract tracing to noninvasive diffusion imaging, and to impose multiple dynamical systems, from simple spiking neurons to memristive dynamics. The versatility of the `conn2res` toolbox allows us to ask new questions at the confluence of neuroscience and artificial intelligence. By reconceptualizing function as computation, `conn2res` sets the stage for a more mechanistic understanding of structure-function relationships in brain networks.

4.3 Introduction

Our brains are complex networks of anatomically connected and functionally interacting neurons that have the ability to seamlessly assimilate and interact with the ever-changing external environment (Sporns, 2022). Sensory stimuli elicit signalling events within the network that manifest as patterned neural activity. These emergent neural dynamics are thought to support the computations that underlie cognition and adaptive behaviour. However, a computational framework that describes how information processing and functional specialization occur in brain networks remains elusive. Developing such a framework would require an understanding of the multiple levels of processing involved along the information processing hierarchy, from how the brain's network architecture shapes the complex activity patterns elicited by external stimuli, to how neural circuits extract from these evoked activity patterns the necessary information to compute with time-varying inputs.

How network structure gives rise to spatiotemporal patterns of neural activity, and how these neural dynamics are used to perform the computations that underlie specific cognitive functions and behaviours are questions that allude to the old problem of how structure shapes function in brain networks. An important piece of the puzzle in elucidating this link between structure and function has been the connectomics revolution (Sporns et al., 2005). Technological and analytic advances in neuroimaging methods have made it possible to map and trace the wiring patterns of nervous systems, yielding high-resolution connectomes of brains in multiple species (Assaf et al., 2020; Heuvel et al., 2016; Insel et al., 2013; Suarez et al., 2022). The availability of connectomes has led to the formulation of a variety of models that aim to map network architecture to various functional aspects of the brain (Suárez et al., 2020), such as emergent neural dynamics (Breakspear, 2017; Uddin, 2020), neural co-activation patterns (Cabral et al., 2017) and inter-individual differences in behaviour (Melozzi et al., 2019; Mišić and Sporns, 2016; Seguin et al., 2020). Multiple network features appear to be correlated with emergent functional phenomena (Bettinardi et al., 2017; Fletcher and Wennekers, 2018; Goñi et al., 2014; Sethi et al., 2017; Sporns, 2013; Zhang and Saggar, 2020), but how does network architecture support the computations underlying cognition and behaviour?

Furthermore, descriptive studies of the connectome across different species provide evidence that structural connectivity networks display nontrivial topological features that are thought to shape the flow, integration and segregation of information in the network (Bertolero et al., 2018). For instance, the simultaneous presence of a highly clustered

architecture of segregated modules that promotes specialized information processing (Bassett and Bullmore, 2006; Bertolero et al., 2015; Betzel et al., 2017; Chen et al., 2008; Hilgetag and Kaiser, 2004; Sporns and Zwi, 2004; Watts and Strogatz, 1998), and a densely interconnected core of high-degree hubs that shortens communication pathways and promotes the integration of information from distributed specialized domains (Heuvel et al., 2012; Zamora-López et al., 2010). How these ubiquitous organization principles of the architecture of the brain confer computational capacity remains unknown.

Alternative ways to approach the link between structure and function in brain networks that take into account computation are offered by the more recent artificial intelligence revolution (Marblestone et al., 2016; Richards et al., 2019). Within the expanding spectrum of artificial neural network models, reservoir computing is an ideal paradigm to describe how recurrent neural circuits extract information from a continuous stream of external stimuli and how they approximate complex time-varying functions (Buonomano and Maass, 2009; Maass et al., 2002). In this regard, machine-learning and artificial intelligence algorithms offer new ways to study structure-function relationships in brain networks by conceptualizing function as a computational property (Richards et al., 2019; Suárez et al., 2021).

Here we review the fundamentals of reservoir computing and how it can be applied to gain mechanistic insight about the information-processing of biological neural circuits. We then present `conn2res` (`https://github.com/netneurolab/conn2res.git`), an open-source Python toolbox that implements connectomes as reservoirs to perform cognitive tasks. In the spirit of open-science, `conn2res` builds on top of and is interoperable with other third-party resources and research initiatives to offer a comprehensive corpus of tasks spanning a wide spectrum of computational and behavioral paradigms that researchers can experiment with. One of the hallmark features of the `conn2res` toolbox is the inclusion of multiple local neuron models. We have included a general use-case tutorial to illustrate the flexibility of the toolbox in terms of network architecture, local and global network dynamics, task paradigm, learning algorithm and performance metrics. While being inclusive of different modeling traditions, from micro-circuits to whole-brain network models, `conn2res` contributes a novel way for researchers to explore the link between structure and function in biological brain networks.

The present report has been conceived as a modular manuscript with 3 standalone components: (1) fundamentals of reservoir computing, (2) how reservoir computing has been applied to model brain phenomena and (3) an overview and tutorial of the `conn2res` toolbox. Readers who are new to the world of reservoir computing or curious how the

paradigm can be applied to gain mechanistic insight into the information-processing properties of biological neural circuits can start with the review sections. Readers who are familiar with reservoir computing but wish to use the toolbox can skip ahead to the toolbox and tutorial sections.

4.4 Fundamentals of reservoir computing

The conventional reservoir computing (RC) architecture consists of an input layer, followed by the reservoir and a readout module (Fig. 4.1) (Jaeger, 2001; Maass et al., 2002; Verstraeten et al., 2007). Typically, the reservoir is a recurrent neural network (RNN) of nonlinear units, while the readout module is a simple linear model. The readout module is trained to read the activation states of the reservoir — elicited by an external input signal — and map them to the desired target output in a supervised manner. In contrast to traditional artificial RNNs, the recurrent connections within the reservoir are fixed; only the connections between the reservoir and the readout module are learned (Lukoševičius and Jaeger, 2009).

So, how does RC work? RC capitalizes on the nonlinear response of high-dimensional dynamical systems, referred to as reservoirs. The reservoir performs a nonlinear projection of the input into a high-dimensional space. This transformation of the input converts nonlinearly separable signals into linearly separable ones such that a linear model in the readout module can be trained to map the transformed input to the desired output (Lukoševičius and Jaeger, 2009). As long as the reservoir has sufficient built-in dynamical complexity and rich dynamics, a large variety of input-output mappings can be realized, including the approximation of complex time-varying functions, such as forecasting chaotic time series, considered to be a problem of high computational complexity. Under certain conditions, such as the presence of fading memory and separation properties, reservoirs can act as universal function approximators (Legenstein and Maass, 2007a,b; Maass and Markram, 2004; Maass et al., 2002). The computational capabilities of the reservoir are determined by its dynamics, which arise from the interaction between the fixed architecture of the reservoir and the equations or rules governing the time evolution of its internal units. Importantly, unlike traditional artificial neural networks, in RC the network architecture can be set and the dynamics can be tuned by the experimenter. The RC paradigm thus offers the advantages that arbitrary architectures and dynamics can be superimposed on the reservoir, providing a tool for neuroscientists to investigate how connectome organization and neural dynamics interact to support learning in biologically-informed reservoirs.

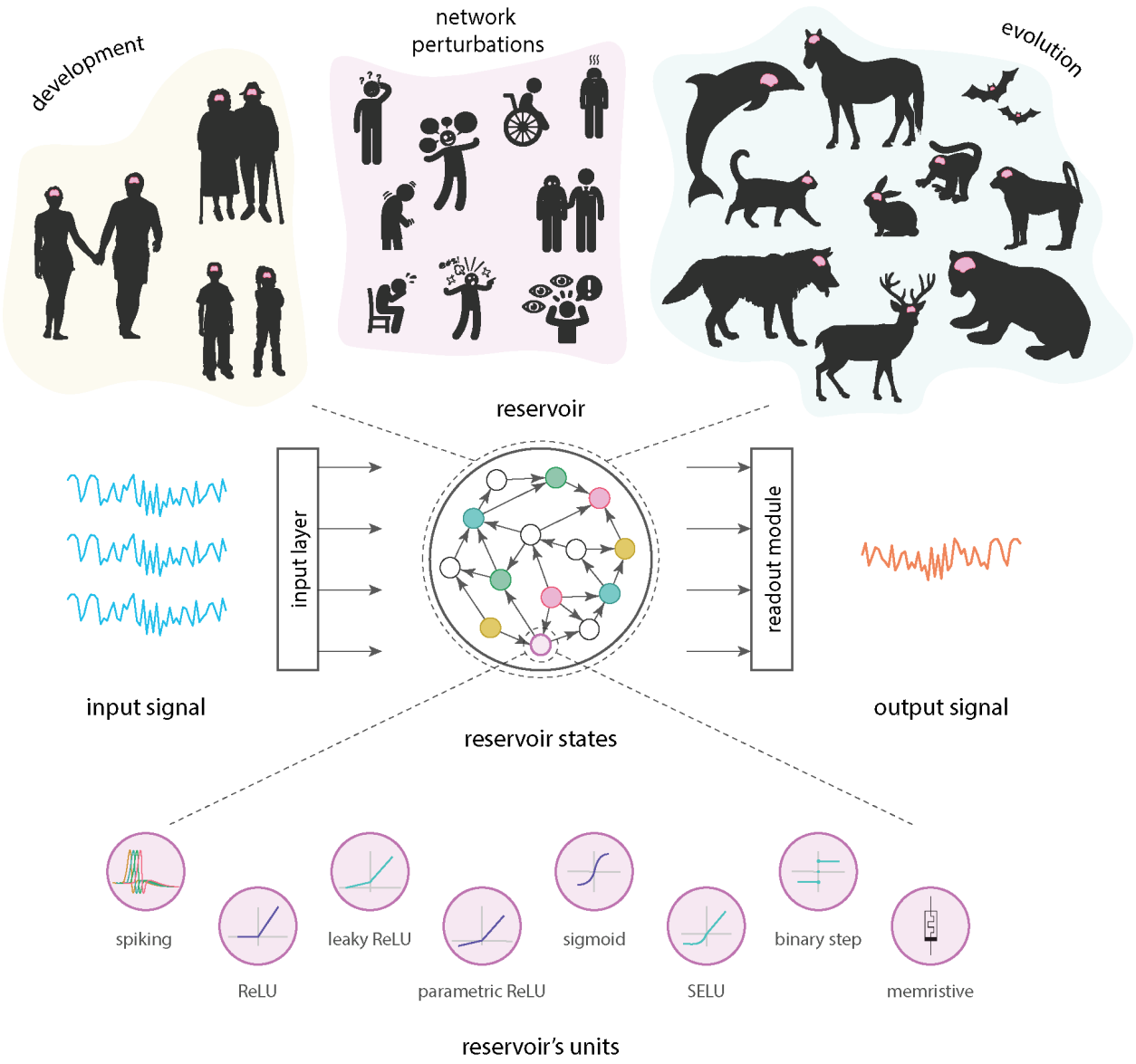

Figure 4.1: **Reservoir computing** | The conventional reservoir computing architecture consists of an input layer, followed by a hidden layer, or *reservoir*, which is typically a recurrent neural network of nonlinear units, and the readout module, which is a simple linear model. In contrast to traditional artificial RNNs, the recurrent connections within the reservoir are fixed; only the connections between the reservoir and the readout module are trained. More importantly, RC allows arbitrary network architecture and network dynamics to be implemented by the experimenter. Hence, biologically-plausible wiring patterns (top panel) and different types of local dynamics (bottom panel) can be superimposed on the reservoir. In this way, the RC paradigm offers a tool for neuroscientists to investigate how network organization and neural dynamics interact to support learning in biologically-informed reservoirs.

The fact that RC can be used with arbitrary network architectures and dynamics, plus the possibility of performing a variety of tasks spanning multiple cognitive domains — from perceptual-motor functions, memory and learning, to complex attention and executive functions — makes it ideal to investigate how specific network attributes and dynamics influence the neural computations that support cognition (Molano-Mazon et al., 2022). By implementing multiple tasks along the spectrum of cognitive domains, connectome-informed reservoirs allow us to systematically map network structure and dynamics to a unique set of identifiable computational properties exclusive to the task at hand. In this way, the RC framework allows us to build a comprehensive structural-functional ontology, relating network structure and dynamics to fundamental blocks of computation and, ultimately, to cognitive function.

The application of this hybrid approach between artificial intelligence and neuroscience goes beyond exploring the link between structure and function in the healthy brain. For instance, it can be applied in the clinical setting to study how neurological diseases affect learning in the network. By comparing the performance of reservoirs informed by clinical populations against those informed by healthy controls, this framework allows us to investigate whether cognitive/computational decline can be explained by measurable changes in network architecture due to neurodegeneration. Another relevant application of the RC framework is the exploration of how the link between structure and function changes throughout adaptive processes such as development or evolution. For example, by implementing connectomes corresponding to different developmental phases, or species, as reservoirs, this framework allows us to investigate how variations in network architecture translate into differences in cognition/computational capacity across ontogeny and phylogeny, respectively. In all cases, the RC framework allows for statistical significance testing by benchmarking empirical neural network architectures against random or null network models. The architectural flexibility of RC is multi-scale: reservoirs can be informed by connectomes reconstructed at different spatial scales, from micro-circuits to meso- and macro-scale networks. Depending on the context, the units of the reservoir represent either populations of neurons or entire brain regions.

Compared to traditional RNNs, in which global network dynamics are determined by connectivity changes due to learning, the dynamical aspect of RC networks is equally flexible to their static structural counterpart. RC allows us to impose not only different types of local dynamics, but also global dynamics governing the population-level behaviour can be controlled. This means that the dynamical regime of the reservoir can be tuned to progressively transition from stable to chaotic dynamics, thus passing through a critical

phase transition, or *criticality*. By parametrically tuning the dynamics to be closer or further from criticality, RC allows us to investigate the effects of qualitatively different neural trajectories near this critical point on the computational performance of the reservoir (Bertschinger and Natschläger, 2004; Langton, 1990). An additional advantage of the dynamical and structural flexibility of RC is the possibility to enforce computational priors in the form of either functional or structural inductive biases (Subramoney et al., 2021). Therefore, RC allows us to explore the functional consequences of information-processing strategies, such as critical dynamics or the presence of computational priors, thought to be exploited by biological brains (Cocchi et al., 2017; Deco and Jirsa, 2012; Kitzbichler et al., 2009; O'Byrne and Jerbi, 2022; Tagliazucchi et al., 2012).

Apart from the advantages that RC offers to the neuroscience community, this paradigm also seems promising from an engineering point of view. Reservoirs can be realized using physical systems, substrates or devices, as opposed to – generally time- and energy-consuming — simulated RNNs (Nakajima, 2020; Tanaka et al., 2019). In this regard, the architecture of these neuromorphic chips could benefit from the emerging understanding of connection patterns in biological networks (Fu et al., 2020; Loeffler et al., 2021, 2023). For instance, systematically mapping combinations of network attributes and dynamical regimes to a range of computational functions could assist the design of *ad hoc* or problem-specific tailored architectures. Due to their physical nature, neuromorphic systems are limited by spatial, material and energetic constraints, akin to biological neural networks. Because of this, insights gained about the economical organization of brain networks could contribute to the cost-effective design of these information processing systems (Suárez et al., 2021). Furthermore, the fact that training only occurs at the readout stage makes RC an extraordinarily computationally efficient learning approach. In addition to this, parallel information-processing can be achieved by simultaneously training multiple readout modules to perform various parallel tasks. Therefore, physical RC and RC in general, provide a powerful method for faster and simpler multi-task learning, compared to other RNNs. Thanks to the dynamical and versatile nature of the reservoir, the RC paradigm is perfectly suited for a wide range of supervised tasks involving the processing of temporal and sequential data. These include: time series prediction, dynamical pattern generation, classification and segmentation, control, signal processing, and monitoring of rare events, among others (Lukoševičius et al., 2012). Because of all these reasons, physical RC systems have become ideal candidates for the development of novel brain-inspired computing architectures (Dale et al., 2021).

4.5 The brain as a reservoir

RC originated independently in the fields of machine-learning and computational neuroscience in the early 2000s with the seminal works of Herbert Jaeger on echo-state networks (Jaeger, 2001), and Wolfgang Maass on liquid state machines (Maass et al., 2002). More broadly the ideas encompassed by the RC paradigm had been around in different forms for more than two decades prior. A series of electrophysiological (Barone and Joseph, 1989), behavioral (Barone and Joseph, 1989; Stadler, 1993), and anatomical (Alexander et al., 1986; Dominey and Arbib, 1992; Goldman-Rakic, 2011; Markov et al., 2011; Selemon and Goldman-Rakic, 1985; Selemon and Goldman-Rakic, 1988) empirical findings in the late 80's and 90's gave rise to what would be later known as RC. Importantly, RC has been used to model biological mechanisms at multiple scales and here we briefly trace the origins and myriad applications of RC to different phenomena in neuroscience.

To develop a brain-inspired system that could explain physiological and behavioral phenomena observed in primates performing a sensorimotor sequence learning task (Barone and Joseph, 1989), Peter Dominey implemented the first RC model (Dominey et al., 1995; Dominey, 1995). This new model was built on a previous network model to understand saccadic movements in the primate corticostriatal oculomotor system (Dominey and Arbib, 1992). The initial model, involving the posterior parietal cortex, frontal eye fields, superior colliculus and basal ganglia, was capable of reproducing the saccades observed in primates. To endow this circuit with the ability to display conditioned behavior in which the correct saccade target is selected among many, Dominey included the prefrontal cortex, which he modeled as an RNN with fixed excitatory and inhibitory connections, and added adaptive projections from the prefrontal cortex to the caudate, which could be trained through reward-based learning. And so the first RC system was born: the prefrontal cortex — the *reservoir* — transformed visuospatial input from the posterior parietal cortex into activity sequences that were then associated with saccade sequences in the caudate — the *readout* — through dopamine-related reward learning. This circuit could reproduce the behavioral responses observed in a sensorimotor sequence learning task. Interestingly, the activation of the reservoir's internal units resembled those observed in the primate cortex while performing the same task (Dominey et al., 1995; Dominey, 1995).

This new computational model proved to be versatile: it was sensitive to sequential and temporal structure (Dominey et al., 1995; Dominey, 1995, 1998a,b), and could also learn more abstract structures like arbitrary syntax rules (Dominey et al., 2003; Dominey and Ramus, 2000). The model was also capable of higher cognitive functions such as language

acquisition and processing (Dominey and Inui, 2009), grammatical construction (Dominey, 2013; Dominey et al., 2009), language production (Hinaut et al., 2015) and narrative (Mealier et al., 2017), and even complex non-linguistic tasks such as exploration-exploitation (Enel et al., 2016) and optimized spatial navigation (Cazin et al., 2018). Remarkably, across all these different tasks, the activation of the units in the reservoir, and sometimes the readout, display a striking resemblance to what is observed in the living primate cortex under the same task contexts (Enel et al., 2016). One such similarity is the activation of the reservoir's units to complex nonlinear combinations of task dimensions, thus demonstrating a form of *mixed selectivity*, recently shown to be a computational strategy highly exploited by biological brains (Rigotti et al., 2013). Altogether, these studies open an exciting possibility: that the cortex could be conceived as a set of "reservoirs organized in parallel interdigitated subsystems" (Dominey, 2021).

A related notion of a reservoir as a delay-coupled recurrent oscillator network has been put forward by Wolf Singer as a conceptual framework to explain a variety of cortical phenomena (Singer, 2021). First, recurrently connected networks have the propensity to engage in oscillatory activity (Börgers and Kopell, 2008; Buzsáki and Wang, 2012; Gray and Singer, 1989; Whittington et al., 2000), generating temporally structured activity. This behaviour becomes useful in a variety of scenarios. For instance, it allows for pattern completion in the presence of partial information (Falandays et al., 2021), supports the formation of novel associations (Wang et al., 2011), and permits the precise control of motor movements (Sussillo et al., 2015; Wyffels and Schrauwen, 2009). Second, oscillatory activity can introduce precise but variable temporal relations between interconnected nodes in the network, including phase synchrony and phase shifts. Given the sensitivity of Hebbian-like learning mechanisms to temporal relations (Artola et al., 1990; Bi and Poo, 1998; Hebb, 2005; Markram et al., 1997), the synchronization of oscillatory activity can favour the formation of synaptic connections and hence can be used for establishing associations. In this way, as posited by the "binding by synchrony" hypothesis (Singer, 1993, 1999; Singer and Gray, 1995), synchronous oscillations act as a binding mechanism for distributed nodes in the network that represent features of the same cognitive object, thus serving as a general code of relatedness (Singer, 1999). Likewise, phase shifts can lead to rapid reversals of the direction of information flow, thus serving as gating mechanisms for information transfer according to the "communication through coherence" hypothesis (Fries, 2005). Finally, imposing delays in recurrently connected networks gives rise to highly complex nonlinear dynamics that can be exploited for a variety of computational purposes. Low-dimensional stimuli are nonlinearly projected into a higher-dimensional

space, converting nonlinearly separable stimuli into linearly separable. This allows the fast and effective classification of complex spatiotemporal input patterns (Singer, 2021). Furthermore, the recurrent nature of the connections endows the network with a fading memory (Singer, 2021), that is, information about a stimulus persists for some time after the stimulus has disappeared. Therefore, information about multiple stimuli can be integrated over time, allowing for the encoding of temporal sequences (Dominey, 2021). Collectively these features showcase the versatility of the RC paradigm to capture the computational flexibility of the cortex.

Building on these early ideas, Wolfgang Maass proposed a related computational paradigm termed liquid computing (Haeusler and Maass, 2007; Maass et al., 2002). This framework was motivated by the question of how cortical columns in the brain seamlessly assimilate and process the spatial and temporal features of sensory stimuli (Haeusler and Maass, 2007; Maass et al., 2002). Maass and colleagues proposed a computational model whose construction was task-independent. The model comprised a recurrent network of spiking neurons in which only the connections of the readout neurons to the readout module are trained for the task at hand, while the recurrent connections within the network are fixed and randomly determined (Maass et al., 2002). Connection probabilities are assigned based on the connectivity between laminae and neural populations (Maass et al., 2002). These liquid state machines were shown to be successful for a variety of learning tasks involving the real-time processing of time-varying inputs (Maass et al., 2002). Around the same time and independently, Herbert Jaeger developed echo-state networks (Jaeger, 2001), a similar framework conceived for artificial neural networks. Given their common goal of computing with nonlinear, high-dimensional dynamical systems, these two frameworks were brought together under the name of reservoir computing (Verstraeten et al., 2007).

More recently, advances in imaging and tracing technologies make it possible to reconstruct the wiring diagrams of multiple species, opening new opportunities to identify features of brain networks that theoretically enhance information-processing, such as modularity and small-worldness. Traditionally, reservoirs are randomly wired; by imposing some structure to this random connectivity we can explore how specific features of brain networks contribute to computational capacity. Modularity, for instance, affects information transmission in the network as well as its memory capacity (Rodriguez et al., 2019; Suárez et al., 2021). In random modular networks there is an optimal modularity where a balance between local cohesion and global communication is established, allowing the network to remember longer (Rodriguez et al., 2019). The same is true for empirical brain networks: the mesoscale modular organization of the human connectome, defined

by intrinsic functional networks (Bellec et al., 2010; Damoiseaux et al., 2006; Power et al., 2011; Schaefer et al., 2018; Smith et al., 2009; Thomas Yeo et al., 2011), and its underlying macroscale network topology, enhance the memory capacity of the reservoir, in particular when dynamics are critical (Suárez et al., 2021). Hence, in both random and empirical modular networks, there is an optimal level of modularity that delivers a balance between integration and segregation in the network (Shine et al., 2018), supporting optimal memory capacity (Rodriguez et al., 2019; Suárez et al., 2021). Similarly, small-world topology (Bassett and Bullmore, 2006; Sporns and Zwi, 2004; Watts and Strogatz, 1998) — prevalent across biological networks (Suarez et al., 2022) — contributes to the echo-state property of the reservoir (Kawai et al., 2019), a measure of how flexibly network dynamics can unmoor/untether from initial conditions, and promotes efficient signal propagation along the network (Kawai et al., 2017). Besides improving our understanding on how network architecture and dynamics affect the computational capacity of biological brain networks, implementing reservoirs informed by empirical connectomes can also be used for practical engineering purposes such as designing brain-like artificial neural network models or neuromorphic hardware (Damicelli et al., 2022; Goulas et al., 2021; Loeffler et al., 2021).

Alternatively, the conventional RC architecture can be modified in unconventional ways to model different functional and structural aspects of the cortex. For example, a collaborative multimodal RC model can offer a mechanistic explanation to multisensory integration at early stages of the cortical processing hierarchy (Kanemura and Kitano, 2023). Multi-timescale changes in connectivity that occur through evolutionary and developmental processes can also be modeled using alternative learning paradigms, such as the Learning-to-Learn algorithm on modular and temporarily adaptive RC architectures (Subramoney et al., 2021). These enforced structural priors — or pre-optimized reservoir's hyper-parameters — facilitate subsequent learning in multi-task learning contexts (Márton et al., 2021; Subramoney et al., 2021). More recently, the concept of spatially-embedded recurrent neural networks was introduced (Achterberg et al., 2022). These are recurrent networks with adaptive weights, confined within a 3D Euclidean space, and whose learning is constrained by biological optimization processes, like the minimization of wiring costs or the optimization of inter-regional communicability, in addition to the maximization of computational performance. When the pruning of the network is guided by these biological optimization principles, the resulting network architecture displays characteristic features of biological brain networks, including a modular structure with a small-world topology, and the emergence of functionally specialized regions that are spatially co-localized and implement an energetically-efficient, mixed-selective code (Achterberg et al., 2022; Rigotti

et al., 2013). Altogether, reservoir computing and recurrent neural networks in general open a world of possibilities to provide mechanistic explanations for the way computations take place in real brain networks.

4.6 The `conn2res` toolbox

`conn2res` is an open-source Python toolbox that allows users to implement biological neural networks as reservoirs to perform cognitive tasks (https://github.com/netneurolab/conn2res.git). The toolbox is built on top of the following well established, documented and maintained Python package dependencies: `NumPy` (https://numpy.org; (Harris et al., 2020; Oliphant, 2006; Walt et al., 2011)), `SciPy` (https://scipy.org; (Virtanen et al., 2020)), `pandas` (https://pandas.pydata.org; (McKinney et al., 2010)), `Scikit-Learn` (https://scikit-learn.org; (Pedregosa et al., 2011)), `Gym` (https://www.gymlibrary.dev; (Brockman et al., 2016)), `NeuroGym` (https://neurogym.github.io; (Molano-Mazon et al., 2022)), `bctpy` (https://github.com/aestrivex/bctpy; (Rubinov and Sporns, 2010)), `Seaborn` (https://seaborn.pydata.org; (Waskom et al., 2016)) and `Matplotlib` (https://matplotlib.org; (Hunter, 2007)). The toolbox is also interoperable with other relevant Python packages including `The Virtual Brain` (https://www.thevirtualbrain.org; (Ritter et al., 2013)), `bio2art` (https://github.com/AlGoulas/bio2art; (Goulas et al., 2021)), `NeuroSynth` (https://neurosynth.org; (Yarkoni et al., 2011)), `Neuromaps` (https://neuromaps-main.readthedocs.io; (Markello et al., 2022)) and the `Enigma Toolbox` (https://enigma-toolbox.readthedocs.io; (Larivière et al., 2021)).

Besides its extensive interoperability with other Python packages, a major strength of the `conn2res` toolbox is its flexibility in the choice of the different components that are part of the main RC workflow, in particular, the possibility to implement arbitrary network architectures and different types of local dynamics, which to our knowledge are typically fixed in other RC packages. The baseline `conn2res` workflow requires the following input arguments (Fig. 4.2a): ***(i)* task name or dataset:** the name of the task to be performed, or a labeled dataset of input-target pairs for supervised learning can also be provided. `conn2res` is a wrapper of `NeuroGym` (Molano-Mazon et al., 2022), a curated collection of behavioural paradigms that were designed to facilitate the training of neural network models, and that are relevant for the neuroscience community. All of the 20+ tasks available in `NeuroGym` are also available in `conn2res`; ***(ii)* connectome:** the connectivity matrix, which serves as the reservoir's network architecture. The toolbox supports binary and weighted connectivity matrices of both directed and undirected networks; ***(iii)* input**

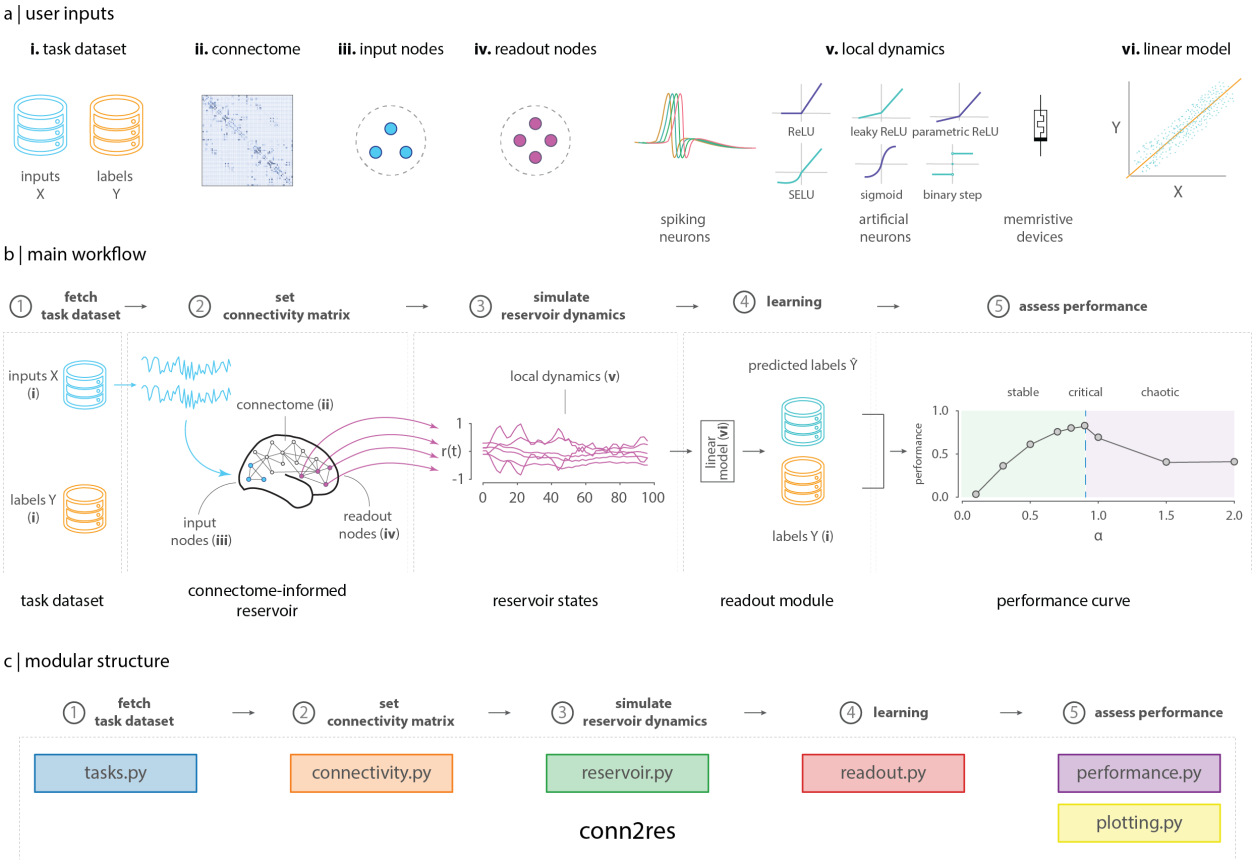

Figure 4.2: `conn2res` **toolbox** | (a) The general `conn2res` workflow requires the following parameters to be provided by the user: *i*) a task name or a supervised learning dataset; *ii*) a connectome or connectivity matrix; *iii*) a set of input nodes; *iv*) a set of readout nodes or modules; *v*) the type of local dynamics, which can be either spiking neurons, artificial neurons (with a variety of activation functions), or memristive devices (for the simulation of physical reservoirs); and *vi*) the linear model to be trained in the readout module. (b) In the mainstream `conn2res` workflow the input signal (X) is introduced to the reservoir through the input nodes (blue nodes). The signal propagates through the network, activating the states of the units within the reservoir. The activation states of the readout nodes (purple nodes) are then retrieved and used to train a linear model to approximate the target signal (Y). Depending on the type of the reservoir, the performance can be a single score or a curve of performance as a function of a parameter that tunes the dynamics of the reservoir. (c) The `conn2res` toolbox has a modular architecture. It consists of six modules, each one comprising functions that support a specific step along the `conn2res` pipeline.

nodes: the set of nodes that receive the external input signals concerning the task at hand; **(*iv*) readout nodes:** the set of nodes or modules from which information will be retrieved to train the linear model in the readout module; **(*v*) reservoir local dynamics:** the type of dynamics governing the activation of the reservoir's units. Right now only discrete-time, linear and nonlinear dynamics can be implemented. These include artificial neuron models with different activation functions such as ReLU, leaky ReLU, sigmoid or hyperbolic tangent. In the future, continuous-time nonlinear dynamical models will be implemented, including different spiking neuron models; and lastly the type of **(*vi*) linear model:** specified as an instance of a linear model estimator from the `Scikit-Learn` library to be implemented for learning by the readout module (Pedregosa et al., 2011).

The typical `conn2res` workflow is depicted in Fig. 4.2b. In the first stage, **fetch task dataset**, a supervised dataset consisting of input-label pairs is either fetched from the `conn2res` repository, if the name of the task is provided by the user, or directly loaded if an external path is provided instead. In the second stage, **set connectivity matrix**, an instance of a reservoir object is created, and its network architecture and dynamics are set based on the connectivity matrix and the type of local dynamics specified by the user, respectively. In the third stage, **simulate reservoir dynamics**, the task inputs from the previous stage are introduced as external signals to the reservoir through the set of input nodes specified by the user. The dynamical models in the `conn2res` toolbox simulate the time evolution of the reservoir's internal units (which are activated thanks to the propagation of the external input signals), and generate time series activity for each node in the reservoir. In the fourth stage, **learning**, the time series activity of the readout nodes or modules specified by the user are retrieved and passed on to the readout module, together with the task labels from the first stage. Both of these are used to train the linear model in the readout module. Finally, during the fifth and last stage, **assess performance**, depending on the nature of the reservoir, the final output can be either a single performance score, or a performance curve that displays performance as a function of the parameter that controls for the qualitative behavior of the reservoir's dynamics (i.e., stable, critical or chaotic). Various performance metrics are currently available depending on whether the task requires a classification or a regression model. To facilitate the user's experience, the toolbox provides several example scripts that illustrate use-case driven workflows.

The `conn2res` toolbox has a modular design. It consists of six modules, each one containing functions that support a specific step along the mainstream `conn2res` pipeline (Fig. 4.2c). The wrapper functions and classes used to generate the task datasets can be found in the ***tasks.py*** module. All types of manipulations on the connectivity matrix, such

as binarization, weight scaling, normalization and rewiring, are handled by the Conn class in the ***connectivity.py*** module. All the reservoir's features including its network architecture, local dynamics and retrieval of reservoir's activation states, are handled by the Reservoir class in the ***reservoir.py*** module. The functions in charge of the training and test of the linear model in the readout module are contained in the ***readout.py*** and ***performance.py*** modules, respectively. Finally, the ***plotting.py*** module offers a set of plotting tools that assist with the visualization of the different types of data generated along the pipeline, including the task input-output data, the 2D connectivity matrix of the reservoir's network architecture, the simulated reservoir states, the decision function of the readout module, and the performance curve.

4.6.1 A use-case tutorial

In this section we present a toy example in which we use `conn2res` to evaluate the effect of different types of local and global dynamics on the performance of a connectome-informed reservoir across two cognitive tasks: perceptual decision making (Britten et al., 1992) and context decision making (Mante et al., 2013). To do so, we implement an echo-state network (Jaeger, 2001) whose connections are constrained by a human connectome reconstructed from diffusion-weighted MRI data. To select the set of input and readout nodes, we use a functional connectivity-based partition of the connectome into intrinsic networks (Thomas Yeo et al., 2011). We define input nodes as a set of randomly selected brain regions from the visual system, and for the readout nodes we select all brain regions in the somatomotor system. Local dynamics are determined by the activation function of the reservoir's units. Here we use sigmoid and hyperbolic tangent activation functions. Global network dynamics are set by parametrically tuning α, which corresponds to the spectral radius of the connectivity matrix (Seung, 1996). The dynamics of the reservoir are considered to be stable if $\alpha < 1$, and chaotic if $\alpha > 1$. When $\alpha \approx 1$, the dynamics are said to be critical (O'Byrne and Jerbi, 2022). Because both tasks can be treated as supervised classification problems, we use a Ridge classifier model to train the readout module. We generate 1000 trials per task (70% training, 30% test), and we perform each task using 50 different realizations of the task's labeled dataset. The distribution of performance scores is reported across the 50 instances of the task dataset.

Next we walk the reader through each of the steps along the main `conn2res` pipeline, and use the visualization tools included in the ***plotting.py*** module to depict the main output at each stage, facilitating the conceptual understanding of the workflow. Details about the practical implementation can be found in the *examples* folder of the `conn2res`

toolbox. Results for the perceptual and context decision making tasks are shown on the left and right columns of Fig. 4.3, respectively. The first top panel in Fig. 4.3 consists of a single plot that displays the time series of the input (x_i) and target labels (y) obtained during the task dataset fetching process. The perceptual decision making task is a two-alternative forced choice task in which the reservoir must be able to integrate two stimuli to decide which one is higher on average (left column in Fig. 4.3). In the context decision making task the reservoir has to perform one of two different perceptual discriminations, indicated by a contextual cue in every trial (right column in Fig. 4.3). Trials are delimited by vertical black dotted lines.

The second panel in Fig. 4.3 from top to bottom is a toy representation of the assignment of the connectome-based connectivity matrix to the reservoir's network (center); it also shows the input nodes (left) used for the introduction of the external input signal into the reservoir during the simulation of the reservoir's dynamics, and the readout nodes (right) used for the retrieval of information from the reservoir during the learning phase. The third panel in Fig. 4.3 depicts the simulation of the reservoir's dynamics and it consists of two plots: the top plot presents the time series of the input signals (x), while the bottom plot shows the simultaneous reservoir's activation state at every time step. These plots help the user visualize how reservoir states evolve as a function of the external inputs. The fourth panel in Fig. 4.3 makes reference to the learning process of the readout module during training. This panel contains three plots: the time series of the input signal (top), the decision function of the Ridge classifier (middle), and the predicted versus the ground truth target signals (bottom). Finally, the fifth panel in Fig. 4.3 shows the performance of the reservoir as a function of both local and global network dynamics. This panel presents two plots, each one corresponding to a different classification performance metric: balanced accuracy (top) and F1 score (bottom). Each plot displays two curves that indicate how performance varies as a function of α, and each curve corresponds to a different activation function: hyperbolic tangent (pink) and sigmoid (green).

Results in Fig. 4.3 suggest that both local and global network dynamics have an impact on task performance. At the local level, both tasks, perceptual and context decision making, benefit from having a hyperbolic tangent activation function, compared to the sigmoid. However, dependence of task performance on global network dynamics varies from one task to the other. Computations required in the perceptual decision making task take advantage of stable network dynamics if the local nonlinearity is hyperbolic tangent, whereas with a sigmoid nonlinearity the network does not show a strong dependence with respect to global network dynamics. Contrary, performance in the context decision making

task improves as global network dynamics transition from stable to chaotic, regardless of the type of local activation function. As expected, the effect of local and global network dynamics on task performance depends on the type of computations required by the task at hand.

This example helps us to illustrate the flexibility of the `conn2res` toolbox in terms of the choice of network architecture, local and global network dynamics, computational properties, performance metrics and learning algorithms. Even though the type of experiments that the `conn2res` toolbox has been designed for have more of an exploratory character, we are hoping that as imaging technologies improve together with our understanding of the anatomical structure of biological brains, more hypothesis-driven type of experiments can be carried out with `conn2res`.

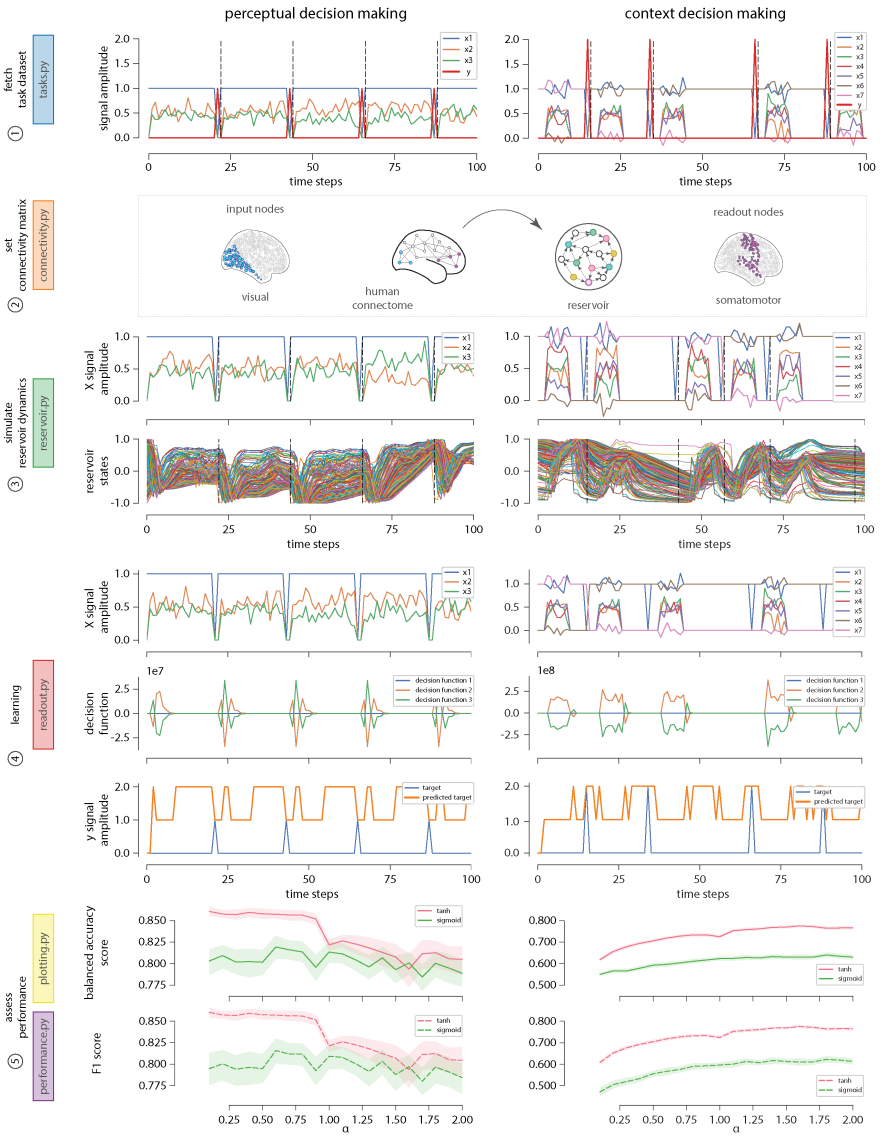

Figure 4.3: **Use-case tutorial: effect of local and global dynamics on the performance of perceptual and context decision making tasks** | Perceptual decision making (left column): is a two-alternative forced choice task ($y = \{1, 2\}$) in which the reservoir must be able to integrate two stimuli (x_2 and x_3; x_1 serves as a bias) to decide which one is higher on average. Context decision making task (right column): in this task the reservoir has to perform one of two different perceptual discriminations ($y = \{1, 2\}$), indicated by a contextual cue in every trial (determined by x_1 to x_7). From top to bottom: the first panel displays the time series of the input (x_i) and target (y) signals obtained during the task dataset fetching step. The second panel presents a toy representation of the assignment of a connectome-based connectivity matrix to the reservoir's network (center). It also shows the set of input (left) and readout (right) nodes selected for the analysis. The third panel displays the simulated reservoir's dynamics; the top plot shows the time series of the input signals and the bottom plot shows the simultaneous activation states of the readout nodes within the reservoir (results shown here correspond to the simulated reservoir states with hyperbolic tangent as activation function). The fourth panel illustrates the learning process that takes place in the readout module during training. At every time step, the top plot shows the input signals, the middle plot shows the decision function of the classifier — in the readout module —, and the bottom plot shows the predicted versus the target signal. Finally, the fifth panel shows the performance curves as a function of both local (hyperbolic tangent in pink and sigmoid in green) and global (varying α) network dynamics. Two metrics were used to measure the performance of the classification: balanced accuracy (top - solid line) and F1 score (bottom - dotted line).

4.7 Concluding remarks

Despite common roots, modern neuroscience and artificial intelligence have followed diverging paths. The advent of high-resolution connectomics and the incredible progress of artificial neural networks in recent years present fundamentally new and exciting opportunities for the convergence of these vibrant and fast-paced fields. Here we briefly summarized the principles of the RC paradigm, reviewed various ways in which it can be applied to model diverse cortical phenomena, and introduced `conn2res`, an open-source code initiative designed to promote cross-pollination of ideas and bridge multiple disciplines, including neuroscience, psychology, engineering, artificial intelligence, physics and dynamical systems. Below we look outward and speculate how the `conn2res` toolbox can be used to address emerging questions in these fields.

The `conn2res` toolbox embodies the versatility of the RC paradigm itself. By allowing arbitrary network architecture and dynamics to be superimposed on the reservoir, `conn2res` can be applied to investigate a wide range of neuroscience problems: from understanding the link between structure and function, studying individual differences in behaviour, to exploring the functional consequences of network perturbations, such as disease or stimulation, or the computational benefits of specific architectural features, such as hierarchies and modules. The `conn2res` toolbox can readily accommodate network reconstructions at different spatial scales, from microcircuits to large-scale brain networks, and obtained using different imaging modalities, such as tract-tracing or diffusion MRI. Networks reconstructed at different points in either development and evolution can also be implemented in the toolbox to study, for instance, how structural adaptations across ontogeny and phylogeny shape computational capacity in brain networks. Collectively, `conn2res` offers new and numerous possibilities to discover how computation and functional specialization emerge from the brain's anatomical network structure.

RC is often presented as a unified framework to train RNNs, but in a broader sense, it is a general framework to compute with high-dimensional, nonlinear dynamical systems, regardless of the choice of reservoir! Since any high-dimensional physical system with nonlinear dynamics could serve as reservoir — and these are abundant in both natural and man-made systems — a new field of applied research has emerged: physical reservoir computing. Here the goal is to exploit the rich dynamics of complex physical systems as information-processing devices. Physical substrates used for reservoirs are quite diverse: from analog circuits (Appeltant et al., 2011; Li et al., 2018; Soriano et al., 2014; Zhao et al., 2016), field programmable gate arrays (Alomar et al., 2014; Antonik, 2018; Antonik et al.,

2015; Wang et al., 2017), photonic opto-electronic devices (Katumba et al., 2017, 2018; Laporte et al., 2018; Vandoorne et al., 2008, 2014; Zhang et al., 2014), spintronics (Nomura et al., 2021; Riou et al., 2021; Taniguchi et al., 2021), quantum dynamics (Fujii and Nakajima, 2021; Negoro et al., 2021), nanomaterials (Bennett et al., 2017; Du et al., 2017; Kendall et al., 2018; Kulkarni and Teuscher, 2012; Sillin et al., 2013; Suárez et al., 2018; Yang et al., 2016), biological materials and organoids (Nakajima et al., 2013), mechanics and robotics (Caluwaerts et al., 2013; Dion et al., 2021; Hauser, 2021), up to liquids or fluids (Nakajima and Aoyagi, 2015; Natschläger et al., 2002), and most recently, origami structures (Bhovad and Li, 2021). As physical reservoir computing becomes more popular, we envision the use of `conn2res` as a workbench to explore the effect of network interactions on the computational properties of physical reservoirs. Anticipating this, `conn2res` is currently equipped with a dedicated class for physical reservoirs, which allows memristive networks — a promising alternative for neuromorphic computing (Kulkarni and Teuscher, 2012) — to be implemented as reservoirs. In this sense, the paradigm and the `conn2res` toolbox can be applicable to a wide variety of problems in adjacent scientific disciplines. From the neuroconnectomics perspective, `conn2res` offers new and numerous possibilities to discover how structure and function are linked in biological brain networks. From the artificial intelligence perspective, reverse-engineering biological networks will provide insights and novel design principles for re-engineering artificial, brain-inspired RC architectures and systems.

Altogether, `conn2res` is an easy-to-use toolbox that allows biological neural networks to be implemented as artificial neural networks. By combining connectomics and AI, the RC paradigm allows us to address new questions in a variety of scales of description and many adjacent fields. We hope that by reconceptualizing function as computation, `conn2res` allows us to take the next step towards understanding structure-function relationships in brain networks.

4.8 Bibliography

Achterberg, J. et al. (2022). "Spatially-embedded recurrent neural networks reveal widespread links between structural and functional neuroscience findings". *bioRxiv*, pp. 2022–11.

Alexander, G. E., M. R. DeLong, and P. L. Strick (1986). "Parallel organization of functionally segregated circuits linking basal ganglia and cortex". *Annual review of neuroscience*, 9(1), pp. 357–381.

Alomar, M. L. et al. (2014). "Low-cost hardware implementation of reservoir computers". In: *2014 24th International Workshop on Power and Timing Modeling, Optimization and Simulation (PATMOS)*. IEEE, pp. 1–5.

Antonik, P. (2018). *Application of FPGA to Real-Time Machine Learning: Hardware Reservoir Computers and Software Image Processing*. Springer.

Antonik, P. et al. (2015). "FPGA implementation of reservoir computing with online learning". In: *24th Belgian-Dutch Conference on Machine Learning*.

Appeltant, L. et al. (2011). "Information processing using a single dynamical node as complex system". *Nature communications*, 2(1), pp. 1–6.

Artola, A., S Bröcher, and W. Singer (1990). "Different voltage-dependent thresholds for inducing long-term depression and long-term potentiation in slices of rat visual cortex". *Nature*, 347(6288), pp. 69–72.

Assaf, Y. et al. (2020). "Conservation of brain connectivity and wiring across the mammalian class". *Nat Neurosci*, 23(7), pp. 805–808.

Barone, P and J. P. Joseph (1989). "Prefrontal cortex and spatial sequencing in macaque monkey". *Experimental brain research*, 78, pp. 447–464.

Bassett, D. S. and E. Bullmore (2006). "Small-world brain networks". *The neuroscientist*, 12(6), pp. 512–523.

Bellec, P. et al. (2010). "Multi-level bootstrap analysis of stable clusters in resting-state fMRI". *NeuroImage*, 51(3), pp. 1126–1139.

Bennett, C. H., D. Querlioz, and J.-O. Klein (2017). "Spatio-temporal learning with arrays of analog nanosynapses". In: *2017 IEEE/ACM International Symposium on Nanoscale Architectures (NANOARCH)*. IEEE, pp. 125–130.

Bertolero, M. A., B. T. Yeo, and M. D'Esposito (2015). "The modular and integrative functional architecture of the human brain". *Proc Natl Acad Sci USA*, 112(49), E6798–E6807.

Bertolero, M. A. et al. (2018). "A mechanistic model of connector hubs, modularity and cognition". *Nat Hum Behav*, 2(10), pp. 765–777.

Bertschinger, N. and T. Natschläger (2004). "Real-time computation at the edge of chaos in recurrent neural networks". *Neural computation*, 16(7), pp. 1413–1436.

Bettinardi, R. G. et al. (2017). "How structure sculpts function: unveiling the contribution of anatomical connectivity to the brain's spontaneous correlation structure". *Chaos: An Interdisciplinary Journal of Nonlinear Science*, 27(4), p. 047409.

Betzel, R. F. et al. (2017). "The modular organization of human anatomical brain networks: Accounting for the cost of wiring". *Net Neurosci*, 1(1), pp. 42–68.

Bhovad, P. and S. Li (2021). "Physical reservoir computing with origami and its application to robotic crawling". *Scientific Reports*, 11(1), p. 13002.

Bi, G.-q. and M.-m. Poo (1998). "Synaptic modifications in cultured hippocampal neurons: dependence on spike timing, synaptic strength, and postsynaptic cell type". *Journal of neuroscience*, 18(24), pp. 10464–10472.

Börgers, C. and N. J. Kopell (2008). "Gamma oscillations and stimulus selection". *Neural computation*, 20(2), pp. 383–414.

Breakspear, M. (2017). "Dynamic models of large-scale brain activity". *Nat Neurosci*, 20(3), p. 340.

Britten, K. H. et al. (1992). "The analysis of visual motion: a comparison of neuronal and psychophysical performance". *Journal of Neuroscience*, 12(12), pp. 4745–4765.

Brockman, G. et al. (2016). "Openai gym". *arXiv preprint arXiv:1606.01540*.

Buonomano, D. V. and W. Maass (2009). "State-dependent computations: spatiotemporal processing in cortical networks". *Nature Reviews Neuroscience*, 10(2), p. 113.

Buzsáki, G. and X.-J. Wang (2012). "Mechanisms of gamma oscillations". *Annual review of neuroscience*, 35, pp. 203–225.

Cabral, J., M. L. Kringelbach, and G. Deco (2017). "Functional connectivity dynamically evolves on multiple time-scales over a static structural connectome: Models and mechanisms". *NeuroImage*, 160, pp. 84–96.

Caluwaerts, K. et al. (2013). "Locomotion without a brain: physical reservoir computing in tensegrity structures". *Artificial life*, 19(1), pp. 35–66.

Cazin, N. et al. (2018). "Prefrontal cortex creates novel navigation sequences from hippocampal place-cell replay with spatial reward propagation". *bioRxiv*, p. 466920.

Chen, Z. J. et al. (2008). "Revealing modular architecture of human brain structural networks by using cortical thickness from MRI". *Cerebral cortex*, 18(10), pp. 2374–2381.

Cocchi, L. et al. (2017). "Criticality in the brain: A synthesis of neurobiology, models and cognition". *Progress in neurobiology*, 158, pp. 132–152.

Dale, M. et al. (2021). "Reservoir computing in material substrates". *Reservoir Computing: Theory, Physical Implementations, and Applications*, pp. 141–166.

Damicelli, F., C. C. Hilgetag, and A. Goulas (2022). "Brain connectivity meets reservoir computing". *PLoS Computational Biology*, 18(11), e1010639.

Damoiseaux, J. et al. (2006). "Consistent resting-state networks across healthy subjects". *Proc Natl Acad Sci USA*, 103(37), pp. 13848–13853.

Deco, G. and V. K. Jirsa (2012). "Ongoing cortical activity at rest: criticality, multistability, and ghost attractors". *Journal of Neuroscience*, 32(10), pp. 3366–3375.

Dion, G. et al. (2021). "Reservoir Computing in MEMS". *Reservoir Computing: Theory, Physical Implementations, and Applications*, pp. 191–217.

Dominey, P., M. Arbib, and J.-P. Joseph (1995). "A model of corticostriatal plasticity for learning oculomotor associations and sequences". *Journal of cognitive neuroscience*, 7(3), pp. 311–336.

Dominey, P. F. (1995). "Complex sensory-motor sequence learning based on recurrent state representation and reinforcement learning". *Biological cybernetics*, 73(3), pp. 265–274.

— (2013). "Recurrent temporal networks and language acquisition—from corticostriatal neurophysiology to reservoir computing". *Frontiers in psychology*, 4, p. 500.

Dominey, P. F. and M. A. Arbib (1992). "A cortico-subcortical model for generation of spatially accurate sequential saccades". *Cerebral cortex*, 2(2), pp. 153–175.

Dominey, P. F. and T. Inui (2009). "Cortico-striatal function in sentence comprehension: Insights from neurophysiology and modeling". *Cortex*, 45(8), pp. 1012–1018.

Dominey, P. F. et al. (2003). "Neurological basis of language and sequential cognition: evidence from simulation, aphasia, and ERP studies". *Brain and language*, 86(2), pp. 207–225.

Dominey, P. F. (1998a). "A shared system for learning serial and temporal structure of sensori-motor sequences? Evidence from simulation and human experiments". *Cognitive Brain Research*, 6(3), pp. 163–172.

— (1998b). "Influences of temporal organization on sequence learning and transfer: Comments on Stadler (1995) and Curran and Keele (1993)." *Journal of Experimental Psychology: Learning, Memory, and Cognition*, 24(1), p. 234.

— (2021). "Cortico-striatal origins of reservoir computing, mixed selectivity, and higher cognitive function". *Reservoir Computing: Theory, Physical Implementations, and Applications*, pp. 29–58.

Dominey, P. F., T. Inui, and M. Hoen (2009). "Neural network processing of natural language: II. Towards a unified model of corticostriatal function in learning sentence comprehension and non-linguistic sequencing". *Brain and language*, 109(2-3), pp. 80–92.

Dominey, P. F. and F. Ramus (2000). "Neural network processing of natural language: I. Sensitivity to serial, temporal and abstract structure of language in the infant". *Language and Cognitive Processes*, 15(1), pp. 87–127.

Du, C. et al. (2017). "Reservoir computing using dynamic memristors for temporal information processing". *Nature communications*, 8(1), pp. 1–10.

Enel, P. et al. (2016). "Reservoir computing properties of neural dynamics in prefrontal cortex". *PLoS computational biology*, 12(6), e1004967.

Falandays, J. B., B. Nguyen, and M. J. Spivey (2021). "Is prediction nothing more than multi-scale pattern completion of the future?" *Brain Research*, 1768, p. 147578.

Fletcher, J. M. and T. Wennekers (2018). "From structure to activity: Using centrality measures to predict neuronal activity". *International journal of neural systems*, 28(02), p. 1750013.

Fries, P. (2005). "A mechanism for cognitive dynamics: neuronal communication through neuronal coherence". *Trends in cognitive sciences*, 9(10), pp. 474–480.

Fu, K. et al. (2020). "Reservoir computing with neuromemristive nanowire networks". In: *2020 International Joint Conference on Neural Networks (IJCNN)*. IEEE, pp. 1–8.

Fujii, K. and K. Nakajima (2021). "Quantum reservoir computing: a reservoir approach toward quantum machine learning on near-term quantum devices". *Reservoir Computing: Theory, Physical Implementations, and Applications*, pp. 423–450.

Goldman-Rakic, P. S. (2011). "Circuitry of primate prefrontal cortex and regulation of behavior by representational memory". *Comprehensive physiology*, pp. 373–417.

Goñi, J. et al. (2014). "Resting-brain functional connectivity predicted by analytic measures of network communication". *Proc Natl Acad Sci USA*, 111(2), pp. 833–838.

Goulas, A., F. Damicelli, and C. C. Hilgetag (2021). "Bio-instantiated recurrent neural networks: Integrating neurobiology-based network topology in artificial networks". *Neural Networks*, 142, pp. 608–618.

Gray, C. M. and W. Singer (1989). "Stimulus-specific neuronal oscillations in orientation columns of cat visual cortex." *Proceedings of the National Academy of Sciences*, 86(5), pp. 1698–1702.

Haeusler, S. and W. Maass (2007). "A statistical analysis of information-processing properties of lamina-specific cortical microcircuit models". *Cerebral cortex*, 17(1), pp. 149–162.

Harris, C. R. et al. (2020). "Array programming with NumPy". *Nature*, 585(7825), pp. 357–362.

Hauser, H. (2021). "Physical reservoir computing in robotics". *Reservoir Computing: Theory, Physical Implementations, and Applications*, pp. 169–190.

Hebb, D. O. (2005). *The organization of behavior: A neuropsychological theory*. Psychology Press.

Heuvel, M. P. Van den, E. T. Bullmore, and O. Sporns (2016). "Comparative connectomics". *Trends Cognitive Science*, 20(5), pp. 345–361.

Heuvel, M. P. van den et al. (2012). "High-cost, high-capacity backbone for global brain communication". *Proc Natl Acad Sci USA*, 109(28), pp. 11372–11377.

Hilgetag, C. C. and M. Kaiser (2004). "Clustered organization of cortical connectivity". *Neuroinformatics*, 2(3), pp. 353–360.

Hinaut, X. et al. (2015). "Corticostriatal response selection in sentence production: Insights from neural network simulation with reservoir computing". *Brain and language*, 150, pp. 54–68.

Hunter, J. D. (2007). "Matplotlib: A 2D graphics environment". *Computing in science & engineering*, 9(3), pp. 90–95.

Insel, T. R., S. C. Landis, and F. S. Collins (2013). "The NIH brain initiative". *Science*, 340(6133), pp. 687–688.

Jaeger, H. (2001). "The "echo state" approach to analysing and training recurrent neural networks-with an erratum note". *Bonn, Germany: German National Research Center for Information Technology GMD Technical Report*, 148(34), p. 13.

Kanemura, I. and K. Kitano (2023). "Association between different sensory modalities based on concurrent time series data obtained by a collaborative reservoir computing model". *Scientific Reports*, 13(1), p. 173.

Katumba, A. et al. (2017). "A multiple-input strategy to efficient integrated photonic reservoir computing". *Cognitive Computation*, 9(3), pp. 307–314.

Katumba, A. et al. (2018). "Low-loss photonic reservoir computing with multimode photonic integrated circuits". *Scientific reports*, 8(1), pp. 1–10.

Kawai, Y., J. Park, and M. Asada (2019). "A small-world topology enhances the echo state property and signal propagation in reservoir computing". *Neural Networks*, 112, pp. 15–23.

Kawai, Y. et al. (2017). "Echo in a small-world reservoir: Time-series prediction using an economical recurrent neural network". In: *2017 Joint IEEE International Conference on Development and Learning and Epigenetic Robotics (ICDL-EpiRob)*. IEEE, pp. 126–131.

Kendall, J. D., J. C. Nino, and L. E. Suárez (2018). *Deep learning in bipartite memristive networks*. US Patent App. 15/985,212.

Kitzbichler, M. G. et al. (2009). "Broadband criticality of human brain network synchronization". *PLoS Comput Biol*, 5(3), e1000314.

Kulkarni, M. S. and C. Teuscher (2012). "Memristor-based reservoir computing". In: *2012 IEEE/ACM international symposium on nanoscale architectures (NANOARCH)*. IEEE, pp. 226–232.

Langton, C. (1990). "Computation at the edge of chaos: Phase transition and emergent computation". *Physica D: nonlinear phenomena*, 42, pp. 12–37.

Laporte, F. et al. (2018). "Numerical demonstration of neuromorphic computing with photonic crystal cavities". *Optics express*, 26(7), pp. 7955–7964.

Larivière, S. et al. (2021). "The ENIGMA Toolbox: multiscale neural contextualization of multisite neuroimaging datasets". *Nature Methods*, 18(7), pp. 698–700.

Legenstein, R. and W. Maass (2007a). "Edge of chaos and prediction of computational performance for neural circuit models". *Neural Networks*, 20(3), pp. 323–334.

— (2007b). "What makes a dynamical system computationally powerful". *New directions in statistical signal processing: From systems to brain*, pp. 127–154.

Li, J. et al. (2018). "A deep learning based approach for analog hardware implementation of delayed feedback reservoir computing system". In: *2018 19th International Symposium on Quality Electronic Design (ISQED)*. IEEE, pp. 308–313.

Loeffler, A. et al. (2021). "Modularity and multitasking in neuro-memristive reservoir networks". *Neuromorphic Computing and Engineering*, 1(1), p. 014003.

Loeffler, A. et al. (2023). "Neuromorphic learning, working memory, and metaplasticity in nanowire networks". *Science Advances*, 9(16), eadg3289.

Lukoševičius, M. and H. Jaeger (2009). "Reservoir computing approaches to recurrent neural network training". *Computer Science Review*, 3(3), pp. 127–149.

Lukoševičius, M., H. Jaeger, and B. Schrauwen (2012). "Reservoir computing trends". *KI-Künstliche Intelligenz*, 26, pp. 365–371.

Maass, W. and H. Markram (2004). "On the computational power of circuits of spiking neurons". *Journal of computer and system sciences*, 69(4), pp. 593–616.

Maass, W., T. Natschläger, and H. Markram (2002). "Real-time computing without stable states: A new framework for neural computation based on perturbations". *Neural computation*, 14(11), pp. 2531–2560.

Mante, V. et al. (2013). "Context-dependent computation by recurrent dynamics in prefrontal cortex". *nature*, 503(7474), pp. 78–84.

Marblestone, A. H., G. Wayne, and K. P. Kording (2016). "Toward an integration of deep learning and neuroscience". *Frontiers in computational neuroscience*, p. 94.

Markello, R. D. et al. (2022). "Neuromaps: structural and functional interpretation of brain maps". *Nature Methods*, 19(11), pp. 1472–1479.

Markov, N. T. et al. (2011). "Weight consistency specifies regularities of macaque cortical networks". *Cerebral cortex*, 21(6), pp. 1254–1272.

Markram, H. et al. (1997). "Regulation of synaptic efficacy by coincidence of postsynaptic APs and EPSPs". *Science*, 275(5297), pp. 213–215.

Márton, C. D. et al. (2021). "Efficient and robust multi-task learning in the brain with modular latent primitives". *arXiv preprint arXiv:2105.14108*.

McKinney, W. et al. (2010). "Data structures for statistical computing in python". In: *Proceedings of the 9th Python in Science Conference*. Vol. 445. Austin, TX, pp. 51–56.

Mealier, A.-L. et al. (2017). "Narrative constructions for the organization of self experience: Proof of concept via embodied robotics". *Frontiers in psychology*, 8, p. 1331.

Melozzi, F. et al. (2019). "Individual structural features constrain the functional connectome". *Proc Natl Acad Sci USA*, 116, pp. 26961–26969.

Mišić, B. and O. Sporns (2016). "From regions to connections and networks: new bridges between brain and behavior". *Curr Opin Neurobiol*, 40, pp. 1–7.

Molano-Mazon, M. et al. (2022). "NeuroGym: An open resource for developing and sharing neuroscience tasks".

Nakajima, K. (2020). "Physical reservoir computing—an introductory perspective". *Japanese Journal of Applied Physics*, 59(6), p. 060501.

Nakajima, K. and T. Aoyagi (2015). "The memory capacity of a physical liquid state machine". *IEICE Technical Report; IEICE Tech. Rep.*, 115(300), pp. 109–112.

Nakajima, K. et al. (2013). "A soft body as a reservoir: case studies in a dynamic model of octopus-inspired soft robotic arm". *Frontiers in computational neuroscience*, 7, p. 91.

Natschläger, T., W. Maass, and H. Markram (2002). "The" liquid computer": A novel strategy for real-time computing on time series". *Telematik*, 8(ARTICLE), pp. 39–43.

Negoro, M. et al. (2021). "Toward NMR quantum reservoir computing". *Reservoir Computing: Theory, Physical Implementations, and Applications*, pp. 451–458.

Nomura, H., H. Kubota, and Y. Suzuki (2021). "Reservoir computing with dipole-coupled nanomagnets". *Reservoir Computing: Theory, Physical Implementations, and Applications*, pp. 361–374.

Oliphant, T. E. (2006). *A guide to NumPy*. Vol. 1. Trelgol Publishing USA.

O'Byrne, J. and K. Jerbi (2022). "How critical is brain criticality?" *Trends in Neurosciences*.

Pedregosa, F. et al. (2011). "Scikit-learn: Machine learning in Python". *Journal of machine Learning research*, 12, pp. 2825–2830.

Power, J. D. et al. (2011). "Functional network organization of the human brain". *Neuron*, 72(4), pp. 665–678.

Prince, L. Y. et al. (2021). "Current State and Future Directions for Learning in Biological Recurrent Neural Networks: A Perspective Piece". *arXiv preprint arXiv:2105.05382*.

Richards, B. A. et al. (2019). "A deep learning framework for neuroscience". *Nat Neurosci*, 22(11), pp. 1761–1770.

Rigotti, M. et al. (2013). "The importance of mixed selectivity in complex cognitive tasks". *Nature*, 497(7451), pp. 585–590.

Riou, M. et al. (2021). "Reservoir computing leveraging the transient non-linear dynamics of spin-torque nano-oscillators". *Reservoir Computing: Theory, Physical Implementations, and Applications*, pp. 307–329.

Ritter, P. et al. (2013). "The virtual brain integrates computational modeling and multimodal neuroimaging". *Brain connectivity*, 3(2), pp. 121–145.

Rodriguez, N., E. Izquierdo, and Y.-Y. Ahn (2019). "Optimal modularity and memory capacity of neural reservoirs". *Network Neuroscience*, 3(2), pp. 551–566.

Rubinov, M. and O. Sporns (2010). "Complex network measures of brain connectivity: uses and interpretations". *Neuroimage*, 52(3), pp. 1059–1069.

Schaefer, A. et al. (2018). "Local-global parcellation of the human cerebral cortex from intrinsic functional connectivity MRI". *Cereb Cortex*, 28(9), pp. 3095–3114.

Seguin, C., Y. Tian, and A. Zalesky (2020). "Network communication models improve the behavioral and functional predictive utility of the human structural connectome". *Network Neuroscience*, (X), pp. 1–40.

Selemon, L. and P. Goldman-Rakic (1985). "Longitudinal topography and interdigitation of corticostriatal projections in the rhesus monkey". *Journal of Neuroscience*, 5(3), pp. 776–794.

Selemon, L. D. and P. S. Goldman-Rakic (1988). "Common cortical and subcortical targets of the dorsolateral prefrontal and posterior parietal cortices in the rhesus monkey: evidence for a distributed neural network subserving spatially guided behavior". *Journal of Neuroscience*, 8(11), pp. 4049–4068.

Sethi, S. S. et al. (2017). "Structural connectome topology relates to regional BOLD signal dynamics in the mouse brain". *Chaos*, 27(4), p. 047405.

Seung, H. S. (1996). "How the brain keeps the eyes still". *Proceedings of the National Academy of Sciences*, 93(23), pp. 13339–13344.

Shine, J. M. et al. (2018). "The modulation of neural gain facilitates a transition between functional segregation and integration in the brain". *eLife*, 7, e31130.

Sillin, H. O. et al. (2013). "A theoretical and experimental study of neuromorphic atomic switch networks for reservoir computing". *Nanotechnology*, 24(38), p. 384004.

Singer, W. (1993). "Synchronization of cortical activity and its putative role in information processing and learning". *Annual review of physiology*, 55(1), pp. 349–374.

— (1999). "Neuronal synchrony: a versatile code for the definition of relations?" *Neuron*, 24(1), pp. 49–65.

Singer, W. (2021). "The Cerebral Cortex: A Delay-Coupled Recurrent Oscillator Network?" *Reservoir Computing: Theory, Physical Implementations, and Applications*, pp. 3–28.

Singer, W. and C. M. Gray (1995). "Visual feature integration and the temporal correlation hypothesis". *Annual review of neuroscience*, 18(1), pp. 555–586.

Smith, S. M. et al. (2009). "Correspondence of the brain's functional architecture during activation and rest". *Proc Natl Acad Sci USA*, 106(31), pp. 13040–13045.

Soriano, M. C. et al. (2014). "Delay-based reservoir computing: noise effects in a combined analog and digital implementation". *IEEE transactions on neural networks and learning systems*, 26(2), pp. 388–393.

Sporns, O. (2013). "Network attributes for segregation and integration in the human brain". *Current opinion in neurobiology*, 23(2), pp. 162–171.

— (2022). "Structure and function of complex brain networks". *Dialogues in clinical neuroscience*.

Sporns, O., G. Tononi, and R. Kötter (2005). "The human connectome: a structural description of the human brain". *PLoS Comput Biol*, 1(4), e42.

Sporns, O. and J. D. Zwi (2004). "The small world of the cerebral cortex". *Neuroinformatics*, 2(2), pp. 145–162.

Stadler, M. A. (1993). "Implicit serial learning: Questions inspired by Hebb (1961)". *Memory & cognition*, 21, pp. 819–827.

Suárez, L. E., J. D. Kendall, and J. C. Nino (2018). "Evaluation of the computational capabilities of a memristive random network (MN3) under the context of reservoir computing". *Neural Networks*, 106, pp. 223–236.

Suárez, L. E. et al. (2020). "Linking structure and function in macroscale brain networks". *Trends in Cognitive Sciences*, 24(4), pp. 302–315.

Suárez, L. E. et al. (2021). "Learning function from structure in neuromorphic networks". *Nature Machine Intelligence*, 3(9), pp. 771–786.

Suarez, L. E. et al. (2022). "A connectomics-based taxonomy of mammals". *Elife*, 11, e78635.

Subramoney, A., F. Scherr, and W. Maass (2021). "Reservoirs learn to learn". *Reservoir Computing: Theory, Physical Implementations, and Applications*, pp. 59–76.

Sussillo, D. et al. (2015). "A neural network that finds a naturalistic solution for the production of muscle activity". *Nature neuroscience*, 18(7), pp. 1025–1033.

Tagliazucchi, E. et al. (2012). "Criticality in large-scale brain fMRI dynamics unveiled by a novel point process analysis". *Frontiers in physiology*, 3, p. 15.

Tanaka, G. et al. (2019). "Recent advances in physical reservoir computing: A review". *Neural Networks*, 115, pp. 100–123.

Taniguchi, T. et al. (2021). "Reservoir Computing Based on Spintronics Technology". *Reservoir Computing: Theory, Physical Implementations, and Applications*, pp. 331–360.

Thomas Yeo, B. et al. (2011). "The organization of the human cerebral cortex estimated by intrinsic functional connectivity". *J Neurophysiol*, 106(3), pp. 1125–1165.

Uddin, L. Q. (2020). "Bring the noise: Reconceptualizing spontaneous neural activity". *Trends Cogn Sci*.

Vandoorne, K. et al. (2008). "Toward optical signal processing using photonic reservoir computing". *Optics express*, 16(15), pp. 11182–11192.

Vandoorne, K. et al. (2014). "Experimental demonstration of reservoir computing on a silicon photonics chip". *Nature communications*, 5(1), pp. 1–6.

Verstraeten, D. et al. (2007). "An experimental unification of reservoir computing methods". *Neural networks*, 20(3), pp. 391–403.

Virtanen, P. et al. (2020). "SciPy 1.0: fundamental algorithms for scientific computing in Python". *Nature methods*, 17(3), pp. 261–272.

Walt, S. v. d., S. C. Colbert, and G. Varoquaux (2011). "The NumPy array: a structure for efficient numerical computation". *Computing in science & engineering*, 13(2), pp. 22–30.

Wang, H. et al. (2011). "Recurrent neural networks: Associative memory and optimization". *Journal of Information Technology and Software Engineering*, 1(104), p. 2.

Wang, Q. et al. (2017). "Energy efficient parallel neuromorphic architectures with approximate arithmetic on FPGA". *Neurocomputing*, 221, pp. 146–158.

Waskom, M. et al. (2016). "seaborn: v0. 7.0 (January 2016)". *zenodo10*, 5281.

Watts, D. J. and S. H. Strogatz (1998). "Collective dynamics of small-world networks". *Nature*, 393(6684), p. 440.

Whittington, M. A. et al. (2000). "Inhibition-based rhythms: experimental and mathematical observations on network dynamics". *International journal of psychophysiology*, 38(3), pp. 315–336.

Wyffels, F. and B. Schrauwen (2009). "Design of a central pattern generator using reservoir computing for learning human motion". In: *2009 Advanced Technologies for Enhanced Quality of Life*. IEEE, pp. 118–122.

Yang, X., W. Chen, and F. Z. Wang (2016). "Investigations of the staircase memristor model and applications of memristor-based local connections". *Analog Integrated Circuits and Signal Processing*, 87(2), pp. 263–273.

Yarkoni, T et al. (2011). "NeuroSynth: a new platform for large-scale automated synthesis of human functional neuroimaging data Frontiers in Neuroinformatics Conference Abstract: 4th INCF Congress of Neuroinformatics". In: *Boston, United States. doi: 10.3389/conf. fninf*. Vol. 58.

Zamora-López, G., C. Zhou, and J. Kurths (2010). "Cortical hubs form a module for multisensory integration on top of the hierarchy of cortical networks". *Front Neuroinform*, 4, p. 1.

Zhang, H. et al. (2014). "Integrated photonic reservoir computing based on hierarchical time-multiplexing structure". *Optics express*, 22(25), pp. 31356–31370.

Zhang, M. and M. Saggar (2020). "Complexity of intrinsic brain dynamics shaped by multiscale structural constraints". *BioRxiv*, pp. 2020–05.

Zhao, C. et al. (2016). "Novel spike based reservoir node design with high performance spike delay loop". In: *Proceedings of the 3rd ACM International Conference on Nanoscale Computing and Communication*, pp. 1–5.

Chapter 5

A connectomics-based taxonomy of mammals

Laura E. Suárez[1,5], Yossi Yovel[2], Martijn P. van den Heuvel[3], Olaf Sporns[4], Yaniv Assaf[2], Guillaume Lajoie[5], & Bratislav Misic[1]

[1]McConnell Brain Imaging Centre, Montréal Neurological Institute, McGill University, Montréal, Canada [2]School of Neurobiology, Biochemistry and Biophysics, Tel Aviv University, Tel Aviv, Israel [3]Center for Neurogenomics and Cognitive Research, Vrije Universiteit Amsterdam, Amsterdam, Netherlands [4]Psychological and Brain Sciences, Indiana University, IN, USA [5]Mila, Quebec Artificial Intelligence Institute, Montréal, QC, Canada

Published in:
eLife: https://doi.org/10.7554/eLife.78635

5.1 Preface

Whereas previous chapters investigated the link between structure and function with an emphasis on the computational properties of biological connectomes, this chapter examines the link between structure and function through the lenses of evolution. Natural selection shapes cognitive abilities and behavior in the same way it shapes morphological traits (Bendesky and Bargmann, 2011; Yokoyama et al., 2021; York, 2018). Therefore, understanding differences and similarities in connectome architecture across phylogeny is also an important piece in the puzzle of understanding the link between structure and function

in brain networks. Early taxonomical systems classified animals species based on morphological and functional similarities (Darwin, 1959). Thanks to advances in whole-genome sequencing technologies, many of these classification schemes have been recently validated by genetic data (Álvarez-Carretero et al., 2021; Consortium et al., 2020; Murphy et al., 2021; Seehausen et al., 2014). Using the comprehensive MaMI data set (Assaf et al., 2020), which encompasses MRI connectomes of more than a hundred different species of mammals, this study explores the hypothesis of whether variations in connectome architecture, byproduct of speciation events in the genome, are concomitant with adaptations in cognition and behaviour. To do so, I quantify inter-species similarities based on brain wiring and assess the extent to which they reflect already established taxonomic relationships based on morphology, genetics and behaviour. Drawing compelling conclusions in previous studies comparing connectomes across species was hindered by the restricted number of samples and the fact that connectomes had been obtained through different imaging techniques or reconstructed at spatial scales that were not comparable (Heuvel et al., 2016). A major advantage of the MaMI dataset is that most connectomes were obtained with the same scanner, using uniform acquisition and reconstruction protocols, not to mention the larger sample size. All these factors make for a more reasonable and founded comparison. Altogether, this work highlights the importance of combining multimodal data, including genomics, connectomics and behavioural data, to develop a more mechanistic understanding of how genes manifest in diverse neural circuit architectures, and ultimately, giving rise to species-specific cognitive and behavioral adaptations.

5.2 Abstract

Mammalian taxonomies are conventionally defined by morphological traits and genetics. How species differ in terms of neural circuits and whether inter-species differences in neural circuit organization conform to these taxonomies is unknown. The main obstacle for the comparison of neural architectures have been differences in network reconstruction techniques, yielding species-specific connectomes that are not directly comparable to one another. Here we comprehensively chart connectome organization across the mammalian phylogenetic spectrum using a common reconstruction protocol. We analyze the mammalian MRI (MaMI) data set, a database that encompasses high-resolution *ex vivo* structural and diffusion magnetic resonance imaging (MRI) scans of 124 species across 12 taxonomic orders and 5 superorders, collected using a unified MRI protocol. We assess similarity between species connectomes using two methods: similarity of Laplacian eigenspectra

and similarity of multiscale topological features. We find greater inter-species similarities among species within the same taxonomic order, suggesting that connectome organization reflects established taxonomic relationships defined by morphology and genetics. While all connectomes retain hallmark global features and relative proportions of connection classes, inter-species variation is driven by local regional connectivity profiles. By encoding connectomes into a common frame of reference, these findings establish a foundation for investigating how neural circuits change over phylogeny, forging a link from genes to circuits to behaviour.

5.3 Introduction

Anatomical projections between brain regions form a complex network of polyfunctional neural circuits (Sporns et al., 2005). Signaling on the brain's connectome is thought to support cognition and the emergence of adaptive behaviour. Advances in imaging technologies have made it increasingly feasible to reconstruct the wiring diagram of biological neural networks. Thanks to extensive international data sharing efforts, these detailed reconstructions of the nervous system's connection patterns have been made available in humans and in multiple model organisms (Heuvel et al., 2016), including invertebrate (Chiang et al., 2011; Towlson et al., 2013; White et al., 1986; Worrell et al., 2017), avian (Shanahan et al., 2013), rodent (Bota et al., 2015; Oh et al., 2014; Rubinov et al., 2015), feline (Beul et al., 2015; Reus and Heuvel, 2013; Scannell et al., 1995) and primate species (Liu et al., 2020; Majka et al., 2016; Markov et al., 2012).

The rising availability of connectomics data facilitates cross-species comparative studies that identify commonalities in brain network topology and universal principles of connectome evolution (Barker, 2021; Barsotti et al., 2021; Heuvel et al., 2016). A common thread throughout these studies is the existence of non-random topological attributes that theoretically enhance the capacity for information processing (Sporns, 2013). These include a highly clustered architecture with segregated modules that promote specialized information processing (Hilgetag and Kaiser, 2004; Watts and Strogatz, 1998), as well as a densely interconnected core of high-degree hubs that shortens communication pathways (Heuvel et al., 2012), promoting the integration of information from distributed specialized domains (Avena-Koenigsberger et al., 2018; Zamora-López et al., 2010). These universal organizational features suggest that connectome evolution has been shaped by two opposing and competitive pressures: maintaining efficient communication while minimizing neural resources used for connectivity (Bullmore and Sporns, 2012).

While comparative analysis can focus on commonalities among mammalian connectomes and identify universal wiring principles, it can also be used to systematically explore differences among connectomes that confer specific adaptive advantages. Indeed, despite commonalities, architectural variations are also observed even among closely related species (Barker, 2021). Factors such as the external environment, genetics and distinct gene expression programs also account for diversity in neural connectivity patterns (Martinez and Sprecher, 2020). Subtle variations in connectome organization may potentially account for species-specific adaptations in behaviour and cognitive function.

But how does the connectome vary over phylogeny? Traditionally, mammalian taxonomies were built on morphological differences among species (Darwin, 1959). Besides physical commonalities, species within the same taxonomic group also tend to share similar behavioural repertoires (Bendesky and Bargmann, 2011; Yokoyama et al., 2021; York, 2018). Modern high-throughput whole-genome sequencing has further delineated phylogenetic links and relationships among mammalian species (Álvarez-Carretero et al., 2021; Consortium et al., 2020; Murphy et al., 2021; Seehausen et al., 2014). In addition to refining the overall classification of mammals, whole-genome comparative analyses have established the genetic basis of phenotypic variation across phylogeny (Murphy et al., 2021). Whether inter-species differences in the organization of connectome wiring conform to this taxonomy remains unknown. How do genes sculpt behaviour across evolution? Could speciation events in the genome leading to variations in connectome architecture be the missing link between genomics and behaviour? Rigorously addressing these questions is challenging due to the lack of methodological consistency in the acquisition and reconstruction of neural circuits, or the limited number of available species.

Here we comprehensively chart connectome organization across the mammalian phylogenetic spectrum. We analyze the mammalian MRI (MaMI) data set, a comprehensive database that encompasses high-resolution *ex vivo* diffusion and structural (T1- and T2-weighted) MRI scans of 124 species (a total of 225 scans including replicas) (Assaf et al., 2020). All images were acquired using the same scanner and protocol. All connectomes were reconstructed using a uniform parcellation scheme consisting of 200 brain areas, including cortical and subcortical regions. Notably, the MaMI data set spans a wide range of categories across different taxa levels of morphologic and phylogenetic mammalian taxonomies (Assaf et al., 2020). Specifically, it includes animal species across 5 different superorders (Afrotheria, Euarchontoglires, Laurasiatheria, Xenarthra and Marsupialia) and 12 different orders (Cetartiodactyla, Carnivora, Chiroptera, Eulipotyphla, Hyracoidea, Lagomorpha, Marsupialia, Perissodactyla, Primates, Rodentia, Scandentia and Xenarthra).

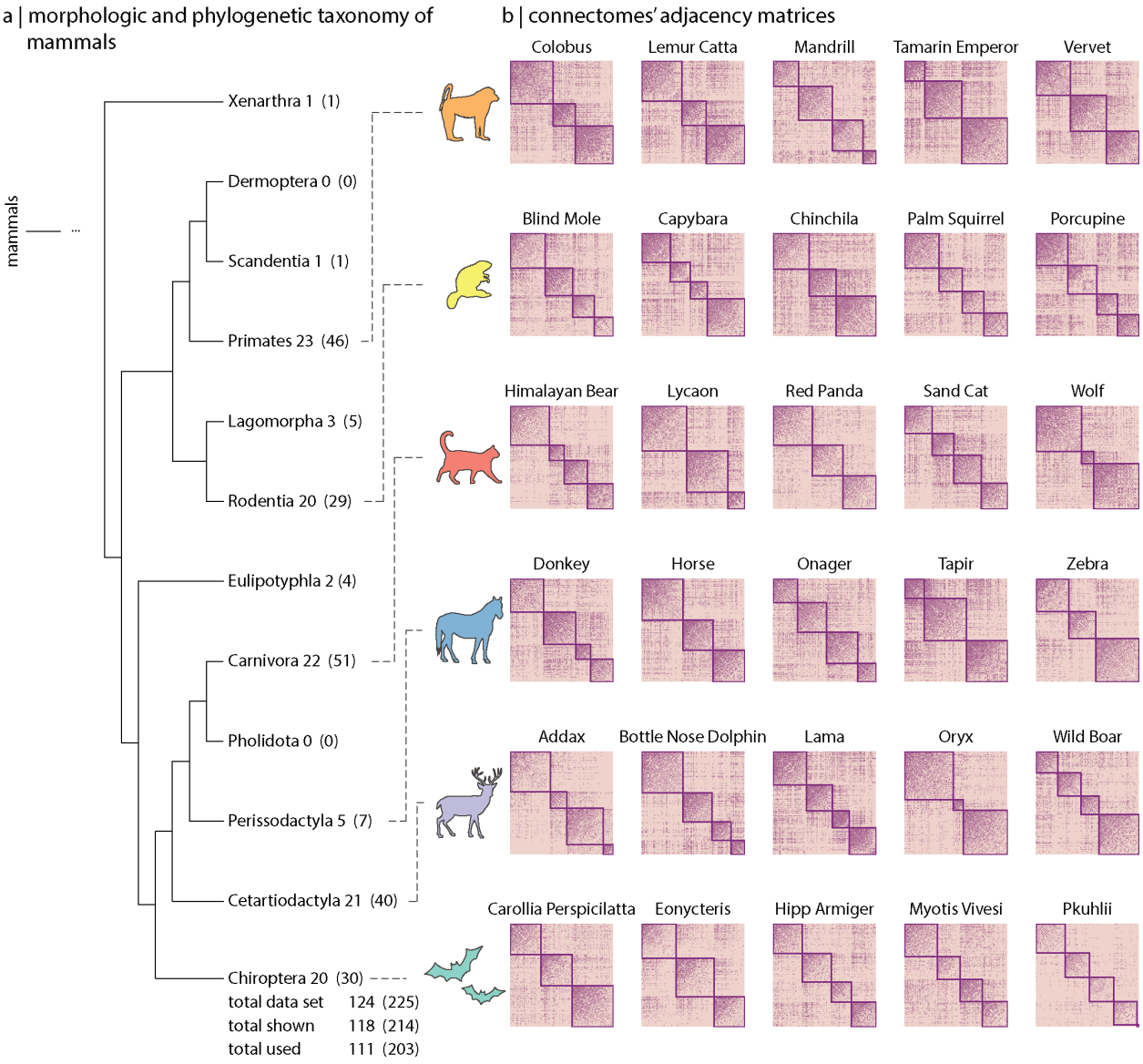

Figure 5.1: **MaMI data set** | The MaMI data set encompasses high-resolution *ex vivo* structural and diffusion MRI scans of 124 animal species spanning 12 morphologically and phylogenetically defined taxonomic orders: Cetartiodactyla, Carnivora, Chiroptera, Eulipotyphla, Hyracoidea, Lagomorpha, Marsupialia, Perissodactyla, Primates, Rodentia, Scandentia and Xenarthra. (a) Hierarchical relationships across 10 (out of the 12 included in the data set) morphologic and phylogenetic taxonomic orders. Numbers outside the parenthesis correspond to the number of unique species within each order and numbers inside the parenthesis correspond to the number of samples (including replicas). (b) Connectivity matrices for 5 randomly-chosen sample species within each of the six orders included in the analyses (i.e. Cetartiodactyla, Carnivora, Chiroptera, Perissodactyla, Primates and Rodentia). Only orders with at least 5 different species were included for the analyses. Nodes are organized according to their community affiliation obtained from consensus clustering applied on the connectivity matrix (see *Methods*). Communities in (b) correspond to the partition for which the resolution parameter $\gamma = 1.0$ (Fig. S5.1).

Taking advantage of the harmonized imaging and reconstruction protocols, we quantitatively assess the similarity of species' connectomes to construct data-driven phylogenetic relationships based on brain wiring. We compare these inter-species wiring similarities with conventional morphologically and genetically defined mammalian taxonomies. We determine the extent to which connectome topology conforms to established taxonomic classes, and identify network features that are associated with speciation.

5.4 Results

The MaMI data set consists of high-resolution *ex vivo* diffusion and structural (T1- and T2-weighted) MRI scans of 124 species. Since there is no species-specific template, all connectomes were reconstructed using a uniformly applied 200-node parcellation. Having equally sized networks facilitates graph comparison but also implies a lack of direct correspondence between nodes across species. However, because our focus is on the statistics of connectomes' topology, this does not impact our analyses. As the size of the network is kept constant across all species, voxel size is normalized to brain volume. Fig. 5.1 shows the distribution of connectomes across ten mammalian orders (out of the twelve present in the data set). We focus on the six orders that contain 5 or more distinct species (within the Laurasiatheria and Euarchontoglires superorders); these include Chiroptera, Rodentia, Cetartiodactyla, Carnivora, Perissodactyla and Primates, resulting in a total of 111 different animal species and 203 brain scans. A complete list of the animal species included in the data set is provided in Table S5.1.

5.4.1 Connectome-based inter-species distances

Similarity between species' network architectures is estimated using two network-based distance metrics: spectral distance, based on the eigenspectrum of the normalized Laplacian of the connectivity matrix (see Fig. S5.2; (Lange et al., 2014)), and topological distance, based on a combination of multiscale graph features of the binary and weighted connectivity matrices (Fig. S5.3 and Fig. S5.4 show the distribution of individual local and global graph features, respectively; (Rubinov and Sporns, 2010). For completeness, Fig. S5.5 and Fig. S5.6 show the cumulative distribution of binary and weighted local features, respectively, for individual species). Both methods measure how similar the architectures of two connectomes are. To identify brain connectivity differences across species, we need to be able to analyze data in a shared frame of reference. The normalized Laplacian eigenspectrum and the graph features of the connectivity matrix allow us to translate

connectomes into a common feature space in which they are comparable, despite the fact that they come from different species, and that the nodes do not correspond to one another (Mars et al., 2021). To account for the fact that some of the species have more than one scan, we randomly select one sample per species and estimate (spectral and topological) inter-species distances. We repeat this procedure 10,000 times and report the average across iterations.

Fig. 5.2a shows the spectral distances between species' connectomes. In general we observe smaller distances among members of the same order (outlined in yellow). Fig. 5.2b confirms this intuition by showing that spectral distances within orders (i.e. values along the diagonal) tend to be smaller than distances between orders (i.e. values off the diagonal). Fig. 5.2c shows the distributions of intra- and inter-order distances. The mean/median intra-order distance is significantly smaller than the mean/median inter-order distance (two-sample Welch's t-test: mean intra- and inter-order distances are 0.43 and 0.55, respectively, $P < 10^{-4}$ two-tailed, and Cohen's d effect size = 0.67; two-sample Mann-Whitney U test: median intra- and inter-order distances are 0.44 and 0.55, respectively, $P < 10^{-4}$ two-tailed, and common-language effect size = 68%; Fig. 5.2c). We find comparable results when estimating species similarity using topological distance (two-sample Welch's t-test: mean intra- and inter-order distances are 0.41 and 0.53, respectively, $P < 10^{-4}$ two-tailed, and Cohen's d effect size = 0.59; two-sample Mann-Whitney U test: median intra- and inter-order distances are 0.41 and 0.53, respectively, $P < 10^{-4}$ two-tailed, and common-language effect size = 66%; Fig. 5.2d-f). Fig. S5.7 shows the same results as in Fig. 5.2, but using all samples including replicas (i.e. without random resampling). Altogether, results suggest that species with similar genetics, morphology and behavior tend to have similar connectome architecture. In other words, variations in connectome architecture reflect phylogeny.

5.4.2 Architectural features differentiate species

Next we consider which network features contribute to the differentiation (Fig. S5.3 and Fig. S5.4 show the distributions of local and global graph features, respectively). To address this question we recompute inter-species topological distances using different sets of graph features (Fig. 5.3). We find that the difference between intra- and inter-order topological distances tends to be larger when only local (node-level) features are included in the estimation of the topological distance (i.e. degree, clustering coefficient, betweenness and closeness; Fig. 5.3b,e), compared to when only global features are considered (i.e. characteristic path length, transitivity and assortativity; Fig. 5.3c,f). This is the case for

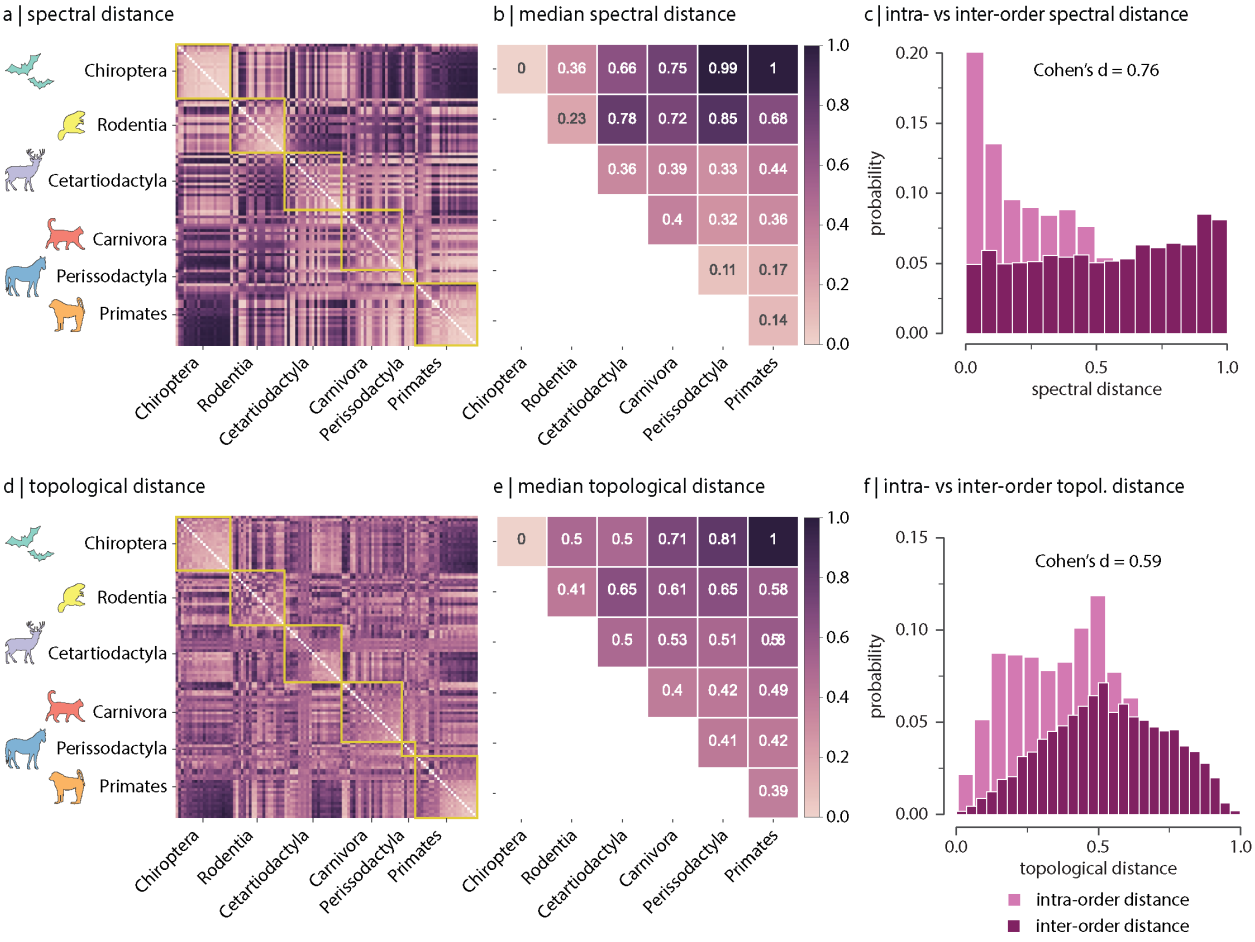

Figure 5.2: **Spectral and topological distance between orders** | (a) Spectral distance between species-specific connectomes. Lower distances indicate greater similarity. Yellow outlines indicate morphologically and genetically-defined orders. (b) Median spectral distance within and between all constituent members of each order. (c) Distribution of intra- and inter-order spectral distances. (d) Topological distance between species-specific connectomes. Lower distances indicate greater similarity. Yellow outlines indicate morphologically and genetically-defined orders. (e) Median topological distance within and between all constituent members of each order. (f) Distribution of intra- and inter-order topological distances. Effect sizes in (c) and (f) are Cohen's d estimator corresponding to a two-sample Welch's t-test ($P < 10^{-4}$). Equivalent conclusions are drawn if common-language effects sizes from the two-sample Mann-Whitney U test are used.

both the binary and weighted versions of these features (top and bottom rows in Fig. 5.3, respectively). Fig. S5.8 shows the same results as in Fig. 5.3, but using all samples including replicas (i.e. without random resampling). These results suggest that differentiation of orders is better explained by differences in local network topology; conversely, global network topology appears to be conserved across species. An illustration of this principle is depicted in Fig. S5.9 showing that the relative local connectivity of the anterior and the posterior ends of the cortex changes across taxonomic orders (Barrett et al., 2020; Krubitzer and Kaas, 2005; Krubitzer and Kahn, 2003).

A similar conclusion can be drawn when the eigenvalue distributions of the (normalized) Laplacian of the connectivity matrices are compared across species (Fig. S5.2). In spectral graph theory, the presence of eigenvalues with high multiplicities or eigenvalues symmetric around $\lambda_i = 1$ provide information about the network's local organization that results from the recursive manipulation of connectivity motifs (Banerjee and Jost, 2008, 2009; Lange et al., 2014). For instance, node duplication (i.e. the presence of nodes with the same connectivity profile) results in an increase of $\lambda_i = 1$. The duplication of edge motifs (i.e. the multiple presence of pairs of connected nodes with the same connectivity profile), on the other hand, produces eigenvalues at equal distances to $\lambda_i = 1$. Visually inspecting their Laplacian eigenspectra, one can notice that, across taxonomic orders, species tend to differ mostly around the interval $0.5 \leq \lambda_i \leq 1.5$, both in terms of the multiplicity of $\lambda_i = 1$, as well as in the width of the bell-shaped curve around $\lambda_i = 1$. While differences in the multiplicity of $\lambda_i = 1$ indicate differential amounts of duplicated node motifs present in the network, differences in the value and multiplicity of eigenvalues around $\lambda_i = 1$ indicate the presence of distinct edge motifs with disparate numbers of duplications in the network. Therefore, differences across taxonomic orders are most likely due to the presence of different local connectivity fingerprints in the connectivity matrix (Fig. S5.2) (Lange et al., 2014; Mars et al., 2018a,b). Determining which are specifically these node and edge motifs cannot be done by simply examining the Laplacian eigenspectra, and is out of the scope of the present study. Additional evidence supporting the idea that spectral distance captures mostly differences in local network topology is the fact that the correlation between spectral and topological distance is maximum when only local features are included in the estimation of the topological distance (Fig. S5.10).

We also observe that that the difference between intra- and inter-order topological distances is greater for binary than for weighted features (Fig. 5.3 a–c and d–f, respectively), independently of being local or global. This suggests that the strength of the connections is less important than the binary architecture of the connectivity matrix.

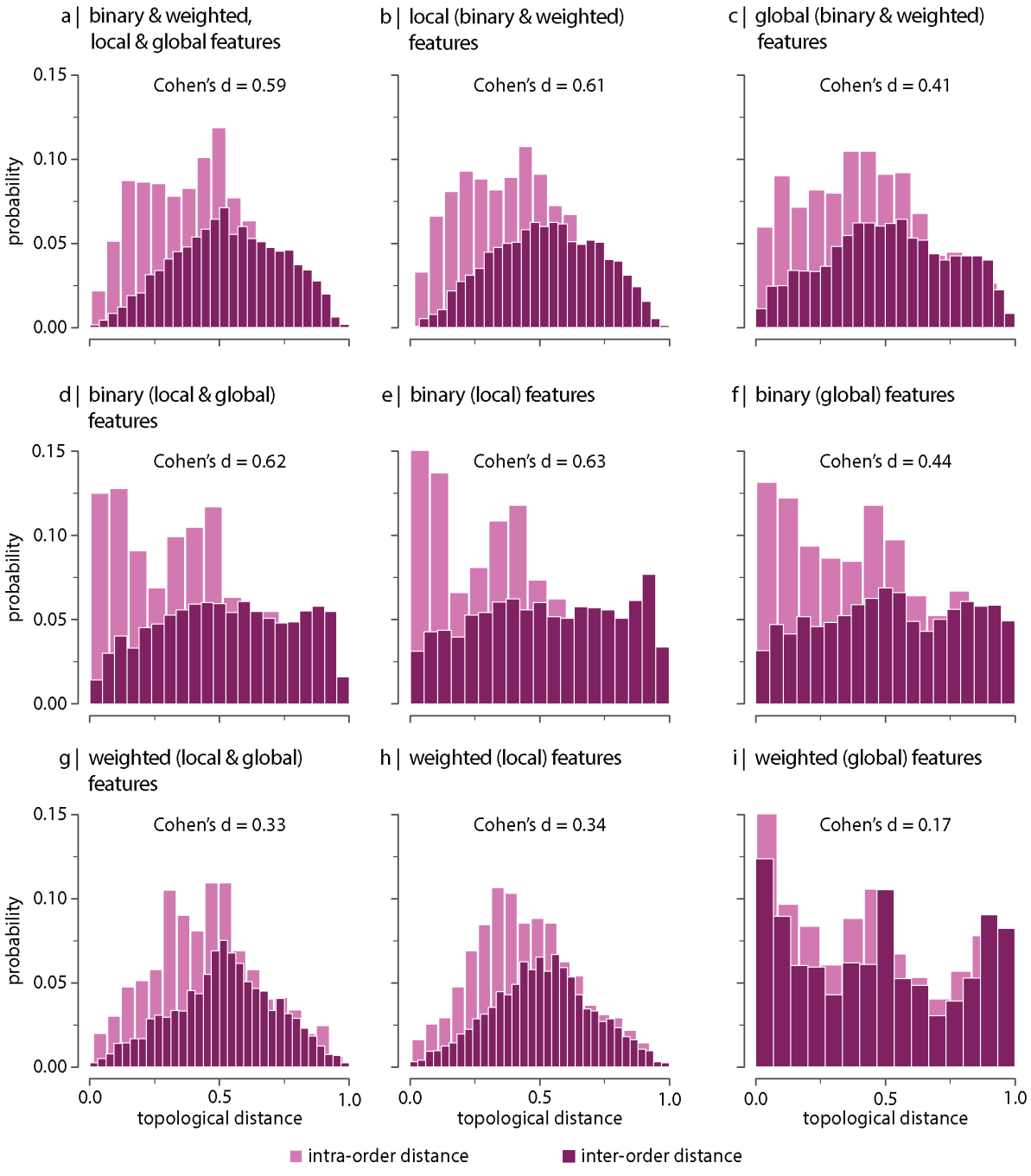

Figure 5.3: **Contribution of network features** | Topological distance can be computed using different combinations of local and global, binary and weighted connectome features. Histograms show intra- and inter-order distance distributions when using (a) all (binary, weighted, local and global), (b) all local (binary and weighted), (c) all global (binary and weighted), (d) all binary (local and global), (e) only binary local, (f) only binary global, (g) all weighted (local and global), (h) only weighted local and (i) only weighted global features. Local features include (the average and standard deviation of) degree, clustering, betweenness, and closeness. Global features include characteristic path length, transitivity, and assortativity. For definitions please see *Methods*. Effect sizes correspond to Cohen's d estimator from a two-sample Welch's t-test. Equivalent conclusions are drawn if common-language effects sizes from a two-sample Mann-Whitney U test are used. In all cases, the difference in the mean and median of intra- and inter-order distance distributions is statistically significant ($P < 10^{-4}$). The same conclusions can be drawn after controlling for network density (Fig. S5.13).

Some of the features used for the estimation of the topological distance depend on network density, which varies across taxonomic orders (Fig. S5.11). To determine whether the observed differences between intra- and inter-order distances are above and beyond differences due to network density, we perform the same analysis shown in Fig. 5.3, after controlling for density (Fig. S5.12). Results, shown in Fig. S5.13, suggest that differences between intra- and inter-order topological distances are not driven by differences in network density, but variations in wiring patterns, as captured by topological features, play a role in the observed phylogenetic variations in connectome organization.

Altogether, our results show that the subset of features that best differentiate species across taxonomic orders are the binary local topological features. We perform a set of complementary analyses to assess which subset of features produces the best partition of animal species relative to traditional taxonomies. To do so, we a) project the data on a 2D plane using multidimensional scaling (Fig. S5.14), and b) apply hierarchical clustering to inter-species distance matrices (Fig. S5.15). Visual inspection of these results suggests that, consistent with our previous results (Fig. 5.3), local features compared to global features (ignoring panel a, center vs right column, respectively, in Fig. S5.14 and Fig. S5.15), as well as binary features compared to weighted features (ignoring panel a, center vs bottom row, respectively, in Fig. S5.14 and Fig. S5.15), yield species partitions that more closely reflect established phylogenetic relationships, further supporting the idea that connectome organization recapitulates traditional taxonomic relationships that are based on morphology and genetics.

5.4.3 Conservation of small-world architecture

Anatomical brain networks are thought to simultaneously reconcile the opposing demands of functional integration and segregation by combining the presence of functionally specialized clusters with short polysynaptic communication pathways (Bassett and Bullmore, 2006; Sporns, 2013; Sporns et al., 2005; Tononi et al., 1994). Such architecture is often referred to as small-world, and is observed in a wide variety of naturally occurring and engineered networks (Watts and Strogatz, 1998). Here we explore whether these principles of segregation and integration in global connectome organization are consistent across phylogeny. To do so, we estimate for each species the ratio of clustering coefficient to characteristic path length, normalized relative to a set of randomly rewired graphs that preserve the degree sequence of the nodes (Humphries and Gurney, 2008; Maslov and Sneppen, 2002; Rubinov and Sporns, 2010) (Fig. 5.4). Consistent with previous reports in individual species' connectomes (Bassett and Bullmore, 2006; Hilgetag and Kaiser,

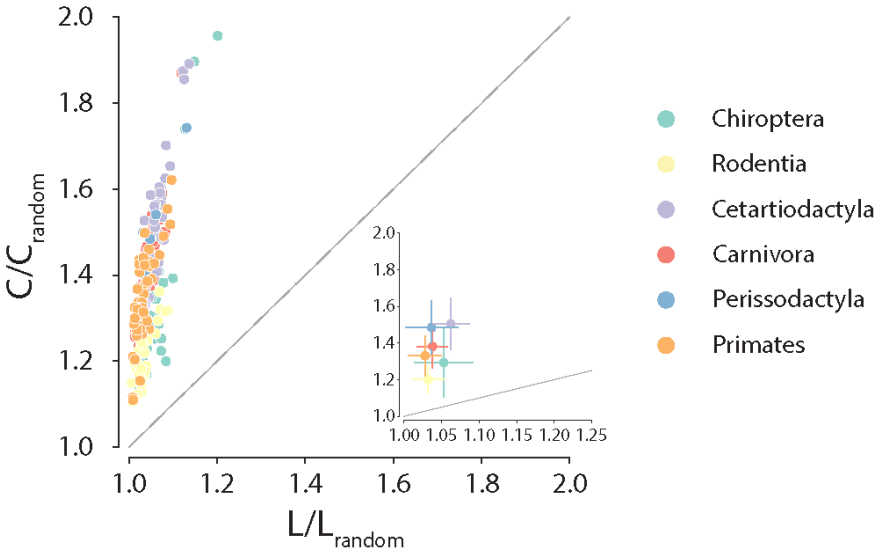

Figure 5.4: **Conservation of small-world architecture** | Clustering coefficient vs characteristic path length normalized relative to a set of 1000 randomly rewired graphs that preserve the degree sequence of the nodes (Maslov and Sneppen, 2002). For definitions of each graph measure, see *Methods*. Each data point represents a different animal species. Data points above the identity line are said to have small-world architecture. The inset on the right bottom corner is a zoom on the abscissa.

2004; Sporns and Zwi, 2004), we find that all connectomes display high and diverse levels of small-worldness, suggesting that simultaneously highly segregated and integrated networks is a global trait conserved across mammalian brains.

5.4.4 Conservation of edge classes across species

The topological and spatial arrangement of connections in connectomes is thought to shape the segregation and integration of information and, ultimately, their computational capacity (Faskowitz et al., 2021). To investigate inter-species differences in the topological and spatial distribution of connections, we stratify edges into different classes in four commonly studied partitions. Partitions include: inter- and intra-modular connections (Fig. 5.5a), inter- and intra-hemispheric connections (Fig. 5.5b), connection length distribution (short, medium and long-range connections; Fig. 5.5c and Fig. S5.16)), and rich-club (rich-club, feeder and peripheral connections; Fig. 5.5d). Overall, we find that, along the four partitions, the relative proportions of each connection class are conserved across taxonomic orders, despite differences in connection density. Collectively, this is consistent with the results from the previous sections showing that global architectural features of connectomes are consistent across phylogeny.

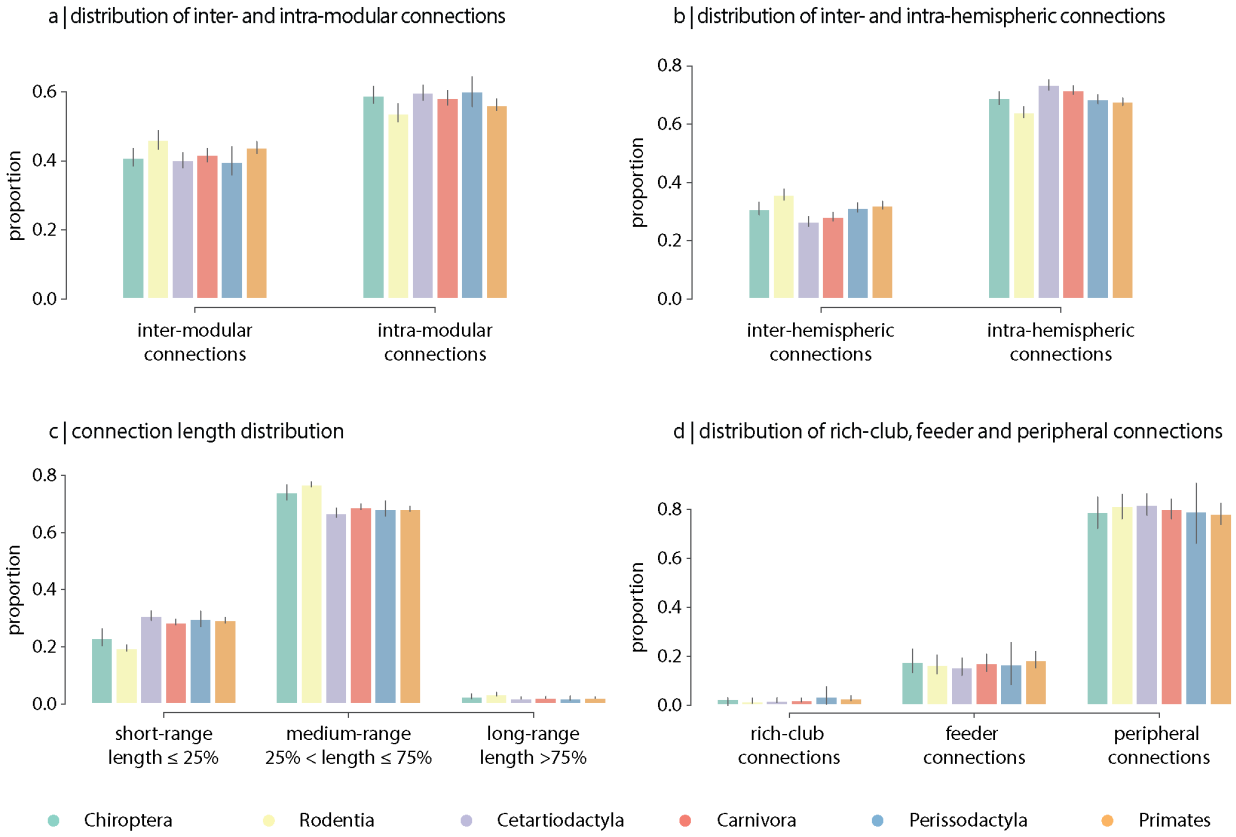

Figure 5.5: **Contribution of edge types** | (a) Connection density distribution for each taxononomic order. (b) Mean proportion of intra- and inter-hemispheric connections. (c) Mean proportion of short (length $\leq$ 25%), medium (25% $<$ length $\leq$ 75%) and long connections (length $\geq$ 75%). (d) Mean proportion of rich-club (connecting two rich club nodes), feeder (connecting one rich club and one non-rich club node) and peripheral (connecting two non-rich club nodes) connections. Error bars indicate 95% confidence intervals.

5.5 Discussion

In the present study we chart the organization of whole-brain neural circuits across 111 mammalian species and 5 superorders. We find that connectome organization recapitulates to a large extent traditional taxonomies. While all connectomes retain hallmark global features and relative proportions of edge classes, inter-species variation is driven by local regional connection profiles.

Conventional mammalian taxonomies are delineated based on the concept that a species is a group of organisms that can reproduce naturally with one another and create fertile offspring (Mallet, 1995). As a result, classical taxonomies based on animal morphology have largely been reconciled with emerging evidence from whole-genome sequencing (Baker and Bradley, 2006); namely, organisms with similar genomes display similar physical characteristics and behaviour. Our work shows that inter-species similarity – as defined by morphology, behaviour and genetics – is concomitant with the organization of neural circuits. Specifically, species that are part of the same taxonomic order tend to display similar connectome architecture, suggesting that brain network organization is under selection pressure (see also (Butler and King, 2004; Lande, 1976; Wright, 1931) for an alternative mechanism of trait evolution characterized by pure drift models based on Brownian motion), analogous to size, weight or color.

Which network features drive differences across taxonomic orders? Interestingly, all connectomes display consistent global hallmarks that were previously documented in tract-tracing studies, including high clustering and near-minimal path length characteristic of small-world organization, as well as segregated network communities and densely-interconnected hub nodes (Heuvel et al., 2016). The conservation in global wiring and organizational principles is further supported by a reduced difference between intra- and inter-order topological distances estimated exclusively from global features, compared to the case in which only local features are considered. Thus, relative differences between connectomes across taxonomic orders are mainly driven by local regional features. These results are in line with the idea that a brain region's functional fingerprint — the specific computation or function that it performs by virtue of its unique firing patterns and dynamics — is determined by its underlying cortico-cortical connectional fingerprint (Mars et al., 2021, 2016, 2018b; Passingham et al., 2002). Accordingly, inter-species differences in functional and behavioural repertoire are likely supported by changes in local connectivity patterns. Along the same lines, our results are also consistent with the notion that neural circuit evolution involves random local circuit modifications that may have provided

species with behavioral adaptations, allowing them to face specific challenges (Barker, 2021), such as extreme environmental pressures Eigenbrod et al., 2019; Park et al., 2008; Smith et al., 2011, or to support specific behaviours, such as courtship (Barkan et al., 2018; Ding et al., 2016, 2019; Khallaf et al., 2020; Markow and O'Grady, 2005; O'Grady and DeSalle, 2018; Seeholzer et al., 2018; York et al., 2019), social bonding (Insel and Shapiro, 1992; Jaggard et al., 2020; Loomis et al., 2019; Winslow et al., 1993), or foraging (Pantoja et al., 2020; Vanwalleghem et al., 2018). How computations and cognitive functions emerge from these species-specific circuit modifications remains a key question in the field (Buckner and Krienen, 2013; Suárez et al., 2021).

These results highlight the importance of developing species-specific, anatomical based parcellations, as well as new ways to align connectomes from different species. Understanding how homologous regions correspond to one another will allow further investigation of regional inter-species differences in connectome topology, which is a fundamental step for advancing comparative connectomics. A variety of emerging methods are contributing to further resolve correspondence between brain regions across species, facilitating fine-grained comparisons at the level of individual regions. These methods implement regional comparisons based on different data modalities including measures of cytoarchitecture (Bianchi et al., 2013; Garey, 1999), receptor distribution (Levant, 1998), functional and structural connectivity fingerprints (Mars et al., 2016, 2018b; Passingham et al., 2002), patterns of gene expression (Beauchamp et al., 2022; Warrington et al., 2022), and macro scale gradients of functional activation (Buckner and Margulies, 2019).

It is noteworthy that the relative proportion of edge classes (inter- vs intra-modular, inter- vs intra-hemispheric, short- vs medium- vs long-range and rich-club vs feeder vs peripheral) are preserved across species. This result is reminiscent of recent work on allometric scaling that investigates how white matter connectivity scales with brain size (Bullmore and Sporns, 2012). For example, species with fewer commissural inter-hemispheric connections exhibit lower hemispheric mean-shortest-path (i.e. stronger intra-hemispheric connectivity), suggesting a similar connectivity conservation principle (Assaf et al., 2020). Likewise, using diffusion-weighted MRI data across 14 different primate species, another study reported negative allometric scaling of cortical surface area with white matter volume and corpus callosum cross-sectional area (Ardesch et al., 2021). This scaling results in less space for white matter connectivity with increasing brain size, translating into larger brains with a relatively higher proportion of short-range connections than long-range connections when compared with smaller brains (Ardesch et al., 2021). These results, however, do not contradict studies showing a positive allometric scaling

between white matter and gray matter volume (Frahm et al., 1982; Schlenska, 1974; Theunissen, 1988; Zhang and Sejnowski, 2000); while the proportion of total volume devoted to cerebral white matter is higher in larger brains, it does not keep pace with the rapid cortical expansion that occurs with larger brain size. Collectively these studies highlight that the architecture of neural circuits and their physical embedding are intertwined, and the distribution of connections is such that it retains consistent global architectural features across phylogeny.

The present results contribute to the emerging field of comparative connectomics (Barker, 2021; Heuvel et al., 2016; Mars et al., 2021, 2018a; Tendler et al., 2021). Adopting a harmonized imaging protocol in a large number of mammalian species facilitates a rigorous quantitative comparison of neural circuits. Central to this are network analytic methods that map connectomes to a common space, and quantify similarities across local and global levels of organization (Bassett and Sporns, 2017; Lange et al., 2014; Lange et al., 2016; Mars et al., 2021, 2018b; Warrington et al., 2022). By comprehensively charting taxonomies of connectome architectures we may uncover the principles that govern the wiring of neural circuits (Avena-Koenigsberger et al., 2015). In particular, quantitative analysis of connectome architecture across phylogeny may help to link genomics and behaviour (Mišić and Sporns, 2016). Traditionally, taxonomic groups were defined in terms of physical morphology and behavioural repertoire (Burke, 1968), but these are now understood to be driven by speciation events in the genome (Álvarez-Carretero et al., 2021; Consortium et al., 2020; Murphy et al., 2021). However, we do not yet understand how genes influence neural circuit architecture, which in turn shapes the behavioural repertoire of an organism. By understanding how neural circuits change over phylogeny we can fill this gap and forge a link from genes to circuits to behaviour. Ultimately, the confluence of genomics, connectomics and behaviour may help to triangulate towards a more well-rounded view of speciation (Hernández-Hernández et al., 2021), and their simultaneous investigation can further illuminate the link between structure and function in brain networks (Bassett et al., 2010; Stiso and Bassett, 2018; Suárez et al., 2020).

The present work must be considered with respect to multiple limitations. First, uniformly parcellating brains of different size into the same number of nodes facilitates comparison of network architecture, but potentially obscures biologically important regional differences. Second, many species are represented by a single individual. Although we focus on orders rather than individual species and there is high within-species reliability (Assaf et al., 2020), the analyses do not capture individual variability within species. Third, all connectomes are reconstructed using diffusion weighted imaging, which

is subject to both systematic false positives and false negatives (Maier-Hein et al., 2017; Schilling et al., 2019). While a uniform, high-resolution *ex vivo* scanning protocol allows for systematic comparisons among species, and our results recapitulate findings from tract tracing studies, future work in comparative connectomics will benefit from technological and analytical advances in neural circuit mapping. Fourth, evolutionary circuit modifications may not occur at the level of large-scale white matter, but at finer scales involving smaller nuclei or physiological events not accessible by diffusion imaging, such as up- or down-regulation of neurotransmitter receptors (Barker, 2021). Nevertheless, the strikingly consistent taxonomic and phylogenetic relationships revealed by connectome analysis remain, and suggest that macroscale connectivity, as measured by diffusion MRI, is informative of species similarities and differences across taxonomic orders.

By encoding connectomes into a common frame of reference, we quantitatively assess neural circuit architecture across the mammalian phylogeny. We find that connectome organization recapitulates previously established taxonomic relationships. Collectively, these findings set the stage for future mechanistic studies to trace the link between genes to neural circuits and ultimately to behaviour, and offer new opportunities to explore how changes in brain network structure across phylogeny translate into changes in function and behavior.

5.6 Materials and Methods

5.6.1 Brain samples

The mammalian MRI (MaMI) database includes a total of 225 ex vivo diffusion and T2- and T1-weighted brain scans of 125 different animal species (Table S5.1). No animals were deliberately euthanized for the present study. All brains were collected based on incidental death of animals in zoos in Israel or natural death collected abroad, and with the permission of the national park authority (approval no. 2012/38645) or its equivalent in the relevant countries. All scans were performed on excised and fixated tissue. Animals' brains were extracted within 24 h of death and placed in formaldehyde (10 percent) for a fixation period of a few days to a few weeks (depending on the brain size). Approximately 24 h before the MRI scanning session, the brains were placed in phosphate-buffered saline for rehydration. Given the limited size of the bore, small brains were scanned using a 7-T 30/70 Biospec Avance Bruker system, whereas larger brains were scanned using a 3-T Siemens Prisma system. To minimize image artifacts caused by magnet susceptibility

effects, the brains were immersed in fluorinated oil (Flourinert, 3M) inside a plastic bag during the MRI scanning session.

5.6.2 MRI acquisition

A unified MRI protocol was implemented for all species. The protocol included high-resolution anatomical scans (T2- or T1-weighted MRI), which were used as an anatomical reference, and diffusion MR scans. Diffusion MRI data were acquired using high angular resolution diffusion imaging (HARDI), which consists of a series of diffusion-weighted, spin-echo, echo-planar-imaging images covering the whole brain, scanned in either 60 (in the 7-T scanner) or 64 gradient directions (in the 3-T scanner) with an additional 3 non-diffusion-weighted images (B0). The b value was 1,000 smm^{-2} in all scans. In the 7-T scans, TR was longer than 12,000 ms (depending on the number of slices), TE was 20 ms and Δ/δ = 10/4.5 ms. In the 3-T scans, TR was 3,500 ms, with a TE of 47 ms and Δ/δ = 17/23 ms.

To linearly scale according to brain size the two-dimensional image pixel resolution (per slice), the size of the matrix remained constant across all species (128 x 96). Due to differences in brain shape, the number of slices varied between 46 and 68. Likewise, the number of scan repetitions and the acquisition time were different for each species, depending on brain size and desired signal to noise ratio (SNR) levels. To keep SNR levels above 20, an acquisition time of 48 h was used for small brains ($\sim$ 0.15ml), and 25 min for large brains ($>$ 1,000 ml). SNR was defined as the ratio of mean signal strength to the standard deviation of the noise (an area in the non-brain part of the image). Full details are provided in Assaf et al. (2020).

5.6.3 Connectome reconstruction

The ExploreDTI software was used for diffusion analysis and tractography (Leemans et al., 2009). The following steps were used to reconstruct fiber tracts:

1. To reduce noise and smooth the data, anisotropic smoothing with a 3-pixel Gaussian kernel was applied.

2. Motion, susceptibility and eddy current distortions were corrected in the native space of the HARDI acquisition.

3. A spherical harmonic deconvolution approach was used to generate fiber-orientation density functions per pixel (Tournier et al., 2004), yielding multiple (n>=1) fiber orientations per voxel. Spherical harmonics of up to fourth order were used.

4. Whole-brain tractography was performed using a constrained spherical deconvolution (CSD) seed point threshold similar for all samples (0.2) and a step length half the pixel size.

The end result of the tractography analysis is a list of streamlines starting and ending between pairs of voxels. Recent studies have shown that fiber tracking tends to present a bias where the vast majority of end-points reside in the white matter (Tournier et al., 2004). To avoid this, the CSD tracking implemented here insures that approximately 90% of the end-points reside in the cortical and subcortical grey matter.

5.6.4 Network generation and analysis

Before the reconstruction of the networks, certain fiber tracts were removed from the final list of tracts. These include: external projection fibers that pass through the cerebral peduncle, as well as cerebellar connections. Inner-hemispheric projections, such as the thalamic radiation, were included in the analysis. Brains were parcellated into 200 nodes using a *k*-means clustering algorithm. All the fiber end-point positions were used as input, and cluster assignment was done based on the similarity in connectivity profile between pairs of end-points. Therefore, vertices with similar connectivity profile have a higher chance of grouping together. The clustering was performed twice, once for each hemisphere. Nodes were defined as the mass center of the resulting 200 clusters. Connectivity matrices were generated by indexing the number of streamlines between any two nodes (Assaf et al., 2020). The resulting connectivity matrices are hence sparse and weighted adjacency matrices. For the analysis of the Laplacian eigenspectrum, connectivity matrices were binarized by setting connectivity values to 1 if the connection exists and 0 otherwise.

Even though the sizes of the regions differ across species, we opted for a uniform parcellation scheme (i.e. 200 nodes) for several reasons. First, to our knowledge, there is no MRI parcellation for the brains of the majority of the species studied here. Second, how brain regions correspond to one another across species (i.e. homologs) is still not completely understood for many regions and for many species. Third, comparing networks of different sizes introduces numerous analytical biases because most network measures trivially depend on size, making the comparison challenging. We therefore opted to implement a

uniform parcellation scheme across species, allowing us to translate connectomes into a common reference feature space in which they can be compared (see *Spectral distance* and *Topological distance* sections). Note that this approach does not take into account species-specific regional delinations, nor does it capture homologies between nodes across species, which are still not completely understood. To ensure that the results are not idiosyncratic to the choice of parcellation and parcellation scale, we replicated all results using a lower resolution (100 node; Fig. S5.17) and Fig. S5.18) and higher resolution (300 node; Fig. S5.19) and Fig. S5.20) parcellation.

5.6.5 Controlling for the scanning resolution and acquisition parameters

As the size of the matrix was kept constant across species (i.e. 200 nodes), voxel dimensions were linearly scaled with brain volume, thus resulting in different scanning resolutions across the samples. To verify that this was a reasonable assumption, several tests were performed: (1) The diffusion-based connectome of the mouse was previously compared against one derived from tract-tracing (see (Assaf et al., 2020) for details), obtaining a strong correlation between both networks. (2) Results on the connectivity conservation principle presented in (Assaf et al., 2020) were invariant to different scanning and parcellation parameters across nine different species. (3) The diffusion weighted imaging method was able to reconstruct specific ground truth fiber systems across brains, and these fiber bundles scaled in size with brain volume.

5.6.6 Spectral distance

To estimate similarities between species' connectome organization, we computed the Laplacian eigenspectrum of each graph. The Laplacian eigenspectrum acts like a spectroscopy of the graph and summarizes distinct aspects of the underlying topology (Banerjee and Jost, 2008, 2009; Das, 2004; Grone and Merris, 1994; Grone et al., 1990; Newman, 2001). We considered the normalized Laplacian matrix L for undirected graphs with binary adjacency matrix A. L is defined as $L = I - D^{-1}A$, where D is a diagonal matrix with $D(i,i) = \deg i$, and $\deg i$ is the binary degree of vertex i.

$$L(i,j) = \begin{cases} 1 & \text{if } i = j \\ -\frac{1}{\deg i} & \text{if } i \text{ and } j \text{ are connected} \\ 0 & \text{otherwise} \end{cases}$$

with i and j representing two vertices of the graph. The Laplacian spectrum is then given by the set of all the eigenvalues of L. Importantly, the eigenspectrum of the normalized Laplacian has the advantage that all eigenvalues are in the range $[0, 2]$ (Chung, 1996), facilitating comparison across species. Furthermore, the normalized Laplacian is unitarily equivalent to the symmetric normalized Laplacian (Chung, 1996), i.e. $L_{symm} = I - D^{-\frac{1}{2}}AD^{\frac{1}{2}}$, thus the eigenvalues of both Laplacians are real. The spectral distance between every pair of animal species was then estimated as 1 minus the cosine similarity of their Laplacian eigenvalue distributions, where eigenvalue distributions were assumed to be vectors in a high dimensional space.

To allow comparison of our results with previous reports (Lange et al., 2014), in addition to comparing species using their connectome's Laplacian eigenspectra straightaway, we smoothed the eigenvalue distribution (i.e. λ_1, λ_2, ..., λ_n) by convolving eigenvalue frequencies with a Gaussian kernel. The new estimated density is given by:

$$\Gamma(x) = \sum_{i=1}^{n} \frac{1}{\sqrt{2\pi\sigma^2}} \exp\left(-\frac{|x - \lambda_i|^2}{2\sigma^2}\right)$$

with n being the number of eigenvalues in the approximated distribution, and σ being a smoothing factor of 0.015. We used a step of 0.001, which resulted in a total of $n = 2000$ points. The approximated distribution was normalized such that area under the curve is 1. For the smoothing, we used the*KernelDensity* function in the *neighbors* module of the *Scikit-learn* Python package Pedregosa et al., 2011. Details of the implementation can be found in the publicly available code repository. As with the Laplacian eigenspectrum, the spectral distance between every pair of animal species was estimated as 1 minus the cosine similarity of their smoothed (normalized) Laplacian eigenvalue distributions. Results of this supplementary analysis can be found in Fig. S5.21.

5.6.7 Topological distance

An alternative way to estimate inter-species distances in connectome organization is to compute the correlation between their network features. We estimated a set of local and global graph theory measures of the connectivity matrix. Local measures include node degree, clustering coefficient, node betweenness and closeness. Global measures include characteristic path length, transitivity and assortativity. We included both the binary and the weighted versions of these measures. We constructed a vector of local and global topological features for every animal species. Because there are as many local features as nodes in a network, we only used the average and the standard deviation of

these measures. Similar to the spectral distance, the topological distance between every pair of animal species was estimated as 1 minus the cosine similarity of their topological feature vectors. All local and global features were estimated using the Python version of the Brain Connectivity Toolbox (https://github.com/aestrivex/bctpy; Rubinov and Sporns, 2010). Definitions of these topological metrics can be found below.

Local features

- *Degree (bin)*. Number of connections that a node participates in:

$$k_i = \sum_{j \neq i} a_{ij} \qquad \forall i \in N$$

  where $a_{ij} = 1$ if nodes i and j are connected, otherwise $a_{ij} = 0$. N corresponds to the set of all nodes in the graph (Rubinov and Sporns, 2010).

- *Degree (wei)*. Sum of connection weights that a node participates in:

$$s_i = \sum_{j \neq i} w_{ij} \qquad \forall i \in N$$

  where w_{ij} corresponds to the connection weight between nodes i and j. N corresponds to the set of all nodes in the graph (Rubinov and Sporns, 2010).

- *Clustering (bin)*. Proportion of transitive closures (closed triangles) around a node, i.e. the fraction of neighbor nodes that are neighbors of each other:

$$c_i(A) = \frac{\frac{1}{2} \sum_{j \neq i} \sum_{h \neq (i,j)} a_{ij} a_{ih} a_{jh}}{\frac{1}{2} k_i (k_i - 1)}$$

$$= \frac{(A^3)_{ii}}{k_i (k_i - 1)} \qquad \forall i \in N$$

  where A corresponds to the binary adjacency matrix of the graph, $(A^3)_{ii}$ is the i-th element of the main diagonal of $A^3 = A \cdot A \cdot A$, and k_i is the degree of node i (Rubinov and Sporns, 2010; Watts and Strogatz, 1998).

- *Clustering (wei)*. Mean "intensity" of triangles around a node:

$$c_i(W) = \frac{\frac{1}{2}\sum_{j\neq i}\sum_{h\neq(i,j)} w_{ij}^{\frac{1}{3}} w_{ih}^{\frac{1}{3}} w_{jh}^{\frac{1}{3}}}{\frac{1}{2}k_i(k_i-1)}$$

$$= \frac{(W^{[\frac{1}{3}]})_{ii}^3}{k_i(k_i-1)} \qquad \forall i \in N$$

where W corresponds to the weighted connectivity matrix, $(W^{[\frac{1}{3}]})_{ii}^3$ is the i-th element of the main diagonal of $(W^{[\frac{1}{3}]})^3 = W^{\frac{1}{3}} \cdot W^{\frac{1}{3}} \cdot W^{\frac{1}{3}}$, and k_i is the degree of node i (**onnela2005physrev**; Rubinov and Sporns, 2010).

- *Shortest path length (bin)*. Minimum geodesic distance between pairs of nodes:

$$d_{ij} = \sum_{a_{uv}\in g_{i\leftrightarrow j}} a_{uv}$$

where $g_{i\leftrightarrow j}$ is the shortest geodesic path between nodes i and j. Note that $d_{ij} = \infty$ for all disconnected pairs i, j (Rubinov and Sporns, 2010).

- *Shortest path length (wei)*. Minimum weighted distance between pairs of nodes:

$$d_{ij}^{\mathrm{w}} = \sum_{a_{uv}\in g_{i\leftrightarrow j}} f(w_{uv})$$

where f is a map (e.g., the inverse) from weight to length and $g_{i\leftrightarrow j}$ is the shortest weighted path between nodes i and j (Rubinov and Sporns, 2010).

- *Betweenness (bin)*. Proportion of shortest (geodesic) paths in the graph that traverse a node:

$$b_i = \frac{1}{(n-1)(n-2)} \sum_{j\neq i} \sum_{h\neq(i,j)} \frac{\rho_{hj}(i)}{\rho_{hj}} \qquad \forall i \in N$$

where ρ_{hj} is the number of shortest (geodesic) paths between nodes h and j, $\rho_{hj}(i)$ is the number of shortest (geodesic) paths between nodes h and j that pass through i, and n is the number of nodes in the graph (Brandes, 2001; Freeman, 1978; Kintali, 2008; Rubinov and Sporns, 2010).

- *Betweenness (wei)*. Same as *betweenness (bin)*, but shortest paths are estimated on the respective weighted graph (Brandes, 2001; Freeman, 1978; Kintali, 2008; Rubinov and Sporns, 2010).

- *Closeness (bin)*. Mean shortest (geodesic) path length from a node to all other nodes in the network:

$$e_i(A) = \frac{\sum_{j \neq i} \sum_{h \neq (i,j)} a_{ij} a_{ih} [d_{jh}(N_i)]^{-1}}{k_i(k_i - 1)} \qquad \forall i \in N$$

  where $d_{jh}(N_i)$ is the shortest (geodesic) path length between nodes j and h, that contains only neighbors of i, and is estimated on the corresponding binary adjacency matrix A (Latora and Marchiori, 2001; Rubinov and Sporns, 2010).

- *Closeness (wei)*. Mean shortest (weighted) path from a node to all other nodes in the network:

$$e_i(W) = \frac{\sum_{j \neq i} \sum_{h \neq (i,j)} (w_{ij} w_{ih} [d^{\mathrm{w}}_{jh}(N_i)]^{-1})^{\frac{1}{3}}}{k_i(k_i - 1)} \qquad \forall i \in N$$

  where $d^{\mathrm{w}}_{jh}(N_i)$ is the length of the shortest (weighted) path between nodes j and h, that contains only neighbors of i, and is estimated on the corresponding weighted adjacency matrix W (Latora and Marchiori, 2001; Rubinov and Sporns, 2010).

Global features

- *Characteristic path length (bin)*. Average shortest (geodesic) path length between all pairs of nodes in the graph:

$$L = \frac{1}{n} \sum_{i \in N} \frac{\sum_{j \neq i} d_{ij}}{n - 1}$$

  where d_{ij} is the shortest (geodesic) path length between nodes i and j, and n is the number of nodes in the graph (Rubinov and Sporns, 2010; Watts and Strogatz, 1998).

- *Characteristic path length (wei)*. Average shortest (weighted) path length between all pairs of nodes in the graph:

$$L^{\mathrm{w}} = \frac{1}{n} \sum_{i \in N} \frac{\sum_{j \neq i} d^{\mathrm{w}}_{ij}}{n - 1}$$

where d_{ij}^{w} is the shortest (weighted) path length between nodes i and j, and n is the number of nodes in the graph (Rubinov and Sporns, 2010; Watts and Strogatz, 1998).

- *Transitivity (bin).* Ratio between the observed number of closed triangles and the maximum possible number of closed triangles:

$$T(A) = \frac{\sum_{i \in N} \sum_{j,h \in N} a_{ij} a_{ih} a_{jh}}{\sum_{i \in N} k_i (k_i - 1)}$$

$$= \frac{\sum_{i \in N} (A^3)_{ii}}{\sum_{i \in N} k_i (k_i - 1)}$$

where A is the binary adjacency matrix, and k_i is the degree of node i (Newman, 2003; Rubinov and Sporns, 2010).

- *Transitivity (wei).* Ratio between the "intensity" of observed closed triangles and the maximum possible "intensity" of closed triangles:

$$T(W) = \frac{\sum_{i \in N} \sum_{j,h \in N} w_{ij}^{\frac{1}{3}} w_{ih}^{\frac{1}{3}} w_{jh}^{\frac{1}{3}}}{k_i (k_i - 1)}$$

$$= \frac{\sum_{i \in N} (W^{[\frac{1}{3}]})_{ii}^{3}}{\sum_{i \in N} k_i (k_i - 1)}$$

where W is the weighted connectivity matrix, and k_i is the degree of node i (Newman, 2003; Rubinov and Sporns, 2010).

- *Assortativity (bin).* Correlation coefficient between the degree of a node and the mean degree of its neighbours:

$$r = \frac{l^{-1} \sum_{(i,j) \in L} k_i k_j - [l^{-1} \sum_{(i,j) \in L} \frac{1}{2} (k_i + k_j)]^2}{l^{-1} \sum_{(i,j) \in L} \frac{1}{2} (k_i^2 + k_j^2) - [l^{-1} \sum_{(i,j) \in L} \frac{1}{2} (k_i + k_j)]^2}$$

where l^{-1} is the inverse of the number of links in the graph, k_i is the degree of node i, and L is the set of links in the graph (Newman, 2002; Rubinov and Sporns, 2010).

- *Assortativity (wei).* Correlation coefficient between the weighted degree of a node and the mean wighted degree of its neighbour:

$$r^{w} = \frac{l^{-1}\sum_{(i,j)\in L} w_{ij}s_i s_j - [l^{-1}\sum_{(i,j)\in L}\frac{1}{2}w_{ij}(s_i + s_j)]^2}{l^{-1}\sum_{(i,j)\in L}\frac{1}{2}w_{ij}(s_i^2 + s_j^2) - [l^{-1}\sum_{(i,j)\in L}\frac{1}{2}w_{ij}(s_i + s_j)]^2}$$

where l^{-1} is the inverse of the number of links in the graph, s_i is the weighted degree of node i, and L is the set of links in the graph (Leung and Chau, 2007; Rubinov and Sporns, 2010).

5.6.8 Small-world organization

We use the index proposed in (Humphries and Gurney, 2008) to measure connectomes' small-worldness level. The index is given by:

$$\gamma = \frac{C}{C_{rand}}$$

$$\lambda = \frac{L}{L_{rand}}$$

$$S = \frac{\gamma}{\lambda}$$

where L and C are the corresponding characteristic path length and clustering coefficient of each connectome, respectively, and L_{rand} and C_{rand} are the corresponding average quantities for a set of 1000 randomly rewired graphs that preserve the degree sequence and distribution of the nodes (Maslov and Sneppen, 2002). A network is said to possess a small world architecture if $S \geq 1$, that is, if it situates above the identity line in a γ vs λ plot.

5.6.9 Multi-resolution community detection

We used the Louvain algorithm to determine the optimal community structure of connectomes (Blondel et al., 2008). Briefly, this algorithm extracts communities from large networks by optimizing a modularity score. Here we use the Q-metric as the objective function (Blondel et al., 2008; Fortunato and Barthelemy, 2007):

$$Q(\gamma) = \frac{1}{2m}\sum_{ij}\left[A_{ij} - \gamma\frac{k_i k_j}{2m}\right]\delta(c_i, c_j)$$

where A corresponds to the adjacency matrix of the network, k_i is the degree of node i, m is the sum of all connections in the graph, c_i is the community affiliation of node i, and δ is the Kronecker delta function (i.e. $\delta(x, y) = 1 \quad \text{if} \quad x = y, \quad 0 \quad \text{otherwise}$). The size of the partition is controlled by a resolution parameter γ (higher γ values result in a larger number of modules). Because the Louvain method is a greedy algorithm, we first found multiple (250) optimal partitions at $\gamma = 1$, and then we determined a single partition using a consensus clustering approach (Bassett et al., 2013).

5.6.10 Classification of edges

Connectomes's connections were classified into different categories based on four criteria. The first criterion is based on the modular structure of the network and classifies connections depending on whether they link brain regions within the same module (i.e. intra-modular) or regions across different modules (i.e. inter-modular); the second criterion is whether connections link brain regions within the same hemisphere (i.e. intra-hemispheric connections) or across hemispheres (inter-hemispheric connections); the third criterion is based on the physical length of the connections (i.e. short-, medium- and long-range connections), and the fourth criterion is based on the rich-club structure of the network (i.e. rich-club, feeder and peripheral connections).

Inter- vs intra-modular connections

To classify connections as being either inter- or intra-modular, a consensus clustering algorithm was applied on each connectome to determine a partition of the network into different modules (see *Community detection*). Once modules are identified, inter-modular connections correspond to those linking brain regions across different modules, whereas intra-modular connections correspond to those linking brain regions belonging to the same module.

Connection length

Euclidean distance between regions' centers was used as a proxy for connection length. To subdivide connections into short-, medium- and long-range, connection lengths were estimated as a percentage with respect to the maximum distance between regions. Short-range connections correspond to those that are less or equal to 25% of the maximum distance; medium-range connections are above 25% but less than or equal to 75% of the

maximum distance; and long-range connections are those above 75% of the maximum distance.

Rich-club vs feeder vs peripheral connections

To classify edges as being either rich-club, feeder or peripheral connections, it is necessary to identify first the rich-club of hubs in the network, that is, the densely interconnected core of nodes that have a disproportionately high number of connections (Heuvel and Sporns, 2011; Heuvel et al., 2012). To do so, we compute the rich-club coefficients $\Phi(k)$ across a range of degree k of the unweighted (binary) connectomes. For binary networks, all nodes that show a degree $\leq k$ are removed from the network, and for the remaining set of nodes (i.e. a sub-graph), the rich club coefficient is estimated as the ratio of connections present in the sub-graph, to the total number of possible connections that would be present if the resulting sub-graph was fully connected. Formally, the rich-club coefficient is given by (Colizza et al., 2006; McAuley et al., 2007; Zhou and Mondragón, 2004):

$$\phi(k) = \frac{2E_{>k}}{N_{>k}(N_{>k} - 1)}$$

In random networks, such as the Erdős-Rényi model, nodes with a higher degree have a higher probability of being interconnected by chance alone, thus showing an increasing function of $\Phi(k)$. For this reason, the rich-club coefficient is typically normalized relative to a set of m comparable random networks of equal size and node degree sequence and distribution (Colizza et al., 2006; Maslov and Sneppen, 2002; McAuley et al., 2007). The normalized rich-club coefficient is then given by:

$$\phi_{norm}(k) = \frac{\phi(k)}{\phi_{random}(k)}$$

where ϕ_{random} corresponds to the average rich-club coefficient over the m random networks. In our particular case $m = 1000$. An increasing normalized coefficient $\Phi_{norm} > 1$ over a range of k reflects the existence of rich-club organization.

To assess the statistical significance of rich-club organization we used permutation testing (Bassett and Bullmore, 2009; Heuvel et al., 2010). Briefly, the population of the m random networks yields a null distribution of rich-club coefficients. For the range of k expressing rich-club organization (i.e. $\Phi_{norm} > 1$), we tested whether $\phi(k)$ significantly exceeds $\Phi_{random}(k)$. Next, we identify the k^{th} level at which the maximum significant Φ_{norm} occurs. Nodes with a degree $\geq k$ are said to belong to the k^{th}-core of the network. Next, we identify the hubs, that is, nodes whose degree is above the average degree of the

network plus one standard deviation. Therefore, rich-club nodes were identified as those nodes that are both hubs and belong to the k^{th}-core of the network.

Once rich-club nodes are identified, rich-club connections are defined as edges between rich-club nodes; feeder connections are edges connecting rich-club to non-rich-club nodes, and peripheral connections are edges between non-rich-club nodes.

5.6.11 Controlling for replicas

Because some of the species have multiple scans, this could bias the distribution of intra- and inter-order distances, which could be dominated by those species with a large number of replicas. To account for that, we randomly sample a single connectome per species, and we calculated inter-species distances. We repeated this procedure iteratively 10,000 times. The reported intra- and inter-order distance distributions correspond to the average distances across iterations.

5.6.12 Controlling for density

Some of the graph features used for the estimation of the topological distance are highly dependant on the density of the network. To regress out the effects of network density on a graph feature, a univariate linear and an exponential model are fitted using density as the explanatory variable, and each feature as response variable. That is:

$$\text{Linear:} \quad y = ax + b$$

$$\text{Exponential:} \quad y = ae^{bx} + c$$

where y represents network features and x corresponds to density. Network features are then replaced by the residuals of the model. The decision to fit either a linear, an exponential or no model at all was based on the variance explained by the model or R^2. The model with the largest R^2 is selected. Only those features with $R^2 > 0.1$ were controlled to account for density (features in Fig. S5.12 with a regression line).

5.7 Data availability

The MaMI data set was originally collected and analyzed by Assaf and colleagues in (Assaf et al., 2020). We have included the connectivity matrices used in this study in a public

repository available at https://doi.org/10.5281/zenodo.7143143.

5.8 Code availability

All code used for data analysis and figure generation is publicly available on GitHub (https://github.com/netneurolab/suarez_connectometaxonomy), and is built on top of the following open-source Python packages: rnns (https://github.com/estefanysuarez/rnns.git; https://doi.org/10.5281/zenodo.4913398), Netneurotools (https://github.com/netneurolab/netneurotools), Numpy Harris et al., 2020; Oliphant, 2006; Walt et al., 2011, Scipy Virtanen et al., 2020, Pandas McKinney et al., 2010, Scikit-learn Pedregosa et al., 2011, bctpy (https://github.com/aestrivex/bctpy) Rubinov and Sporns, 2010, Matplotlib Hunter, 2007, and Seaborn Waskom et al., 2016.

5.9 Acknowledgments

BM acknowledges support from the Natural Sciences and Engineering Research Council of Canada (NSERC), Canadian Institutes of Health Research (CIHR), Brain Canada Foundation Future Leaders Fund, the Canada Research Chairs (CRC) Program and the Healthy Brains for Healthy Lives (HBHL) initiative. GL acknowlegdes support from NSERC, the CRC Program, and the Canada CIFAR AI Cahir Program.

5.10 Bibliography

Álvarez-Carretero, S. et al. (2021). "A Species-Level Timeline of Mammal Evolution Integrating Phylogenomic Data". *Nature*, pp. 1–8.

Ardesch, D. J. et al. (2021). "Scaling principles of white matter connectivity in the human and nonhuman primate brain". *Cereb Cortex*.

Assaf, Y. et al. (2020). "Conservation of brain connectivity and wiring across the mammalian class". *Nat Neurosci*, 23(7), pp. 805–808.

Avena-Koenigsberger, A., B. Misic, and O. Sporns (2018). "Communication dynamics in complex brain networks". *Nat Rev Neurosci*, 19(1), p. 17.

Avena-Koenigsberger, A. et al. (2015). "Network morphospace". *J Roy Soc Interface*, 12(103), p. 20140881.

Baker, R. J. and R. D. Bradley (2006). "Speciation in mammals and the genetic species concept". *J Mammal*, 87(4), pp. 643–662.

Banerjee, A. and J. Jost (2008). "On the spectrum of the normalized graph Laplacian". *Linear algebra and its applications*, 428(11-12), pp. 3015–3022.

— (2009). "Graph spectra as a systematic tool in computational biology". *Discrete Applied Mathematics*, 157(10), pp. 2425–2431.

Barkan, C. L., D. B. Kelley, and E. Zornik (2018). "Premotor neuron divergence reflects vocal evolution". *J Neurosci*, 38(23), pp. 5325–5337.

Barker, A. J. (2021). "Brains and speciation: Control of behavior". *Curr Opin Neurobiol*, 71, pp. 158–163.

Barrett, R. L. et al. (2020). "Differences in frontal network anatomy across primate species". *J Neurosci*, 40(10), pp. 2094–2107.

Barsotti, E., A. Correia, and A. Cardona (2021). "Neural architectures in the light of comparative connectomics". *Curr Opin Neurobiol*, 71, pp. 139–149.

Bassett, D. S. and E. T. Bullmore (2009). "Human brain networks in health and disease". *Current opinion in neurology*, 22(4), p. 340.

Bassett, D. S. and O. Sporns (2017). "Network neuroscience". *Nature neuroscience*, 20(3), pp. 353–364.

Bassett, D. S. et al. (2010). "Efficient physical embedding of topologically complex information processing networks in brains and computer circuits". *PLoS Comput Biol*, 6(4), e1000748.

Bassett, D. S. et al. (2013). "Robust detection of dynamic community structure in networks". *Chaos: An Interdisciplinary Journal of Nonlinear Science*, 23(1), p. 013142.

Bassett, D. S. and E. Bullmore (2006). "Small-world brain networks". *The neuroscientist*, 12(6), pp. 512–523.

Beauchamp, A. et al. (2022). "Whole-brain comparison of rodent and human brains using spatial transcriptomics". *bioRxiv*.

Bendesky, A. and C. I. Bargmann (2011). "Genetic contributions to behavioural diversity at the gene–environment interface". *Nature Reviews Genetics*, 12(12), pp. 809–820.

Beul, S. F., S. Grant, and C. C. Hilgetag (2015). "A predictive model of the cat cortical connectome based on cytoarchitecture and distance". *Brain Struct Funct*, 220(6), pp. 3167–3184.

Bianchi, S. et al. (2013). "Dendritic morphology of pyramidal neurons in the chimpanzee neocortex: regional specializations and comparison to humans". *Cereb Cortex*, 23(10), pp. 2429–2436.

Blondel, V. D. et al. (2008). "Fast unfolding of communities in large networks". *Journal of statistical mechanics: theory and experiment*, 2008(10), P10008.

Bota, M., O. Sporns, and L. W. Swanson (2015). "Architecture of the cerebral cortical association connectome underlying cognition". *Proc Natl Acad Sci USA*, 112(16), E2093–E2101.

Brandes, U. (2001). "A faster algorithm for betweenness centrality". *Journal of mathematical sociology*, 25(2), pp. 163–177.

Buckner, R. L. and F. M. Krienen (2013). "The evolution of distributed association networks in the human brain". *Trends Cogn Sci*, 17(12), pp. 648–665.

Buckner, R. L. and D. S. Margulies (2019). "Macroscale cortical organization and a default-like apex transmodal network in the marmoset monkey". *Nat Commun*, 10(1), pp. 1–12.

Bullmore, E. and O. Sporns (2012). "The economy of brain network organization". *Nat Rev Neurosci*, 13(5), p. 336.

Burke, J. D. (1968). "A Brief History of the Taxonomy of Mammals". *MCV/Q, Medical College of Virginia Quarterly*, 4(2), pp. 77–80.

Butler, M. A. and A. A. King (2004). "Phylogenetic comparative analysis: a modeling approach for adaptive evolution". *The American Naturalist*, 164(6), pp. 683–695.

Chiang, A.-S. et al. (2011). "Three-dimensional reconstruction of brain-wide wiring networks in Drosophila at single-cell resolution". *Curr Biol*, 21(1), pp. 1–11.

Chung, F. (1996). "Spectral graph theory. Fresno". *Proceedings of the American Mathematical Society*.

Colizza, V. et al. (2006). "Detecting rich-club ordering in complex networks". *Nature physics*, 2(2), pp. 110–115.

Consortium, Z. et al. (2020). "A comparative genomics multitool for scientific discovery and conservation". *Nature*, 587(7833), p. 240.

Darwin, C. (1959). *On the origin of species*. Routledge.

Das, K. C. (2004). "The Laplacian spectrum of a graph". *Computers & Mathematics with Applications*, 48(5-6), pp. 715–724.

Ding, Y. et al. (2016). "Natural courtship song variation caused by an intronic retroelement in an ion channel gene". *Nature*, 536(7616), pp. 329–332.

Ding, Y. et al. (2019). "Neural evolution of context-dependent fly song". *Current biology*, 29(7), pp. 1089–1099.

Eigenbrod, O. et al. (2019). "Rapid molecular evolution of pain insensitivity in multiple African rodents". *Science*, 364(6443), pp. 852–859.

Faskowitz, J., R. F. Betzel, and O. Sporns (2021). "Edges in Brain Networks: Contributions to Models of Structure and Function". *arXiv preprint arXiv:2105.07069*.

Fortunato, S. and M. Barthelemy (2007). "Resolution limit in community detection". *Proceedings of the national academy of sciences*, 104(1), pp. 36–41.

Frahm, H., H Stephan, and M Stephan (1982). "Comparison of brain structure volumes in Insectivora and Primates. I. Neocortex." *J Hirnforsch*, 23(4), pp. 375–389.

Freeman, L. C. (1978). "Centrality in social networks conceptual clarification". *Social networks*, 1(3), pp. 215–239.

Garey, L. J. (1999). *Brodmann's' localisation in the cerebral cortex'*. World Scientific.

Grone, R. and R. Merris (1994). "The Laplacian spectrum of a graph II". *SIAM Journal on discrete mathematics*, 7(2), pp. 221–229.

Grone, R., R. Merris, and V. Sunder (1990). "The Laplacian spectrum of a graph". *SIAM Journal on matrix analysis and applications*, 11(2), pp. 218–238.

Harris, C. R. et al. (2020). "Array programming with NumPy". *Nature*, 585(7825), pp. 357–362.

Hernández-Hernández, T. et al. (2021). "Speciation across the T ree of L ife". *Biological Reviews*, 96(4), pp. 1205–1242.

Heuvel, M. P. Van den, E. T. Bullmore, and O. Sporns (2016). "Comparative connectomics". *Trends Cognitive Science*, 20(5), pp. 345–361.

Heuvel, M. P. van den and O. Sporns (2011). "Rich-club organization of the human connectome". *Journal of Neuroscience*, 31(44), pp. 15775–15786.

Heuvel, M. P. van den et al. (2010). "Aberrant frontal and temporal complex network structure in schizophrenia: a graph theoretical analysis". *Journal of Neuroscience*, 30(47), pp. 15915–15926.

Heuvel, M. P. van den et al. (2012). "High-cost, high-capacity backbone for global brain communication". *Proc Natl Acad Sci USA*, 109(28), pp. 11372–11377.

Hilgetag, C. C. and M. Kaiser (2004). "Clustered organization of cortical connectivity". *Neuroinformatics*, 2(3), pp. 353–360.

Humphries, M. D. and K. Gurney (2008). "Network 'small-world-ness': a quantitative method for determining canonical network equivalence". *PloS one*, 3(4), e0002051.

Hunter, J. D. (2007). "Matplotlib: A 2D graphics environment". *Computing in science & engineering*, 9(3), pp. 90–95.

Insel, T. R. and L. E. Shapiro (1992). "Oxytocin receptor distribution reflects social organization in monogamous and polygamous voles". *Proceedings of the National Academy of Sciences*, 89(13), pp. 5981–5985.

Jaggard, J. B. et al. (2020). "Cavefish brain atlases reveal functional and anatomical convergence across independently evolved populations". *Sci Adv*, 6(38), eaba3126.

Khallaf, M. A. et al. (2020). "Mate discrimination among subspecies through a conserved olfactory pathway". *Sci Adv*, 6(25), eaba5279.

Kintali, S. (2008). "Betweenness centrality: Algorithms and lower bounds". *arXiv preprint arXiv:0809.1906*.

Krubitzer, L. and J. Kaas (2005). "The evolution of the neocortex in mammals: how is phenotypic diversity generated?" *Curr Opin Neurobiol*, 15(4), pp. 444–453.

Krubitzer, L. and D. M. Kahn (2003). "Nature versus nurture revisited: an old idea with a new twist". *Prog Neurobiol*, 70(1), pp. 33–52.

Lande, R. (1976). "Natural selection and random genetic drift in phenotypic evolution". *Evolution*, pp. 314–334.

Lange, S. de, M. de Reus, and M. van den Heuvel (2014). "The Laplacian spectrum of neural networks". *Front Comput Neurosci*, 7, p. 189.

Lange, S. C. de, M. P. van den Heuvel, and M. A. de Reus (2016). "The role of symmetry in neural networks and their Laplacian spectra". *NeuroImage*, 141, pp. 357–365.

Latora, V. and M. Marchiori (2001). "Efficient behavior of small-world networks". *Physical review letters*, 87(19), p. 198701.

Leemans, A. et al. (2009). "ExploreDTI: a graphical toolbox for processing, analyzing, and visualizing diffusion MR data". In: *Proc Intl Soc Mag Reson Med*. Vol. 17. 1, p. 3537.

Leung, C. and H. Chau (2007). "Weighted assortative and disassortative networks model". *Physica A: Statistical Mechanics and its Applications*, 378(2), pp. 591–602.

Levant, B. (1998). "Differential distribution of D3 dopamine receptors in the brains of several mammalian species". *Brain Res*, 800(2), pp. 269–274.

Liu, Z.-Q., Y.-Q. Zheng, and B. Misic (2020). "Network topology of the marmoset connectome". *Network Neurosci*, (-), pp. 1–26.

Loomis, C. et al. (2019). "An adult brain atlas reveals broad neuroanatomical changes in independently evolved populations of Mexican cavefish". *Frontiers in neuroanatomy*, 13, p. 88.

Maier-Hein, K. H. et al. (2017). "The challenge of mapping the human connectome based on diffusion tractography". *Nat Commun*, 8(1), p. 1349.

Majka, P. et al. (2016). "Towards a comprehensive atlas of cortical connections in a primate brain: Mapping tracer injection studies of the common marmoset into a reference digital template". *J Com Neurol*, 524(11), pp. 2161–2181.

Mallet, J. (1995). "A species definition for the modern synthesis". *Trends in Ecology & Evolution*, 10(7), pp. 294–299.

Markov, N. T. et al. (2012). "A weighted and directed interareal connectivity matrix for macaque cerebral cortex". *Cereb Cortex*, 24(1), pp. 17–36.

Markow, T. A. and P. M. O'Grady (2005). "Evolutionary genetics of reproductive behavior in Drosophila: connecting the dots". *Annu. Rev. Genet.*, 39, pp. 263–291.

Mars, R. B., S. Jbabdi, and M. F. Rushworth (2021). "A common space approach to comparative neuroscience". *Annual Review of Neuroscience*, 44.

Mars, R. B., R. E. Passingham, and S. Jbabdi (2018a). "Connectivity fingerprints: from areal descriptions to abstract spaces". *Trends in cognitive sciences*, 22(11), pp. 1026–1037.

Mars, R. B. et al. (2016). "Comparing brains by matching connectivity profiles". *Neuroscience & Biobehavioral Reviews*, 60, pp. 90–97.

Mars, R. B. et al. (2018b). "Whole brain comparative anatomy using connectivity blueprints". *Elife*, 7, e35237.

Martinez, P. and S. G. Sprecher (2020). "Of circuits and brains: The origin and diversification of neural architectures". *Frontiers in Ecology and Evolution*, 8, p. 82.

Maslov, S. and K. Sneppen (2002). "Specificity and stability in topology of protein networks". *Science*, 296(5569), pp. 910–913.

McAuley, J. J., L. da Fontoura Costa, and T. S. Caetano (2007). "Rich-club phenomenon across complex network hierarchies". *Applied Physics Letters*, 91(8), p. 084103.

McKinney, W. et al. (2010). "Data structures for statistical computing in python". In: *Proceedings of the 9th Python in Science Conference*. Vol. 445. Austin, TX, pp. 51–56.

Mišić, B. and O. Sporns (2016). "From regions to connections and networks: new bridges between brain and behavior". *Curr Opin Neurobiol*, 40, pp. 1–7.

Murphy, W. J. et al. (2021). "Phylogenomics and the Genetic Architecture of the Placental Mammal Radiation". *Annual Review of Animal Biosciences*, 9, pp. 29–53.

Newman, M. E. (2002). "Assortative mixing in networks". *Physical review letters*, 89(20), p. 208701.

— (2003). "The structure and function of complex networks". *SIAM review*, 45(2), pp. 167–256.

Newman, M. W. (2001). "The Laplacian spectrum of graphs". MA thesis. University of Manitoba.

Oh, S. W. et al. (2014). "A mesoscale connectome of the mouse brain". *Nature*, 508(7495), p. 207.

Oliphant, T. E. (2006). *A guide to NumPy*. Vol. 1. Trelgol Publishing USA.

O'Grady, P. M. and R. DeSalle (2018). "Phylogeny of the genus Drosophila". *Genetics*, 209(1), pp. 1–25.

Pantoja, C. et al. (2020). "Rapid effects of selection on brain-wide activity and behavior". *Current Biology*, 30(18), pp. 3647–3656.

Park, T. J. et al. (2008). "Selective inflammatory pain insensitivity in the African naked mole-rat (Heterocephalus glaber)". *PLoS biology*, 6(1), e13.

Passingham, R. E., K. E. Stephan, and R. Kötter (2002). "The anatomical basis of functional localization in the cortex". *Nat Rev Neurosci*, 3(8), pp. 606–616.

Pedregosa, F. et al. (2011). "Scikit-learn: Machine learning in Python". *Journal of machine Learning research*, 12, pp. 2825–2830.

Reus, M. A. de and M. P. van den Heuvel (2013). "Rich club organization and intermodule communication in the cat connectome". *J Neurosci*, 33(32), pp. 12929–12939.

Rubinov, M. and O. Sporns (2010). "Complex network measures of brain connectivity: uses and interpretations". *Neuroimage*, 52(3), pp. 1059–1069.

Rubinov, M. et al. (2015). "Wiring cost and topological participation of the mouse brain connectome". *Proc Natl Acad Sci USA*, 112(32), pp. 10032–10037.

Scannell, J. W., C. Blakemore, and M. P. Young (1995). "Analysis of connectivity in the cat cerebral cortex". *J Neurosci*, 15(2), pp. 1463–1483.

Schilling, K. G. et al. (2019). "Limits to anatomical accuracy of diffusion tractography using modern approaches". *NeuroImage*, 185, pp. 1–11.

Schlenska, G (1974). "Volumen-und oberflachenmessungen an gehirnen verschiedener saugetiere im vergleich zu einem errechneten modell". *J Hirnforsch*, 15, pp. 401–408.

Seehausen, O. et al. (2014). "Genomics and the origin of species". *Nat Rev Genet*, 15(3), pp. 176–192.

Seeholzer, L. F. et al. (2018). "Evolution of a central neural circuit underlies Drosophila mate preferences". *Nature*, 559(7715), pp. 564–569.

Shanahan, M. et al. (2013). "Large-scale network organization in the avian forebrain: a connectivity matrix and theoretical analysis". *Front Comput Neurosci*, 7, p. 89.

Smith, E. S. J. et al. (2011). "The molecular basis of acid insensitivity in the African naked mole-rat". *Science*, 334(6062), pp. 1557–1560.

Sporns, O. (2013). "Network attributes for segregation and integration in the human brain". *Current opinion in neurobiology*, 23(2), pp. 162–171.

Sporns, O., G. Tononi, and R. Kötter (2005). "The human connectome: a structural description of the human brain". *PLoS Comput Biol*, 1(4), e42.

Sporns, O. and J. D. Zwi (2004). "The small world of the cerebral cortex". *Neuroinformatics*, 2(2), pp. 145–162.

Stiso, J. and D. S. Bassett (2018). "Spatial embedding imposes constraints on neuronal network architectures". *Trends in cognitive sciences*, 22(12), pp. 1127–1142.

Suárez, L. E. et al. (2020). "Linking structure and function in macroscale brain networks". *Trends in Cognitive Sciences*, 24(4), pp. 302–315.

Suárez, L. E. et al. (2021). "Learning function from structure in neuromorphic networks". *Nature Machine Intelligence*, 3(9), pp. 771–786.

Tendler, B. C. et al. (2021). "The Digital Brain Bank: an open access platform for post-mortem datasets". *bioRxiv*.

Theunissen, L. (1988). *Eugène Dubois and the Ape-man from Java: The history of the first 'missing link'and its discoverer*. Springer Science & Business Media.

Tononi, G., O. Sporns, and G. M. Edelman (1994). "A measure for brain complexity: relating functional segregation and integration in the nervous system". *Proceedings of the National Academy of Sciences*, 91(11), pp. 5033–5037.

Tournier, J.-D. et al. (2004). "Direct estimation of the fiber orientation density function from diffusion-weighted MRI data using spherical deconvolution". *NeuroImage*, 23(3), pp. 1176–1185.

Towlson, E. K. et al. (2013). "The rich club of the C. elegans neuronal connectome". *J Neurosci*, 33(15), pp. 6380–6387.

Vanwalleghem, G. C., M. B. Ahrens, and E. K. Scott (2018). "Integrative whole-brain neuroscience in larval zebrafish". *Current opinion in neurobiology*, 50, pp. 136–145.

Virtanen, P. et al. (2020). "SciPy 1.0: fundamental algorithms for scientific computing in Python". *Nature methods*, 17(3), pp. 261–272.

Walt, S. v. d., S. C. Colbert, and G. Varoquaux (2011). "The NumPy array: a structure for efficient numerical computation". *Computing in science & engineering*, 13(2), pp. 22–30.

Warrington, S et al. (2022). "Concurrent mapping of brain ontogeny and phylogeny within a common connectivity space". *bioRxiv*.

Waskom, M. et al. (2016). "seaborn: v0. 7.0 (January 2016)". *zenodo10*, 5281.

Watts, D. J. and S. H. Strogatz (1998). "Collective dynamics of small-world networks". *Nature*, 393(6684), p. 440.

White, J. G. et al. (1986). "The structure of the nervous system of the nematode Caenorhabditis elegans". *Philos Trans R Soc Lond B Biol Sci*, 314(1165), pp. 1–340.

Winslow, J. T. et al. (1993). "A role for central vasopressin in pair bonding in monogamous prairie voles". *Nature*, 365(6446), pp. 545–548.

Worrell, J. C. et al. (2017). "Optimized connectome architecture for sensory-motor integration". *Net Neurosci*, 1(4), pp. 415–430.

Wright, S. (1931). "Evolution in Mendelian populations". *Genetics*, 16(2), p. 97.

Yokoyama, C. et al. (2021). "Comparative connectomics of the primate social brain". *NeuroImage*, 245, p. 118693.

York, R. A. (2018). "Assessing the genetic landscape of animal behavior". *Genetics*, 209(1), pp. 223–232.

York, R. A. et al. (2019). "Behavioral evolution contributes to hindbrain diversification among Lake Malawi cichlid fish". *Scientific reports*, 9(1), pp. 1–9.

Zamora-López, G., C. Zhou, and J. Kurths (2010). "Cortical hubs form a module for multisensory integration on top of the hierarchy of cortical networks". *Front Neuroinform*, 4, p. 1.

Zhang, K. and T. J. Sejnowski (2000). "A universal scaling law between gray matter and white matter of cerebral cortex". *Proceedings of the National Academy of Sciences*, 97(10), pp. 5621–5626.

Zhou, S. and R. J. Mondragón (2004). "The rich-club phenomenon in the Internet topology". *IEEE communications letters*, 8(3), pp. 180–182.

Table S5.1: List of animal species

Id	Order	Species	Name	Filename
1	Cetartiodactyla	Addax Nasomaculatus	Addax	Addax
2	Rodentia	Dasyprocta leporina	Agouti	Agouti1
3	Rodentia	Dasyprocta leporina	Agouti	Agouti2
4	Chiroptera	Artibeus jamaicensis	Artibeus Jamacien	ArtibeusJamacien
5	Chiroptera	Asellia tridens	Asellia	Asellia
6	Carnivora	Amblonyx cinerea	Asian Otter	AsianOtter
7	Primates	Baboon	Baboon	Baboon1
8	Primates	Baboon	Baboon	Baboon2
9	Primates	Baboon	Baboon	Baboon3
10	Primates	Papio hamadryas (Baboon)	Baboon	Baboon4
11	Primates		Baboon	Baboon5
12	Cetartiodactyla		Bactrian Deer	BactrianDeer1
13	Cetartiodactyla		Bactrian Deer	BactrianDeer2
14	Carnivora	Vulpes cana	Blanford Fox	BlanfordFox
15	Rodentia	Spalax ehrenbergi	Blind Mole	BlindMole1
16	Rodentia	Spalax ehrenbergi	Blind Mole	BlindMole2
17	Cetartiodactyla	Tursiops truncatus	Bottle Nose Dolphin	BottleNoseDolphin
18	Primates	Brown Lemur	Brown Lemur	BrownLemur1
19	Primates	Brown Lemur	Brown Lemur	BrownLemur2
20	Primates		Brown Lemur	BrownLemur3
21	Cetartiodactyla	Capra Nubiana	Capra Nubiana	CapraNubiana1
22	Cetartiodactyla	Capra Nubiana	Capra Nubiana	CapraNubiana2
23	Cetartiodactyla	Capra Nubiana	Capra Nubiana	CapraNubiana3
24	Cetartiodactyla	Capra Nubiana	Capra Nubiana	CapraNubiana4
25	Primates	Capuchin	Capuchin	Capuchin1
26	Primates	Capuchin	Capuchin	Capuchin2
27	Primates	Capuchin	Capuchin	Capuchin3
28	Rodentia	Hydrochoerus hydrochaeris	Capybara	Capybara
29	Carnivora		Caracal	Caracal
30	Chiroptera		Carollia Perspicilatta	CarolliaPerspicilatta1
31	Chiroptera		Carollia Perspicilatta	CarolliaPerspicilatta2
32	Carnivora	Felis Catus	Cat	Cat1
33	Carnivora	Felis Catus	Cat	Cat2

Continued on next page

Id	Order	Species	Name	Filename
34	Carnivora	Felis Catus	Cat	Cat3
35	Carnivora	Felis Catus	Cat	Cat4
36	Carnivora	Felis Catus	Cat	Cat5
37	Carnivora		Cat	Cat6
38	Rodentia		Caucasian Squirrel	CaucasianSquirrel
39	Chiroptera	Chaerephon plicata	Chaerephon Plicata	ChaerephonPlicata
40	Primates	Pan troglodytes (Chimpanzee)	Chimpanzee	Chimpanzee
41	Rodentia	Chinchilla chinchilla	Chinchila	Chinchila
42	Cetartiodactyla	Axis Axis	Chital	Chital1
43	Cetartiodactyla	Axis Axis	Chital	Chital2
44	Primates	Angola Colobus	Colobus	Colobus2
45	Carnivora		Common Fox	CommonFox
46	Cetartiodactyla	Bos taurus	Cow	Cow1
47	Rodentia	Myocastor Coypus	Coypu	Coypu
48	Chiroptera	Cynopterus brachyotis	Cynopterus	Cynopterus
49	Cetartiodactyla	Gazella Gazella	Deer	Deer1
50	Cetartiodactyla	Gazella Gazella	Deer	Deer2
51	Rodentia	Ocotdon degus	Dego	Dego
52	Cetartiodactyla		Dik Dik	DikDik
53	Carnivora	Canis lupus familiaris	Dog	Dog1
54	Carnivora	Canis lupus familiaris	Dog	Dog2
55	Carnivora	Canis lupus familiaris	Dog	Dog3
56	Carnivora	Canis lupus familiaris	Dog	Dog4
57	Carnivora	Canis lupus familiaris	Dog	Dog5
58	Carnivora	Canis lupus familiaris	Dog	Dog6
59	Carnivora	Canis lupus familiaris	Dog	Dog7
60	Perissodactyla	Equus africanus asinus	Donkey	Donkey
61	Chiroptera	Eonycteris spelaea	Eonycteris	Eonycteris1
62	Chiroptera	Eonycteris spelaea	Eonycteris	Eonycteris2
63	Chiroptera	Eptesicus fuscus	Eptesicus	Eptesicus1
64	Chiroptera		Eptesicus	Eptesicus2
65	Cetartiodactyla	Dama Dama	Fallow Deer	FallowDeer1
66	Cetartiodactyla	Dama Dama	Fallow Deer	FallowDeer2
67	Cetartiodactyla	Dama Dama	Fallow Deer	FallowDeer3
68	Carnivora	Vulpes zerda	Fennek Fox	FennekFox
69	Carnivora	Mustela putorius furo	Ferret	Ferret1
70	Carnivora	Mustela putorius furo	Ferret	Ferret2

Continued on next page

Id	Order	Species	Name	Filename
71	Carnivora	Mustela putorius furo	Ferret	Ferret3
72	Carnivora	Mustela putorius furo	Ferret	Ferret4
73	Chiroptera	Rousettus aegyptiacus	Fruit Bat	FruitBat1
74	Chiroptera	Rousettus aegyptiacus	Fruit Bat	FruitBat2
75	Chiroptera	Rousettus aegyptiacus	Fruit Bat	FruitBat3
76	Chiroptera	Rousettus aegyptiacus	Fruit Bat	FruitBat4
77	Chiroptera	Rousettus aegyptiacus	Fruit Bat	FruitBat5
78	Rodentia	Psammomys obesus	Gerbil	Gerbil
79	Cetartiodactyla	Giraffa camelopardalis	Giraffe	Giraffe1
80	Cetartiodactyla	Giraffa camelopardalis	Giraffe	Giraffe2
81	Cetartiodactyla	Giraffa camelopardalis	Giraffe	Giraffe3
82	Cetartiodactyla	Capra aegagrus hircus	Goat	Goat1
83	Cetartiodactyla	Capra aegagrus hircus	Goat	Goat2
84	Cetartiodactyla	Capra aegagrus hircus	Goat	Goat3
85	Rodentia	Acomys russatus	Golden Spiny Mouse	GoldenSpinyMouse
86	Primates	Gorilla gorilla	Gorilla	Gorilla
87	Primates	Green Monkey	Green Monkey	GreenMonkey1
88	Primates		Green Monkey	GreenMonkey2
89	Carnivora	Ursus arctos isabellinus	Himalian Bear	HimalianBear
90	Chiroptera	Hipposideros armiger	Hipp Armiger	HippArmiger
91	Carnivora	Mellivora capensis	Honey Badger	HoneyBadger
92	Perissodactyla	Equus ferus caballus	Horse	Horse1
93	Perissodactyla	Equus ferus caballus	Horse	Horse2
94	Primates		Howler Monkey	HowlerMonkey1
95	Primates		Howler Monkey	HowlerMonkey2
96	Carnivora	Hyaena hyaena	Hyaena	Hyaena1
97	Carnivora	Hyaena hyaena	Hyaena	Hyaena2
98	Cetartiodactyla	Hyelaphus porcinus	Ind Hog Deer	IndHogDeer
99	Carnivora	Felis chaus	Jungle Cat	JungleCat
100	Cetartiodactyla		Lama	Lama1
101	Cetartiodactyla		Lama	Lama2
102	Primates	Lemur Catta	Lemur Catta	LemurCatta1
103	Primates	Lemur Catta	Lemur Catta	LemurCatta2
104	Carnivora		Leopard	Leopard1
105	Carnivora		Leopard	Leopard2
106	Carnivora	Lycaon pictus	Lycaon	Lycaon1
107	Carnivora	Lycaon pictus	Lycaon	Lycaon2

Continued on next page

Id	Order	Species	Name	Filename
108	Carnivora	Lycaon pictus	Lycaon	Lycaon3
109	Primates	Crab-Eating Macaque	Macaque	Macaque1
110	Primates	Crab-Eating Macaque	Macaque	Macaque10
111	Primates	Crab-Eating Macaque	Macaque	Macaque2
112	Primates	Crab-Eating Macaque	Macaque	Macaque3
113	Primates	Crab-Eating Macaque	Macaque	Macaque4
114	Primates	Crab-Eating Macaque	Macaque	Macaque5
115	Primates	Crab-Eating Macaque	Macaque	Macaque7
116	Primates	Crab-Eating Macaque	Macaque	Macaque9
117	Primates	Black Macaque	Macaque Black	MacaqueBlack
118	Primates		Macaque Lion Tail	MacaqueLionTail
119	Primates	Pig Tailed Macaque	Macaque P T	MacaquePT
120	Primates	Mandrill	Mandrill	Mandrill1
121	Primates	Mandrill	Mandrill	Mandrill2
122	Primates	Mangabey	Mangebi	Mangebi
123	Rodentia	D. Salinociola	Mara	Mara
124	Primates	Cebuella pygmaea (Pygmy marmoset)	Marmoset	Marmoset
125	Carnivora	Suricata suricata	Meerkat	Meerkat1
126	Carnivora	Suricata suricata	Meerkat	Meerkat2
127	Carnivora	Suricata suricata	Meerkat	Meerkat3
128	Carnivora	Suricata suricata	Meerkat	Meerkat4
129	Carnivora	Suricata suricata	Meerkat	Meerkat5
130	Rodentia	Meriones tristrami	Merion	Merion
131	Chiroptera	Miniopterus schreibersii	Miniopterus Schreibersii	MiniopterusSchreibersii1
132	Carnivora	Herpestes ichneumon	Mongoose	Mongoose
133	Rodentia	Mus musculus	Mouse	Mouse
134	Chiroptera	Myotis emarginatus	Myotis Emargenitus	MyotisEmargenitus
135	Chiroptera	Myotis myotis	Myotis Myotis	MyotisMyotis
136	Chiroptera	Myotis Vivesi	Myotis Vivesi	MyotisVivesi1
137	Carnivora	Nasua nasua	Nasua	Nasua1
138	Carnivora	Nasua nasua	Nasua	Nasua2
139	Carnivora	Nasua nasua	Nasua	Nasua3
140	Perissodactyla	Equus hemionus	Onager	Onager
141	Primates	Pongo borneo	Orangutan	Orangutan1
142	Primates	Pongo borneo	Orangutan	Orangutan2
143	Primates		Orangutan	Orangutan3
144	Cetartiodactyla	Oryx leucoryx	Oryx	Oryx1

Continued on next page

Id	Order	Species	Name	Filename
145	Cetartiodactyla	Oryx Gazella	Oryx	Oryx2
146	Cetartiodactyla	Oryx Gazella	Oryx	Oryx3
147	Carnivora	Lutra lutra	Otter	Otter1
148	Carnivora	Lutra lutra	Otter	Otter2
149	Carnivora	Lutra lutra	Otter	Otter3
150	Rodentia	Funambulus palmarum	Palm Squirrel	PalmSquirrel
151	Cetartiodactyla	Pecari	Pecari	Pecari1
152	Cetartiodactyla	Pecari	Pecari	Pecari2
153	Chiroptera	Pipistrellus kuhlii	Pkuhlii	Pkuhlii2
154	Chiroptera	Pipistrellus kuhlii	Pkuhlii	Pkuhlii3
155	Cetartiodactyla	Sus Scrofa	Porcine	Porcine1
156	Cetartiodactyla	Sus Scrofa	Porcine	Porcine2
157	Rodentia	Hystrix Indica	Porcupine	Porcupine1
158	Rodentia	Hystrix Indica	Porcupine	Porcupine2
159	Rodentia	Cynomys ludovicianus	Prairie Dog	PrairieDog
160	Chiroptera	Pteropus lylei	Pteropus Lylei	PteropusLylei
161	Rodentia	Rattus norvegicus	Rat	Rat1
162	Rodentia	Rattus norvegicus	Rat	Rat2
163	Rodentia	Rattus norvegicus	Rat	Rat3
164	Rodentia	Rattus norvegicus	Rat	Rat4
165	Rodentia	Rattus norvegicus	Rat	Rat5
166	Rodentia	Rattus norvegicus	Rat	Rat6
167	Carnivora	Ailurus fulgens	Red Panda	RedPanda
168	Chiroptera	Rhinolophus ferrumequinum	Rhinolophus	Rhinolophus
169	Chiroptera	Rhinopoma hardwickii	Rhinopoma	Rhinopoma
170	Carnivora	Felis margarita	Sand Cat	SandCat1
171	Carnivora	Felis margarita	Sand Cat	SandCat2
172	Cetartiodactyla	Ovis aries	Sheep	Sheep
173	Primates		Siamang	Siamang1
174	Rodentia	Cavia porcellus	Skinny Pig	SkinnyPig
175	Rodentia	Acomys cahirinus	Spiny Mouse	SpinyMouse
176	Primates	Saimiri sciureus	Squirrel Monkey	SquirrelMonkey1
177	Cetartiodactyla	Stenella coeruleoalba	Stripped Dolphin	StrippedDolphin1
178	Cetartiodactyla	Stenella coeruleoalba	Stripped Dolphin	StrippedDolphin2
179	Chiroptera	Sturnira lilium	Sturnira Lilium	SturniraLilium
180	Chiroptera	Tadarida teniotis	Tadarida Teniotis	TadaridaTeniotis1
181	Chiroptera	Tadarida teniotis	Tadarida Teniotis	TadaridaTeniotis2

Continued on next page

Id	Order	Species	Name	Filename
182	Primates	Saguinus oedipus	Tamarin Cotton Top	TamarinCottonTop1
183	Primates	Saguinus oedipus	Tamarin Cotton Top	TamarinCottonTop2
184	Primates	Emperor Tamarin	Tamarin Emperor	TamarinEmperor1
185	Primates	Emperor Tamarin	Tamarin Emperor	TamarinEmperor2
186	Primates	Golden Handed Tamarin	Tamarin Golden Hands	TamarinGoldenHands
187	Perissodactyla	nan	Tapir	Tapir1
188	Perissodactyla		Tapir	Tapir2
189	Cetartiodactyla	Eudorcas thomosonii	Thomson Gazelle	ThomsonGazelle
190	Carnivora		Tiger	Tiger
191	Chiroptera	Desmodus rotundus	Vampire Bat	VampireBat1
192	Chiroptera	Desmodus rotundus	Vampire Bat	VampireBat2
193	Primates	Vervet	Vervet	Vervet
194	Rodentia	Microfus arvalis	Vole	Vole
195	Cetartiodactyla	Sus Scrofa	Wild Boar	WildBoar1
196	Cetartiodactyla	Sus Scrofa	Wild Boar	WildBoar2
197	Cetartiodactyla	Wilderbeest	Wilderbeest	Wilderbeest
198	Rodentia	Rattus norvegicus	Wild Rat	WildRat1
199	Rodentia		Wild Rat	WildRat2
200	Carnivora	Canis lupus	Wolf	Wolf1
201	Carnivora	Canis lupus	Wolf	Wolf2
202	Carnivora	Canis lupus	Wolf	Wolf3
203	Perissodactyla	Equus zebra	Zebra	Zebra

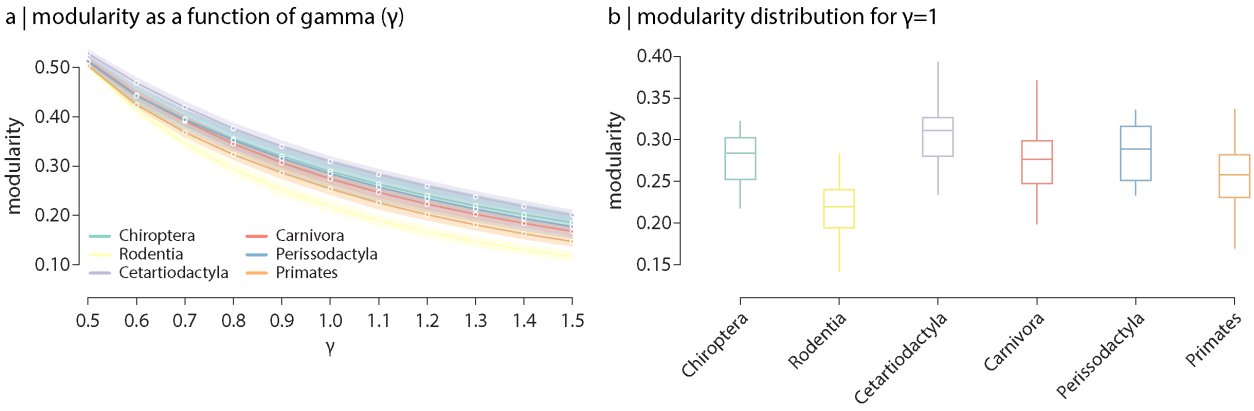

Figure S5.1: **Modularity** | (a) Modularity as a function of resolution the resolution parameter γ, which controls for the size of the identified modules (see *Multi-resolution community detection*). (b) Modularity distributions for each taxonomic order ($\gamma = 1$).

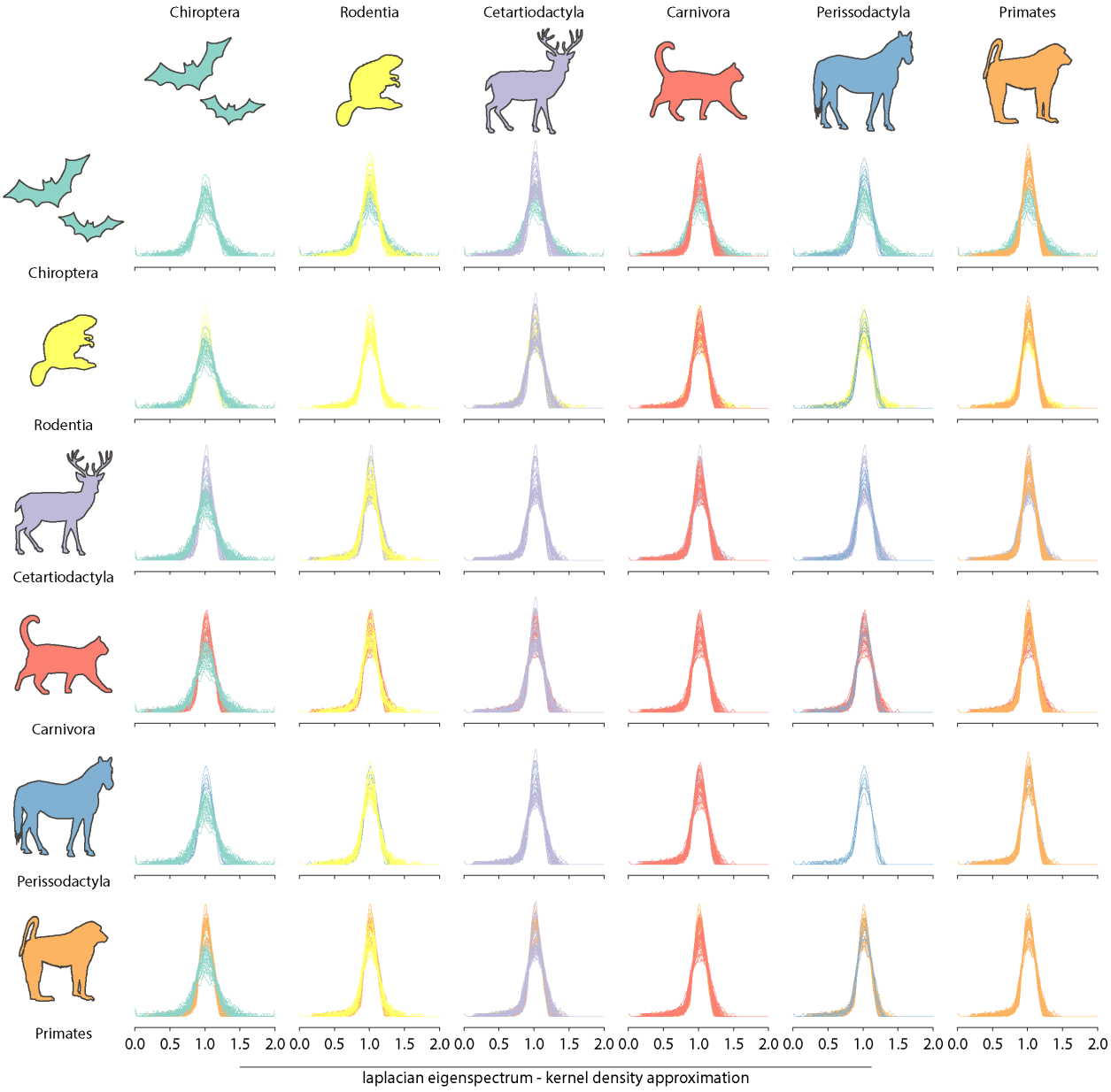

Figure S5.2: **Laplacian eigenspectra** | Spectral plots were obtained by convolving the eigenspectrum of the normalized Laplacian matrix of the graph with a Gaussian kernel. The eigenvalues of the normalized Laplacian of the connectivity matrix, and their multiplicities, capture distinct topological properties of the graph (Banerjee and Jost, 2008, 2009; Das, 2004; Grone and Merris, 1994; Grone et al., 1990; Newman, 2001), thus acting like a spectroscopy of its underlying topology. More importantly, it has the advantage of situating graphs of different sizes and with non-homologous node correspondence in a common frame of reference in which they can be compared.

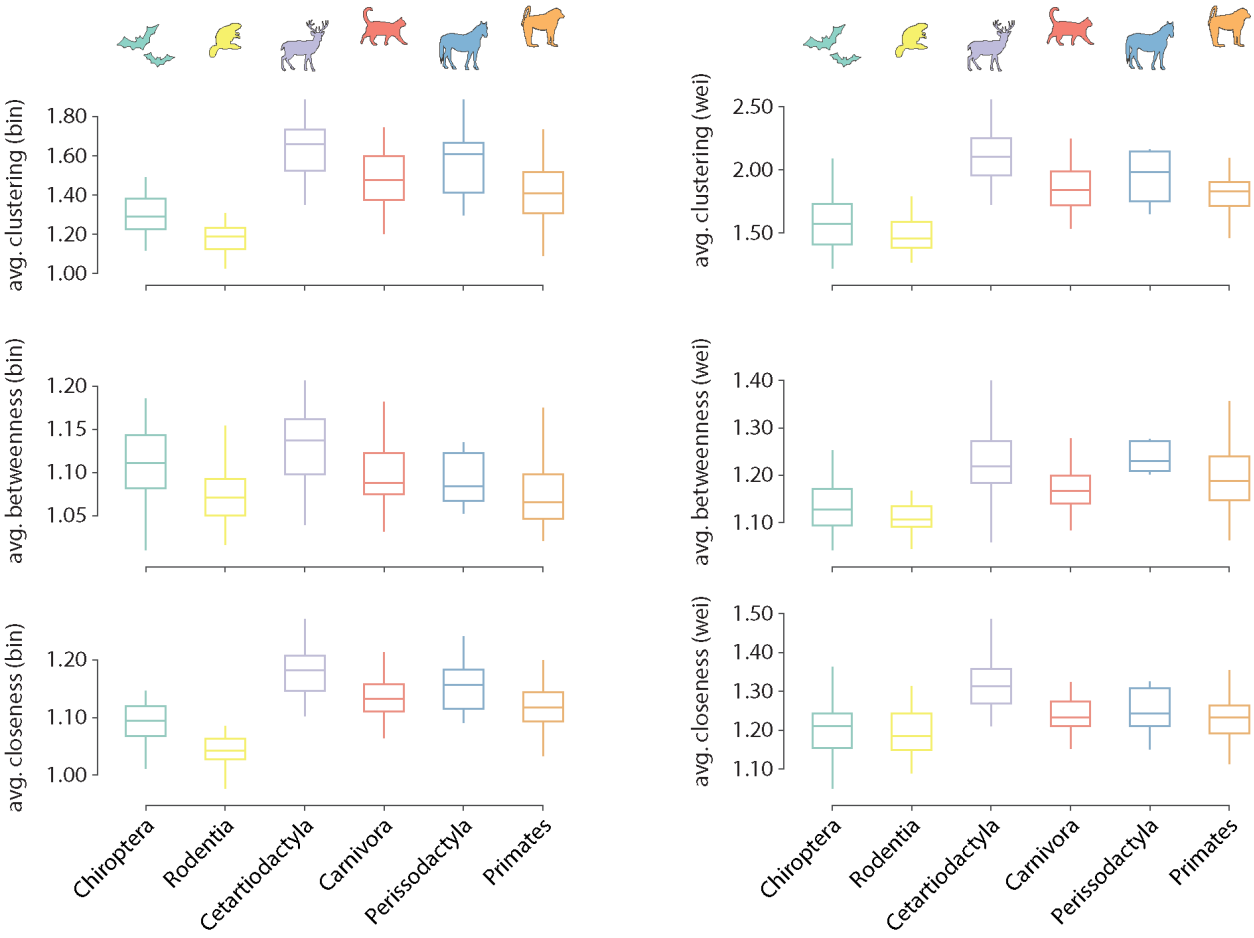

Figure S5.3: **Distribution of local graph features across taxonomic orders** | Distributions of average local features are shown for each order. Features are normalized relative to a set of 1000 randomly rewired graphs that preserve the degree sequence and distribution of the nodes (Maslov and Sneppen, 2002). Features are computed for both the binary (left) and weighted (right) connectomes.

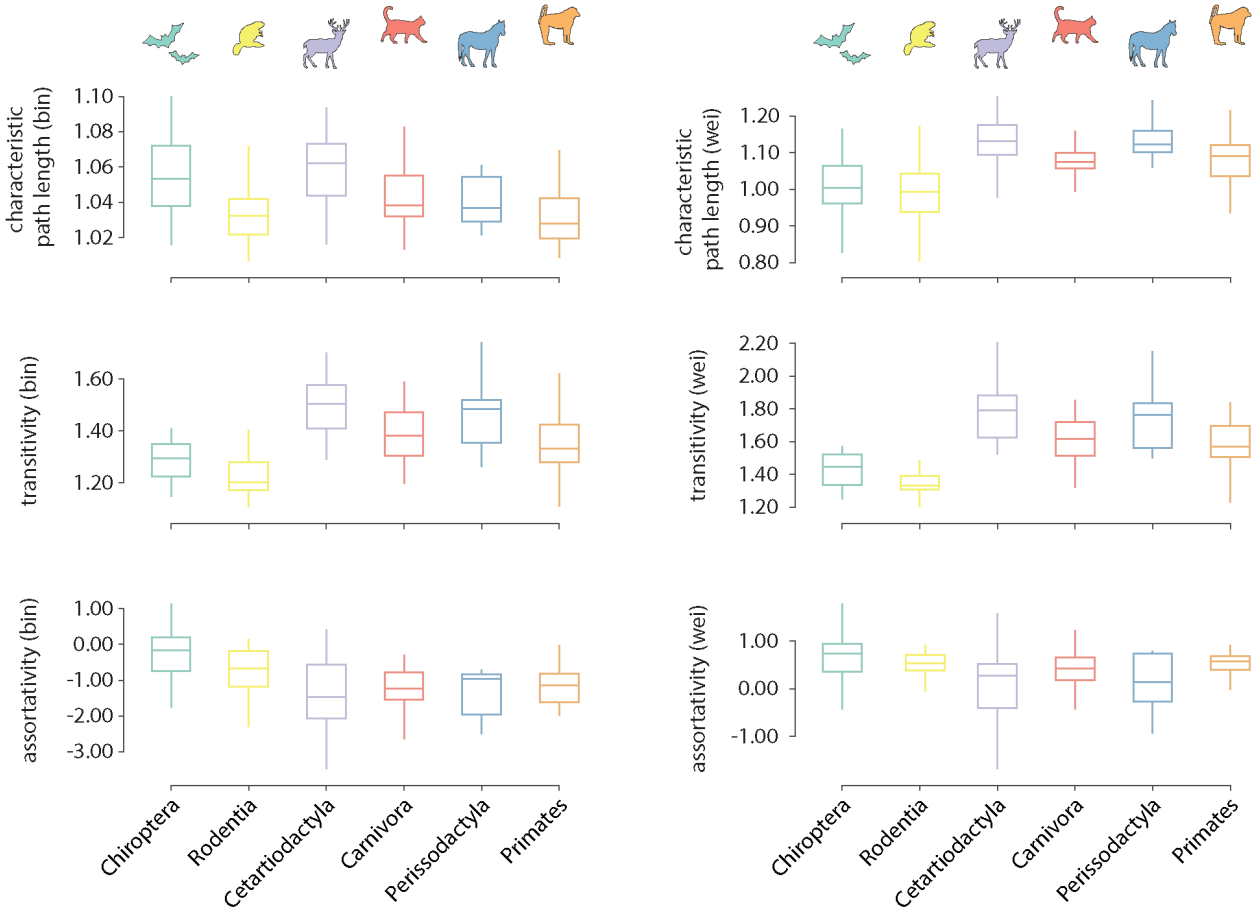

Figure S5.4: **Distribution of global graph features across taxonomic orders** | Distributions of global features are shown for each order. Features are normalized relative to a set of 1000 randomly rewired graphs that preserve the degree sequence and distribution of the nodes (Maslov and Sneppen, 2002). Features are computed for both the binary (left) and weighted (right) connectomes.

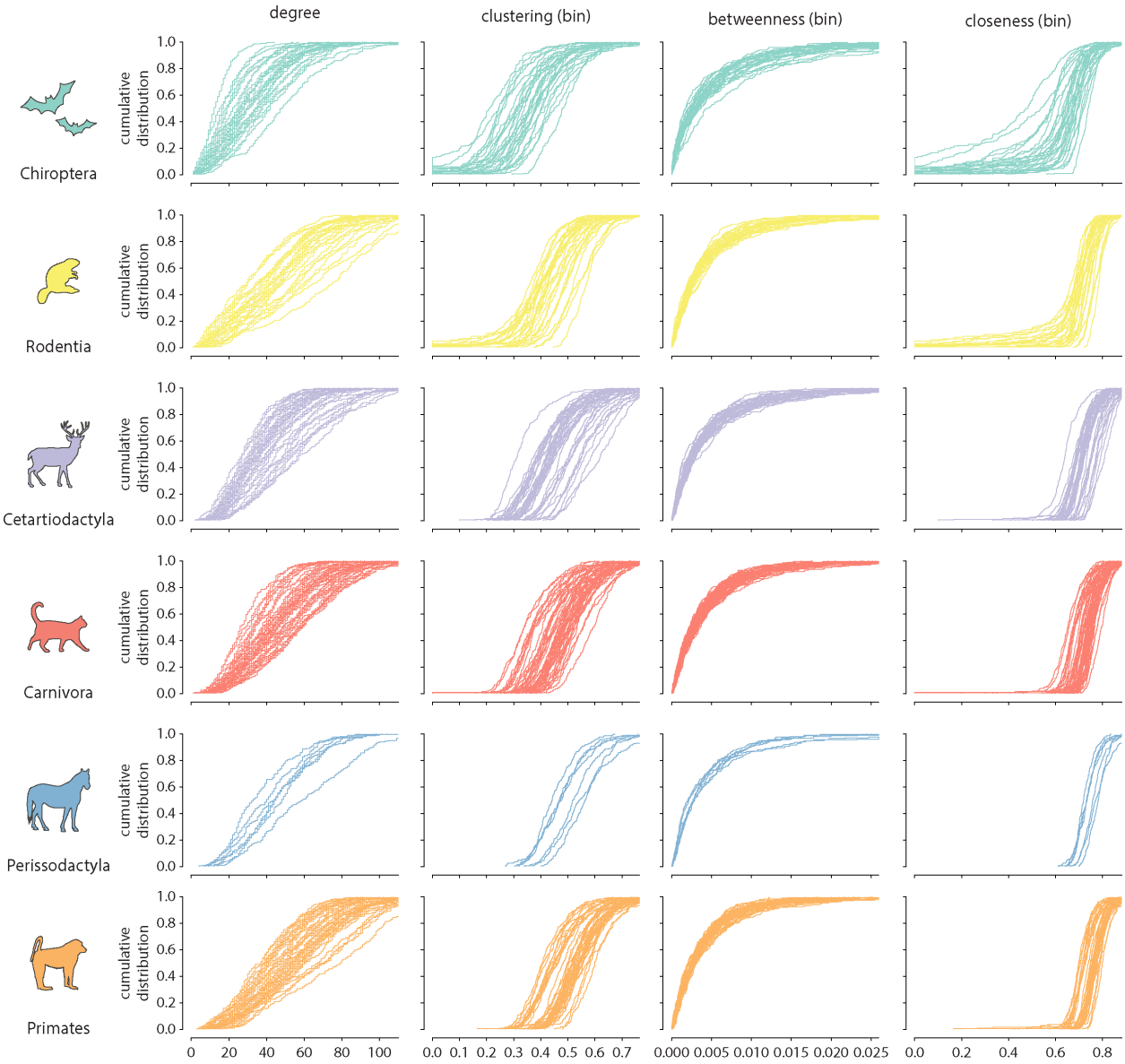

Figure S5.5: **Cumulative distribution of binary local graph features across taxonomic orders** | The cumulative distributions of individual features are shown for each individual sample within each order.

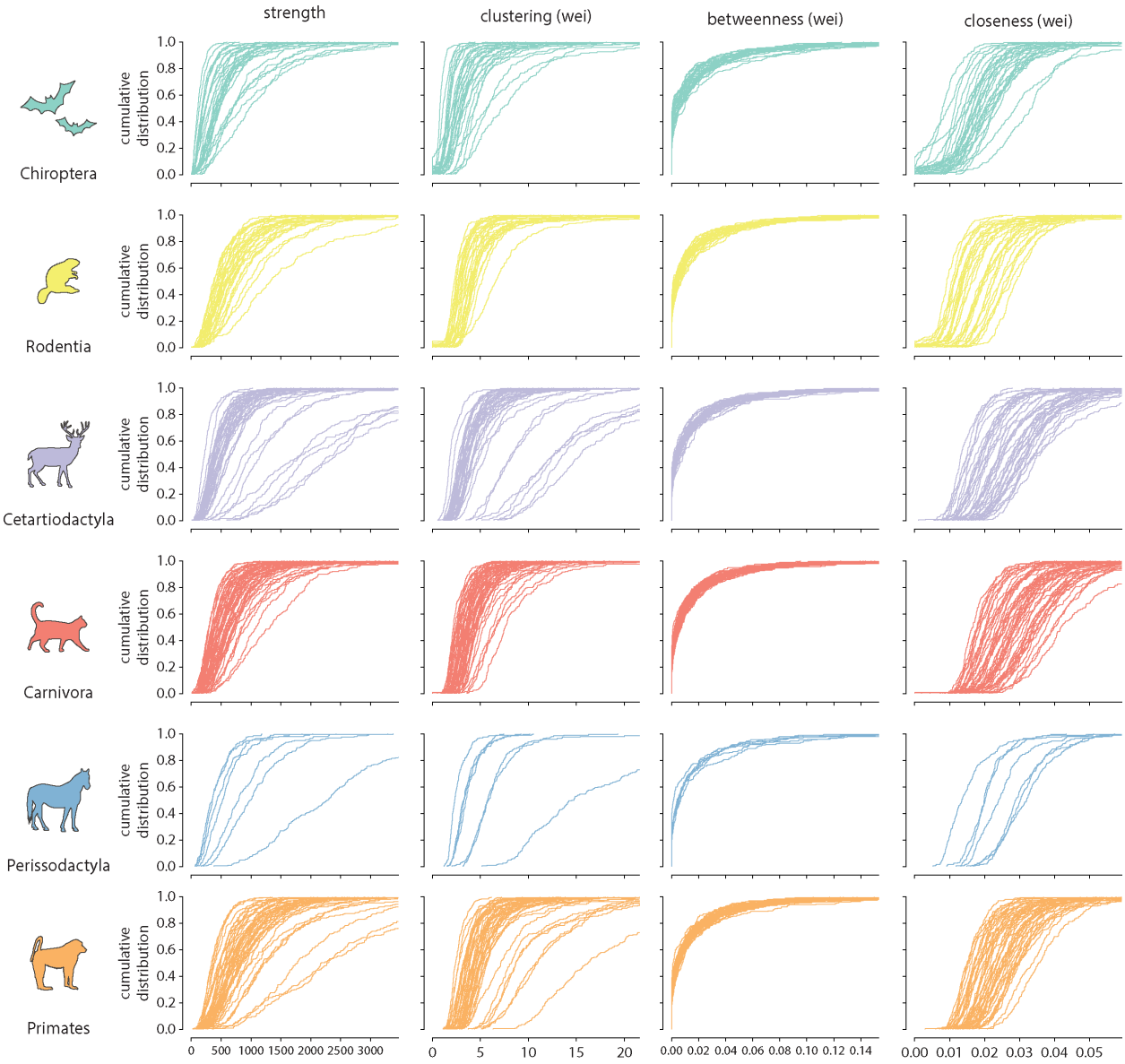

Figure S5.6: **Cumulative distribution of weighted local graph features across taxonomic orders** | The cumulative distributions of individual features are shown for each individual sample within each order.

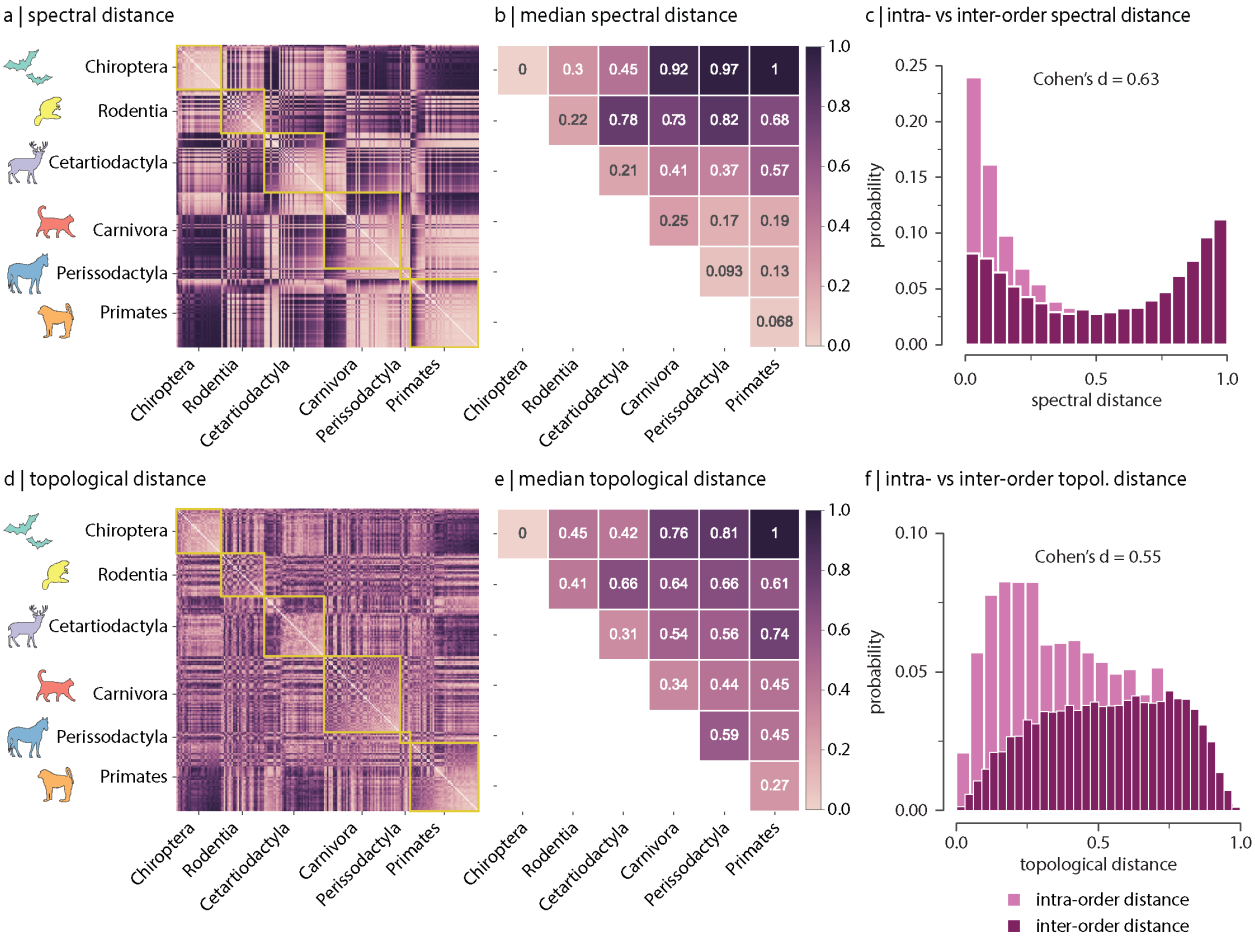

Figure S5.7: **Effect of using replicated samples on the topological and spectral distance between orders** | All samples, including replicas, were used to estimate inter-species spectral and topological distance. (a) Spectral distance between species-specific connectomes. (b) Median spectral distance within and between all constituent members of each order. (c) Distribution of intra- and inter-order spectral distances. (d) Topological distance between species-specific connectomes. (e) Median topological distance within and between all constituent members of each order. (f) Distribution of intra- and inter-order topological distances. Effect sizes in (c) and (f) are Cohen's d estimator corresponding to a two-sample Welch's t-test ($P < 10^{-4}$). Equivalent conclusions are drawn if common-language effects sizes from the two-sample Mann-Whitney U test are used.

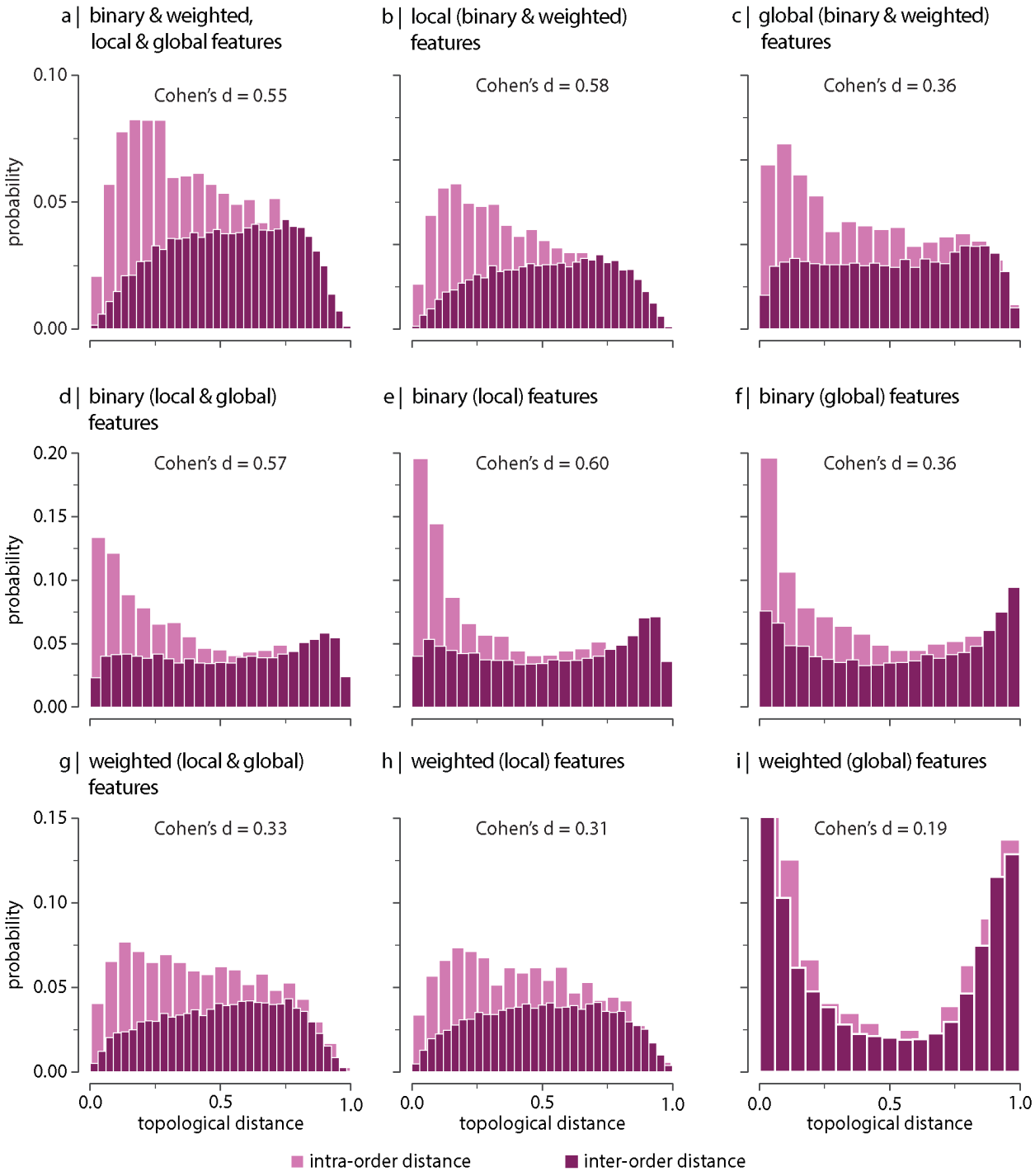

Figure S5.8: **Effect of using replicated samples on the contribution of network features** | All samples, including replicas, were used to estimate inter-species topological distance. Topological distance can be computed using different combinations of local and global, binary and weighted connectome features. Histograms show intra- and inter-order distance distributions when using (a) all (binary, weighted, local and global), (b) all local (binary and weighted), (c) all global (binary and weighted), (d) all binary (local and global), (e) only binary local, (f) only binary global, (g) all weighted (local and global), (h) only weighted local and (i) only weighted global features. Local features include (the average and standard deviation of) degree, clustering, betweenness, and closeness. Global features include characteristic path length, transitivity, and assortativity. Effect sizes correspond to Cohen's d estimator from a two-sample Welch's t-test. Equivalent conclusions are drawn if common-language effects sizes from a two-sample Mann-Whitney U test are used. In all cases, the difference in the mean and median of intra- and inter-order distance distributions is statistically significant ($P < 10^{-4}$).

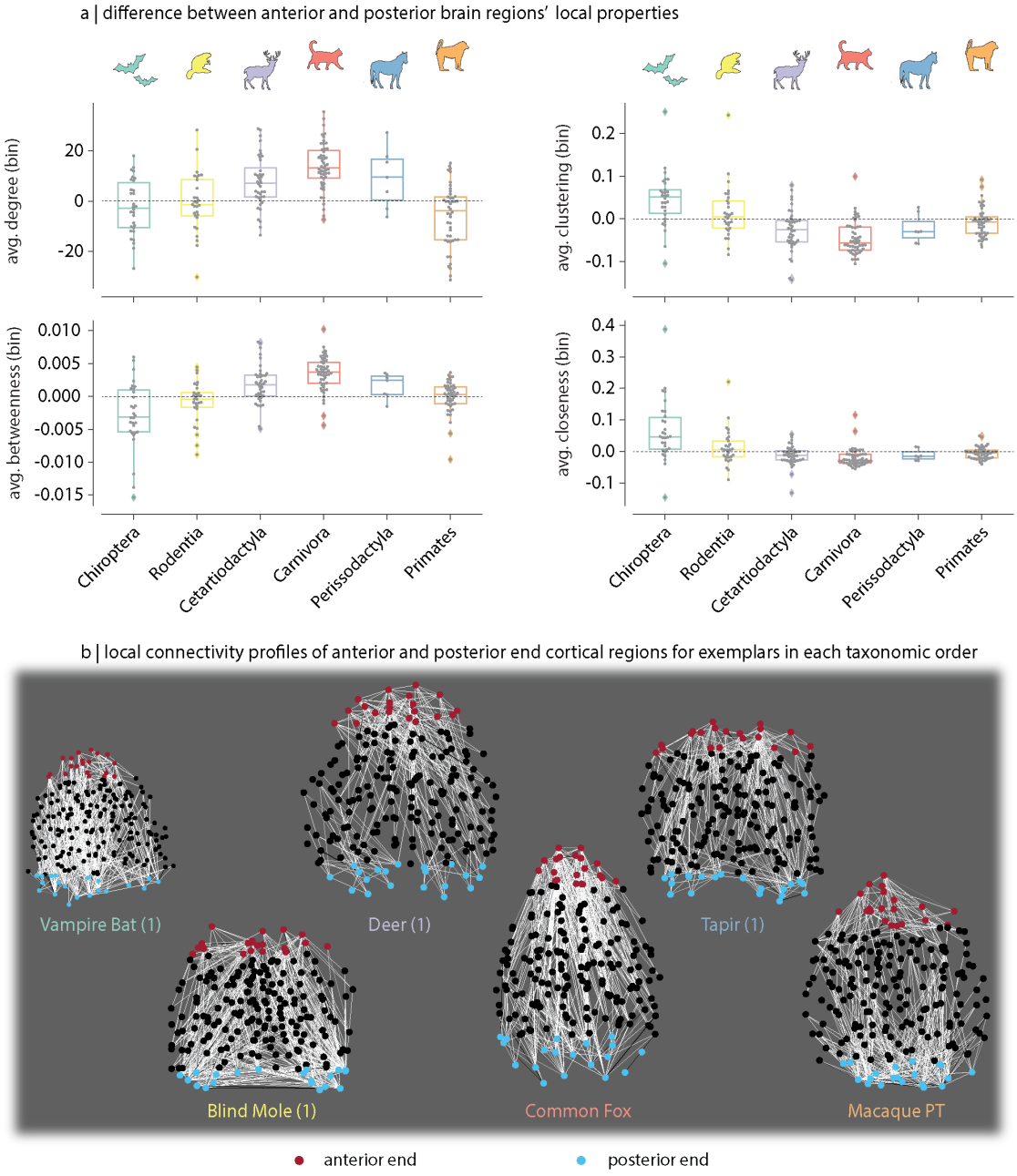

Figure S5.9: **Changes in local topology along the frontal-occipital axis** | (a) Distribution across taxonomic orders of the difference in average local network topology between the 10% most anterior and the 10% most posterior brain regions (i.e. the anterior - posterior difference). Local features considered include: binary (average) degree, clustering, betweenness centrality and closeness. (b) Top 5% strongest connections of the 10% most anterior (red) and the 10% most posterior (blue) brain regions for exemplar species within each taxonomic order. Separate one-way ANOVAs were performed to compare the effect of taxonomic order on anterior-posterior differences in local: i) degree: $F_5 = 20.29$, $P = 2.57 \times 10^{-16}$, ii) clustering: $F_5 = 15.88$, $P = 3.88 \times 10^{-13}$, iii) betweenness: $F_5 = 17.97$, $P = 1.14 \times 10^{-14}$ and iv) closeness: $F_5 = 13.54$, $P = 2.36 \times 10^{-11}$.

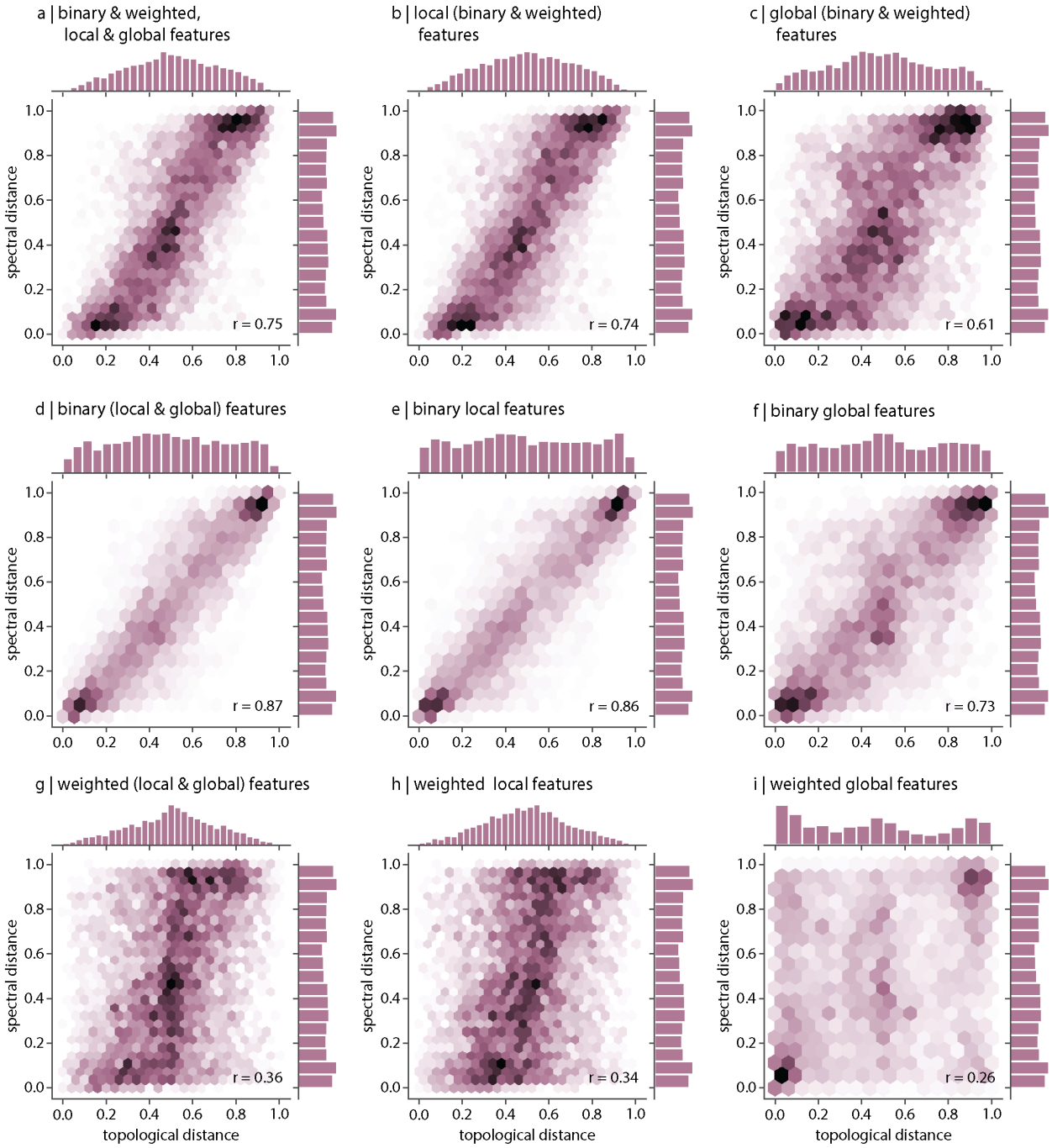

Figure S5.10: **Relationship between spectral and topological distance** | Correlations between inter-species distances computed using topological distance (abscissa) and spectral distance (ordinate). Correlations are shown for (a) binary local and global features, (b) binary local features, (c) binary global features, (d) weighted local and global features, (e) weighted local features and (f) weighted global features.

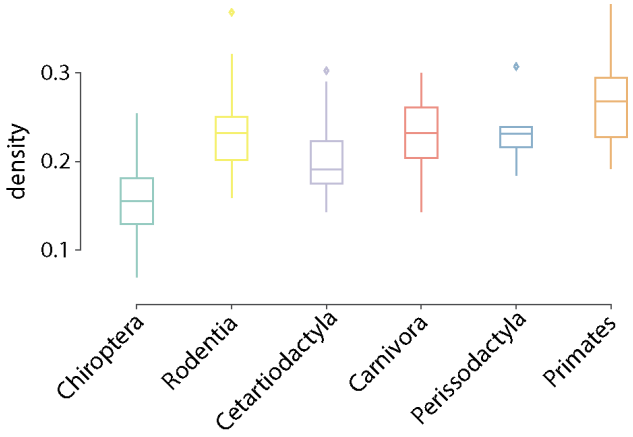

Figure S5.11: **Network density** | Distribution of network density is shown for each taxonomic order. Connection density is estimated as the ration of existent connections to the total number of possible connections.

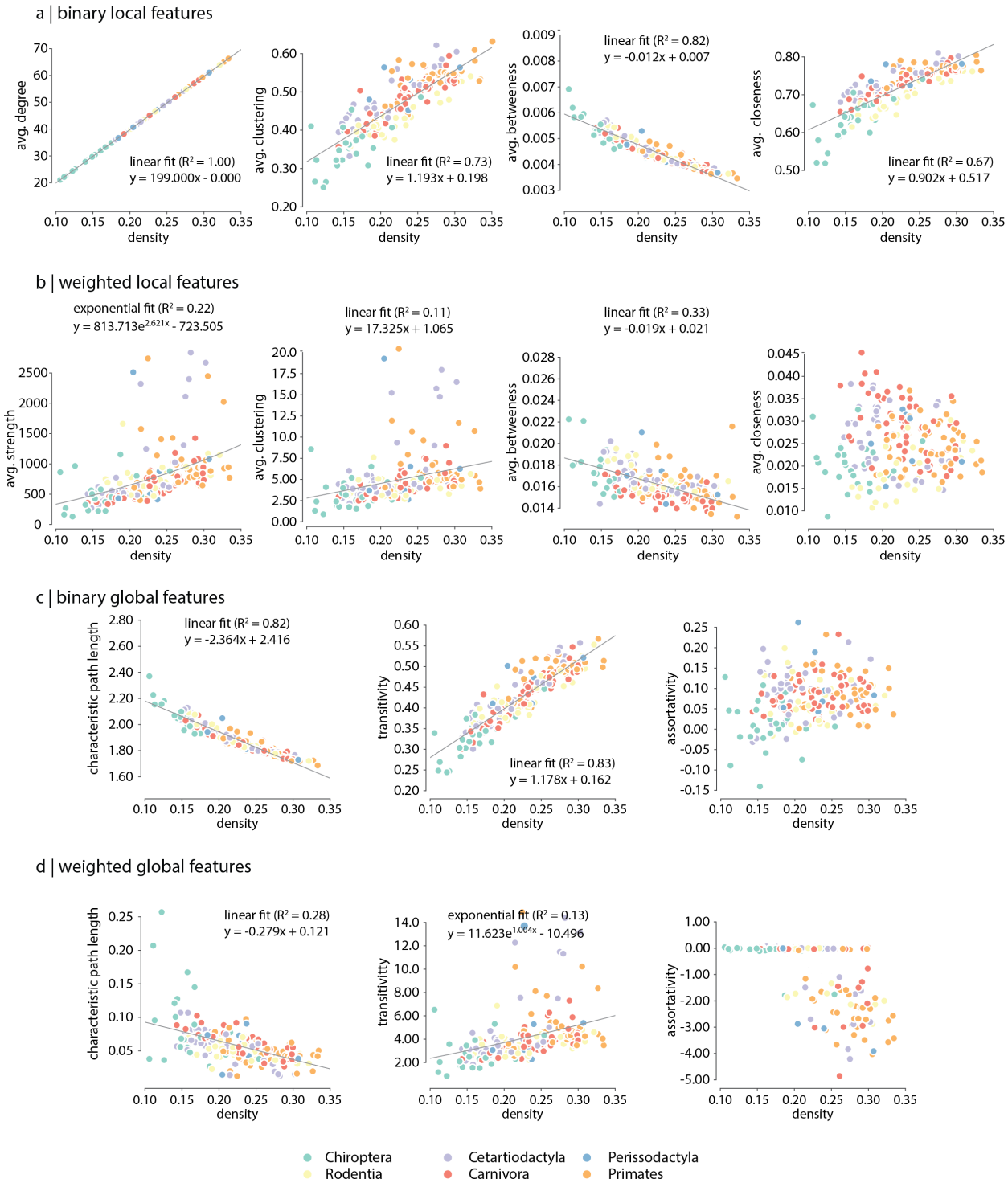

Figure S5.12: **Controlling for network density** | Network density is regressed out from topological features (see *Methods*).

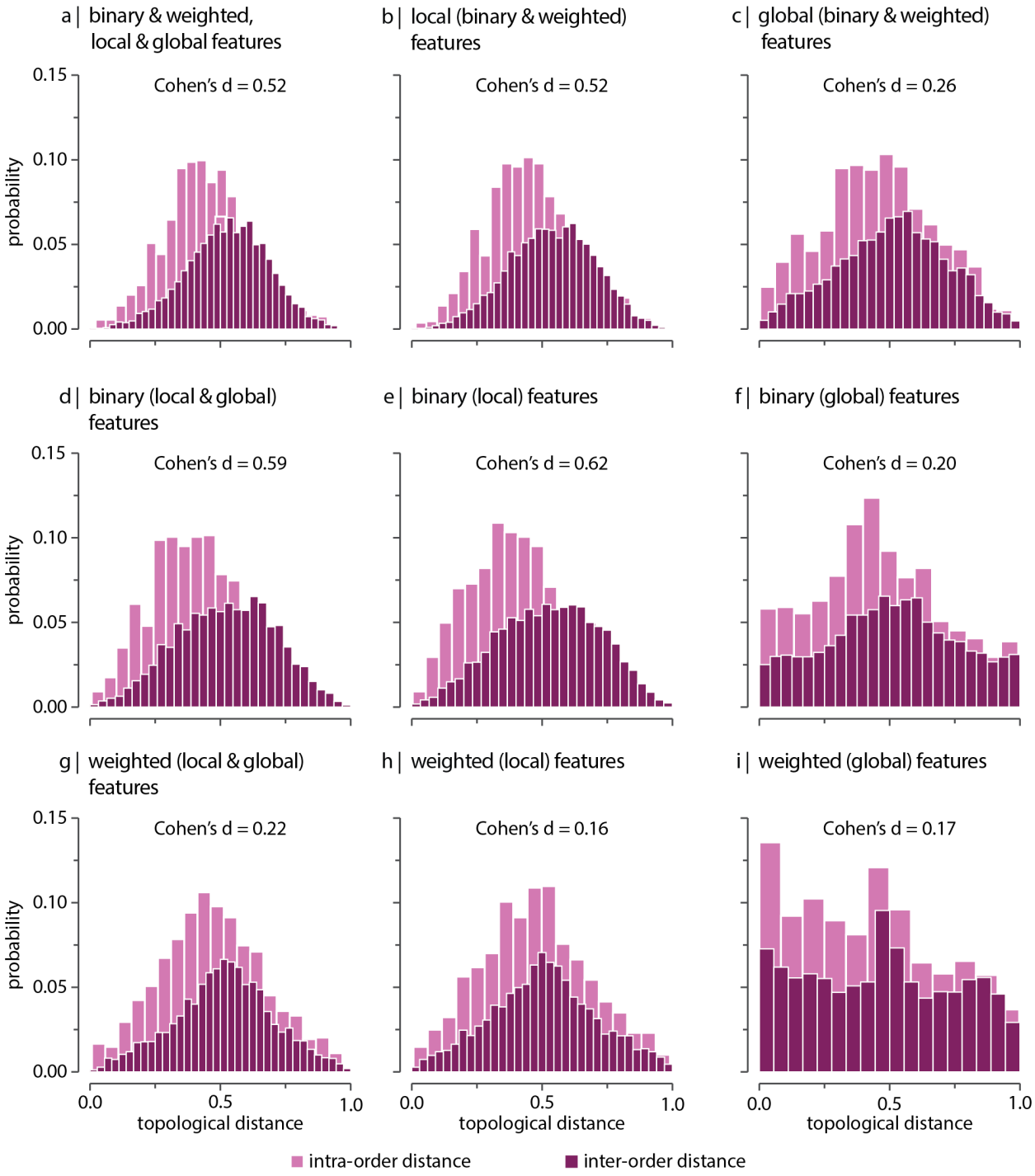

Figure S5.13: **Contribution of network features after controlling for connection density** | Network density is regressed out from topological features (see *Methods*), and topological distance is computed using multiple local and global connectome features. Histograms show intra- and inter-order distance distributions when using (a) all (binary, weighted, local and global), (b) all local (binary and weighted), (c) all global (binary and weighted), (d) all binary (local and global), (e) only binary local, (f) only binary global, (g) all weighted (local and global), (h) only weighted local and (i) only weighted global features. Local features include (the average and standard deviation of) degree, clustering, betweenness, and closeness. Global features include characteristic path length, transitivity, and assortativity. For definitions please see *Methods*. Effect sizes correspond to Cohen's d estimator from a two-sample Welch's t-test. Equivalent conclusions are drawn if common-language effects sizes from a two-sample Mann-Whitney U test are used. In all cases, the difference in the mean and median of intra- and inter-order distance distributions is statistically significant ($P < 10^{-4}$).

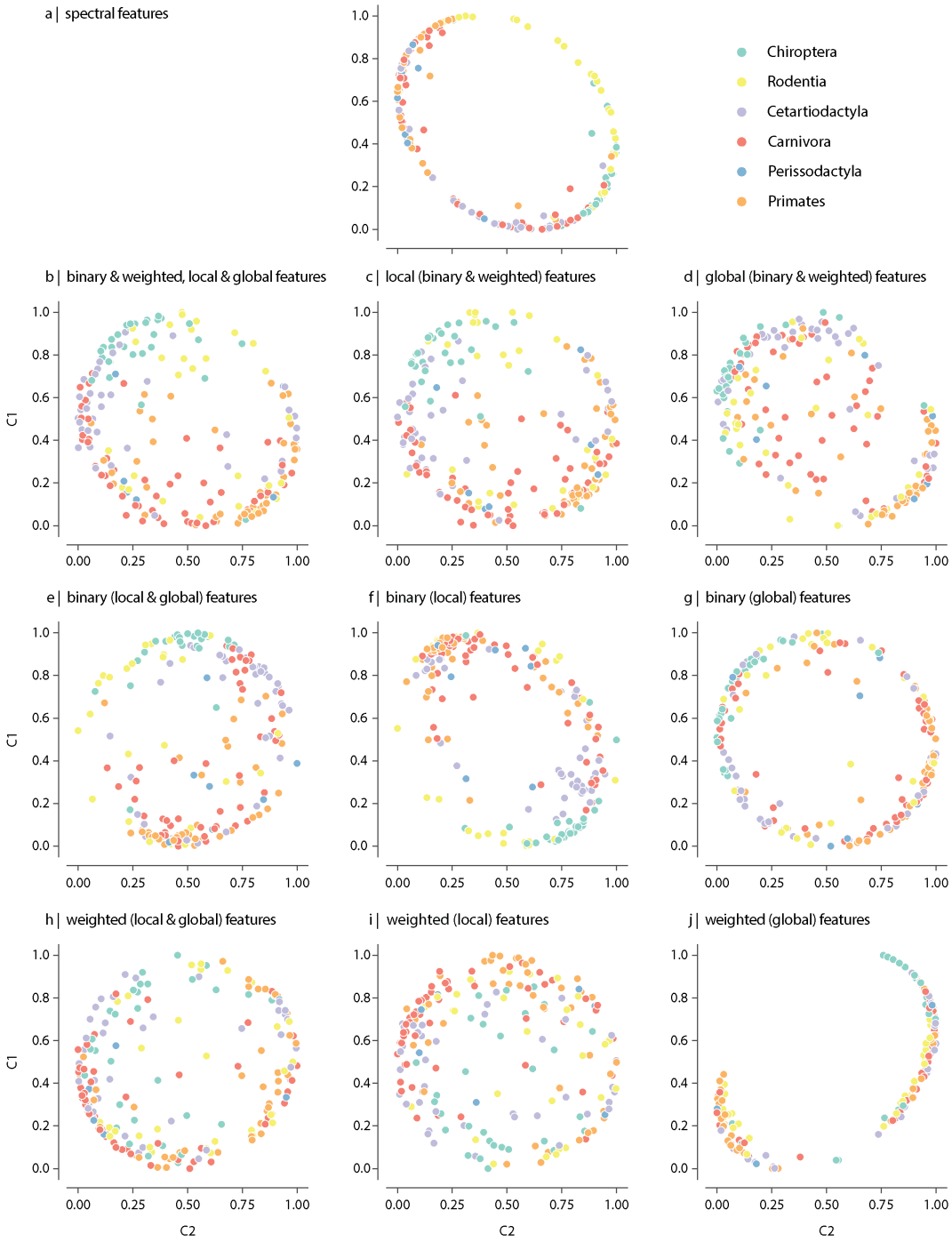

Figure S5.14: **Taxonomic order separation in low-dimensional space** | Multidimensional scaling (MDS) with cosine distance is applied to (a) spectral and (b-j) topological features to generate a low-dimensional (2D) projection of the data set. MDS was implemented using the *MDS* function in the *manifold* module of the *Scikit-learn* Python package Pedregosa et al., 2011. Details of the implementation can be found in the publicly available code repository. Specifically, MDS was applied to (a) the Laplacian eigenspectra, (b) all (binary, weighted, local and global), (c) all local (binary and weighted), (d) all global (binary and weighted), (e) all binary (local and global), (f) only binary local, (g) only binary global, (h) all weighted (local and global), (i) only weighted local and (j) only weighted global features. Local features include (the average and standard deviation of) degree, clustering, betweenness, and closeness. Global features include characteristic path length, transitivity, and assortativity. Each dot in the scatter plots represents a sample from a different order. Visual inspection of the 2D projections shows that, generally speaking, local features tend to provide a better class separation compared to global features.

Figure S5.15: **Connectome-based clustering of mammals** | Hierarchical clustering was applied to the (a) spectral and (b-j) topological distance matrices to assess the extent to which data-driven clustering of mammalian species recapitulates traditional taxonomies based on morphology and genetics. Hierarchical clustering was implemented using the *hierarchy.linkage* function in the *cluster* module of the *Scipy* Python package Virtanen et al., 2020. Details of the implementation can be found in the publicly available code repository. Specifically, hierarchical clustering was applied to the inter-species distance matrix estimated using (a) the Laplacian eigenspectra, (b) all (binary, weighted, local and global), (c) all local (binary and weighted), (d) all global (binary and weighted), (e) all binary (local and global), (f) only binary local, (g) only binary global, (h) all weighted (local and global), (i) only weighted local and (j) only weighted global topological features. Local features include (the average and standard deviation of) degree, clustering, betweenness, and closeness. Global features include characteristic path length, transitivity, and assortativity. Each heat map represents an inter-species distance matrix. Colored rectangles represent the order each sample belongs to. Visual inspection of the results shows that, generally speaking, local features tend to provide a clustering solution that resembles more traditional taxonomies.

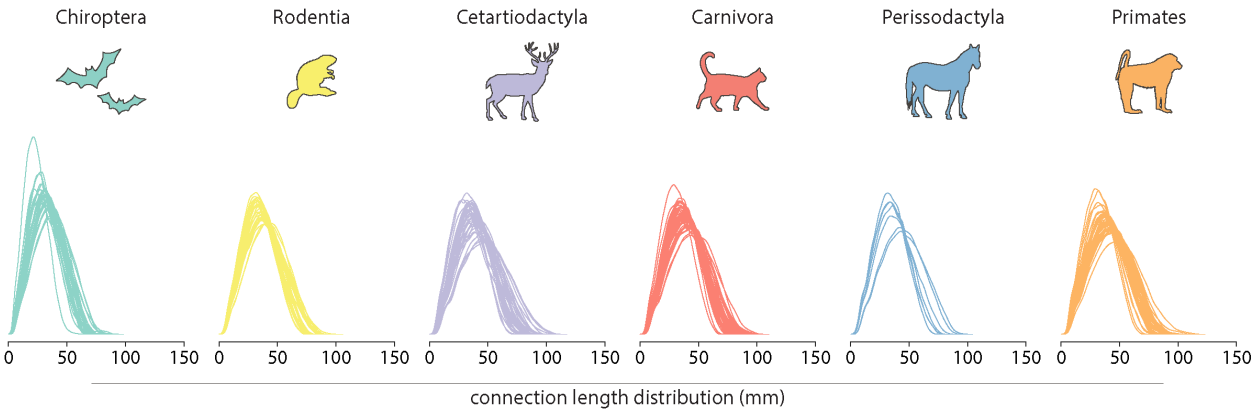

Figure S5.16: **Connection length distribution** | The connection length distributions of individual species for each taxonomic order.

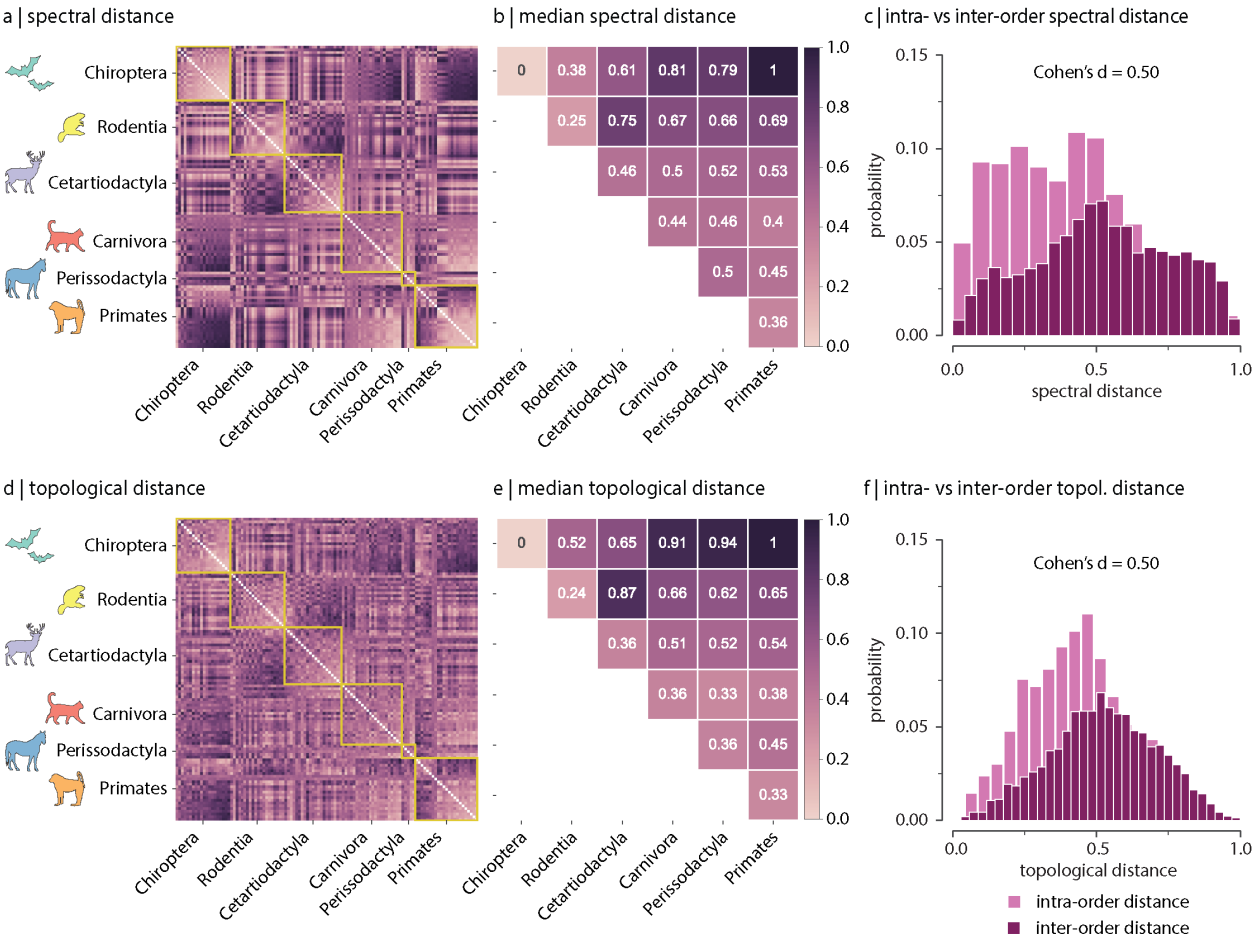

Figure S5.17: **Effect of (decreasing) parcellation resolution on the spectral and topological inter-species distance** | Results were replicated using a 100-node parcellation. (a) Spectral distance between species-specific connectomes. (b) Median spectral distance within and between all constituent members of each order. (c) Distribution of intra- and inter-order spectral distances. (d) Topological distance between species-specific connectomes. (e) Median topological distance within and between all constituent members of each order. (f) Distribution of intra- and inter-order topological distances. Effect sizes in (c) and (f) are Cohen's d estimator corresponding to a two-sample Welch's t-test ($P < 10^{-4}$). Equivalent conclusions are drawn if common-language effects sizes from the two-sample Mann-Whitney U test are used.

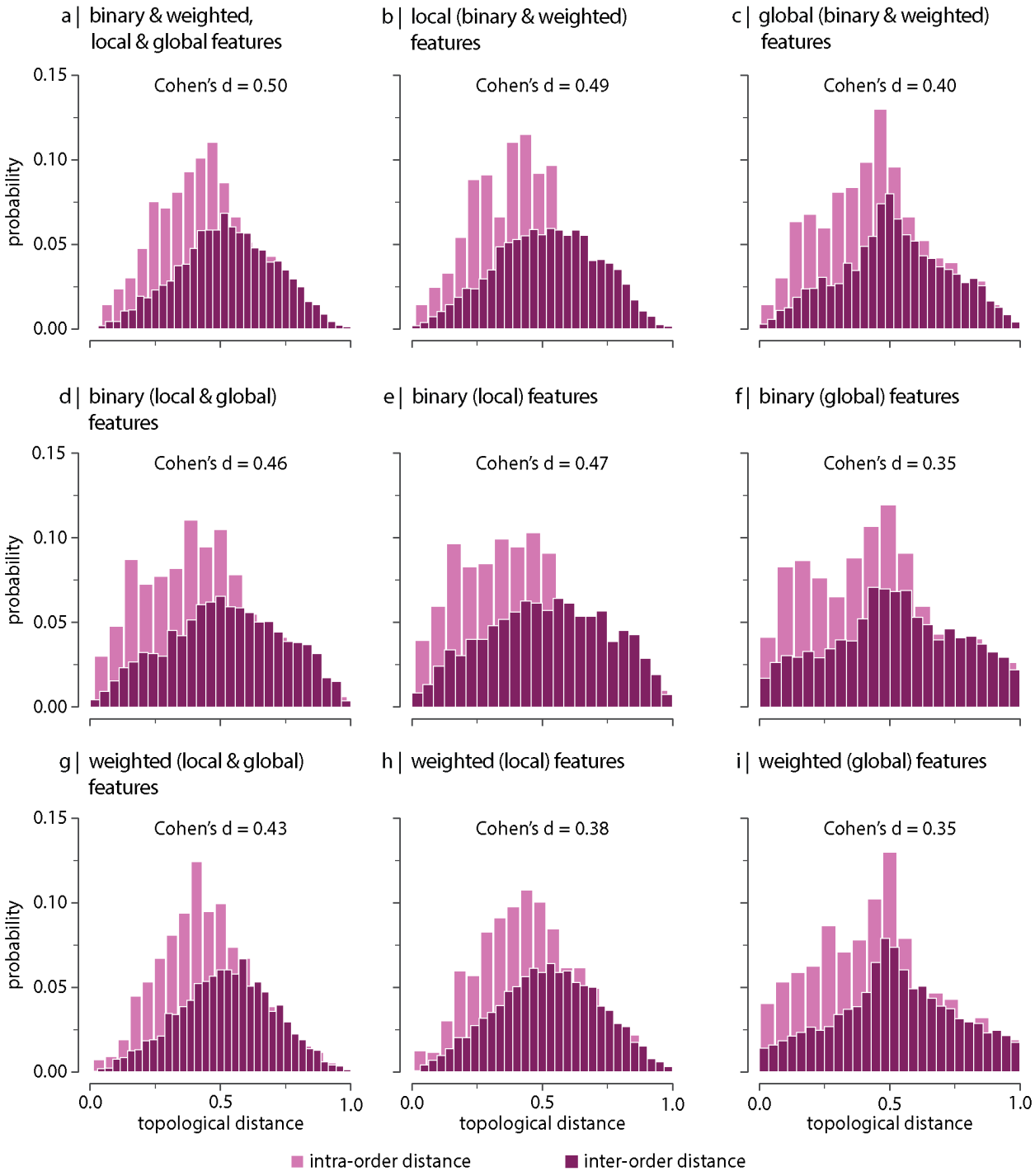

Figure S5.18: **Effect of (decreasing) parcellation resolution on the contribution of topological network features** | Results were replicated using a 100-node parcellation. Topological distance can be computed using different combinations of local and global, binary and weighted connectome features. Histograms show intra- and inter-order distance distributions when using (a) all (binary, weighted, local and global), (b) all local (binary and weighted), (c) all global (binary and weighted), (d) all binary (local and global), (e) only binary local, (f) only binary global, (g) all weighted (local and global), (h) only weighted local and (i) only weighted global features. Local features include (the average and standard deviation of) degree, clustering, betweenness, and closeness. Global features include characteristic path length, transitivity, and assortativity. For definitions please see *Methods*. Effect sizes correspond to Cohen's d estimator from a two-sample Welch's t-test. Equivalent conclusions are drawn if common-language effects sizes from a two-sample Mann-Whitney U test are used. In all cases, the difference in the mean and median of intra- and inter-order distance distributions is statistically significant ($P < 10^{-4}$).

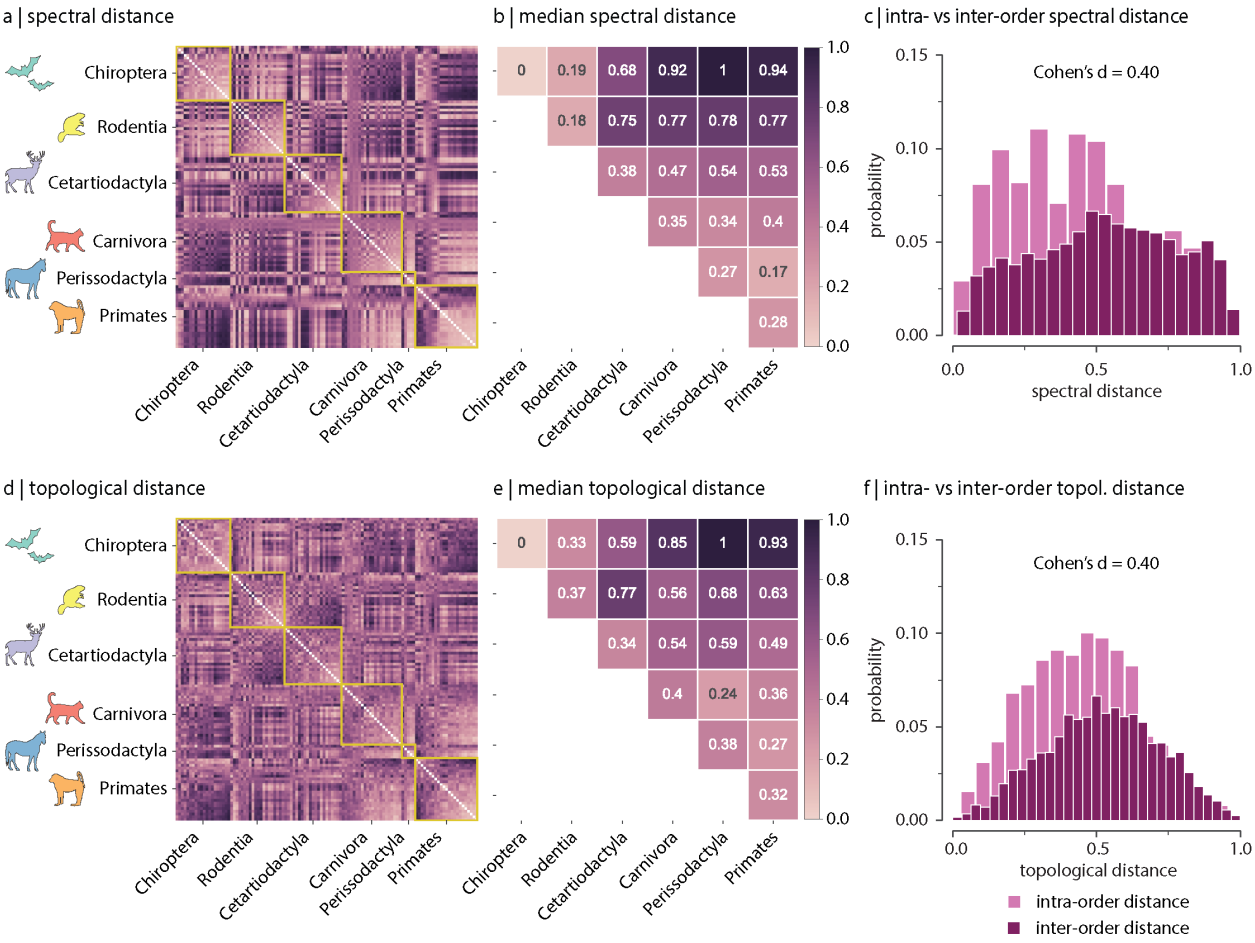

Figure S5.19: **Effect of (increasing) parcellation resolution on the spectral and topological inter-species distance** | Results were replicated using a 300-node parcellation. (a) Spectral distance between species-specific connectomes. (b) Median spectral distance within and between all constituent members of each order. (c) Distribution of intra- and inter-order spectral distances. (d) Topological distance between species-specific connectomes. (e) Median topological distance within and between all constituent members of each order. (f) Distribution of intra- and inter-order topological distances. Effect sizes in (c) and (f) are Cohen's d estimator corresponding to a two-sample Welch's t-test ($P < 10^{-4}$). Equivalent conclusions are drawn if common-language effects sizes from the two-sample Mann-Whitney U test are used.

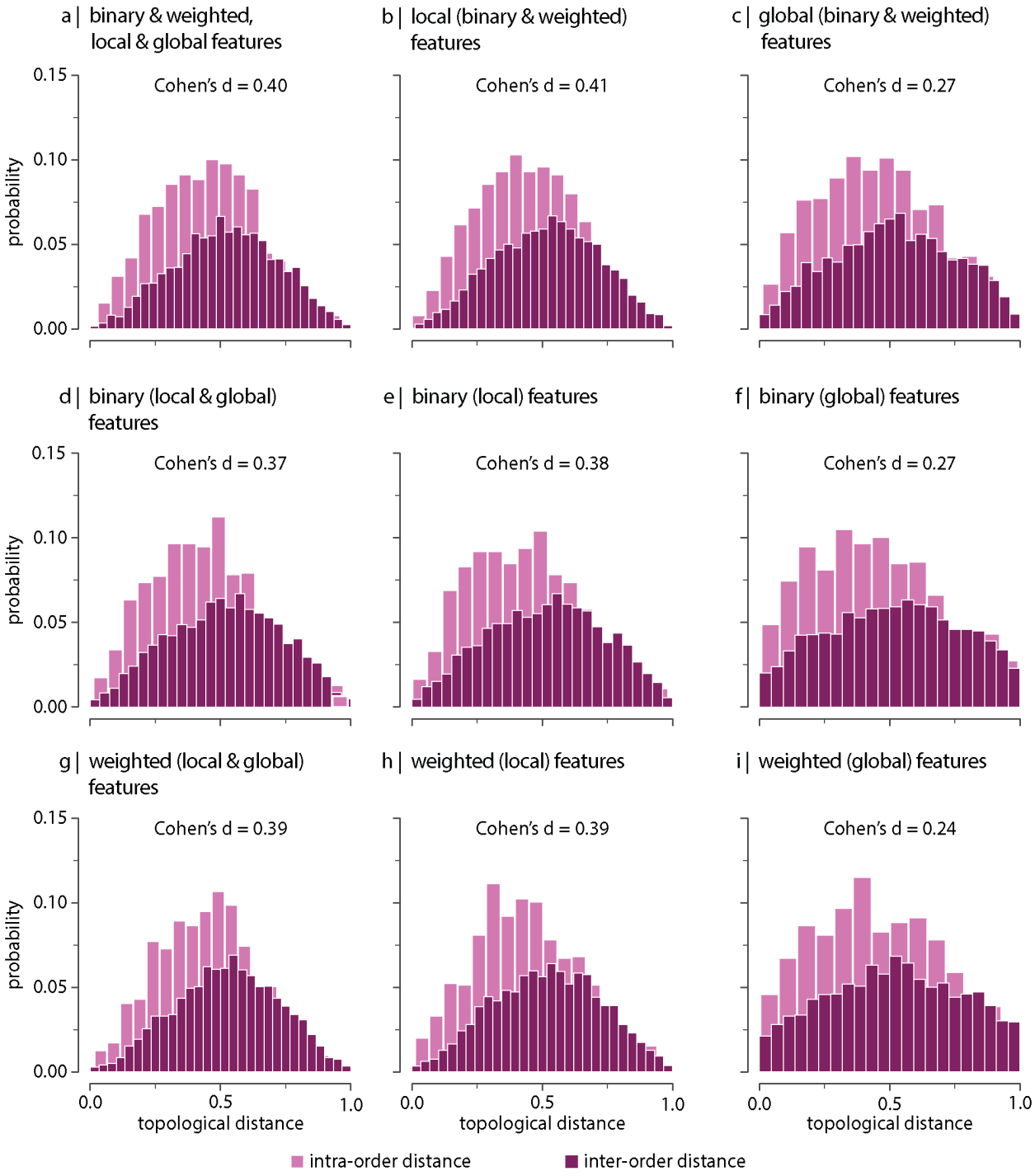

Figure S5.20: **Effect of (increasing) parcellation resolution on the contribution of topological network features** | Results were replicated using a 300-node parcellation. Topological distance can be computed using different combinations of local and global, binary and weighted connectome features. Histograms show intra- and inter-order distance distributions when using (a) all (binary, weighted, local and global), (b) all local (binary and weighted), (c) all global (binary and weighted), (d) all binary (local and global), (e) only binary local, (f) only binary global, (g) all weighted (local and global), (h) only weighted local and (i) only weighted global features. Local features include (the average and standard deviation of) degree, clustering, betweenness, and closeness. Global features include characteristic path length, transitivity, and assortativity. For definitions please see *Methods*. Effect sizes correspond to Cohen's d estimator from a two-sample Welch's t-test. Equivalent conclusions are drawn if common-language effects sizes from a two-sample Mann-Whitney U test are used. In all cases, the difference in the mean and median of intra- and inter-order distance distributions is statistically significant ($P < 10^{-4}$).

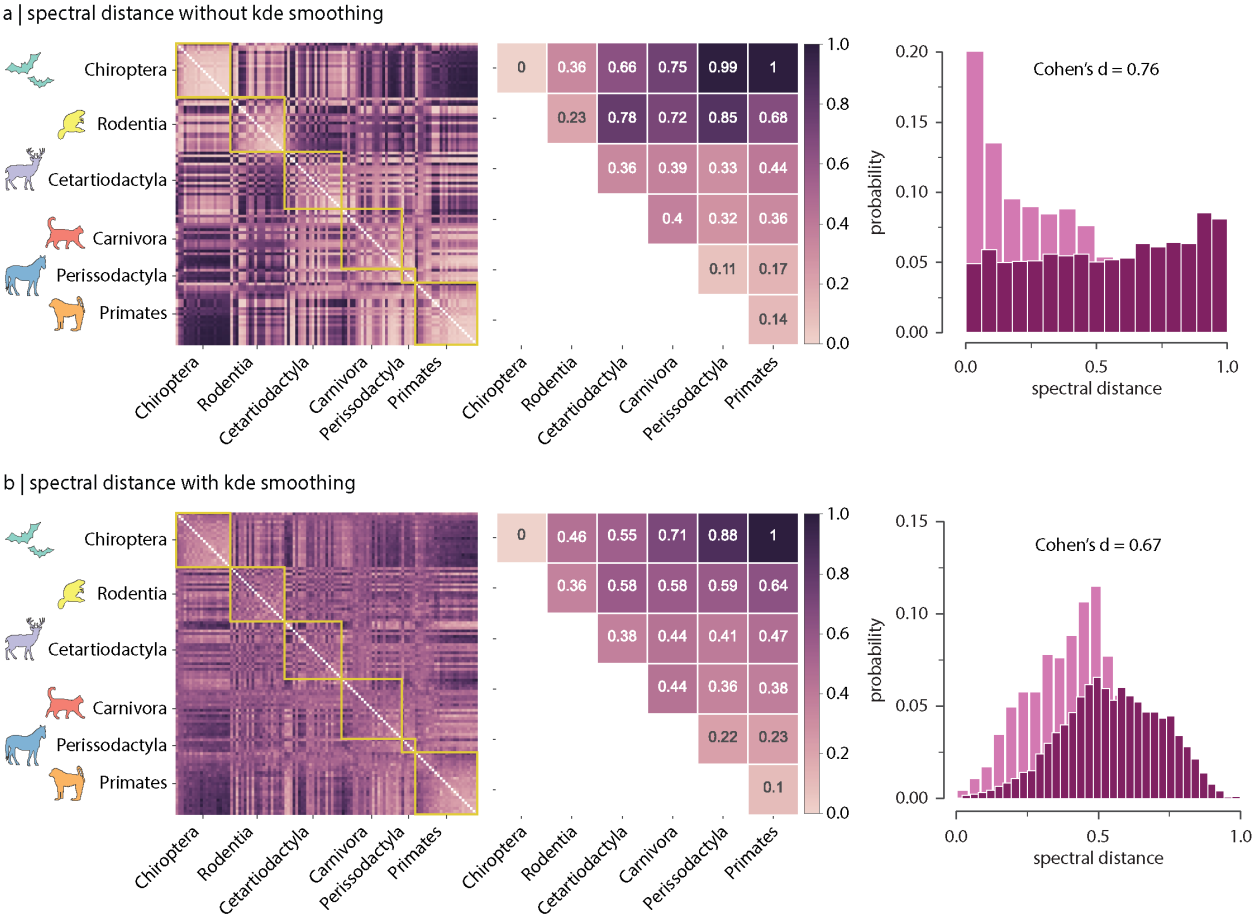

Figure S5.21: **Effect of kernel density estimation (kde) on inter-species spectral distances** | To allow comparison with previous reports, Gaussian kde smoothing is applied to the Laplacian eigenspectrum of individual species, before estimating inter-species distances. Spectral distance with (a) and without (b) kernel density estimation smoothing. Left: inter-species spectral distance. Center: median inter-species spectral distance. Right: intra- vs inter-order spectral distance distributions. Effect sizes correspond to Cohen's d estimator from a two-sample Welch's t-test ($P < 10^{-4}$).

Chapter 6

Discussion

6.1 Summary of findings and contributions

The research projects presented in this thesis investigate unique aspects of the link between structure and function in brain networks. However, against the conventional notion of *function*, understood as inter-regional co-activation patterns of neural activity, or *functional connectivity*, this thesis takes a small step forward, and deals with *function* in a way that its notion is closer to what we would generally consider as cognition and behaviour. Chapter 3 and chapter 4 introduce an interdisciplinary framework that brings together artificial intelligence and neuroscience to explore structure-function relationships in brain networks, but with a focus on the computational and information-processing aspects of the brain. Chapter 5 examines whether variations in cognition and behavior across phylogeny are concomitant with variations in connectome architecture, and hence the notion of *function* is implicitly represented by the set of behaviours and cognitive abilities that are shared across species with similar genetics and morphology. Below I highlight the main scientific findings and contributions of each chapter.

Chapter 3 highlights the computational consequences of different topological attributes in human connectome organization. In this study I combine MRI connectomics and reservoir computing to investigate how network architecture and dynamics jointly support memory capacity in biological connectomes. I reconstruct human connectomes using diffusion-weighted MRI data, implement them as artificial reservoirs, and train them to perform a memory task. By comparing these connectome-informed reservoirs against random architectures, I demonstrate that the computational advantages granted by the unique macro-scale network topology of the human connectome, and its meso-scale

modular organization, are exclusively optimized when the dynamics of the network are critical. This is in line with experimental and theoretical studies suggesting that the brain operates at a *criticality*, a dynamical regime that is thought to confer optimal information-processing (Cocchi et al., 2017). Throughout this work I adopted intrinsic networks to typify functional modules. Intrinsic networks are a functional connectivity based partition of the connectome into regions that co-activate during rest and during task, and tend to share a similar function (Thomas Yeo et al., 2011). Despite their widespread use in cognitive neuroscience, the specific contribution of intrinsic networks to computation in the brain is unknown. Here I provide evidence that intrinsic functional networks constitute computationally relevant components of the human connectome. This study also explores the economy of the human connectome; I show that, regardless of global network dynamics, human connectomes maximize memory capacity while minimizing metabolic and material costs associated to the growth and maintenance of inter-areal axonal projections. Consistently, findings emphasize the idea that network structure and dynamics interact to support and modulate the computational capacity of connectome-informed reservoirs, suggesting a potential mechanism to explain how a spectrum of computational capabilities emerge from the *invariant* anatomical macroscale network of the brain.

Chapter 4 expands on the previous chapter and presents this hybrid approach between artificial intelligence and neuroscience as a more general framework aimed to address structure-function relationships, with an emphasis on the computational properties of biological neural networks. Specifically, I combine connectomics and reservoir computing to allow scientists to implement biologically derived network architectures or connectomes as artificial neural networks, and train them to perform a variety of cognitive tasks. Given its flexibility in terms of network architecture, dynamics and task paradigm, this inter-disciplinary approach opens new and exciting opportunities to explore multiple aspects of the link between structure and function in brain networks. For instance, comparing reservoirs informed by healthy versus clinical populations could help us get insight into how disruptions in network architecture affect cognitive capacity. An equally intriguing question that could be addressed using this framework is how variations in connectome architecture, either throughout development or evolution, give rise to different cognitive capacities. These are just a few examples among the myriad applications that this framework can support. Beyond its potential scientific contributions, this work makes unique technical contributions via an openly-developed and free-available software package, `conn2res` (`https://github.com/netneurolab/conn2res.git`), facilitating the use of this

framework by the wide neuroscience community. In summary, by moving away from a *phenomenological* notion of function and shifting the focus towards the computational properties of the brain, the framework I propose can take us a step closer to understanding how cognition and behaviour emerge from the underlying anatomical structure of the brain. In addition to contributing new perspectives on the link between structure and function, this framework provides mechanistic insights into how computations arise from the dynamics that unfold upon the structural connectome, as opposed to purely statistical relations between measures of structure and function. Finally, despite common interests, neuroscience and artificial intelligence have followed diverging paths. The framework here proposed aims to act as a bridge between these two exciting and fast-pacing fields, thus stimulating the cross-pollination of ideas.

Chapter 5 demonstrates that variations in connectome architecture reflect already-established taxonomic relationships among a wide range of mammalian species. In this study I comprehensively chart connectome organization across the mammalian phylogenetic spectrum. I present a comparative analysis in which I quantitatively assess inter-species connectome similarities, and construct data-driven derived phylogenetic relationships based on brain wiring. Results show that these newly derived, connectome-based phylogenetic relations conform to traditional taxonomies based on morphology, genetics and behavior. Specifically, species that are part of the same taxonomic order tend to display similar connectome architecture. This supports the hypothesis that variations in connectome architecture, byproduct of speciation events in the genome, shape the cognitive and behavioural repertoire of an organism, thus suggesting a potential link between genomics and behaviour (York, 2018). Comparative analyses also indicate that, while hallmark global architectural features tend to be preserved, inter-species variations in connectome architecture are mainly driven by regional connectivity profiles. These findings validate previous studies suggesting that functional and behavioural adaptations across species are likely supported by changes in local connectivity patterns. Collectively, results from this work set the stage for future mechanistic studies linking genes to neural circuits and ultimately behaviour, offering new opportunities to explore how changes in brain network structure across phylogeny translate into changes in cognitive function and behavior. Altogether, this study emphasizes the impact that simultaneously investigating genomics, connectomics and behavior can have on our understanding of the link between structure and function in brain networks.

6.2 Function as computation

Chapter 3 and chapter 4 of this thesis are devoted to promoting an interdisciplinary framework that combines artificial intelligence and neuroscience to explore structure-function relationships in brain networks. This hybrid approach, while still being inclusive of the traditional notion of function, associated to emergent dynamical and functional phenomena, it puts a stronger emphasis on the computational and information-processing of biological neural networks. Through the development of an open-source software package, `conn2res`, I made this framework available to the neuroscience community, giving researchers the possibility to explore the opportunities that this framework offers. Below I discuss some of the limitations of this approach, and propose future research directions to improve our understanding of how structure and function are linked in biological brains. Throughout the discussion, I will use the name of the toolbox, `conn2res`, as a general reference to this combined framework.

6.2.1 Annotating artificial reservoirs

Convergent lines of evidence demonstrate a link between structural and functional connectivity networks. However, the correspondence between the two is far from perfect. While it is true that anatomical structural connections shape how information propagates throughout the brain, multiple other factors including transcription profiles, cytoarchitecture, receptor densities, laminar differentiation and intrinsic temporal dynamics, modulate how and when information is transmitted along the brain's axonal highways (Betzel et al., 2019; Huntenburg et al., 2017; Paquola et al., 2019; Seidlitz et al., 2018; Shafiei et al., 2018; Shine et al., 2019). The degree to which each of these factors is expressed throughout the cortex varies from one brain region to the other, following a dominant axis of variation — or *gradient* — that spans from unimodal to transmodal regions (Huntenburg et al., 2018; Margulies et al., 2016; Mesulam, 1998). The heterogeneous manifestation of these factors not only impacts the coupling between structure and function across the cortex (Baum et al., 2019; Paquola et al., 2019; Preti and Van De Ville, 2019; Vazquez-Rodriguez et al., 2019), but it also promotes functional specialization of brain areas (Fornito et al., 2019; Hansen et al., 2021), suggesting that the local computations that take place in cortical circuits are equally affected by the regional expression of these variables (Deco et al., 2020; Shine et al., 2019). Currently, the dynamical models implemented in `conn2res` do not necessarily take into account any of these variables and assume that local dynamics are homogeneous across the entire network. Thanks to extensive international data sharing efforts, increasingly

detailed maps of cortical features have been made available in humans an other organisms (Hawrylycz et al., 2012; Markello et al., 2022). These brain maps could be used to enrich the models that govern the local dynamics of each brain region in the artificial reservoir's network. This would open new opportunities to explore how the concerted interaction between network structure and micro-architecture shapes the computational properties of neural circuits.

6.2.2 Plastic reservoirs

Plasticity is an essential and critical feature of biological brains (Magee and Grienberger, 2020). Plasticity refers to the ability of the brain to adapt to the continuously changing environment. Although various forms of plasticity have been reported in the literature, including synaptic, structural and functional plasticity (Citri and Malenka, 2008), generally speaking, all of them reflect the malleability of neuronal circuitry and patterns of activity. Importantly, plasticity-driven modifications of structural and functional connectivity have been crucial for our understanding of learning and memory in neural circuits (Abbott and Nelson, 2000; Tsodyks, 2002). Reservoir computing, the artificial neural network model which `conn2res` has been built upon, is characterized by the fact that the reservoir's connection weights remain fixed throughout learning. While this is advantageous to assess the effect of network architecture on learning, it could also lead to misleading conclusions. Plasticity is described as a multiscale phenomena (Power and Schlaggar, 2017). The structural and functional reorganization of cortical micro-circuits can occur in a matter of milliseconds but can also extend throughout the lifespan of an organism (Power and Schlaggar, 2017). In contrast, large-scale reorganizations of the patterning and connectivity of the cortex take place almost exclusively early during development, with some exceptions found in the adult brain in the presence of brain injury or disease (Kambi et al., 2014; Makin and Flor, 2020; Siuda-Krzywicka et al., 2016). Therefore, depending on the scale under consideration, the assumption of a fixed reservoir could be problematic or not. For instance, if the connectome architecture used to inform the reservoir represents long-range, inter-areal axonal projections, like is the case of most MRI-derived connectomes, the assumption of a fixed network may still hold valid. However, if the connectome architecture represents a micro-cortical circuit, then the assumption of a fixed network is not valid anymore. In `conn2res`, this problem can be overcome by implementing adaptive weights that change according to local, activity-dependant learning rules (Zhang et al., 2017). Previous works have demonstrated that using hebbian-like synapses can actually improve the performance of reservoir computing models (Morales et al., 2021; Schrauwen et al., 2008; Zhang et al.,

2017). Adding this extra dimension to the `conn2res` framework can further improve our understanding of how neural circuit structure relates to function but from a computational point of view.

6.2.3 Promoting the synergy between AI and neuroscience

One of the goals of `conn2res` is to help reduce the gap between artificial intelligence and neuroscience, and to promote the cross-pollination of ideas between fields. `conn2res` integrates artificial recurrent neural network models with connectomics data to simulate, even if simplified, cognitive and behavioral phenomena. Using `conn2res`, one could envision the construction of a comprehensive structure-function ontology. We can systematically assess the computational performance of connectome-informed reservoirs in a variety of tasks spanning multiple cognitive domains. This would allow us to build a dictionary of key-value pairs, in which the keys correspond to different combinations of network architectures and dynamics, and the values correspond to the emerging computational property. Such level of apprehension of the link between structure and function can have a major impact beyond advancing our understanding of biological brains. Artificial intelligence and neuromorphic computing are currently hot areas of research. In particular, the design of memristive networks, a specific type of neuromorphic hardware, could benefit from our understanding on how computations arise in artificial reservoirs with biologically-plausible dynamics and connectivity patterns. In this regard, the construction of a structure-function ontology could serve as a look-up table to inform the architectural design of these brain-inspired memristive networks (Loeffler et al., 2021, 2023). The advantage of memristive networks compared to current neural network algorithms is that they can significantly reduce the computational and energy costs associated to training (Deng et al., 2015). This can be achieved thanks to the fact that, in contrast to modern von Neumann computer architectures -currently used to implement neural network algorithms-, in which there are dedicated components for memory storage and processing, in memristive networks these processes are combined. Memristive connections have the potential of simultaneously storing and processing information while altering their conductance due to local electric activity, quite similar to synaptic plasticity mechanisms in biological brains (Huang et al., 2021). As artificial and neuromorphic systems improve so does our capacity to analyze neuroimaging data. This of course can further our understanding of the brain.

6.3 Linking structure to ~~function~~ computation across phylogeny

Chapter 5 of this thesis showed that connectome-based, data-driven derived phylogenetic relationships, among a broad range of mammalian species, conform to traditional taxonomies based on morphological, genetic and functional traits. This suggests that variations in connectome architecture are concomitant with variations in morphology and genetics (Arnatkeviciute et al., 2021; Fornito et al., 2019), but more importantly, with variations in cognition and behavior. In this work the concept of *function* was implicitly represented by the set of shared behaviours among species belonging to the same taxonomic order. One important aspect of how structure leads to function in brain networks is understanding how connectome variations across phylogeny support species-specific cognitive and behavioral adaptations. Using the same comprehensive data set used for this study, which encompasses the connectomes of more than a hundred mammalian species, and the computation-related notion of *function* proposed by `conn2res`, one could directly assess how variations in connectome architecture across phylogeny account for variations in computational performance, bringing us one step closer to understanding how the connectome has rewired itself to accommodate different cognitive and behavioral repertoires, allowing animal species to adapt to different environmental conditions and habitats.

6.4 Conclusions

A full comprehension of how structure determines function in brain networks requires uncovering each of the steps along the information processing hierarchy. At an elementary level, local connectivity patterns and neuronal intrinsic dynamics shape population level dynamics. Computation and functional specialization of cortical micro-circuits are thought to arise from this neural population activity. At the next level, the brain's meso- and macro-scale structural connections determine how distant, functionally-specialized neural populations talk to one another, giving rise to inter-regional co-activation patterns that we capture via functional connectivity networks. These emergent functional interactions integrate multimodal information from functionally specialized segregated populations, thus supporting computations of a higher complexity. At the top of the processing hierarchy, there seems to be a correspondence between these inter-regional functional interactions and observable cognitive functions and behaviours. A large part of the neuroimaging

literature has been devoted to understanding how the anatomical network structure of the brain shapes micro-scale population dynamics and emerging meso- and macroscale functional interactions, but it remains unclear how these multi-scale emergent dynamical and functional phenomena support the computations that underlie cognition and behaviour. The projects here proposed aim to give a step forward in that direction. The main contribution of this thesis is therefore to shift the focus from dynamical and functional phenomena to the computational and information-processing aspects of biological brains. It proposes to do so by combining modern neuroimaging tools and advances in artificial intelligence, two currently exciting and fast-pacing fields.

Bibliography

Abbott, L. F. and S. B. Nelson (2000). "Synaptic plasticity: taming the beast". *Nature neuroscience*, 3(11), pp. 1178–1183.

Abdelnour, F., H. U. Voss, and A. Raj (2014). "Network diffusion accurately models the relationship between structural and functional brain connectivity networks". *NeuroImage*, 90, pp. 335–347.

Abdelnour, F. et al. (2018). "Functional brain connectivity is predictable from anatomic network's Laplacian eigen-structure". *Neuroimage*, 172, pp. 728–739.

Aceituno, P. V., G. Yan, and Y.-Y. Liu (2020). "Tailoring Echo State Networks for Optimal Learning". *Iscience*, 23(9), p. 101440.

Achterberg, J. et al. (2022). "Spatially-embedded recurrent neural networks reveal widespread links between structural and functional neuroscience findings". *bioRxiv*, pp. 2022–11.

Adachi, Y. et al. (2011). "Functional connectivity between anatomically unconnected areas is shaped by collective network-level effects in the macaque cortex". *Cereb Cortex*, 22(7), pp. 1586–1592.

Alavash, M. et al. (2018). "Dopaminergic modulation of hemodynamic signal variability and the functional connectome during cognitive performance". *NeuroImage*, 172, pp. 341–356.

Alexander, G. E., M. R. DeLong, and P. L. Strick (1986). "Parallel organization of functionally segregated circuits linking basal ganglia and cortex". *Annual review of neuroscience*, 9(1), pp. 357–381.

Alexander-Bloch, A. F. et al. (2018). "On testing for spatial correspondence between maps of human brain structure and function". *Neuroimage*, 178, pp. 540–551.

Alomar, M. L. et al. (2014). "Low-cost hardware implementation of reservoir computers". In: *2014 24th International Workshop on Power and Timing Modeling, Optimization and Simulation (PATMOS)*. IEEE, pp. 1–5.

Alonso Montes, C. et al. (2015). "Lagged and instantaneous dynamical influences related to brain structural connectivity". *Front Psychol*, 6, p. 1024.

Álvarez-Carretero, S. et al. (2021). "A Species-Level Timeline of Mammal Evolution Integrating Phylogenomic Data". *Nature*, pp. 1–8.

Alves, P. N. et al. (2019). "An improved neuroanatomical model of the default-mode network reconciles previous neuroimaging and neuropathological findings". *Commun Biol*, 2(1), pp. 1–14.

Antonelo, E. A. and B. Schrauwen (2014). "On learning navigation behaviors for small mobile robots with reservoir computing architectures". *IEEE transactions on neural networks and learning systems*, 26(4), pp. 763–780.

Antonik, P. (2018). *Application of FPGA to Real-Time Machine Learning: Hardware Reservoir Computers and Software Image Processing*. Springer.

Antonik, P. et al. (2015). "FPGA implementation of reservoir computing with online learning". In: *24th Belgian-Dutch Conference on Machine Learning*.

Appeltant, L. et al. (2011). "Information processing using a single dynamical node as complex system". *Nature communications*, 2(1), pp. 1–6.

Ardesch, D. J. et al. (2021). "Scaling principles of white matter connectivity in the human and nonhuman primate brain". *Cereb Cortex*.

Arnatkeviciute, A. et al. (2021). "Where the genome meets the connectome: understanding how genes shape human brain connectivity". *PsyArXiv*.

Arnatkevičiūtė, A. et al. (2018). "Hub connectivity, neuronal diversity, and gene expression in the Caenorhabditis elegans connectome". *PLoS Comput Biol*, 14(2), e1005989.

Artola, A., S Bröcher, and W. Singer (1990). "Different voltage-dependent thresholds for inducing long-term depression and long-term potentiation in slices of rat visual cortex". *Nature*, 347(6288), pp. 69–72.

Assaf, Y. et al. (2020). "Conservation of brain connectivity and wiring across the mammalian class". *Nat Neurosci*, 23(7), pp. 805–808.

Atasoy, S., I. Donnelly, and J. Pearson (2016). "Human brain networks function in connectome-specific harmonic waves". *Nat Commun*, 7, p. 10340.

Auer, T. O. et al. (2020). "Olfactory receptor and circuit evolution promote host specialization". *Nature*, 579(7799), pp. 402–408.

Avena-Koenigsberger, A., B. Misic, and O. Sporns (2018). "Communication dynamics in complex brain networks". *Nat Rev Neurosci*, 19(1), p. 17.

Avena-Koenigsberger, A. et al. (2015). "Network morphospace". *J Roy Soc Interface*, 12(103), p. 20140881.

Avena-Koenigsberger, A. et al. (2017). "Path ensembles and a tradeoff between communication efficiency and resilience in the human connectome". *Brain Struct Funct*, 222(1), pp. 603–618.

Avena-Koenigsberger, A. et al. (2019). "A spectrum of routing strategies for brain networks". *PLoS Comput Biol*, 15(3), e1006833.

Baker, R. J. and R. D. Bradley (2006). "Speciation in mammals and the genetic species concept". *J Mammal*, 87(4), pp. 643–662.

Banerjee, A. and J. Jost (2008). "On the spectrum of the normalized graph Laplacian". *Linear algebra and its applications*, 428(11-12), pp. 3015–3022.

— (2009). "Graph spectra as a systematic tool in computational biology". *Discrete Applied Mathematics*, 157(10), pp. 2425–2431.

Barkan, C. L., D. B. Kelley, and E. Zornik (2018). "Premotor neuron divergence reflects vocal evolution". *J Neurosci*, 38(23), pp. 5325–5337.

Barker, A. J. (2021). "Brains and speciation: Control of behavior". *Curr Opin Neurobiol*, 71, pp. 158–163.

Barone, P and J. P. Joseph (1989). "Prefrontal cortex and spatial sequencing in macaque monkey". *Experimental brain research*, 78, pp. 447–464.

Barrett, R. L. et al. (2020). "Differences in frontal network anatomy across primate species". *J Neurosci*, 40(10), pp. 2094–2107.

Barsotti, E., A. Correia, and A. Cardona (2021). "Neural architectures in the light of comparative connectomics". *Curr Opin Neurobiol*, 71, pp. 139–149.

Bassett, D. S. and E. T. Bullmore (2009). "Human brain networks in health and disease". *Current opinion in neurology*, 22(4), p. 340.

Bassett, D. S. and O. Sporns (2017). "Network neuroscience". *Nature neuroscience*, 20(3), pp. 353–364.

Bassett, D. S., P. Zurn, and J. I. Gold (2018). "On the nature and use of models in network neuroscience". *Nature Reviews Neuroscience*, 19(9), pp. 566–578.

Bassett, D. S. et al. (2010). "Efficient physical embedding of topologically complex information processing networks in brains and computer circuits". *PLoS Comput Biol*, 6(4), e1000748.

Bassett, D. S. et al. (2011). "Conserved and variable architecture of human white matter connectivity". *Neuroimage*, 54(2), pp. 1262–1279.

Bassett, D. S. et al. (2013). "Robust detection of dynamic community structure in networks". *Chaos: An Interdisciplinary Journal of Nonlinear Science*, 23(1), p. 013142.

Bassett, D. S. and E. Bullmore (2006). "Small-world brain networks". *The neuroscientist*, 12(6), pp. 512–523.

Bathellier, B., L. Ushakova, and S. Rumpel (2012). "Discrete neocortical dynamics predict behavioral categorization of sounds". *Neuron*, 76(2), pp. 435–449.

Baum, G. L. et al. (2019). "Development of structure–function coupling in human brain networks during youth". *Proc Natl Acad Sci USA*.

Baum, G. L. et al. (2020). "Development of structure–function coupling in human brain networks during youth". *Proceedings of the National Academy of Sciences*, 117(1), pp. 771–778.

Beauchamp, A. et al. (2022). "Whole-brain comparison of rodent and human brains using spatial transcriptomics". *bioRxiv*.

Bell, P. T. and J. M. Shine (2016). "Subcortical contributions to large-scale network communication". *Neurosci Biobehav Rev*, 71, pp. 313–322.

Bellec, P. et al. (2010). "Multi-level bootstrap analysis of stable clusters in resting-state fMRI". *NeuroImage*, 51(3), pp. 1126–1139.

Bendesky, A. and C. I. Bargmann (2011). "Genetic contributions to behavioural diversity at the gene–environment interface". *Nature Reviews Genetics*, 12(12), pp. 809–820.

Bennett, C. H., D. Querlioz, and J.-O. Klein (2017). "Spatio-temporal learning with arrays of analog nanosynapses". In: *2017 IEEE/ACM International Symposium on Nanoscale Architectures (NANOARCH)*. IEEE, pp. 125–130.

Bertolero, M. A., B. T. Yeo, and M. D'Esposito (2015). "The modular and integrative functional architecture of the human brain". *Proc Natl Acad Sci USA*, 112(49), E6798–E6807.

Bertolero, M. A. et al. (2018). "A mechanistic model of connector hubs, modularity and cognition". *Nat Hum Behav*, 2(10), pp. 765–777.

Bertschinger, N. and T. Natschläger (2004). "Real-time computation at the edge of chaos in recurrent neural networks". *Neural computation*, 16(7), pp. 1413–1436.

Bettinardi, R. G. et al. (2017a). "How structure sculpts function: unveiling the contribution of anatomical connectivity to the brain's spontaneous correlation structure". *Chaos*, 27(4), p. 047409.

— (2017b). "How structure sculpts function: unveiling the contribution of anatomical connectivity to the brain's spontaneous correlation structure". *Chaos: An Interdisciplinary Journal of Nonlinear Science*, 27(4), p. 047409.

Betzel, R. F. and D. S. Bassett (2018). "Specificity and robustness of long-distance connections in weighted, interareal connectomes". *Proceedings of the National Academy of Sciences*, 115(21), E4880–E4889.

Betzel, R. F., J. D. Medaglia, and D. S. Bassett (2018a). "Diversity of meso-scale architecture in human and non-human connectomes". *Nat Commun*, 9(1), p. 346.

Betzel, R. F. et al. (2016). "Generative models of the human connectome". *NeuroImage*, 124, pp. 1054–1064.

Betzel, R. F. et al. (2017a). "Inter-regional ECoG correlations predicted by communication dynamics, geometry, and correlated gene expression". *arXiv preprint arXiv:1706.06088*.

Betzel, R. F. et al. (2017b). "The modular organization of human anatomical brain networks: Accounting for the cost of wiring". *Net Neurosci*, 1(1), pp. 42–68.

Betzel, R. F. et al. (2018b). "Distance-Dependent Consensus Thresholds for Generating Group-Representative Structural Brain Networks". *Net Neurosci*, 3(2), pp. 475–496.

Betzel, R. F. et al. (2019). "Structural, geometric and genetic factors predict interregional brain connectivity patterns probed by electrocorticography". *Nat Biomed Eng*, p. 1.

Beul, S. F., S. Grant, and C. C. Hilgetag (2015). "A predictive model of the cat cortical connectome based on cytoarchitecture and distance". *Brain Struct Funct*, 220(6), pp. 3167–3184.

Bhovad, P. and S. Li (2021). "Physical reservoir computing with origami and its application to robotic crawling". *Scientific Reports*, 11(1), p. 13002.

Bi, G.-q. and M.-m. Poo (1998). "Synaptic modifications in cultured hippocampal neurons: dependence on spike timing, synaptic strength, and postsynaptic cell type". *Journal of neuroscience*, 18(24), pp. 10464–10472.

Bianchi, S. et al. (2013). "Dendritic morphology of pyramidal neurons in the chimpanzee neocortex: regional specializations and comparison to humans". *Cereb Cortex*, 23(10), pp. 2429–2436.

Biswal, B. et al. (1995). "Functional connectivity in the motor cortex of resting human brain using echo-planar MRI". *Magn Reson Med*, 34(4), pp. 537–541.

Blondel, V. D. et al. (2008). "Fast unfolding of communities in large networks". *Journal of statistical mechanics: theory and experiment*, 2008(10), P10008.

Boedecker, J. et al. (2012). "Information processing in echo state networks at the edge of chaos". *Theory in Biosciences*, 131(3), pp. 205–213.

Börgers, C. and N. J. Kopell (2008). "Gamma oscillations and stimulus selection". *Neural computation*, 20(2), pp. 383–414.

Bota, M., O. Sporns, and L. W. Swanson (2015). "Architecture of the cerebral cortical association connectome underlying cognition". *Proc Natl Acad Sci USA*, 112(16), E2093–E2101.

Brandes, U. (2001). "A faster algorithm for betweenness centrality". *Journal of mathematical sociology*, 25(2), pp. 163–177.

Breakspear, M. (2017). "Dynamic models of large-scale brain activity". *Nat Neurosci*, 20(3), p. 340.

Brink, R. L. van den, T. Pfeffer, and T. H. Donner (2019). "Brainstem modulation of large-scale intrinsic cortical activity correlations". *Front Hum Neurosci*.

Brink, R. L. van den et al. (2016). "Catecholaminergic neuromodulation shapes intrinsic MRI functional connectivity in the human brain". *J Neurosci*, 36(30), pp. 7865–7876.

Britten, K. H. et al. (1992). "The analysis of visual motion: a comparison of neuronal and psychophysical performance". *Journal of Neuroscience*, 12(12), pp. 4745–4765.

Brockman, G. et al. (2016). "Openai gym". *arXiv preprint arXiv:1606.01540*.

Brown, A. E. and B. De Bivort (2018). "Ethology as a physical science". *Nat Phys*, p. 1.

Buckner, R. L. and F. M. Krienen (2013). "The evolution of distributed association networks in the human brain". *Trends Cogn Sci*, 17(12), pp. 648–665.

Buckner, R. L. and D. S. Margulies (2019). "Macroscale cortical organization and a default-like apex transmodal network in the marmoset monkey". *Nat Commun*, 10(1), pp. 1–12.

Bullmore, E. and O. Sporns (2012). "The economy of brain network organization". *Nat Rev Neurosci*, 13(5), p. 336.

Buonomano, D. V. and W. Maass (2009). "State-dependent computations: spatiotemporal processing in cortical networks". *Nature Reviews Neuroscience*, 10(2), p. 113.

Burke, J. D. (1968). "A Brief History of the Taxonomy of Mammals". *MCV/Q, Medical College of Virginia Quarterly*, 4(2), pp. 77–80.

Büsing, L., B. Schrauwen, and R. Legenstein (2010). "Connectivity, dynamics, and memory in reservoir computing with binary and analog neurons". *Neural computation*, 22(5), pp. 1272–1311.

Butler, M. A. and A. A. King (2004). "Phylogenetic comparative analysis: a modeling approach for adaptive evolution". *The American Naturalist*, 164(6), pp. 683–695.

Buzsáki, G. and X.-J. Wang (2012). "Mechanisms of gamma oscillations". *Annual review of neuroscience*, 35, pp. 203–225.

Cabral, J., M. L. Kringelbach, and G. Deco (2017). "Functional connectivity dynamically evolves on multiple time-scales over a static structural connectome: Models and mechanisms". *NeuroImage*, 160, pp. 84–96.

Caluwaerts, K. et al. (2013). "Locomotion without a brain: physical reservoir computing in tensegrity structures". *Artificial life*, 19(1), pp. 35–66.

Cammoun, L. et al. (2012). "Mapping the human connectome at multiple scales with diffusion spectrum MRI". *J Neurosci Meth*, 203(2), pp. 386–397.

Cazin, N. et al. (2018). "Prefrontal cortex creates novel navigation sequences from hippocampal place-cell replay with spatial reward propagation". *bioRxiv*, p. 466920.

Chen, Z. J. et al. (2008). "Revealing modular architecture of human brain structural networks by using cortical thickness from MRI". *Cerebral cortex*, 18(10), pp. 2374–2381.

Chiang, A.-S. et al. (2011). "Three-dimensional reconstruction of brain-wide wiring networks in Drosophila at single-cell resolution". *Curr Biol*, 21(1), pp. 1–11.

Chung, F. (1996). "Spectral graph theory. Fresno". *Proceedings of the American Mathematical Society*.

Citri, A. and R. C. Malenka (2008). "Synaptic plasticity: multiple forms, functions, and mechanisms". *Neuropsychopharmacology*, 33(1), pp. 18–41.

Cocchi, L. et al. (2014). "Disruption of structure–function coupling in the schizophrenia connectome". *NeuroImage: Clinical*, 4, pp. 779–787.

Cocchi, L. et al. (2017). "Criticality in the brain: A synthesis of neurobiology, models and cognition". *Progress in neurobiology*, 158, pp. 132–152.

Cole, M. W. et al. (2014). "Intrinsic and task-evoked network architectures of the human brain". *Neuron*, 83(1), pp. 238–251.

Colizza, V. et al. (2006). "Detecting rich-club ordering in complex networks". *Nature physics*, 2(2), pp. 110–115.

Consortium, Z. et al. (2020). "A comparative genomics multitool for scientific discovery and conservation". *Nature*, 587(7833), p. 240.

Cornblath, E. J. et al. (2020). "Temporal sequences of brain activity at rest are constrained by white matter structure and modulated by cognitive demands". *Communications Biology*, 3(1), pp. 1–12.

Crofts, J. J. and D. J. Higham (2009). "A weighted communicability measure applied to complex brain networks". *J Roy Soc Interface*, 6(33), pp. 411–414.

Crossley, N. A. et al. (2013). "Cognitive relevance of the community structure of the human brain functional coactivation network". *Proceedings of the National Academy of Sciences*, 110(28), pp. 11583–11588.

Daducci, A. et al. (2012). "The connectome mapper: an open-source processing pipeline to map connectomes with MRI". *PLoS ONE*, 7(12), e48121.

Dale, M. et al. (2021). "Reservoir computing in material substrates". *Reservoir Computing: Theory, Physical Implementations, and Applications*, pp. 141–166.

Damicelli, F., C. C. Hilgetag, and A. Goulas (2022). "Brain connectivity meets reservoir computing". *PLoS Computational Biology*, 18(11), e1010639.

Damicelli, F. et al. (2017). "Modular topology emerges from plasticity in a minimalistic excitable network model". *Chaos*, 27(4), p. 047406.

Damoiseaux, J. S. and M. D. Greicius (2009). "Greater than the sum of its parts: a review of studies combining structural connectivity and resting-state functional connectivity". *Brain Struct Funct*, 213(6), pp. 525–533.

Damoiseaux, J. et al. (2006). "Consistent resting-state networks across healthy subjects". *Proc Natl Acad Sci USA*, 103(37), pp. 13848–13853.

Darwin, C. (1959). *On the origin of species*. Routledge.

Das, K. C. (2004). "The Laplacian spectrum of a graph". *Computers & Mathematics with Applications*, 48(5-6), pp. 715–724.

Deco, G. and V. K. Jirsa (2012). "Ongoing cortical activity at rest: criticality, multistability, and ghost attractors". *Journal of Neuroscience*, 32(10), pp. 3366–3375.

Deco, G., V. K. Jirsa, and A. R. McIntosh (2011). "Emerging concepts for the dynamical organization of resting-state activity in the brain". *Nat Rev Neurosci*, 12(1), p. 43.

Deco, G. et al. (2009). "Key role of coupling, delay, and noise in resting brain fluctuations". *Proc Natl Acad Sci USA*, 106(25), pp. 10302–10307.

Deco, G. et al. (2018). "Whole-brain multimodal neuroimaging model using serotonin receptor maps explains non-linear functional effects of LSD". *Curr Biol*, 28(19), pp. 3065–3074.

Deco, G. et al. (2020). "Dynamical consequences of regional heterogeneity in the brains transcriptional landscape". *bioRxiv*.

Deligianni, F. et al. (2016). "NODDI and tensor-based microstructural indices as predictors of functional connectivity". *PloS ONE*, 11(4), e0153404.

Demirtas, M. et al. (2010). "Hierarchical heterogeneity across human cortex shapes large-scale neural dynamics". *Neuron*, p. 341966.

Demirtaş, M. et al. (2019). "Hierarchical heterogeneity across human cortex shapes large-scale neural dynamics". *Neuron*, 101(6), pp. 1181–1194.

Deng, L. et al. (2015). "Complex learning in bio-plausible memristive networks". *Scientific reports*, 5(1), pp. 1–10.

Desikan, R. S. et al. (2006). "An automated labeling system for subdividing the human cerebral cortex on MRI scans into gyral based regions of interest". *NeuroImage*, 31(3), pp. 968–980.

Dijkstra, E. W. et al. (1959). "A note on two problems in connexion with graphs". *Numerische mathematik*, 1(1), pp. 269–271.

Ding, Y. et al. (2016). "Natural courtship song variation caused by an intronic retroelement in an ion channel gene". *Nature*, 536(7616), pp. 329–332.

Ding, Y. et al. (2019). "Neural evolution of context-dependent fly song". *Current biology*, 29(7), pp. 1089–1099.

Dion, G. et al. (2021). "Reservoir Computing in MEMS". *Reservoir Computing: Theory, Physical Implementations, and Applications*, pp. 191–217.

Dockès, J. et al. (2020). "NeuroQuery, comprehensive meta-analysis of human brain mapping". *eLife*, 9, e53385.

Dohmatob, E., G. Dumas, and D. Bzdok (2020). "Dark control: The default mode network as a reinforcement learning agent". *Hum Brain Mapp*.

Dominey, P., M. Arbib, and J.-P. Joseph (1995). "A model of corticostriatal plasticity for learning oculomotor associations and sequences". *Journal of cognitive neuroscience*, 7(3), pp. 311–336.

Dominey, P. F. (1995). "Complex sensory-motor sequence learning based on recurrent state representation and reinforcement learning". *Biological cybernetics*, 73(3), pp. 265–274.

— (2013). "Recurrent temporal networks and language acquisition—from corticostriatal neurophysiology to reservoir computing". *Frontiers in psychology*, 4, p. 500.

Dominey, P. F. and M. A. Arbib (1992). "A cortico-subcortical model for generation of spatially accurate sequential saccades". *Cerebral cortex*, 2(2), pp. 153–175.

Dominey, P. F. and T. Inui (2009). "Cortico-striatal function in sentence comprehension: Insights from neurophysiology and modeling". *Cortex*, 45(8), pp. 1012–1018.

Dominey, P. F. et al. (2003). "Neurological basis of language and sequential cognition: evidence from simulation, aphasia, and ERP studies". *Brain and language*, 86(2), pp. 207–225.

Dominey, P. F. (1998a). "A shared system for learning serial and temporal structure of sensori-motor sequences? Evidence from simulation and human experiments". *Cognitive Brain Research*, 6(3), pp. 163–172.

— (1998b). "Influences of temporal organization on sequence learning and transfer: Comments on Stadler (1995) and Curran and Keele (1993)." *Journal of Experimental Psychology: Learning, Memory, and Cognition*, 24(1), p. 234.

Dominey, P. F. (2021). "Cortico-striatal origins of reservoir computing, mixed selectivity, and higher cognitive function". *Reservoir Computing: Theory, Physical Implementations, and Applications*, pp. 29–58.

Dominey, P. F., T. Inui, and M. Hoen (2009). "Neural network processing of natural language: II. Towards a unified model of corticostriatal function in learning sentence comprehension and non-linguistic sequencing". *Brain and language*, 109(2-3), pp. 80–92.

Dominey, P. F. and F. Ramus (2000). "Neural network processing of natural language: I. Sensitivity to serial, temporal and abstract structure of language in the infant". *Language and Cognitive Processes*, 15(1), pp. 87–127.

Du, C. et al. (2017). "Reservoir computing using dynamic memristors for temporal information processing". *Nature communications*, 8(1), pp. 1–10.

Eigenbrod, O. et al. (2019). "Rapid molecular evolution of pain insensitivity in multiple African rodents". *Science*, 364(6443), pp. 852–859.

Elman, J. L. (1990). "Finding structure in time". *Cognitive science*, 14(2), pp. 179–211.

— (1991). "Distributed representations, simple recurrent networks, and grammatical structure". *Machine learning*, 7(2), pp. 195–225.

Enel, P. et al. (2016). "Reservoir computing properties of neural dynamics in prefrontal cortex". *PLoS computational biology*, 12(6), e1004967.

Falandays, J. B., B. Nguyen, and M. J. Spivey (2021). "Is prediction nothing more than multi-scale pattern completion of the future?" *Brain Research*, 1768, p. 147578.

Faskowitz, J., R. F. Betzel, and O. Sporns (2021). "Edges in Brain Networks: Contributions to Models of Structure and Function". *arXiv preprint arXiv:2105.07069*.

Feldman, J. A. and D. H. Ballard (1982). "Connectionist models and their properties". *Cognitive science*, 6(3), pp. 205–254.

Finn, E. S. et al. (2019). "Layer-dependent activity in human prefrontal cortex during working memory". *Nat Neurosci*, 22(10), pp. 1687–1695.

Fletcher, J. M. and T. Wennekers (2018). "From structure to activity: Using centrality measures to predict neuronal activity". *International journal of neural systems*, 28(02), p. 1750013.

Fodor, J. A. and Z. W. Pylyshyn (1988). "Connectionism and cognitive architecture: A critical analysis". *Cognition*, 28(1-2), pp. 3–71.

Fornito, A., A. Arnatkevičiūtė, and B. D. Fulcher (2019). "Bridging the gap between connectome and transcriptome". *Trends in Cognitive Sciences*, 23(1), pp. 34–50.

Fortunato, S. and M. Barthelemy (2007). "Resolution limit in community detection". *Proceedings of the national academy of sciences*, 104(1), pp. 36–41.

Fox, P. T. and J. L. Lancaster (2002). "Mapping context and content: the BrainMap model". *Nature Reviews Neuroscience*, 3(4), pp. 319–321.

Frahm, H., H Stephan, and M Stephan (1982). "Comparison of brain structure volumes in Insectivora and Primates. I. Neocortex." *J Hirnforsch*, 23(4), pp. 375–389.

Freeman, L. C. (1978). "Centrality in social networks conceptual clarification". *Social networks*, 1(3), pp. 215–239.

Fries, P. (2005). "A mechanism for cognitive dynamics: neuronal communication through neuronal coherence". *Trends in cognitive sciences*, 9(10), pp. 474–480.

Fu, K. et al. (2020). "Reservoir computing with neuromemristive nanowire networks". In: *2020 International Joint Conference on Neural Networks (IJCNN)*. IEEE, pp. 1–8.

Fujii, K. and K. Nakajima (2021). "Quantum reservoir computing: a reservoir approach toward quantum machine learning on near-term quantum devices". *Reservoir Computing: Theory, Physical Implementations, and Applications*, pp. 423–450.

Fukushima, M. et al. (2018). "Structure–function relationships during segregated and integrated network states of human brain functional connectivity". *Brain Struct Funct*, 223(3), pp. 1091–1106.

Fulcher, B. D. and A. Fornito (2016). "A transcriptional signature of hub connectivity in the mouse connectome". *Proc Natl Acad Sci USA*, 113(5), pp. 1435–1440.

Gao, R. et al. (2020). "Neuronal timescales are functionally dynamic and shaped by cortical microarchitecture". *Elife*, 9, e61277.

Garey, L. J. (1999). *Brodmann's' localisation in the cerebral cortex'*. World Scientific.

Ghosh, A. et al. (2008). "Noise during rest enables the exploration of the brain's dynamic repertoire". *PLoS Comput Biol*, 4(10), e1000196.

Glasser, M. F. et al. (2014). "Trends and properties of human cerebral cortex: correlations with cortical myelin content". *NeuroImage*, 93, pp. 165–175.

Goldman-Rakic, P. S. (2011). "Circuitry of primate prefrontal cortex and regulation of behavior by representational memory". *Comprehensive physiology*, pp. 373–417.

Gollo, L. L. et al. (2015). "Dwelling quietly in the rich club: brain network determinants of slow cortical fluctuations". *Phil Trans Roy Soc B*, 370(1668), p. 20140165.

Goni, J. et al. (2013). "Exploring the morphospace of communication efficiency in complex networks". *PLoS ONE*, 8(3), e58070.

Goñi, J. et al. (2014). "Resting-brain functional connectivity predicted by analytic measures of network communication". *Proc Natl Acad Sci USA*, 111(2), pp. 833–838.

Good, B. H., Y.-A. De Montjoye, and A. Clauset (2010). "Performance of modularity maximization in practical contexts". *Physical Review E*, 81(4), p. 046106.

Gordon, E. M. et al. (2017). "Precision functional mapping of individual human brains". *Neuron*, 95(4), pp. 791–807.

Goulas, A., F. Damicelli, and C. C. Hilgetag (2021). "Bio-instantiated recurrent neural networks: Integrating neurobiology-based network topology in artificial networks". *Neural Networks*, 142, pp. 608–618.

Graham, D. and D. Rockmore (2011). "The packet switching brain". *J Cogn Neurosci*, 23(2), pp. 267–276.

Gratton, C. et al. (2018). "Functional brain networks are dominated by stable group and individual factors, not cognitive or daily variation". *Neuron*, 98(2), pp. 439–452.

Gray, C. M. and W. Singer (1989). "Stimulus-specific neuronal oscillations in orientation columns of cat visual cortex." *Proceedings of the National Academy of Sciences*, 86(5), pp. 1698–1702.

Grayson, D. S. et al. (2016). "The rhesus monkey connectome predicts disrupted functional networks resulting from pharmacogenetic inactivation of the amygdala". *Neuron*, 91(2), pp. 453–466.

Griffa, A. et al. (2017). "Transient networks of spatio-temporal connectivity map communication pathways in brain functional systems". *NeuroImage*, 155, pp. 490–502.

Grone, R. and R. Merris (1994). "The Laplacian spectrum of a graph II". *SIAM Journal on discrete mathematics*, 7(2), pp. 221–229.

Grone, R., R. Merris, and V. Sunder (1990). "The Laplacian spectrum of a graph". *SIAM Journal on matrix analysis and applications*, 11(2), pp. 218–238.

Gu, S. et al. (2017). "Functional hypergraph uncovers novel covariant structures over neurodevelopment". *Hum Brain Mapp*, 38(8), pp. 3823–3835.

Guimera, R. and L. A. N. Amaral (2005). "Functional cartography of complex metabolic networks". *nature*, 433(7028), pp. 895–900.

Haeusler, S. and W. Maass (2007). "A statistical analysis of information-processing properties of lamina-specific cortical microcircuit models". *Cerebral cortex*, 17(1), pp. 149–162.

Hagberg, A., P. Swart, and D. S Chult (2008). *Exploring network structure, dynamics, and function using NetworkX*. Tech. rep. Los Alamos National Lab.(LANL), Los Alamos, NM (United States).

Hagmann, P. et al. (2008). "Mapping the structural core of human cerebral cortex". *PLoS Biol*, 6(7), e159.

Haimovici, A. et al. (2013). "Brain organization into resting state networks emerges at criticality on a model of the human connectome". *Physical review letters*, 110(17), p. 178101.

Haldeman, C. and J. M. Beggs (2005). "Critical branching captures activity in living neural networks and maximizes the number of metastable states". *Physical review letters*, 94(5), p. 058101.

Hallquist, M. N. and F. G. Hillary (2018). "Graph theory approaches to functional network organization in brain disorders: A critique for a brave new small-world". *Net Neurosci*, 3(1), pp. 1–26.

Hansen, E. C. et al. (2015). "Functional connectivity dynamics: modeling the switching behavior of the resting state". *Neuroimage*, 105, pp. 525–535.

Hansen, J. Y. et al. (2021). "Mapping gene transcription and neurocognition across human neocortex". *Nature Human Behaviour*, pp. 1–11.

Harris, C. R. et al. (2020). "Array programming with NumPy". *Nature*, 585(7825), pp. 357–362.

Hauser, H. (2021). "Physical reservoir computing in robotics". *Reservoir Computing: Theory, Physical Implementations, and Applications*, pp. 169–190.

Hawrylycz, M. et al. (2012). "An anatomically comprehensive atlas of the adult human brain transcriptome". *Nature*, 489(7416), p. 391.

Hebb, D. O. (2005). *The organization of behavior: A neuropsychological theory*. Psychology Press.

Hens, C. et al. (2019). "Spatiotemporal signal propagation in complex networks". *Nat Phys*, 15(4), p. 403.

Hernández-Hernández, T. et al. (2021). "Speciation across the T ree of L ife". *Biological Reviews*, 96(4), pp. 1205–1242.

Heuvel, M. P. Van den, E. T. Bullmore, and O. Sporns (2016). "Comparative connectomics". *Trends Cognitive Science*, 20(5), pp. 345–361.

Heuvel, M. P. van den and O. Sporns (2011). "Rich-club organization of the human connectome". *Journal of Neuroscience*, 31(44), pp. 15775–15786.

Heuvel, M. P. van den and B. T. Yeo (2017). "A spotlight on bridging microscale and macroscale human brain architecture". *Neuron*, 93(6), pp. 1248–1251.

Heuvel, M. P. van den et al. (2010). "Aberrant frontal and temporal complex network structure in schizophrenia: a graph theoretical analysis". *Journal of Neuroscience*, 30(47), pp. 15915–15926.

Heuvel, M. P. van den et al. (2012). "High-cost, high-capacity backbone for global brain communication". *Proc Natl Acad Sci USA*, 109(28), pp. 11372–11377.

Hilgetag, C. C. and M. Kaiser (2004). "Clustered organization of cortical connectivity". *Neuroinformatics*, 2(3), pp. 353–360.

Hilgetag, C.-C. et al. (2000). "Anatomical connectivity defines the organization of clusters of cortical areas in the macaque and the cat". *Philos Trans R Soc Lond B*, 355(1393), pp. 91–110.

Hinaut, X. et al. (2015). "Corticostriatal response selection in sentence production: Insights from neural network simulation with reservoir computing". *Brain and language*, 150, pp. 54–68.

Homma, Y. and M. Hagiwara (2013). "An echo state network with working memories for probabilistic language modeling". In: *International Conference on Artificial Neural Networks*. Springer, pp. 595–602.

Honey, C. J. and O. Sporns (2008). "Dynamical consequences of lesions in cortical networks". *Hum Brain Mapp*, 29(7), pp. 802–809.

Honey, C. J., J.-P. Thivierge, and O. Sporns (2010). "Can structure predict function in the human brain?" *NeuroImage*, 52(3), pp. 766–776.

Honey, C. J. et al. (2007). "Network structure of cerebral cortex shapes functional connectivity on multiple time scales". *Proc Natl Acad Sci USA*, 104(24), pp. 10240–10245.

Honey, C. et al. (2009). "Predicting human resting-state functional connectivity from structural connectivity". *Proc Natl Acad Sci USA*, 106(6), pp. 2035–2040.

Hopfield, J. J. (1982). "Neural networks and physical systems with emergent collective computational abilities". *Proceedings of the national academy of sciences*, 79(8), pp. 2554–2558.

Hori, Y. et al. (2020). "Comparison of resting-state functional connectivity in marmosets with tracer-based cellular connectivity". *NeuroImage*, 204, p. 116241.

Horowitz, A. et al. (2015). "In vivo correlation between axon diameter and conduction velocity in the human brain". *Brain Struct Funct*, 220(3), pp. 1777–1788.

Horvát, S. et al. (2016). "Spatial embedding and wiring cost constrain the functional layout of the cortical network of rodents and primates". *PLoS Biol*, 14(7), e1002512.

Huang, W. et al. (2021). "Memristive artificial synapses for neuromorphic computing". *Nano-Micro Letters*, 13, pp. 1–28.

Humphries, M. D. and K. Gurney (2008). "Network 'small-world-ness': a quantitative method for determining canonical network equivalence". *PloS one*, 3(4), e0002051.

Huntenburg, J. M., P.-L. Bazin, and D. S. Margulies (2018). "Large-scale gradients in human cortical organization". *Trends in cognitive sciences*, 22(1), pp. 21–31.

Huntenburg, J. M. et al. (2017). "A systematic relationship between functional connectivity and intracortical myelin in the human cerebral cortex". *Cereb Cortex*, 27(2), pp. 981–997.

Hunter, J. D. (2007). "Matplotlib: A 2D graphics environment". *Computing in science & engineering*, 9(3), pp. 90–95.

Ijspeert, A. J. (2008). "Central pattern generators for locomotion control in animals and robots: a review". *Neural networks*, 21(4), pp. 642–653.

Insel, T. R., S. C. Landis, and F. S. Collins (2013). "The NIH brain initiative". *Science*, 340(6133), pp. 687–688.

Insel, T. R. and L. E. Shapiro (1992). "Oxytocin receptor distribution reflects social organization in monogamous and polygamous voles". *Proceedings of the National Academy of Sciences*, 89(13), pp. 5981–5985.

Inubushi, M. and K. Yoshimura (2017). "Reservoir computing beyond memory-nonlinearity trade-off". *Scientific reports*, 7(1), pp. 1–10.

Jaeger, H. (2001). "The "echo state" approach to analysing and training recurrent neural networks-with an erratum note". *Bonn, Germany: German National Research Center for Information Technology GMD Technical Report*, 148(34), p. 13.

— (2002). "Short term memory in echo state networks. gmd-report 152". In: *GMD-German National Research Institute for Computer Science (2002), http://www.faculty.jacobs-university.de/hjaeger/pubs/STMEchoStatesTechRep.pdf*. Citeseer.

Jaggard, J. B. et al. (2020). "Cavefish brain atlases reveal functional and anatomical convergence across independently evolved populations". *Sci Adv*, 6(38), eaba3126.

Jirsa, V. K. et al. (2017). "The virtual epileptic patient: individualized whole-brain models of epilepsy spread". *NeuroImage*, 145, pp. 377–388.

Jones, D., T. Knösche, and R Turner (2013). "White matter integrity, fiber count, and other fallacies: the do's and don'ts of diffusion MRI". *NeuroImage*, 73, pp. 239–254.

Ju, H. and D. S. Bassett (2020). "Dynamic representations in networked neural systems". *Nat Neurosci*, pp. 1–10.

Kaiser, M. and C. C. Hilgetag (2006). "Nonoptimal component placement, but short processing paths, due to long-distance projections in neural systems". *PLoS Comput Biol*, 2(7), e95.

Kambi, N. et al. (2014). "Large-scale reorganization of the somatosensory cortex following spinal cord injuries is due to brainstem plasticity". *Nature communications*, 5(1), p. 3602.

Kanemura, I. and K. Kitano (2023). "Association between different sensory modalities based on concurrent time series data obtained by a collaborative reservoir computing model". *Scientific Reports*, 13(1), p. 173.

Katumba, A. et al. (2017). "A multiple-input strategy to efficient integrated photonic reservoir computing". *Cognitive Computation*, 9(3), pp. 307–314.

Katumba, A. et al. (2018). "Low-loss photonic reservoir computing with multimode photonic integrated circuits". *Scientific reports*, 8(1), pp. 1–10.

Kawai, Y., J. Park, and M. Asada (2019). "A small-world topology enhances the echo state property and signal propagation in reservoir computing". *Neural Networks*, 112, pp. 15–23.

Kawai, Y. et al. (2017). "Echo in a small-world reservoir: Time-series prediction using an economical recurrent neural network". In: *2017 Joint IEEE International Conference on Development and Learning and Epigenetic Robotics (ICDL-EpiRob)*. IEEE, pp. 126–131.

Keitel, A. and J. Gross (2016). "Individual human brain areas can be identified from their characteristic spectral activation fingerprints". *PLoS Biol*, 14(6), e1002498.

Kendall, J. D., J. C. Nino, and L. E. Suárez (2018). *Deep learning in bipartite memristive networks*. US Patent App. 15/985,212.

Khallaf, M. A. et al. (2020). "Mate discrimination among subspecies through a conserved olfactory pathway". *Sci Adv*, 6(25), eaba5279.

Khambhati, A. N. et al. (2018). "Modeling and interpreting mesoscale network dynamics". *NeuroImage*, 180, pp. 337–349.

Kintali, S. (2008). "Betweenness centrality: Algorithms and lower bounds". *arXiv preprint arXiv:0809.1906*.

Kitzbichler, M. G. et al. (2009). "Broadband criticality of human brain network synchronization". *PLoS Comput Biol*, 5(3), e1000314.

Knock, S. et al. (2009). "The effects of physiologically plausible connectivity structure on local and global dynamics in large scale brain models". *J Neurosci Meth*, 183(1), pp. 86–94.

Kötter, R., C. C. Hilgetag, and K. E. Stephan (2001). "Connectional characteristics of areas in Walker's map of primate prefrontal cortex". *Neurocomputing*, 38, pp. 741–746.

Krubitzer, L. and J. Kaas (2005). "The evolution of the neocortex in mammals: how is phenotypic diversity generated?" *Curr Opin Neurobiol*, 15(4), pp. 444–453.

Krubitzer, L. and D. M. Kahn (2003). "Nature versus nurture revisited: an old idea with a new twist". *Prog Neurobiol*, 70(1), pp. 33–52.

Kulkarni, M. S. and C. Teuscher (2012). "Memristor-based reservoir computing". In: *2012 IEEE/ACM international symposium on nanoscale architectures (NANOARCH)*. IEEE, pp. 226–232.

Lande, R. (1976). "Natural selection and random genetic drift in phenotypic evolution". *Evolution*, pp. 314–334.

Lange, S. de, M. de Reus, and M. van den Heuvel (2014). "The Laplacian spectrum of neural networks". *Front Comput Neurosci*, 7, p. 189.

Lange, S. C. de, M. P. van den Heuvel, and M. A. de Reus (2016). "The role of symmetry in neural networks and their Laplacian spectra". *NeuroImage*, 141, pp. 357–365.

Langton, C. (1990). "Computation at the edge of chaos: Phase transition and emergent computation". *Physica D: nonlinear phenomena*, 42, pp. 12–37.

Laporte, F. et al. (2018). "Numerical demonstration of neuromorphic computing with photonic crystal cavities". *Optics express*, 26(7), pp. 7955–7964.

Larivière, S. et al. (2018). "Microstructure-informed connectomics: enriching large-scale descriptions of healthy and diseased brains". *Brain Conn*.

Larivière, S. et al. (2021). "The ENIGMA Toolbox: multiscale neural contextualization of multisite neuroimaging datasets". *Nature Methods*, 18(7), pp. 698–700.

Latora, V. and M. Marchiori (2001). "Efficient behavior of small-world networks". *Physical review letters*, 87(19), p. 198701.

Laumann, T. O. et al. (2015). "Functional system and areal organization of a highly sampled individual human brain". *Neuron*, 87(3), pp. 657–670.

Layden, E. A. et al. (2019). "Interhemispheric functional connectivity in the zebra finch brain, absent the corpus callosum in normal ontogeny". *NeuroImage*.

Leemans, A. et al. (2009). "ExploreDTI: a graphical toolbox for processing, analyzing, and visualizing diffusion MR data". In: *Proc Intl Soc Mag Reson Med*. Vol. 17. 1, p. 3537.

Legenstein, R. and W. Maass (2007a). "Edge of chaos and prediction of computational performance for neural circuit models". *Neural Networks*, 20(3), pp. 323–334.

— (2007b). "What makes a dynamical system computationally powerful". *New directions in statistical signal processing: From systems to brain*, pp. 127–154.

Leicht, E. A. and M. E. Newman (2008). "Community structure in directed networks". *Physical review letters*, 100(11), p. 118703.

Leung, C. and H. Chau (2007). "Weighted assortative and disassortative networks model". *Physica A: Statistical Mechanics and its Applications*, 378(2), pp. 591–602.

Levant, B. (1998). "Differential distribution of D3 dopamine receptors in the brains of several mammalian species". *Brain Res*, 800(2), pp. 269–274.

Li, J. et al. (2018). "A deep learning based approach for analog hardware implementation of delayed feedback reservoir computing system". In: *2018 19th International Symposium on Quality Electronic Design (ISQED)*. IEEE, pp. 308–313.

Li, J. and H. Jaeger (2011). "Minimal Energy Control of an ESN Pattern Generator". In:

Lim, S. et al. (2019). "Discordant attributes of structural and functional brain connectivity in a two-layer multiplex network". *Sci Rep*, 9(1), p. 2885.

Liu, Z.-Q., Y.-Q. Zheng, and B. Misic (2020). "Network topology of the marmoset connectome". *Network Neurosci*, (-), pp. 1–26.

Loeffler, A. et al. (2021). "Modularity and multitasking in neuro-memristive reservoir networks". *Neuromorphic Computing and Engineering*, 1(1), p. 014003.

Loeffler, A. et al. (2023). "Neuromorphic learning, working memory, and metaplasticity in nanowire networks". *Science Advances*, 9(16), eadg3289.

Loomis, C. et al. (2019). "An adult brain atlas reveals broad neuroanatomical changes in independently evolved populations of Mexican cavefish". *Frontiers in neuroanatomy*, 13, p. 88.

Lukoševičius, M. and H. Jaeger (2009). "Reservoir computing approaches to recurrent neural network training". *Computer Science Review*, 3(3), pp. 127–149.

Lukoševičius, M., H. Jaeger, and B. Schrauwen (2012). "Reservoir computing trends". *KI-Künstliche Intelligenz*, 26, pp. 365–371.

Lurie, D. J. et al. (2019). "Questions and controversies in the study of time-varying functional connectivity in resting fMRI". *Net Neurosci*, pp. 1–40.

Maass, W. and H. Markram (2004). "On the computational power of circuits of spiking neurons". *Journal of computer and system sciences*, 69(4), pp. 593–616.

Maass, W., T. Natschläger, and H. Markram (2002). "Real-time computing without stable states: A new framework for neural computation based on perturbations". *Neural computation*, 14(11), pp. 2531–2560.

Magee, J. C. and C. Grienberger (2020). "Synaptic plasticity forms and functions". *Annual review of neuroscience*, 43, pp. 95–117.

Maier-Hein, K. H. et al. (2017). "The challenge of mapping the human connectome based on diffusion tractography". *Nat Commun*, 8(1), p. 1349.

Majka, P. et al. (2016). "Towards a comprehensive atlas of cortical connections in a primate brain: Mapping tracer injection studies of the common marmoset into a reference digital template". *J Com Neurol*, 524(11), pp. 2161–2181.

Makin, T. R. and H. Flor (2020). "Brain (re) organisation following amputation: Implications for phantom limb pain". *Neuroimage*, 218, p. 116943.

Mallet, J. (1995). "A species definition for the modern synthesis". *Trends in Ecology & Evolution*, 10(7), pp. 294–299.

Mancini, M. et al. (2018). "Introducing axonal myelination in connectomics: A preliminary analysis of g-ratio distribution in healthy subjects". *NeuroImage*, 182, pp. 351–359.

Mante, V. et al. (2013). "Context-dependent computation by recurrent dynamics in prefrontal cortex". *nature*, 503(7474), pp. 78–84.

Marblestone, A. H., G. Wayne, and K. P. Kording (2016). "Toward an integration of deep learning and neuroscience". *Frontiers in computational neuroscience*, p. 94.

Margulies, D. S. et al. (2016). "Situating the default-mode network along a principal gradient of macroscale cortical organization". *Proceedings of the National Academy of Sciences*, 113(44), pp. 12574–12579.

Marinazzo, D. et al. (2014). "Information transfer and criticality in the Ising model on the human connectome". *PloS one*, 9(4), e93616.

Markello, R. D. and B. Misic (2021). "Comparing spatial null models for brain maps". *NeuroImage*, p. 118052.

Markello, R. D. et al. (2022). "Neuromaps: structural and functional interpretation of brain maps". *Nature Methods*, 19(11), pp. 1472–1479.

Markov, N. T. et al. (2011). "Weight consistency specifies regularities of macaque cortical networks". *Cerebral cortex*, 21(6), pp. 1254–1272.

Markov, N. T. et al. (2012). "A weighted and directed interareal connectivity matrix for macaque cerebral cortex". *Cereb Cortex*, 24(1), pp. 17–36.

Markow, T. A. and P. M. O'Grady (2005). "Evolutionary genetics of reproductive behavior in Drosophila: connecting the dots". *Annu. Rev. Genet.*, 39, pp. 263–291.

Markram, H. et al. (1997). "Regulation of synaptic efficacy by coincidence of postsynaptic APs and EPSPs". *Science*, 275(5297), pp. 213–215.

Marrelec, G. et al. (2016). "Functional connectivity's degenerate view of brain computation". *PLoS Comput Biol*, 12(10), e1005031.

Mars, R. B., S. Jbabdi, and M. F. Rushworth (2021). "A common space approach to comparative neuroscience". *Annual Review of Neuroscience*, 44.

Mars, R. B., R. E. Passingham, and S. Jbabdi (2018a). "Connectivity fingerprints: from areal descriptions to abstract spaces". *Trends in cognitive sciences*, 22(11), pp. 1026–1037.

Mars, R. B. et al. (2016). "Comparing brains by matching connectivity profiles". *Neuroscience & Biobehavioral Reviews*, 60, pp. 90–97.

Mars, R. B. et al. (2018b). "Whole brain comparative anatomy using connectivity blueprints". *Elife*, 7, e35237.

Martinez, P. and S. G. Sprecher (2020). "Of circuits and brains: The origin and diversification of neural architectures". *Frontiers in Ecology and Evolution*, 8, p. 82.

Márton, C. D. et al. (2021). "Efficient and robust multi-task learning in the brain with modular latent primitives". *arXiv preprint arXiv:2105.14108*.

Maslov, S. and K. Sneppen (2002). "Specificity and stability in topology of protein networks". *Science*, 296(5569), pp. 910–913.

Mastrogiuseppe, F. and S. Ostojic (2018). "Linking connectivity, dynamics, and computations in low-rank recurrent neural networks". *Neuron*, 99(3), pp. 609–623.

McAuley, J. J., L. da Fontoura Costa, and T. S. Caetano (2007). "Rich-club phenomenon across complex network hierarchies". *Applied Physics Letters*, 91(8), p. 084103.

McIntosh, A. R. and B. Mišić (2013). "Multivariate statistical analyses for neuroimaging data". *Annu Rev Psychol*, 64, pp. 499–525.

McKinney, W. et al. (2010a). "Data structures for statistical computing in python". In: *Proceedings of the 9th Python in Science Conference*. Vol. 445. Austin, TX, pp. 51–56.

— (2010b). "Data structures for statistical computing in python". In: *Proceedings of the 9th Python in Science Conference*. Vol. 445. Austin, TX, pp. 51–56.

Mealier, A.-L. et al. (2017). "Narrative constructions for the organization of self experience: Proof of concept via embodied robotics". *Frontiers in psychology*, 8, p. 1331.

Medaglia, J. D. et al. (2018). "Functional alignment with anatomical networks is associated with cognitive flexibility". *Nat Hum Behav*, 2(2), p. 156.

Meier, J. et al. (2016). "A mapping between structural and functional brain networks". *Brain Conn*, 6(4), pp. 298–311.

Melozzi, F. et al. (2019). "Individual structural features constrain the functional connectome". *Proc Natl Acad Sci USA*, 116, pp. 26961–26969.

Messé, A., M.-T. Hütt, and C. C. Hilgetag (2018). "Toward a theory of coactivation patterns in excitable neural networks". *PLoS Comput Biol*, 14(4), e1006084.

Messé, A. et al. (2014). "Relating structure and function in the human brain: relative contributions of anatomy, stationary dynamics, and non-stationarities". *PLoS Comput Biol*, 10(3), e1003530.

Messé, A. et al. (2015). "Predicting functional connectivity from structural connectivity via computational models using MRI: an extensive comparison study". *NeuroImage*, 111, pp. 65–75.

Mesulam, M (1994). "Neurocognitive networks and selectively distributed processing." *Revue neurologique*.

Mesulam, M.-M. (1998). "From sensation to cognition." *Brain*, 121(6), pp. 1013–1052.

Mišić, B. and O. Sporns (2016). "From regions to connections and networks: new bridges between brain and behavior". *Curr Opin Neurobiol*, 40, pp. 1–7.

Mišić, B. et al. (2014a). "A network convergence zone in the hippocampus". *PLoS Comput Biol*, 10(12), e1003982.

Mišić, B. et al. (2014b). "The functional connectivity landscape of the human brain". *PLoS ONE*, 9(10), e111007.

Mišić, B. et al. (2015). "Cooperative and competitive spreading dynamics on the human connectome". *Neuron*, 86(6), pp. 1518–1529.

Mišić, B. et al. (2016). "Network-level structure-function relationships in human neocortex". *Cerebral Cortex*, 26(7), pp. 3285–3296.

Mitra, A. et al. (2015). "Lag threads organize the brain's intrinsic activity". *Proc Natl Acad Sci USA*, 112(17), E2235–E2244.

Molano-Mazon, M. et al. (2022). "NeuroGym: An open resource for developing and sharing neuroscience tasks".

Mollink, J. et al. (2019). "The spatial correspondence and genetic influence of interhemispheric connectivity with white matter microstructure". *Nat Neurosci*, pp. –.

Morales, G. B., C. R. Mirasso, and M. C. Soriano (2021). "Unveiling the role of plasticity rules in reservoir computing". *Neurocomputing*, 461, pp. 705–715.

Mueller, S. et al. (2013). "Individual variability in functional connectivity architecture of the human brain". *Neuron*, 77(3), pp. 586–595.

Murphy, A. C. et al. (2016). "Explicitly linking regional activation and function connectivity: community structure of weighted networks with continuous annotation". *arXiv*, p. 1611.07962.

Murphy, W. J. et al. (2021). "Phylogenomics and the Genetic Architecture of the Placental Mammal Radiation". *Annual Review of Animal Biosciences*, 9, pp. 29–53.

Murray, J. D. et al. (2014). "A hierarchy of intrinsic timescales across primate cortex". *Nat Neurosci*, 17(12), p. 1661.

Nakajima, K. (2020). "Physical reservoir computing—an introductory perspective". *Japanese Journal of Applied Physics*, 59(6), p. 060501.

Nakajima, K. and T. Aoyagi (2015). "The memory capacity of a physical liquid state machine". *IEICE Technical Report; IEICE Tech. Rep.*, 115(300), pp. 109–112.

Nakajima, K. et al. (2013). "A soft body as a reservoir: case studies in a dynamic model of octopus-inspired soft robotic arm". *Frontiers in computational neuroscience*, 7, p. 91.

Natschläger, T., W. Maass, and H. Markram (2002). "The" liquid computer": A novel strategy for real-time computing on time series". *Telematik*, 8(ARTICLE), pp. 39–43.

Negoro, M. et al. (2021). "Toward NMR quantum reservoir computing". *Reservoir Computing: Theory, Physical Implementations, and Applications*, pp. 451–458.

Neves, G., S. F. Cooke, and T. V. Bliss (2008). "Synaptic plasticity, memory and the hippocampus: a neural network approach to causality". *Nature Reviews Neuroscience*, 9(1), pp. 65–75.

Newman, M. E. (2002). "Assortative mixing in networks". *Physical review letters*, 89(20), p. 208701.

— (2003). "The structure and function of complex networks". *SIAM review*, 45(2), pp. 167–256.

Newman, M. W. (2001). "The Laplacian spectrum of graphs". MA thesis. University of Manitoba.

Niessing, J. and R. W. Friedrich (2010). "Olfactory pattern classification by discrete neuronal network states". *Nature*, 465(7294), pp. 47–52.

Noble, S., D. Scheinost, and R. T. Constable (2019). "A decade of test-retest reliability of functional connectivity: A systematic review and meta-analysis". *NeuroImage*, p. 116157.

Nomura, H., H. Kubota, and Y. Suzuki (2021). "Reservoir computing with dipole-coupled nanomagnets". *Reservoir Computing: Theory, Physical Implementations, and Applications*, pp. 361–374.

Nooner, K. B. et al. (2012). "The NKI-Rockland sample: a model for accelerating the pace of discovery science in psychiatry". *Front Neurosci*, 6, p. 152.

Oh, S. W. et al. (2014). "A mesoscale connectome of the mouse brain". *Nature*, 508(7495), p. 207.

Oliphant, T. E. (2006). *A guide to NumPy*. Vol. 1. Trelgol Publishing USA.

Onnela, J.-P. et al. (2005). "Intensity and coherence of motifs in weighted complex networks". *Physical Review E*, 71(6), p. 065103.

O'Reilly, J. X. et al. (2013). "Causal effect of disconnection lesions on interhemispheric functional connectivity in rhesus monkeys". *Proc Natl Acad Sci USA*, 110(34), pp. 13982–13987.

O'Byrne, J. and K. Jerbi (2022). "How critical is brain criticality?" *Trends in Neurosciences*.

O'Grady, P. M. and R. DeSalle (2018). "Phylogeny of the genus Drosophila". *Genetics*, 209(1), pp. 1–25.

Pantoja, C. et al. (2020). "Rapid effects of selection on brain-wide activity and behavior". *Current Biology*, 30(18), pp. 3647–3656.

Paquola, C. et al. (2018). "Dissociations between microstructural and functional hierarchies within regions of transmodal cortex". *bioRxiv*, p. 488700.

Paquola, C. et al. (2019). "Microstructural and functional gradients are increasingly dissociated in transmodal cortices". *PLoS Biol*, 17(5), e3000284.

Park, T. J. et al. (2008). "Selective inflammatory pain insensitivity in the African naked mole-rat (Heterocephalus glaber)". *PLoS biology*, 6(1), e13.

Pascanu, R. and H. Jaeger (2011). "A neurodynamical model for working memory". *Neural networks*, 24(2), pp. 199–207.

Passingham, R. E., K. E. Stephan, and R. Kötter (2002). "The anatomical basis of functional localization in the cortex". *Nat Rev Neurosci*, 3(8), pp. 606–616.

Payeur, A., J.-C. Béïque, and R. Naud (2019). "Classes of dendritic information processing". *Curr Opin Neurobiol*, 58, pp. 78–85.

Pedregosa, F. et al. (2011). "Scikit-learn: Machine learning in Python". *Journal of machine Learning research*, 12, pp. 2825–2830.

Petre, P. and J. Cruz-Albrecht (2016). "Neuromorphic mixed-signal circuitry for Asynchronous Pulse Processing". In: *2016 IEEE International Conference on Rebooting Computing (ICRC)*. IEEE, pp. 1–4.

Poldrack, R. A. and T. Yarkoni (2016). "From brain maps to cognitive ontologies: Informatics and the search for mental structure". *Annual Review of Psychology*, 67, pp. 587–612.

Polepalli, A., N. Soures, and D. Kudithipudi (2016). "Digital neuromorphic design of a liquid state machine for real-time processing". In: *2016 IEEE International Conference on Rebooting Computing (ICRC)*. IEEE, pp. 1–8.

Power, J. D. and B. L. Schlaggar (2017). "Neural plasticity across the lifespan". *Wiley Interdisciplinary Reviews: Developmental Biology*, 6(1), e216.

Power, J. D. et al. (2011). "Functional network organization of the human brain". *Neuron*, 72(4), pp. 665–678.

Preti, M. G. and D. Van De Ville (2019). "Decoupling of brain function from structure reveals regional behavioral specialization in humans". *Nat Commun*.

Prince, L. Y. et al. (2021). "Current State and Future Directions for Learning in Biological Recurrent Neural Networks: A Perspective Piece". *arXiv preprint arXiv:2105.05382*.

Proix, T. et al. (2017). "Individual brain structure and modelling predict seizure propagation". *Brain*, 140(3), pp. 641–654.

Reichardt, J. and S. Bornholdt (2006). "When are networks truly modular?" *Physica D: Nonlinear Phenomena*, 224(1-2), pp. 20–26.

Reus, M. A. de and M. P. van den Heuvel (2013a). "Estimating false positives and negatives in brain networks". *NeuroImage*, 70, pp. 402–409.

— (2013b). "Rich club organization and intermodule communication in the cat connectome". *J Neurosci*, 33(32), pp. 12929–12939.

Richards, B. A. et al. (2019). "A deep learning framework for neuroscience". *Nat Neurosci*, 22(11), pp. 1761–1770.

Richiardi, J. et al. (2015). "Correlated gene expression supports synchronous activity in brain networks". *Science*, 348(6240), pp. 1241–1244.

Rigotti, M. et al. (2013). "The importance of mixed selectivity in complex cognitive tasks". *Nature*, 497(7451), pp. 585–590.

Riou, M. et al. (2021). "Reservoir computing leveraging the transient non-linear dynamics of spin-torque nano-oscillators". *Reservoir Computing: Theory, Physical Implementations, and Applications*, pp. 307–329.

Ritter, P. et al. (2013). "The virtual brain integrates computational modeling and multimodal neuroimaging". *Brain connectivity*, 3(2), pp. 121–145.

Roberts, J. A. et al. (2016). "The contribution of geometry to the human connectome". *NeuroImage*, 124, pp. 379–393.

Roberts, J. A. et al. (2017). "Consistency-based thresholding of the human connectome". *NeuroImage*, 145, pp. 118–129.

Roberts, J. A. et al. (2019). "Metastable brain waves". *Nat Commun*, 10(1), p. 1056.

Robinson, E. C. et al. (2018). "Multimodal surface matching with higher-order smoothness constraints". *NeuroImage*, 167, pp. 453–465.

Rodriguez, N., E. Izquierdo, and Y.-Y. Ahn (2019). "Optimal modularity and memory capacity of neural reservoirs". *Network Neuroscience*, 3(2), pp. 551–566.

Roland, J. L. et al. (2017). "On the role of the corpus callosum in interhemispheric functional connectivity in humans". *Proc Natl Acad Sci USA*, 114(50), pp. 13278–13283.

Rosenthal, G. et al. (2018). "Mapping higher-order relations between brain structure and function with embedded vector representations of connectomes". *Nat Commun*, 9(1), p. 2178.

Roy, S., A. Banerjee, and A. Basu (2014). "Liquid state machine with dendritically enhanced readout for low-power, neuromorphic VLSI implementations". *IEEE transactions on biomedical circuits and systems*, 8(5), pp. 681–695.

Rubinov, M. (2016). "Constraints and spandrels of interareal connectomes". *Nat Commun*, 7, p. 13812.

Rubinov, M. and O. Sporns (2010). "Complex network measures of brain connectivity: uses and interpretations". *Neuroimage*, 52(3), pp. 1059–1069.

Rubinov, M. et al. (2015). "Wiring cost and topological participation of the mouse brain connectome". *Proc Natl Acad Sci USA*, 112(32), pp. 10032–10037.

Salehi, M. et al. (2018). "There is no single functional atlas even for a single individual: Parcellation of the human brain is state dependent". *bioRxiv*, p. 431833.

Salmen, M. and P. G. Ploger (2005). "Echo state networks used for motor control". In: *Proceedings of the 2005 IEEE international conference on robotics and automation*. IEEE, pp. 1953–1958.

Sanz-Leon, P. et al. (2015). "Mathematical framework for large-scale brain network modeling in The Virtual Brain". *NeuroImage*, 111, pp. 385–430.

Scannell, J. W., C. Blakemore, and M. P. Young (1995). "Analysis of connectivity in the cat cerebral cortex". *J Neurosci*, 15(2), pp. 1463–1483.

Schaefer, A. et al. (2018). "Local-global parcellation of the human cerebral cortex from intrinsic functional connectivity MRI". *Cereb Cortex*, 28(9), pp. 3095–3114.

Schilling, K. G. et al. (2019a). "Challenges in diffusion MRI tractography–Lessons learned from international benchmark competitions". *Magn Reson Imaging*, 57, pp. 194–209.

Schilling, K. G. et al. (2019b). "Limits to anatomical accuracy of diffusion tractography using modern approaches". *NeuroImage*, 185, pp. 1–11.

Schirner, M. et al. (2018). "Inferring multi-scale neural mechanisms with brain network modelling". *eLife*, 7, e28927.

Schlenska, G (1974). "Volumen-und oberflachenmessungen an gehirnen verschiedener saugetiere im vergleich zu einem errechneten modell". *J Hirnforsch*, 15, pp. 401–408.

Schrauwen, B. et al. (2008). "Improving reservoirs using intrinsic plasticity". *Neurocomputing*, 71(7-9), pp. 1159–1171.

Scoville, W. B. and B. Milner (1957). "Loss of recent memory after bilateral hippocampal lesions". *Journal of neurology, neurosurgery, and psychiatry*, 20(1), p. 11.

Seehausen, O. et al. (2014). "Genomics and the origin of species". *Nat Rev Genet*, 15(3), pp. 176–192.

Seeholzer, L. F. et al. (2018). "Evolution of a central neural circuit underlies Drosophila mate preferences". *Nature*, 559(7715), pp. 564–569.

Seguin, C., Y. Tian, and A. Zalesky (2020). "Network communication models improve the behavioral and functional predictive utility of the human structural connectome". *Network Neuroscience*, (X), pp. 1–40.

Seguin, C., M. P. Van Den Heuvel, and A. Zalesky (2018). "Navigation of brain networks". *Proc Natl Acad Sci USA*, 115(24), pp. 6297–6302.

Seidlitz, J. et al. (2018). "Morphometric similarity networks detect microscale cortical organization and predict inter-individual cognitive variation". *Neuron*, 97(1), pp. 231–247.

Selemon, L. and P. Goldman-Rakic (1985). "Longitudinal topography and interdigitation of corticostriatal projections in the rhesus monkey". *Journal of Neuroscience*, 5(3), pp. 776–794.

Selemon, L. D. and P. S. Goldman-Rakic (1988). "Common cortical and subcortical targets of the dorsolateral prefrontal and posterior parietal cortices in the rhesus monkey: evidence for a distributed neural network subserving spatially guided behavior". *Journal of Neuroscience*, 8(11), pp. 4049–4068.

Sethi, S. S. et al. (2017). "Structural connectome topology relates to regional BOLD signal dynamics in the mouse brain". *Chaos*, 27(4), p. 047405.

Seung, H. S. (1996). "How the brain keeps the eyes still". *Proceedings of the National Academy of Sciences*, 93(23), pp. 13339–13344.

Shafiei, G. et al. (2018). "Dopamine signaling modulates the stability and integration of intrinsic brain networks". *Cereb Cortex*, 29(1), pp. 397–409.

Shafiei, G. et al. (2020). "Topographic gradients of intrinsic dynamics across neocortex". *bioRxiv*.

Shahi, S., F. H. Fenton, and E. M. Cherry (2022). "Prediction of chaotic time series using recurrent neural networks and reservoir computing techniques: A comparative study". *Machine learning with applications*, 8, p. 100300.

Shanahan, M. et al. (2013). "Large-scale network organization in the avian forebrain: a connectivity matrix and theoretical analysis". *Front Comput Neurosci*, 7, p. 89.

Shen, K. et al. (2012). "Information processing architecture of functionally defined clusters in the macaque cortex". *J Neurosci*, 32(48), pp. 17465–17476.

Shen, K. et al. (2015). "Stable long-range interhemispheric coordination is supported by direct anatomical projections". *Proc Natl Acad Sci USA*, 112(20), pp. 6473–6478.

Sherman, S. M. and R. Guillery (2002). "The role of the thalamus in the flow of information to the cortex". *Philosophical Transactions of the Royal Society of London. Series B: Biological Sciences*, 357(1428), pp. 1695–1708.

Shew, W. L. et al. (2009). "Neuronal avalanches imply maximum dynamic range in cortical networks at criticality". *Journal of neuroscience*, 29(49), pp. 15595–15600.

Shine, J. M. (2019). "Neuromodulatory Influences on Integration and Segregation in the Brain". *Trends Cogn Sci*.

Shine, J. M. et al. (2018a). "Catecholaminergic manipulation alters dynamic network topology across cognitive states". *Net Neurosci*, 2(3), pp. 381–396.

Shine, J. M. et al. (2018b). "The modulation of neural gain facilitates a transition between functional segregation and integration in the brain". *eLife*, 7, e31130.

Shine, J. M. et al. (2019). "Human cognition involves the dynamic integration of neural activity and neuromodulatory systems". *Nat Neurosci*, 22(2), p. 289.

Shine, J. M. et al. (2020). "Topological Augmentation of Latent Information Streams in Feed-Forward Neural Networks". *bioRxiv*.

Sillin, H. O. et al. (2013). "A theoretical and experimental study of neuromorphic atomic switch networks for reservoir computing". *Nanotechnology*, 24(38), p. 384004.

Singer, W. (1993). "Synchronization of cortical activity and its putative role in information processing and learning". *Annual review of physiology*, 55(1), pp. 349–374.

— (1999). "Neuronal synchrony: a versatile code for the definition of relations?" *Neuron*, 24(1), pp. 49–65.

— (2021). "The Cerebral Cortex: A Delay-Coupled Recurrent Oscillator Network?" *Reservoir Computing: Theory, Physical Implementations, and Applications*, pp. 3–28.

Singer, W. and C. M. Gray (1995). "Visual feature integration and the temporal correlation hypothesis". *Annual review of neuroscience*, 18(1), pp. 555–586.

Siuda-Krzywicka, K. et al. (2016). "Massive cortical reorganization in sighted Braille readers". *Elife*, 5, e10762.

Sizemore, A. E. et al. (2018). "Cliques and cavities in the human connectome". *Journal of computational neuroscience*, 44(1), pp. 115–145.

Skowronski, M. D. and J. G. Harris (2007). "Automatic speech recognition using a predictive echo state network classifier". *Neural networks*, 20(3), pp. 414–423.

Smith, E. S. J. et al. (2011). "The molecular basis of acid insensitivity in the African naked mole-rat". *Science*, 334(6062), pp. 1557–1560.

Smith, S. M. et al. (2009). "Correspondence of the brain's functional architecture during activation and rest". *Proc Natl Acad Sci USA*, 106(31), pp. 13040–13045.

Soriano, M. C. et al. (2014). "Delay-based reservoir computing: noise effects in a combined analog and digital implementation". *IEEE transactions on neural networks and learning systems*, 26(2), pp. 388–393.

Spiegler, A. et al. (2016). "Selective activation of resting-state networks following focal stimulation in a connectome-based network model of the human brain". *eNeuro*, 3(5).

Sporns, O. (2013). "Network attributes for segregation and integration in the human brain". *Current opinion in neurobiology*, 23(2), pp. 162–171.

— (2022). "Structure and function of complex brain networks". *Dialogues in clinical neuroscience*.

Sporns, O., C. J. Honey, and R. Kötter (2007). "Identification and classification of hubs in brain networks". *PloS one*, 2(10), e1049.

Sporns, O. and R. Kötter (2004). "Motifs in brain networks". *PLoS Biol*, 2(11), e369.

Sporns, O., G. Tononi, and R. Kötter (2005). "The human connectome: a structural description of the human brain". *PLoS Comput Biol*, 1(4), e42.

Sporns, O. and J. D. Zwi (2004). "The small world of the cerebral cortex". *Neuroinformatics*, 2(2), pp. 145–162.

Sporns, O. et al. (2004). "Organization, development and function of complex brain networks". *Trends in cognitive sciences*, 8(9), pp. 418–425.

Stadler, M. A. (1993). "Implicit serial learning: Questions inspired by Hebb (1961)". *Memory & cognition*, 21, pp. 819–827.

Stiso, J. and D. S. Bassett (2018). "Spatial embedding imposes constraints on neuronal network architectures". *Trends in cognitive sciences*, 22(12), pp. 1127–1142.

Strock, A., N. P. Rougier, and X. Hinaut (2018). "A simple reservoir model of working memory with real values". In: *2018 International Joint Conference on Neural Networks (IJCNN)*. IEEE, pp. 1–8.

Suárez, L. E. (2021). *Code for: Learning function from structure in neuromorphic networks*. Version 0.0.1-alpha.

Suárez, L. E., J. D. Kendall, and J. C. Nino (2018). "Evaluation of the computational capabilities of a memristive random network (MN3) under the context of reservoir computing". *Neural Networks*, 106, pp. 223–236.

Suárez, L. E. et al. (2020). "Linking structure and function in macroscale brain networks". *Trends in Cognitive Sciences*, 24(4), pp. 302–315.

Suárez, L. E. et al. (2021). "Learning function from structure in neuromorphic networks". *Nature Machine Intelligence*, 3(9), pp. 771–786.

Suarez, L. E. et al. (2022). "A connectomics-based taxonomy of mammals". *Elife*, 11, e78635.

Subramoney, A., F. Scherr, and W. Maass (2021). "Reservoirs learn to learn". *Reservoir Computing: Theory, Physical Implementations, and Applications*, pp. 59–76.

Supekar, K. et al. (2010). "Development of functional and structural connectivity within the default mode network in young children". *NeuroImage*, 52(1), pp. 290–301.

Sussillo, D. and L. F. Abbott (2009). "Generating coherent patterns of activity from chaotic neural networks". *Neuron*, 63(4), pp. 544–557.

Sussillo, D. et al. (2015). "A neural network that finds a naturalistic solution for the production of muscle activity". *Nature neuroscience*, 18(7), pp. 1025–1033.

Sydnor, V. J. et al. (2021). "Neurodevelopment of the association cortices: Patterns, mechanisms, and implications for psychopathology". *Neuron*.

Tagliazucchi, E. et al. (2012). "Criticality in large-scale brain fMRI dynamics unveiled by a novel point process analysis". *Frontiers in physiology*, 3, p. 15.

Tagliazucchi, E. et al. (2016). "Increased global functional connectivity correlates with LSD-induced ego dissolution". *Curr Biol*, 26(8), pp. 1043–1050.

Tanaka, G. et al. (2019). "Recent advances in physical reservoir computing: A review". *Neural Networks*, 115, pp. 100–123.

Taniguchi, T. et al. (2021). "Reservoir Computing Based on Spintronics Technology". *Reservoir Computing: Theory, Physical Implementations, and Applications*, pp. 331–360.

Taylor, P et al. (2015). "The global landscape of cognition: hierarchical aggregation as an organizational principle of human cortical networks and functions". *Scientific reports*, 5(1), pp. 1–18.

Tendler, B. C. et al. (2021). "The Digital Brain Bank: an open access platform for post-mortem datasets". *bioRxiv*.

Theunissen, L. (1988). *Eugène Dubois and the Ape-man from Java: The history of the first 'missing link'and its discoverer*. Springer Science & Business Media.

Thomas, C. et al. (2014). "Anatomical accuracy of brain connections derived from diffusion MRI tractography is inherently limited". *Proc Natl Acad Sci USA*, 111(46), pp. 16574–16579.

Thomas Yeo, B. et al. (2011). "The organization of the human cerebral cortex estimated by intrinsic functional connectivity". *J Neurophysiol*, 106(3), pp. 1125–1165.

Tong, M. H. et al. (2007). "Learning grammatical structure with echo state networks". *Neural networks*, 20(3), pp. 424–432.

Tononi, G., G. M. Edelman, and O. Sporns (1998). "Complexity and coherency: integrating information in the brain". *Trends in cognitive sciences*, 2(12), pp. 474–484.

Tononi, G., O. Sporns, and G. M. Edelman (1994). "A measure for brain complexity: relating functional segregation and integration in the nervous system". *Proceedings of the National Academy of Sciences*, 91(11), pp. 5033–5037.

Tournier, J.-D. et al. (2004). "Direct estimation of the fiber orientation density function from diffusion-weighted MRI data using spherical deconvolution". *NeuroImage*, 23(3), pp. 1176–1185.

Towlson, E. K. et al. (2013). "The rich club of the C. elegans neuronal connectome". *J Neurosci*, 33(15), pp. 6380–6387.

Tsodyks, M. (2002). "Spike-timing-dependent synaptic plasticity–The long road towards understanding neuronal mechanisms of learning and memory". *Trends in neurosciences*, 25(12), pp. 599–600.

Uddin, L. Q. (2020). "Bring the noise: Reconceptualizing spontaneous neural activity". *Trends Cogn Sci*.

Uddin, L. Q., B. T. Yeo, and R. N. Spreng (2019). "Towards a universal taxonomy of macro-scale functional human brain networks". *Brain topography*, pp. 1–17.

Uddin, L. Q. et al. (2008). "Residual functional connectivity in the split-brain revealed with resting-state fMRI". *Neuroreport*, 19(7), p. 703.

Uddin, L. Q. et al. (2011). "Dynamic reconfiguration of structural and functional connectivity across core neurocognitive brain networks with development". *J Neurosci*, 31(50), pp. 18578–18589.

Vaishnavi, S. N. et al. (2010). "Regional aerobic glycolysis in the human brain". *Proceedings of the National Academy of Sciences*, 107(41), pp. 17757–17762.

Van Den Heuvel, M. P. et al. (2009). "Functionally linked resting-state networks reflect the underlying structural connectivity architecture of the human brain". *Human brain mapping*, 30(10), pp. 3127–3141.

Van Essen, D. C. (2005). "A population-average, landmark-and surface-based (PALS) atlas of human cerebral cortex". *NeuroImage*, 28(3), pp. 635–662.

Van Essen, D. C. et al. (2013). "The WU-Minn human connectome project: an overview". *NeuroImage*, 80, pp. 62–79.

Vandoorne, K. et al. (2008). "Toward optical signal processing using photonic reservoir computing". *Optics express*, 16(15), pp. 11182–11192.

Vandoorne, K. et al. (2014). "Experimental demonstration of reservoir computing on a silicon photonics chip". *Nature communications*, 5(1), pp. 1–6.

Vanwalleghem, G. C., M. B. Ahrens, and E. K. Scott (2018). "Integrative whole-brain neuroscience in larval zebrafish". *Current opinion in neurobiology*, 50, pp. 136–145.

Váša, F. et al. (2018). "Adolescent tuning of association cortex in human structural brain networks". *Cerebral Cortex*, 28(1), pp. 281–294.

Vázquez-Rodríguez, B. et al. (2017). "Stochastic resonance at criticality in a network model of the human cortex". *Scientific reports*, 7(1), pp. 1–12.

Vazquez-Rodriguez, B. et al. (2019). "Gradients of structure-function tethering across neocortex". *Proc Natl Acad Sci USA*.

Verstraeten, D., B. Schrauwen, and D. Stroobandt (2006). "Reservoir-based techniques for speech recognition". In: *The 2006 IEEE International Joint Conference on Neural Network Proceedings*. IEEE, pp. 1050–1053.

Verstraeten, D. et al. (2005). "Isolated word recognition with the liquid state machine: a case study". *Information Processing Letters*, 95(6), pp. 521–528.

Verstraeten, D. et al. (2007). "An experimental unification of reservoir computing methods". *Neural networks*, 20(3), pp. 391–403.

Virtanen, P. et al. (2020). "SciPy 1.0: fundamental algorithms for scientific computing in Python". *Nature methods*, 17(3), pp. 261–272.

Walt, S. v. d., S. C. Colbert, and G. Varoquaux (2011). "The NumPy array: a structure for efficient numerical computation". *Computing in science & engineering*, 13(2), pp. 22–30.

Wang, D. et al. (2015). "Parcellating cortical functional networks in individuals". *Nat Neurosci*, 18(12), p. 1853.

Wang, H. et al. (2011). "Recurrent neural networks: Associative memory and optimization". *Journal of Information Technology and Software Engineering*, 1(104), p. 2.

Wang, P. et al. (2019). "Inversion of a large-scale circuit model reveals a cortical hierarchy in the dynamic resting human brain". *Sci Adv*, 5(1), eaat7854.

Wang, Q. et al. (2017). "Energy efficient parallel neuromorphic architectures with approximate arithmetic on FPGA". *Neurocomputing*, 221, pp. 146–158.

Warrington, S et al. (2022). "Concurrent mapping of brain ontogeny and phylogeny within a common connectivity space". *bioRxiv*.

Waskom, M. et al. (2016). "seaborn: v0. 7.0 (January 2016)". *zenodo10*, 5281.

Watts, D. J. and S. H. Strogatz (1998). "Collective dynamics of small-world networks". *Nature*, 393(6684), p. 440.

White, J. G. et al. (1986). "The structure of the nervous system of the nematode Caenorhabditis elegans". *Philos Trans R Soc Lond B Biol Sci*, 314(1165), pp. 1–340.

Whittington, M. A. et al. (2000). "Inhibition-based rhythms: experimental and mathematical observations on network dynamics". *International journal of psychophysiology*, 38(3), pp. 315–336.

Wig, G. S. (2017). "Segregated systems of human brain networks". *Trends in cognitive sciences*, 21(12), pp. 981–996.

Wills, T. J. et al. (2005). "Attractor dynamics in the hippocampal representation of the local environment". *Science*, 308(5723), pp. 873–876.

Winslow, J. T. et al. (1993). "A role for central vasopressin in pair bonding in monogamous prairie voles". *Nature*, 365(6446), pp. 545–548.

Worrell, J. C. et al. (2017). "Optimized connectome architecture for sensory-motor integration". *Net Neurosci*, 1(4), pp. 415–430.

Wright, S. (1931). "Evolution in Mendelian populations". *Genetics*, 16(2), p. 97.

Wu, D. et al. (2019). "Hierarchy of connectivity-function relationship of the human cortex revealed through predicting activity across functional domains". *bioRxiv*, p. 591776.

Wyffels, F. and B. Schrauwen (2009). "Design of a central pattern generator using reservoir computing for learning human motion". In: *2009 Advanced Technologies for Enhanced Quality of Life*. IEEE, pp. 118–122.

Yang, W. and R. Yuste (2017). "In vivo imaging of neural activity". *Nat Meth*, 14(4), p. 349.

Yang, X., W. Chen, and F. Z. Wang (2016). "Investigations of the staircase memristor model and applications of memristor-based local connections". *Analog Integrated Circuits and Signal Processing*, 87(2), pp. 263–273.

Yarkoni, T et al. (2011a). "NeuroSynth: a new platform for large-scale automated synthesis of human functional neuroimaging data Frontiers in Neuroinformatics Conference Abstract: 4th INCF Congress of Neuroinformatics". In: *Boston, United States. doi: 10.3389/conf. fninf*. Vol. 58.

Yarkoni, T. et al. (2011b). "Large-scale automated synthesis of human functional neuroimaging data". *Nature Methods*, 8(8), p. 665.

Yokoyama, C. et al. (2021). "Comparative connectomics of the primate social brain". *NeuroImage*, 245, p. 118693.

York, R. A. (2018). "Assessing the genetic landscape of animal behavior". *Genetics*, 209(1), pp. 223–232.

York, R. A. et al. (2019). "Behavioral evolution contributes to hindbrain diversification among Lake Malawi cichlid fish". *Scientific reports*, 9(1), pp. 1–9.

Young, M. P. (1993). "The organization of neural systems in the primate cerebral cortex". *J Roy Soc Lond B*, 252(1333), pp. 13–18.

Zador, A. M. (2019). "A Critique of Pure Learning: What Artificial Neural Networks can Learn from Animal Brains". *BioRxiv*, p. 582643.

Zalesky, A. et al. (2016). "Connectome sensitivity or specificity: which is more important?" *NeuroImage*, 142, pp. 407–420.

Zamora-López, G., C. Zhou, and J. Kurths (2010). "Cortical hubs form a module for multisensory integration on top of the hierarchy of cortical networks". *Front Neuroinform*, 4, p. 1.

Zhang, A., W. Zhu, and M. Liu (2017). "Self-organizing reservoir computing based on spiking-timing dependent plasticity and intrinsic plasticity mechanisms". In: *2017 Chinese Automation Congress (CAC)*. IEEE, pp. 6189–6193.

Zhang, H. et al. (2014). "Integrated photonic reservoir computing based on hierarchical time-multiplexing structure". *Optics express*, 22(25), pp. 31356–31370.

Zhang, J. et al. (2016). "Neural, electrophysiological and anatomical basis of brain-network variability and its characteristic changes in mental disorders". *Brain*, 139(8), pp. 2307–2321.

Zhang, K. and T. J. Sejnowski (2000). "A universal scaling law between gray matter and white matter of cerebral cortex". *Proceedings of the National Academy of Sciences*, 97(10), pp. 5621–5626.

Zhang, M. and M. Saggar (2020). "Complexity of intrinsic brain dynamics shaped by multiscale structural constraints". *BioRxiv*, pp. 2020–05.

Zhao, C. et al. (2016). "Novel spike based reservoir node design with high performance spike delay loop". In: *Proceedings of the 3rd ACM International Conference on Nanoscale Computing and Communication*, pp. 1–5.

Zhou, S. and R. J. Mondragón (2004). "The rich-club phenomenon in the Internet topology". *IEEE communications letters*, 8(3), pp. 180–182.

Zimmermann, J., J. D. Griffiths, and A. R. McIntosh (2018). "Unique mapping of structural and functional connectivity on cognition". *J Neurosci*, 38(45), pp. 9658–9667.

Zylberberg, J. and B. W. Strowbridge (2017). "Mechanisms of persistent activity in cortical circuits: possible neural substrates for working memory". *Annual review of neuroscience*, 40.